Queensland University of Technology
Brisbane Australia

This is the author's version of a work that was submitted/accepted for publication in the following source:

Surawski, Nicholas C. (2012) *An investigation of gaseous and particulate emissions from compression ignition engines operated with alternative fuels, injection technologies, and combustion strategies.* PhD by Publication, Queensland University of Technology.

This file was downloaded from: http://eprints.qut.edu.au/54194/

Notice: *Changes introduced as a result of publishing processes such as copy-editing and formatting may not be reflected in this document. For a definitive version of this work, please refer to the published source:*

An investigation of gaseous and particulate emissions from compression ignition engines operated with alternative fuels, injection technologies, and combustion strategies

Nicholas C. Surawski

BEnvSc Hons I (Griffith University), MSc (QUT)

A thesis by publication submitted in partial fulfilment of the requirements for the degree of Doctor of Philosophy (PhD)

School of Chemistry, Physics and Mechanical Engineering

Science and Engineering Faculty

Queensland University of Technology

November 2011

Ye blind guides, which straine at a gnat, and swallow a camel.

Matthew 23:24 (1611 King James Bible)

Statement of original authorship

The work contained in this thesis has not been previously submitted for a degree or diploma at any other higher education institution. To the best of my knowledge and belief, the thesis contains no material previously published or written by another person except where due reference is made.

Signed:…….

Date:…….

Abstract

Whilst the compression ignition (CI) engine exhibits many design advantages relative to its spark ignition engine counterpart; such as: high thermal efficiency, fuel economy and low carbon monoxide and hydrocarbon emissions, the issue of Diesel Particulate Matter (DPM) emissions continues to be an unresolved problem for the CI engine. Primarily, this thesis investigates a range of DPM mitigation strategies such as alternative fuels, injection technologies and combustion strategies conducted with a view to determine their impact on the physico-chemical properties of DPM emissions, and consequently to shed light on their likely human health impacts. Regulated gaseous emissions, Nitric oxide (NO), Carbon monoxide (CO), and Hydrocarbons (HCs), were measured in all experimental campaigns, although the major focus in this research program was on particulate emissions.

Several experimental campaigns were conducted to achieve the primary aims of this thesis. An ethanol fumigation system (which involves intake manifold injection of a secondary fuel) was installed on a direct injection CI engine, where ethanol substitution percentages in the 10-40 % range (by energy) were achieved. Testing was conducted at intermediate speed (1700 rpm) with 4 different load settings. Relative to neat diesel, this study found that $PM_{2.5}$ (PM with an aerodynamic diameter $\leq$ 2.5 μm) emissions changes ranged from a 56 % increase with E10 (i.e. 10 % of total fuel energy from ethanol) at idle mode to an 81 % reduction with E40 at full load. NO emissions reductions ranged from 68 % with E40 at half load, to a 22 % reduction with E10 at idle mode. CO emissions changes ranged from a 13 % decrease with E10 at idle mode, to a near three-fold increase with E40 at half load. The HC emissions followed a similar pattern to CO, with the HC emissions ranging from a 30 % reduction with E10 at idle mode, to a near 2.5 fold increase with E40 at half load. Whilst significant particle mass reductions were generally achieved with ethanol fumigation, the number of particles emitted was increased at most test modes. Particle number emissions ranged from at 31 % reduction with E10 at idle mode, to a 2.5 fold increase with E40 at full load. The measurement of particle number size distributions showed that with ethanol fumigation at full load, a nucleation mode (particle diameter, D_p, > 30 nm) appeared in the size distribution for E40, but only accumulation mode (30 < D_p < 500 nm) particles were observed with neat diesel. Nucleation modes were observed in the particle number size distributions at all other load setting and ethanol substitution percentages. Through a Volatilisation Tandem Differential Mobility Analyser (V-TDMA) analysis, it was shown that

the particle number emissions increases at full load were the result of homogeneous nucleation of volatile (i.e. organic) compounds. To achieve a reduction in all four regulated pollutants, and also to mitigate the volatile particle formation, it is recommended that a diesel oxidation catalyst be used as an after-treatment device.

The second study explored the physico-chemical properties of DPM emissions from an underground mine compression ignition engine operated with 2 injection technologies (mechanical direct injection and common rail injection) and 3 fuels (i.e. ultra-low sulphur diesel, 20 % biodiesel blend, and synthetic diesel) over a 4 point test cycle. The results from this study showed that both fuel type and injection technology have an impact on particle emissions, but injection technology was the more important factor. Significant particle number emission (54%-84%) reductions were achieved at half load operation (1% increase-43% decrease at full load) with the common rail injection system; however, the particles had a significantly higher polycyclic aromatic hydrocarbon (PAH) fraction (by a factor of 2 to 4) and reactive oxygen species (ROS) concentrations (by a factor of 6 to 16) both expressed on a test-cycle averaged basis. Installing a turbocharger on this test engine could be a useful strategy for reducing the elevated PAH and ROS emissions with the common rail injection system.

A third study undertook a physico-chemical characterisation of DPM emissions from an underground mine CI engine operated at intermediate speed and full load with 3 biodiesel fuels made from 3 different feedstocks (i.e. soy, tallow and canola) tested with at least 4 different blend percentages (20-100 %). The particle number size distributions showed strong dependency on feedstock and blend percentage with some fuel types showing increased particle number emissions, whilst others showed particle number reductions. Particle and vapour phase PAHs were generally reduced with biodiesel, with the results being relatively independent of the blend percentage. The ROS concentrations increased monotonically with biodiesel blend percentage, but did not exhibit strong feedstock variability. Furthermore, the ROS concentrations correlated quite well with the organic volume percentage of particles (obtained via a combined Scanning Mobility Particle Sizer-Thermodenuder approach) – a quantity which increased with increasing blend percentage. The results of this study highlighted the importance of considering the surface chemistry of particles when investigating the likely health impacts of DPM emissions.

A significant reduction in the median particle diameter was observed with most of the alternative fuels investigated in the above 3 studies. Whilst observation of particle restructuring of combustion generated particles upon exposure to various organic and water vapours is becoming more common in the literature, hypotheses able to explain this effect remain limited. Consequently, a secondary aim of this thesis was to explore hypotheses related to the restructuring of combustion generated particles involving; the effect of surface tension, wetting of the particle surface by a vapour, and also the role of organics in flocculating elemental carbon containing primary particles. Overall, the results from this investigation show that wetting of the particle surface seems to be responsible for morphological restructuring of some carbonaceous particle types, such as DPM, candle smoke, and a heptane/toluene combustion mixture.

To synthesise the results from this thesis, multi-criteria decision analysis was performed using the Preference Ranking Organisation METHod for Enrichment Evaluations and Graphical Analysis for Interactive Assistance (PROMETHEE-GAIA) algorithm. This analysis ranked different DPM mitigation strategies based on their gaseous, particulate and life cycle greenhouse gas emissions and the analysis also considered engine thermal efficiency. Based on the complete PROMETHEE II outranking provided by this algorithm, alternative fuels were more highly ranked compared to their petroleum diesel counterparts for all experimental datasets. In the GAIA plane a clear demarcation can be observed between DPM physical and chemical properties. In particular, the DPM mitigation strategies investigated in this thesis performed well based on their physical properties (such as particle mass, number etc) but performed relatively poorly with their chemical emissions profile, especially for ROS emissions. Improving the unregulated chemistry of DPM emissions with alternative fuels thus emerges from this analysis as an area requiring improvement in future CI engine emissions studies.

Overall this thesis has delivered a vast body of new information relating common DPM mitigation techniques to their resulting DPM physico-chemical properties.

Keywords

Compression ignition (CI) engine, Diesel Particulate Matter (DPM), Particulate Matter (PM), particle number size distribution, particle number emissions, accumulation mode, nucleation mode, Condensation Particle Counter (CPC), Scanning Mobility Particle Sizer (SMPS), Thermodenuder (TD), SMPS-TD, volatility, Volatilisation Tandem Differential Mobility Analyser (V-TDMA), Count Median Diameter (CMD), particle mass emissions, Dust-Trak, diesel particulate filter, diesel oxidation catalyst, gaseous emissions, Nitrogen Oxides (NOx), Carbon monoxide (CO), Hydrocarbons (HCs), Polycyclic Aromatic Hydrocarbons (PAHs), Reactive Oxygen Species (ROS), gaseous emissions, Life Cycle Analysis (LCA), alternative fuels, biofuels, ethanol, biodiesel, blends, fumigation, mechanical direct injection, common rail injection, Multi Criteria Decision Analysis (MCDA), Preference Ranking Organisation METHod for Enrichment Evaluations and Graphical Analysis for Interactive Assistance (PROMETHEE-GAIA).

List of publications

Ristovski, Z.D., Miljevic, B., Surawski, N.C., Morawska, L., Fong, K.M., Goh, F., Yang, I.A., **2011**. Respiratory health effects of diesel particulate matter. *Respirology* **2012**, 17, (2), 201-212.

Surawski, N. C.; Ristovski, Z. D.; Brown, R. J.; Situ, R., Gaseous and particle emissions from an ethanol fumigated compression ignition engine. *Energy Conversion and Management* **2012**, 54, (1), 145-151.

Surawski, N. C.; Miljevic, B.; Roberts, B. A.; Modini, R. L.; Situ, R.; Brown, R. J.; Bottle, S. E.; Ristovski, Z. D., Particle Emissions, Volatility, and Toxicity from an Ethanol Fumigated Compression Ignition Engine. *Environmental Science & Technology* **2010,** *44*, (1), 229-235.

Surawski, N. C.; Miljevic, B.; Ayoko, G. A.; Roberts, B. A.; Elbagir, S.; Fairfull-Smith, K. E.; Bottle, S. E.; Ristovski, Z. D., Physicochemical Characterization of Particulate Emissions from a Compression Ignition Engine Employing Two Injection Technologies and Three Fuels. *Environmental Science & Technology* **2011,** *45*, (13), 5498-5505.

Surawski, N. C.; Miljevic, B.; Ayoko, G. A.; Elbagir, S.; Stevanovic, S.; Fairfull-Smith, K. E.; Bottle, S. E.; Ristovski, Z. D., A physico-chemical characterisation of particulate emissions from a compression ignition engine: the influence of biodiesel feedstock. *Environmental Science & Technology* **2011**, 45, (24), 10337-10343.

Miljevic, B.; Surawski, N. C.; Bostrom, T.; Ristovski, Z. D., Restructuring of carbonaceous particles upon exposure to organic vapours. *Journal of Aerosol Science* **2012**, 47, 48-57.

Surawski, N.C., Bodisco, T.A., Miljevic, B., Brown, R.J., Ristovski, Z.D., Ayoko, G.A., **2011**. Multi-criteria decision analysis applied to compression ignition engine efficiency and gaseous, particulate and greenhouse gas emissions. Under review, *Environmental Science & Technology*.

Acknowledgements

My first scientific fascination in early childhood was of an aerosols nature, and involved my mother opening the curtains to her bedroom. A beam of light entered the room and the scattered light enabled particles to be observed. I asked my mother why this happened, and did not get a satisfactory response. If the question was answered properly, perhaps, I would not have embarked on a quest to complete doctoral studies in Aerosol Physics - is this all just fate?

I wish to extend many sincere thanks to my supervisors; namely, my principal supervisor Associate Professor Zoran Ristovski and my associate supervisor Associate Professor Richard Brown. They have supported me in ways that this brief acknowledgement could never possibly do justice to. They have opened so many pathways to opportunity, and have been there to provide very sound scientific judgement and personal counsel at all stages of my candidature. Without their continued guidance and patience, this thesis would not have materialised. I would also like to extend thanks to Professor Godwin Ayoko for making me aware of the PROMETHEE-GAIA technique.

I also wish to commend the efforts of Mr Jonathan James who is the supervising technician for the civil and mechanical engineering disciplines in the Faculty of Built Environment and Engineering (BEE) at QUT. Jon is capably supported by a team of technicians who have supported the BERF facility in many ways. Special thanks are reserved especially for Mr Glenn Geary and also Mr Noel Hartnett – they have provided a great deal of technical and practical assistance to make engine testing at QUT a reality.

The dual-fuel project was fortunate to have a technologist (Mr Anthony Morris) involved who was able to provide research support. His mechanical, electrical, and chemical engineering troubleshooting was first-class, and it was a genuine pleasure of my candidature to work with such a highly skilled engineer.

I wish to extend thanks to all of my ILAQH colleagues for their assistance, co-operation, friendship, and occasional humour. In particular, the input of Dr Branka Miljevic, Dr Robin Modini, and Dr Mandana Mazaheri has been a great deal of help to me. The not so

intermittent humour of Dr Luke Knibbs and Dr Rohan Jayaratne, and associated discussions on cricket, were a very welcome distraction from my work.

I wish to extend thanks to the other post-graduate students involved in the dual-fuel project for their assistance; namely, Mr Timothy Bodisco and Mr David Lowe.

Completing a PhD would be by no means possible without financial assistance. The author was fortunate to simultaneously receive an Australian Post-Graduate Award (APA), A Vice-Chancellor's Initiative Scholarship and a Faculty of Built Environment and Engineering Top-Up scholarship. Thanks obviously go to the relevant departments and committee's for making these scholarships available to me; however, ultimately, the hard-working Australian tax-payer makes such funding schemes available.

This thesis would not have materialised with the emotional, moral and financial support of my wife May. May is my best friend, and completing this thesis would not have been possible without her assistance. My three children, Marcel, Veronica and Gwyneth have provided a very welcome distraction during my candidature, a constant source of inspiration, and a newly found symbol of structure and meaning in my life.

Completion of this journey has been a very tortuous process indeed. I wish to thank my father Graham for cultivating positive reading habits as a child through his wonderful collection of books. I also wish to thank my mother Raylene for her financial support. Without her help, I would not have completed the degrees before this one. I wish to thank my brother Michael, and Sisters Tanya and Wendy for helping me to balance my desire for learning with other aspects of life worth living.

Dedication

Like my late sister Andrea, there have been many occasions when a troubled inner thought plagued my existence. For this reason, I dedicate this thesis to all paranoid schizophrenics who do not lead productive lives.

Table of contents

Statement of original authorship iii

Abstract iv

Keywords vii

List of publications viii

Acknowledgements ix

Dedication xi

Table of contents xii

Table of figures xvii

Table of tables xxi

Chapter 1: Introduction 1

1.1 The research problem investigated 1

1.2 Study aim 2

1.3 Specific study objectives 3

1.4 Account of research progress linking the research papers 4

1.5 References 7

Chapter 2: Theoretical considerations 10

2.1 Introduction 10

2.2 The nature of compression ignition engine emissions 10

2.2.1 Introduction 10

2.2.2 Gaseous emissions and health effects 10

2.2.3 The composition and formation of DPM 13

2.2.4 Life cycle greenhouse gas emissions 22

2.2.5 CI engine efficiency 22

2.3 DPM mitigation strategies 23

2.3.1 The case for alternative fuels 23
2.3.2 The case for alternative injection strategies 26
2.3.3 The case for alternative combustion strategies 27
2.4 Health effects of DPM 28
2.4.1 Introduction 28
2.4.2 Inflammation 28
2.4.3 Oxidative stress 29
2.4.4 Physico-chemical properties that drive inflammation and oxidative stress 30
2.4.5 Translocation 31
2.4.6 Health effects review conclusion 32
2.5 Measurement techniques 32
2.5.1 DPM emissions sampling issues 32
2.5.2 Gaseous emissions measurement 34
2.5.3 DPM emissions measurement 35
2.6 Multi-criteria decision analysis techniques 38
2.7 Research needs addressed by this thesis 42
2.7.1 DPM physico-chemistry 42
2.7.2 Particle size reduction with alternative fuels 43
2.7.3 Multi-criteria decision analysis 44
2.8 References 44
Chapter 3: Gaseous and particle emissions from an ethanol fumigated compression ignition engine 61
3.1 Introduction 63
3.2 Methodology 65
3.2.1 Engine and fuel specifications 65
3.2.2 Emissions measurement methodology 67
3.3 Results and discussion 68

3.4 Conclusions 75
3.5 References 76
Chapter 4: Particle emissions, volatility and toxicity from an ethanol fumigated compression ignition engine 80
4.1 Introduction 82
4.2 Methodology 84
4.2.1 Engine, fuel and testing specifications 84
4.2.2 Particle measurement methodology 85
4.2.3 Particle volatility methodology 86
4.2.4 ROS concentration measurement – BPEAnit assay 87
4.3 Results 88
4.3.1 Particle size distributions 88
4.3.2 Particle volatility 91
4.3.3 ROS concentration results 93
4.4 Discussion 95
4.5 References 98
4.6 Supporting information 100
Chapter 5: A physico-chemical characterisation of particulate emissions from a compression ignition engine employing two injection technologies and three fuels 104
5.1 Introduction 106
5.2 Methodology 107
5.2.1 Engine, injection system and fuel specifications 107
5.2.2 Particulate emissions measurement methodology 109
5.2.3 Data analysis 111
5.3 Results and discussion 112
5.3.1 Particle number size distributions 112
5.3.2 PAH emission factors and ROS concentrations 115

5.3.3 Particle volatility 118

5.4 References 119

5.5 Supporting information 123

Chapter 6: A physico-chemical characterisation of particulate emissions from a compression ignition engine: the influence of biodiesel feedstock 130

6.1 Introduction 132

6.2 Methodology 134

6.2.1 Engine and fuel specifications 134

6.2.2 Particulate emissions measurement methodology 135

6.2.3 Data analysis 136

6.3 Results and discussion 137

6.3.1 PM_{10} emission factors 137

6.3.2 Particle number emission factors 137

6.3.3 Particle number size distributions 139

6.3.4 PAH emission factors and ROS concentrations 141

6.3.5 Particle volatility and ROS correlation 143

6.3.6 Particle surface area and organic volume percentage of particles 144

6.4 References 146

6.5 Supporting information 149

Chapter 7: Restructuring of carbonaceous particles upon exposure to organic vapours 153

7.1 Introduction 155

7.2 Materials and methods 157

7.2.1 Particle sources 157

7.2.2 Experimental set-up 158

7.2.3 TEM sampling and analysis 159

7.3 Results 159

7.3.1 TDMA measurements 159

7.3.2 TEM images 163
7.4 Discussion 164
7.5 Conclusions 169
7.6 References 169
Chapter 8: Multi-criteria decision analysis applied to compression ignition engine efficiency and gaseous, particulate and greenhouse gas emissions 172
8.1 Introduction 174
8.2 Methods 176
8.2.1 The PROMETHEE-GAIA algorithm 176
8.2.2 The datasets analysed 180
8.3 Results and discussion 184
8.4 References 192
Chapter 9: Conclusions and further research 195
9.1 Conclusions arising from this study 195
9.2 Recommendations for future research 198
9.3 Concluding remark 201
9.4 References 202

Table of figures

Figure 1.1: A diagram outlining the structure of this PhD research program. 5
Figure 2.1: A graph showing the relationship between particle number, surface and mass distributions, and the deposition of particles in the tracheo-bronchial region of the human lung upon inhalation (adapted from Kittelson et al. (2004)). 17
Figure 2.2: An engineer's depiction of DPM (adopted from (Maricq, 2007). 19
Figure 2.3: Modes and formation mechanisms of the DPM particle number size distribution (Figure adapted from (United States Environmental Protection Agency, 2004; Kittelson et al., 2006a)). 21
Figure 2.4: An illustration of oxidant/anti-oxidant balance *in vivo* and associated biological responses (figure adopted from (Kelly, 2003)). 30
Figure 2.5: A graph showing the dependency of Saturation Ratio on dilution ratio (adapted from (Kittelson et al., 1999)). Note that the saturation ratio threshold has been arbitrarily set to 2. 34
Figure 2.6: Instrument requirements for instant temporal, physical, and chemical characterisation of particles (Figure adapted from (McMurry, 2000b)). 35
Figure 2.7: The temporal, physical, and chemical resolution of the AMS. 36
Figure 2.8: The temporal, physical, and chemical resolution of the SMPS-TD approach. 36
Figure 2.9: The temporal, physical, and chemical resolution of filter based sampling. 37
Figure 2.10: PROMETHEE-GAIA preference function. 40
Figure 3.1: Schematic representation of the experimental set-up used in this study. 66
Figure 3.2: Brake-specific $PM_{2.5}$ and particle number emissions at intermediate speed (1700 rpm) with various load settings and ethanol substitutions. 69
Figure 3.3: Brake-specific NO emissions at intermediate speed (1700 rpm) with various load settings and ethanol substitutions.....71
Figure 3.4: Brake-specific CO emissions at intermediate speed (1700 rpm) with various load settings and ethanol substitutions.....73
Figure 3.5: Brake-specific HC emissions at intermediate speed (1700 rpm) with various load settings and ethanol substitutions.....74
Figure 3.6: Correlation of CO, HC, NO and $PM_{2.5}$ emissions versus excess air factor (λ) at half load operation. Note the logarithmic scale on the ordinate. 75
Figure 4.1: Schematic representation of the experimental configuration used in this study. .86

Figure 4.2: SMPS derived particle number distributions at intermediate speed (1700 rpm), full load, for neat diesel (E0) and 40% ethanol (E40) engine operation. Error bars denote ± one standard error. 89
Figure 4.3: Correlation of particle size (CMD) with the ethanol substitution percentage for tests conducted at 2000 rpm, full load ($\boldsymbol{r}$=-0.939). Error bars denote ± one standard error...90
Figure 4.4: Brake-specific $PM_{2.5}$ emissions at intermediate speed (1700 rpm) with various load settings and ethanol substitutions. Error bars denote ± one standard error.....91
Figure 4.5: Volume fraction remaining (VFR) versus thermodenuder temperature at intermediate speed (1700 rpm). (a) 100% load E0 and E40. (b) 25% load E0 and E20. Note well the linear scale on the ordinate for (a) and the logarithmic scale on the ordinate for (b). Error bars are calculated using the uncertainties in the diameter measurement. 92
Figure 4.6: Percentage of volatile particles at intermediate speed (1700 rpm) and 50%, 25% load and idle mode for various ethanol substitutions. Error bars have been calculated using the statistical uncertainty in the counts ($\boldsymbol{\sigma = 1/\sqrt{n}}$). 93
Figure 4.7: Fluorescence spectra of BPEAnit control (HEPA filtered) and test samples for neat diesel (E0) and 40% ethanol (E40) at intermediate speed (1700 rpm) and full load. 94
Figure 4.8: ROS concentrations at intermediate speed (1700 rpm) with various load settings and ethanol substitutions. Error bars denote ± one standard error. 95
Figure S 4.1: Particle size distribution for different thermodenuder temperatures ($\boldsymbol{T_d}$). (a) 100% load E0. (b) 100% load E40. (c) 50% load E0. (d) 50% load E40. 101
Figure S 4.2: The volume percentage of volatile material that coats non-volatile particles at intermediate speed (1700 rpm) and for various load settings and ethanol substitutions. Error bars are calculated using the uncertainties in the diameter measurement. 102
Figure S 4.3: A calculation of air available for combustion at intermediate speed (1700 rpm), half load, for various ethanol substitutions. Error bars are calculated based using the uncertainties in the fuel consumption and gaseous emissions measurements. 102
Figure S 4.4: OH radical emissions from an AVL Boost simulation conducted at 2000 rpm, full load. 103
Figure 5.1: Particle number size distribution comparison for both injection technologies and all 3 fuels at 1400 rpm 50% load and 1400 rpm 100% load. Note well that particle number size distributions are also presented for B20 with the aerosol passed through a TD set to 300 ^{o}C.....112

Figure 5.2: Particle number size distribution comparison for both injection technologies and all 3 fuels at 2400 rpm 50% load and 2400 rpm 100% load. Note well that particle number size distributions are also presented for B20 with the aerosol passed through a TD set to 300 ^{o}C.....113
Figure 5.3: Test cycle averaged PAH (mg/kWh) emission factors and ROS concentrations (nmol/mg) for both injection technologies and all three fuels. 116
Figure 5.4: Test cycle averaged BaP_{eq} emission factors (mg/kWh) for PAHs for both injection technologies and all three fuels. 117
Figure S 5.1: A schematic of the experimental set-up utilised in this study.....128
Figure S 5.2: A graph demonstrating correlation between the ROS and PAH measurements. Note: both the PAHs and ROS are expressed on a per unit mg of DPM basis. The Pearson correlation co-efficient, $\boldsymbol{r}$, is 0.913. 129
Figure S 5.3: Test cycle averaged volatile volume percentage of particles for both injection technologies, and all three fuels. 129
Figure 6.1: Brake specific PM_{10} emission factors (g/kWh) for the 14 fuel types investigated in this study. 137
Figure 6.2: Brake-specific particle number emissions (#/kWh) for the 14 fuel types investigated in this study.....138
Figure 6.3: Particle number size distributions (corrected for dilution) for all fourteen fuel types (top panel: soy feedstock, middle panel: tallow feedstock, bottom panel: canola feedstock). TD denotes tests where diesel aerosol was passed through a TD set to 300 ^{o}C. 140
Figure 6.4: Count median diameter of particles (derived from a particle number size distribution) for all fourteen fuel types. 141
Figure 6.5: Brake-specific particle phase (top panel) and vapour phase (bottom panel) PAH emissions for the 7 fuel types where chemical analysis was performed. Error bars denote ± one standard error of the mean.....142
Figure 6.6: ROS concentrations (nmol/mg) for the 6 fuel types where a fluorescence signal was obtained.....143
Figure 6.7: A correlation between ROS concentrations and $\boldsymbol{V_{ORG}}$ for particles.....144
Figure 6.8: A graph showing the relationship between the heated particle surface area of DPM, and $\boldsymbol{V_{ORG}}$ for all fuel types investigated. 145
Figure 7.1: A schematic of the experimental set-up used for measurements of mobility diameter of combustion-generated particles upon exposure to organic and water vapours. .159

Figure 7.2: The difference between the initial mobility diameter and the mobility diameter after bubbling (Δd_m) for particles originating from different combustion sources and bubbled through either heptane or water. 160
Figure 7.3: 200 nm pre-selected candle smoke particles (black solid line) after bubbling through water, heptane, ethanol and DMSO/water (1:1 vol%). Note: The total number concentration of particles upon bubbling is smaller due to partial trapping of particles in the liquid. 162
Figure 7.4: A dependence of the geometric standard deviation (σ) of the size distribution with pre-selected particles bubbled through heptane on the initial d_m. Squares present σ of particles' size distributions prior to bubbling and circles present σ after bubbling. 163
Figure 7.5: TEM images of 80 nm preselected diesel exhaust particles prior to bubbling through heptane (a, b, c) and after bubbling through heptane (d, e, f). 164
Figure 7.6: The difference between the initial mobility diameter and the mobility diameter after bubbling (Δd_m) of candle smoke particles bubbled through heptane and sampled without and with thermodenuder placed after the pre-DMA. 167
Figure 7.7: 200 nm pre-selected candle smoke particles before (squares) and after (circles) bubbling through heptane sampled without (A) and with (B) thermodenuder placed in front of the pre-DMA. 169
Figure 8.1: PROMETHEE-GAIA preference function. 178
Figure 8.2: Relationships between criteria in the GAIA plane. 180
Figure 8.3: PROMETHEE II outranking for all 3 datasets. Top panel: alternative fuels and combustion strategy study, middle panel: alternative fuels and injection technologies study, bottom panel: alternative fuels study. 186
Figure 8.4: GAIA biplot of alternatives for all 3 datasets. Top panel: alternative fuels and combustion strategy study, middle panel: alternative fuels and injection technologies study, bottom panel: alternative fuels study. Principal components 1 and 2 explained 76.4 % (top panel), 66.4 % (middle panel), and 68.9 % (bottom panel) of the variance in the 3 datasets respectively. 189
Figure 8.5: GAIA biplot of criteria of the 3 datasets. Top panel: alternative fuels and combustion strategy study, middle panel: alternative fuels and injection technologies study, bottom panel: alternative fuels study. 192

Table of tables

Table 2.1: The PROMETHEE-GAIA evaluation table. ……..39

Table 3.1: Engine performance data for the ethanol fumigation experiments conducted at 1700 rpm. 68

Table 4.1: Speed, load and fuel settings used for both experimental campaigns. 84

Table S 4.1: Test engine specifications. 100

Table S 5.1: Engine specifications. 123

Table S 5.2: Speed and load settings investigated in this study. 123

Table S 5.3: Fuel specifications. 124

Table S 5.4: Tabulated results for all emissions parameters reported in this study. Uncertainties are calculated as ± one standard error of the mean. NC denotes that the standard error was not computed as the measurement was not replicated. 125

Table S 5.5: Weighting factors for the 4 mode test cycle adopted in this study. 128

Table S 6.1: A tabulation of raw results for this study. Uncertainties related to measurement precision (i.e. not measurement accuracy) are calculated as ± one standard error of the mean ($\sigma_x = \sigma/\sqrt{n}$), where σ is the standard deviation and n is the sample size (i.e. number of data points). NA denotes that the quantity was not available (i.e. chemical measurements for B40 and B60). * Indicates that the control fluorescence was greater than the test sample fluorescence, implying that an ROS concentration could not be calculated. 150

Table 7.1: A summary of the experiments. 161

Table 8.1: The PROMETHEE-GAIA evaluation table. 177

Table 8.2: An overview of the measurements conducted in the 3 datasets analysed with the PROMETHEE-GAIA algorithm. Each column refers to a different study, and each row refers to a different CI engine parameter that was measured or calculated. "X" denotes that a given parameter was measured or calculated in a particular study, whereas "-" denotes that this parameter was not measured or calculated. 182

Chapter 1: Introduction

1.1 The research problem investigated

Access to reliable power sources for transportation purposes has been a stumbling block in the progress of humanity historically. The evolution of a vastly larger more interconnected global population that demands reliable, affordable and nearly instant travel options has led to the obsolescence of previous, unsustainable transportation power sources; such as the steam engine (Majewski and Khair, 2006).

Since its invention in 1893 by German engineer Rudolph Diesel, the compression ignition (or diesel) engine has had a profound impact on global transportation (Hesterberg et al., 2005). The CI engine is both reliable and durable and offers a higher thermal efficiency compared to spark ignition engines (Tzamkiozis et al., 2010). It has found application in a range of on-road and off-road transport environments (Matter et al., 1999) and is also used heavily in marine transportation (Petzold et al., 2010). Even though many design advantages exist with the CI engine, perhaps the most objectionable aspect of its operation continues to be the issue of particulate emissions, often referred to as DPM.

DPM emissions are a by-product of incomplete combustion in a CI engine. Whilst CI engines exhibit a relatively high combustion efficiency of greater than 98 % (Heywood, 1988), the small fraction of the un-combusted fuel which forms DPM is responsible for causing many adverse health effects in humans (Pope et al., 2002; Pope and Dockery, 2006) and is also implicated in global warming due to its ability to absorb and scatter light (Ault et al., 2010; Maricq and Maldonado, 2010). To minimise the impacts of DPM on human health and climate, the only acceptable long-term situation enabling the CI engine to continue its role as a dominant power source for transportation purposes is to achieve (near) particle free combustion (Kittelson et al., 2006b). Despite a considerable amount of research addressing the DPM emissions problem, the attainment of particle free combustion is yet to be realised.

Several strategies are however available to assist in the mitigation of DPM emissions. Mechanical DPM mitigation strategies involve controlling the combustion to prevent fuel-rich combustion conditions from arising such as: modifying the injection timing (Sayin et al., 2008) and strategy (Mohammadi et al., 2005), turbocharging the engine to provide an excess of combustion air (Can et al., 2004), as well as alteration of the combustion strategy

(Martinez-Frias et al., 2007). The mitigation of DPM emissions is also possible by retro-fitting after-treatment devices, such as oxidation catalysts (Bugarski et al., 2010) and particle filters (Mayer et al., 2010b), and also by powering the engine with alternative fuels (Heikkilä et al., 2009) that possess vastly different physico-chemical properties to petroleum diesel.

The operation of CI engines with alternative fuels is the subject of considerable research attention at present (Agarwal, 2007; Lapuerta et al., 2008b; Karavalakis et al., 2009b). This situation is driven heavily by the need not only to develop sustainable transportation fuels that do not rely on fossil derived feedstocks, but is also driven by the need to have transportation fuels that minimise the impact of combustion emissions on global warming and human health (Ahlvik, 2003). The intersection of these constraints provides a very difficult problem for the engine researcher to solve. Consequently, exploring strategies to ameliorate DPM emissions that deliver not only benefits to human health and global climate, but also simultaneously maintaining the status of the CI engine as an efficient and reliable transportation power source provides a significant *raison d'être* for the research undertaken in this thesis.

1.2 Study aim

The principal aim of this thesis is to explore the physico-chemical properties of particulate emissions from CI engines operated with various DPM mitigation strategies, such as: alternative fuels, injection technologies and combustion strategies. Emphasis is also placed on technologies that do not sacrifice engine efficiency, or introduce problems associated with increased life cycle greenhouse gas emissions. This primary thesis aim is explored by undertaking a physico-chemical characterisation of DPM using an SMPS–TD arrangement which is able to determine both the semi-volatile and non-volatile component of DPM. The SMPS is used to monitor changes in the particle number size distribution; such as changes in the number of particles emitted or their median size, with different DPM reduction strategies. DPM is then passed through a TD to monitor whether heating the particles shifts the particle number size distribution to smaller particle diameters. The central tenet of the SMPS-TD approach is that the evaporation of semi-volatile material upon heating with a TD could provide important clues about the presence of toxic organic compounds adsorbed or condensed on the DPM particle surface which will cause human health problems.

1.3 Specific study objectives

To achieve the primary aim of this thesis, several experimental campaigns were conducted exploring the role of fuel type, injection configuration and combustion strategy on DPM emissions with different engine speed and load settings. Additionally, gaseous emissions and engine efficiency were monitored during all experimental campaigns. The three experimental campaigns conducted in this research program involved:

1. Exploring the impact of an ethanol fumigation system on gaseous and particulate emissions.
2. Exploring the impact of common rail and mechanical direct injection on particulate emissions for an engine operated with three different fuels (ultra low sulphur diesel, B20 cooking oil methyl ester, and a Fischer-Tropsch diesel blend).
3. Exploring the impact of different biodiesel blend percentages (B20-B100) with Australian biodiesel feedstocks (soy, tallow, and canola) on particulate emissions.

A requirement for all experimental work was to develop a system for characterising particulate emissions with different DPM mitigation strategies. The system needed to take into account:

1. Dilution of the exhaust sample before particulate emissions measurement.
2. A method for calculating the dilution ratio, so that raw exhaust concentrations could be reported.
3. A method for assessing the semi-volatile and non-volatile component of DPM needed to be developed.
4. Measurement of gaseous emissions, namely: CO_2, CO, HC and NO were also required.

Before the first phase of experimental work commenced, an ethanol fumigation system needed to be retro-fitted to the test engine. This involved installing an ethanol injector in the intake manifold of the engine with a controllable injection pressure and duty cycle. A heater was placed downstream of the ethanol injector to ensure that ethanol vapour was supplied to the intake manifold. Subsequent testing explored the impact of different load settings and ethanol substitutions on gaseous and particulate emissions from this engine.

For the second and third phase of experimental testing, engine modifications were performed by the industry partner (Skill Pro services Pty Ltd) along with fuel and oil changes. For these

two experimental campaigns particulate emissions sampling equipment was deployed and characterised particle emissions for various engine, fuel and injection settings.
An observation arising from the first 3 studies showed that all alternative fuels led to DPM with a smaller median particle diameter. Further experiments were then conducted to test hypotheses related to the observed reduction in median particle diameter with a variety of combustion generated particle types (e.g. diesel/petrol exhaust, candle smoke, wood smoke etc) exposed to organic and water vapours.

An MCDA algorithm (PROMETHEE-GAIA) was then applied to the experimental results from the 3 campaigns to assist in making recommendations about which DPM mitigation strategies should be employed to minimise human health impacts, whilst simultaneously not sacrificing engine efficiency, nor introducing unsustainable alternative transport fuels.

1.4 Account of research progress linking the research papers

A flowchart showing the relationship between published works arising from this thesis (Figure 1.1) indicates the coherency of the research program. A discussion of the research outputs and how they form a unified research program is provided below.

The first two manuscripts in this thesis are inter-connected and explore different aspects of gaseous and particulate emissions with an ethanol fumigated diesel engine. This study made use of an alternative fuel (ethanol) and an alternative combustion strategy (pre-mixed combustion) to explore the impacts on the DPM emissions profile.

The first manuscript (accepted for publication in Energy Conversion & Management) focuses on gaseous and particle number emissions from an ethanol fumigated diesel engine. This study showed that whilst PM and NO emissions were significantly reduced with ethanol fumigation, CO, HC and particle number emissions were increased. The emissions profile of this engine showed a strong dependency on load and ethanol substitution percentage. One of the conclusions of this manuscript involved investigating further the reason for increased particle number emissions with ethanol fumigation.

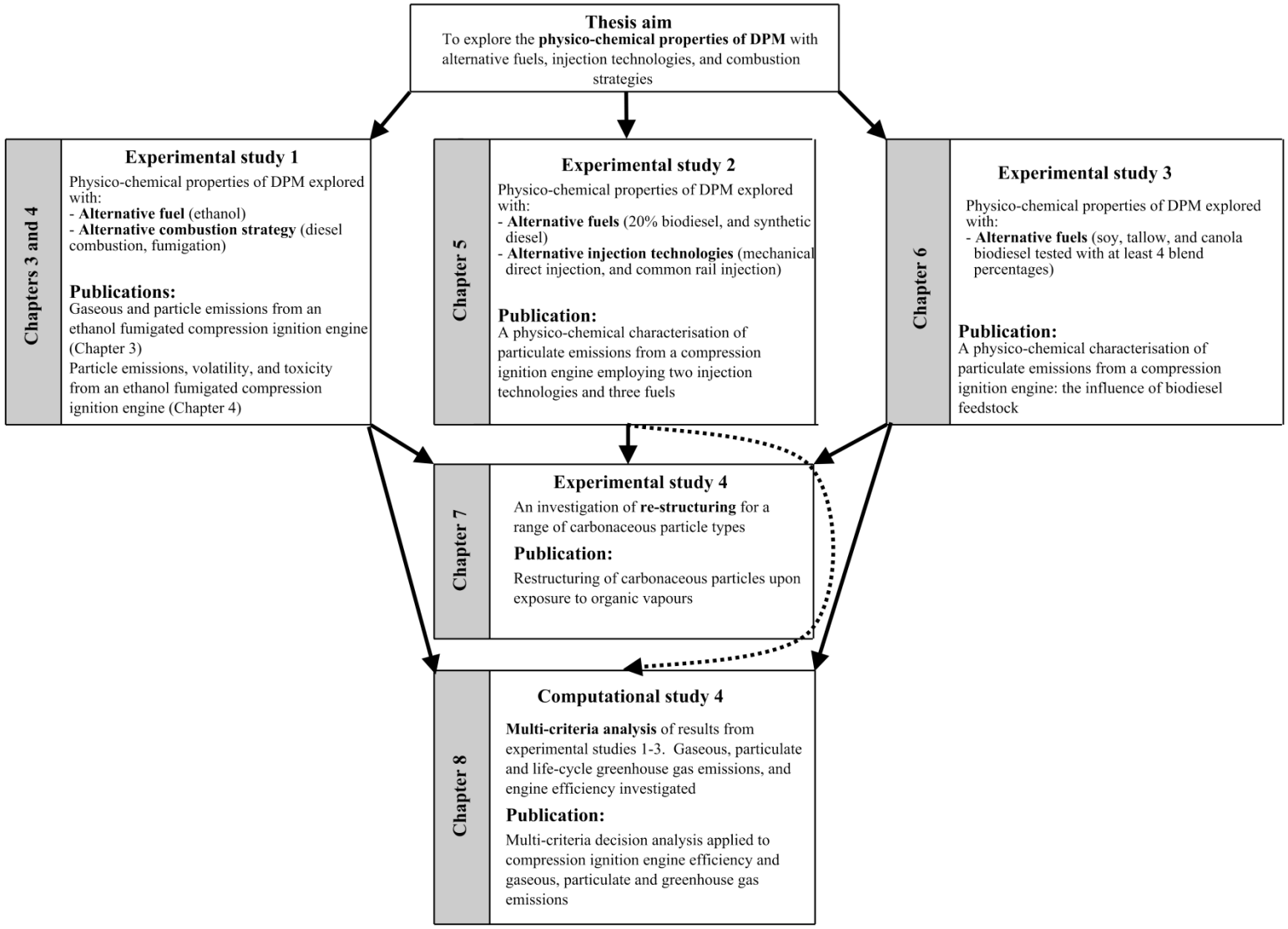

Figure 1.1: A diagram outlining the structure of this PhD research program.

The second manuscript published in Environmental Science & Technology (Surawski et al., 2010b) explored in further detail the increased particle number emissions with ethanol fumigation. Particle number size distributions (with an SMPS) and the volatility of particles were investigated (with a Volatilisation Tandem Differential Mobility Analyser (V-TDMA)). This article showed that the PM reductions with ethanol fumigation were achieved by vastly reducing the accumulation mode surface area – conditions that make homogeneous nucleation more likely in the presence of semi-volatile material. The V-TDMA results showed that ethanol fumigation DPM was characterised by much higher volatility than the diesel DPM, which led to the production of organic nucleation modes with ethanol fumigation.

Investigations were then made into the ability of alternative injection technologies and alternative fuels (other than ethanol) to mitigate DPM emissions. This study was the subject of a third paper published in Environmental Science & Technology (Surawski et al., 2011). This manuscript showed that whilst common rail injection is an effective strategy for reducing particle number emissions, by virtue of greater DPM volatility, this injection technology coated the particles with significantly more genotoxic substances, such as: PAHs and ROS. The alternative fuels investigated were also effective at reducing DPM mass and particle number emissions; however, injection technology was by far the more important factor.

A fourth study was conducted on Australian biodiesel feedstocks (soy, tallow and canola) with various blend percentages (B20-B100) to explore their DPM reduction potential. This article is under review with the journal Environmental Science & Technology. Whilst all blend percentages and feedstocks were very effective at reducing DPM mass, the particle number emissions displayed more complicated results, with the soy and tallow feedstocks reducing particle number emissions for larger blend percentages (> 60 %); however, particle number increases were observed with all canola blends. The semi-volatile organic component of particles was greater with all feedstocks, and the organic component of particles was shown to correlate well with ROS emissions factors.

A reduction in particle diameter was observed for all alternative fuels investigated in the first four studies. This motivated a fifth study which investigated hypotheses related to the

reduction in particle size to be explained. This fifth manuscript has been submitted to the Journal of Aerosol Science.

A sixth manuscript, which is in preparation for submission to Environmental Science & Technology, is a computational study which synthesises the results from the first four manuscripts which were experimentally based. An MCDA program (PROMETHEE-GAIA) aimed to identify different DPM mitigation strategies that minimises human health impacts, whilst also maximising engine efficiency and minimising life cycle greenhouse gas emissions for various alternative transport fuels.

Note that sections of chapter 2 (Theoretical considerations) have been included in a seventh paper which has been submitted for publication in the journal Respirology. There are other aspects requiring discussion in chapter 2; therefore, a literature review has been written independently of the material presented in this seventh journal manuscript.

Overall, this PhD research program investigates technologies that are commonly used in the transportation sector and aims to identify viable technologies based on their DPM related health impacts, engine efficiency and also life cycle greenhouse gas emissions.

1.5 References

Agarwal, A.K., 2007. Biofuels (alcohols and biodiesel) applications as fuels for internal combustion engines. Progress in Energy and Combustion Science 33(3), 233-271.

Ahlvik, P., 2003. Alternative diesel fuels. Dieselnet Technology Guide, Ecopoint Inc, http://www.dieselnet.com/tech/fuel_alt.html, last accessed 16th September 2011.

Ault, A.P., Gaston, C.J., Wang, Y., Dominguez, G., Thiemens, M.H., Prather, K.A., 2010. Characterization of the Single Particle Mixing State of Individual Ship Plume Events Measured at the Port of Los Angeles. Environmental Science & Technology 44(6), 1954-1961.

Brans, J.P., Mareschal, B., 1994. The PROMCALC & GAIA decision-support system for multicriteria decision aid. Decision Support Systems 12(4-5), 297-310.

Bugarski, A.D., Cauda, E.G., Janisko, S.J., Hummer, J.A., Patts, L.D., 2010. Aerosols Emitted in Underground Mine Air by Diesel Engine Fueled with Biodiesel. Journal of the Air & Waste Management Association 60(2), 237-244.

Can, Ö., Çelikten, İ., Usta, N., 2004. Effects of ethanol addition on performance and emissions of a turbocharged indirect injection Diesel engine running at different injection pressures. Energy Conversion and Management 45(15-16), 2429-2440.

Heikkilä, J., Virtanen, A., Rönkkö, T., Keskinen, J., Aakko-Saksa, P., Murtonen, T., 2009. Nanoparticle emissions from a heavy-duty engine running on alternative diesel fuels. Environmental Science & Technology 43(24), 9501-9506.

Hesterberg, T.W., Bunn, W.B., McClellan, R.O., Hart, G.A., Lapin, C.A., 2005. Carcinogenicity studies of diesel engine exhausts in laboratory animals: A review of past studies and a discussion of future research needs. Critical Reviews in Toxicology 35(5), 379-411.

Heywood, J.B., 1988. Internal combustion engine fundamentals. McGraw-Hill, Inc, New York, pp. 1-930.

Karavalakis, G., Stournas, S., Bakeas, E., 2009. Effects of diesel/biodiesel blends on regulated and unregulated pollutants from a passenger vehicle operated over the European and the Athens driving cycles. Atmospheric Environment 43(10), 1745-1752.

Kittelson, D.B., Watts, W.F., Johnson, J.P., Rowntree, C.J., Goodier, S.P., Payne, M.J., Preston, W.H., Warrens, C.P., Ortiz, M., Zink, U., Goersmann, C., Twigg, M.V., Walker, A.P., 2006. Driving down on-highway particulate emissions. Society of Automotive Engineers, SAE Paper No. 2006-01-0916.

Lapuerta, M., Armas, O., Rodríguez-Fernández, J., 2008. Effect of biodiesel fuels on diesel engine emissions. Progress in Energy and Combustion Science 34(2), 198-223.

Majewski, W.A., Khair, M.K., 2006. Diesel emissions and their control. SAE International, Warrendale, pp. 1-561.

Maricq, M.M., Maldonado, H., 2010. Directions for Combustion Engine Aerosol Measurement in the 21st Century. Journal of the Air & Waste Management Association 60(10), 1165-1176.

Martinez-Frias, J., Aceves, S.M., Flowers, D.L., 2007. Improving ethanol life cycle energy efficiency by direct utilization of wet ethanol in HCCI engines. Journal of Energy Resources Technology - Transactions of the ASME 129(4), 332-337.

Matter, U., Siegmann, H.C., Burtscher, H., 1999. Dynamic field measurements of submicron particles from diesel engines. Environmental Science & Technology 33(11), 1946-1952.

Mayer, A., Czerwinski, J., Ulrich, A., Wichser, A., Kasper, M., Mooney, J., 2010. Metal-oxide particles in combustion engine exhaust. Society of Automotive Engineers, SAE Paper No. 2010-01-0792.

Mohammadi, A., Ishiyama, T., Kakuta, T., Kee, S.S., 2005. Fuel injection strategy for clean diesel engine using ethanol blended diesel fuel. Society of Automotive Engineers, SAE Paper No. 2005-01-1725.

Petzold, A., Weingartner, E., Hasselbach, J., Lauer, P., Kurok, C., Fleischer, F., 2010. Physical Properties, Chemical Composition, and Cloud Forming Potential of Particulate Emissions from a Marine Diesel Engine at Various Load Conditions. Environmental Science & Technology 44(10), 3800-3805.

Pope, C.A., III, Burnett, R.T., Thun, M.J., Calle, E.E., Krewski, D., Ito, K., Thurston, G.D., 2002. Lung cancer, cardiopulmonary mortality, and long-term exposure to fine particulate air pollution. JAMA-Journal of the American Medical Association 287(9), 1132-1141.

Pope, C.A., III, Dockery, D.W., 2006. Health effects of fine particulate air pollution: lines that connect. Journal of the Air & Waste Management Association 56(6), 709-742.

Sayin, C., Uslu, K., Canakci, M., 2008. Influence of injection timing on the exhaust emissions of a dual-fuel CI engine. Renewable Energy 33(6), 1314-1323.

Surawski, N.C., Miljevic, B., Roberts, B.A., Modini, R.L., Situ, R., Brown, R.J., Bottle, S.E., Ristovski, Z.D., 2010. Particle emissions, volatility, and toxicity from an ethanol fumigated compression ignition engine. Environmental Science & Technology 44(1), 229-235.

Tzamkiozis, T., Ntziachristos, L., Samaras, Z., 2010. Diesel passenger car PM emissions: From Euro 1 to Euro 4 with particle filter. Atmospheric Environment 44(7), 909-916.

Chapter 2: Theoretical considerations

2.1 Introduction

This chapter provides a review of the theoretical concepts utilised in this thesis. A review of gaseous and particulate emissions formation, sampling, and health impacts in CI engines is provided, along with a rationale for investigating alternative fuels, injection technologies and combustion strategies. The methodology of life cycle greenhouse gas emissions is reviewed as well as multi-criteria decision analysis theory which is used to synthesise the results from this thesis.

2.2 The nature of compression ignition engine emissions

2.2.1 Introduction

The CI engine is a type of internal combustion engine that converts the chemical energy stored in a fuel to mechanical power by injecting a small amount of fuel into compressed air (Majewski and Khair, 2006). This can be contrasted with a spark ignition engine which relies on an electrical discharge to combust the air-fuel mixture. The high temperatures associated with compression enable the injected fuel to evaporate where upon mixing with air, the air-fuel mixture reaches its auto-ignition temperature (Atkins, 2009). The subsequent burning process, consisting of pre-mixed and diffusion flame combustion (Heywood, 1988), enables the chemical energy stored in the fuel to be released.

Complete combustion of a fuel containing hydrocarbons yields only CO_2 and H_2O as combustion products. Whilst CI engines offer a relatively high combustion efficiency ($\geq$ 98 %), in terms of the percentage of fuel that is burnt (Heywood, 1988), the small fraction of unburnt fuel and lubricating oil yield a great number of incomplete combustion products that affect human health, urban air quality and global climate (Majewski and Khair, 2006). A variety of incomplete combustion products are produced by CI engines, many of them are organic in nature, with the total number of exhaust products postulated to be around 20 000 chemical compounds (Sehlstedt et al., 2007). It is the purpose of this section to enumerate these incomplete combustion products, and to provide a theoretical description of how they are formed as well as the potential to ameliorate these emissions through a range of different approaches.

2.2.2 Gaseous emissions and health effects

From a regulatory perspective, gaseous emissions from CI engines have received a great deal of attention. Emissions of CO, NOx, and HCs have featured as regulated gaseous emissions

since the first CI engine emissions standards were introduced by the United States Environmental Protection Agency (USEPA) in 1988 (Hesterberg et al., 2009). This sub-section draws heavily on the material presented in a text book by Majewski and Khair (2006), with updated information on these topics available from the dieselnet website (http://www.dieselnet.com/).

The oxidation of nitrogen (from the intake air) under high temperature conditions is responsible for the formation of a class of compounds referred to as Nitrogen oxides, or NOx. NOx collectively refers to two chemical compounds, namely: Nitric oxide (NO) and nitrogen dioxide (NO_2). Standard chemical practice dictates that NO is quantified as an NO_2 equivalent, so NOx is not obtained by directly summing the concentration of these two pollutants (Majewski and Khair, 2006). Whilst NO is a colourless and odourless gas, NO_2 is a very toxic gas with a reddish-brown colour and has an irritating odour (Majewski, 2010). Both NO and NO_2 are respiratory irritants, however, NO_2 is the more toxic gas with exposures above 200 $\mu g/m^3$ leading to serious respiratory health effects (World Health Organization, 2005), and exposures above 200 ppm leading to fatality (Majewski, 1999). From an environmental perspective, NOx emissions are very important as they are ozone precursors and consequently play a critical role in the production of photochemical smog (Wallington et al., 2006).

Along with DPM emissions, the mitigation of NOx emissions remains a considerable challenge for the engine researcher to solve (McCormick, 2007). This situation is compounded by a phenomenon known as the NOx-DPM trade-off, whereby measures targeting the reduction of one pollutant (DPM for example) leads to an increase in the other pollutant (NOx); with the converse case holding true as well. A range of after-treatment technologies are available for NOx mitigation including: exhaust gas recirculation, selective catalytic reduction and NOx adsorber catalysts (Majewski, 2007).

The NO_2/NOx ratio depends heavily on the engine technology and after-treatment system utilised. Whilst older, naturally aspirated CI engines have an NO_2/NOx ratio of 0.05, Khalek et al. (2009) found NO_2/NOx ratios of 0.33-0.64 with modern engine technologies equipped with advanced after-treatment. Since engines without after-treatment are investigated in this thesis, the NO_2/NOx will be quite small, therefore the theory of NOx formation is best

commenced by discussing the well known extended Zeldovich mechanism, which consists of the following 3 chemical equations (Heywood, 1988):

$$O + N_2 \leftrightarrow NO + N,$$
$$N + O_2 \leftrightarrow NO + O,$$
$$N + OH \leftrightarrow NO + H.$$

A notable feature of these 3 chemical equations is there strong temperature sensitivity. The forward reactions in this mechanism do not contribute appreciably until the start of heat release in-cylinder, once the flame temperature has reached approximately 2000 K (Majewski and Jääskeläinen, 2008). Other mechanisms are responsible for NO formation, such as: the N_2O pathway, the Fenimore mechanism and contributions from fuel nitrogen but will not be discussed as the Zeldovich mechanism is primarily responsible for NO formation in CI engines without after-treatment (Majewski and Jääskeläinen, 2008).

The hydroperoxyl radical (HO_2) plays a critical role in NO_2 formation in CI engines as suggested by the following chemical formula:

$$NO + HO_2 \leftrightarrow NO_2 + OH.$$

At flame temperatures, NO_2 is easily oxidised back to NO (Majewski and Jääskeläinen, 2008), but below temperatures of 1200 K, NO_2 is exhausted from the tailpipe without further chemical modification (Klimstra and Westing, 1995). The presence of NO_2 in the exhaust gas also provides the opportunity to react with water producing nitric acid aerosol (HNO_3) (Harris et al., 1987).

Incomplete oxidation of the carbonaceous component of hydrocarbon fuels to carbon dioxide under conditions of low exhaust gas temperatures is responsible for the formation of CO (Majewski and Jääskeläinen, 2008). CO is an odourless, colourless and very toxic gas, with short-term exposure to concentrations above 1 % leading to fatality (Majewski, 1999; 2010). CO interferes with the ability of haemoglobin to transport oxygen to the human lung, as haemoglobin has a strong affinity for CO forming carboxy-haemoglobin (Majewski, 1999; 2010). The primary parameter that governs the formation of CO in internal combustion engines is the air-fuel ratio (Heywood, 1988). Fuel rich conditions are responsible for forming CO as there is insufficient oxygen available to fully oxidise carbon to CO_2. Because CI engines typically operate under lean combustion conditions, CO emissions are considerably less than those from spark ignition engines; which utilise near stoichiometric

combustion mixtures (Heywood, 1988). Oxidation catalysts are very effective at removing CO emissions from CI engine exhaust, especially under high load conditions once the catalyst light-off temperature has been reached (Zhang et al., 2010b).

HCs are another incomplete combustion product found in CI engine exhaust. The primary cause of HC emissions is due to the preparation of an over-rich or over-lean air-fuel mixture that is not able to support complete combustion (Heywood, 1988). Over-leaning predominates under idle and light load conditions; however, over-fuelling can occur under high load operation due to decreases in the air-fuel ratio in the spray core and near the combustion chamber walls (Majewski and Jääskeläinen, 2008). The formation of quench layers near combustion chamber surfaces also contribute to HC emissions (Majewski and Jääskeläinen, 2008). Many HCs have an irritating odour and are a considerable public health concern due to the carcinogenicity of benzene (International Agency for Research on Cancer, 1987) and formaldehyde, which is a carbonyl emitted in CI engine exhaust (United States Environmental Protection Agency, 2002b).

The formation of other, unregulated, gaseous emissions occur in the CI engine with sulphur dioxide (SO_2) being a notable example. SO_2 is a colourless gas that can cause respiratory irritation and also has an unpleasant odour (Majewski, 1999; 2010). SO_2 is formed by the oxidation of sulphur present in the fuel and lubricating oil, with the SO_2 emission rate correlating well with fuel consumption (Majewski, 2010). Whilst fuel sulphur content has undergone a dramatic reduction in recent years (Dieselnet, 2006b), primarily to facilitate the use of advanced after-treatment technologies such as the diesel particulate filter (DPF), the contribution of sulphur from lubricating oil (~ 20-50 ppm) is becoming more substantial (Khalek et al., 2000). Therefore, the burden of SO_2 emissions from CI engines continues to this day. If oxidation of SO_2 to SO_3 occurs, a process which is promoted by oxidation catalysts (Vaaraslahti et al., 2006; Keskinen and Rönkkö, 2010), SO_3 and H_2O can participate in binary homogeneous nucleation to produce sulphuric acid aerosol (H_2SO_4) (Baumgard and Johnson, 1996; Kittelson, 1998). This mechanism highlights the coupled nature of gaseous and particulate emissions in CI engines.

2.2.3 The composition and formation of DPM

2.2.3.1 An introduction to DPM

The primary cause of DPM emissions is due to the presence of a fuel-rich mixture, characterised by a high equivalence ratio (i.e. fuel-air ratio) (Kittelson, 1998). CI engines

operate on the principle of internal mixture preparation, whereby fuel is injected into the combustion chamber, and subsequently has to mix with an oxidant (i.e. intake air) before combustion can commence (Heywood, 1988). As a result, the CI engine combustion process is characterised by a great degree of heterogeneity, a process that is described in the literature as diffusion flame combustion due to the requirement of this air-fuel mixing process. Diffusion flame combustion is the primary cause of particulate emissions in a CI engine. This situation may be contrasted to that of external mixture preparation, which involves the fuel and oxidant being pre-mixed in the intake manifold. Pre-mixed combustion, like that traditionally used in spark ignition engines, prepares the air-fuel mixture before combustion, consequently greatly reducing the particulate emissions burden. This simple distinction has been blurred somewhat in recent years through the advent of direct injection gasoline engines which employ internal mixture preparation in a spark ignition engine (Zhan et al., 2010), and also homogeneous charge compression ignition (HCCI) in CI engines which pre-mix the fuel and oxidant before combustion takes place (Yao et al., 2009).

In a regulatory sense, Diesel Particulate Matter (DPM) is defined as any substance that is collected on a sampling filter at a temperature below 52 ^{o} C (Majewski and Jääskeläinen, 2008). One can note from this definition that DPM is not a chemically well defined substance. It is a very complicated pollutant not only in terms of its composition, formation and control, but also in terms of the measurement techniques required to characterise this pollutant successfully.

2.2.3.2 DPM composition and formation mechanisms

DPM composition

Diesel Particulate Matter (DPM) is a complex, multi-pollutant mixture of solid and liquid particles suspended in a gas (Eastwood, 2008b). DPM is a very dynamic physical and chemical system that exhibits very strong spatial and temporal dependency in terms of its composition (Wilt, 2007). The composition of DPM depends on many factors, such as: the level of dilution and its subsequent atmospheric processing after being emitted from the tailpipe (Samy and Zielinska, 2010; Zielinska et al., 2010), the engine operating condition (e.g. speed/load, injection timing and strategy), the presence of after-treatment devices (such as a Diesel Particle Filter) (Konstandopoulos et al., 2007), the maintenance status of the engine (Davies, 2002), as well as the type of fuel and lubricants used. This sub-section reviews the physical and chemical properties of DPM, and the formation mechanisms responsible for its observed physico-chemical composition and structure. Reviewing the

physico-chemical properties of DPM is necessary from a theoretical perspective, as knowledge of DPM formation can potentially play a role in DPM mitigation and control, but knowledge of DPM physico-chemical properties is also necessary from a health effects perspective. A paper by Giechaskiel et al. (2009) highlighted that the health impacts (or biological activity) of DPM are influenced by both physical and chemical factors, hence, it is appropriate to review the physical and chemical properties of DPM that are responsible for causing health effects in humans upon inhalation.

2.2.3.3 DPM physical properties

The physical properties of DPM include factors that describe the size and structure of particles such as: their mass, surface area, their number/size distribution and also their physical mixing state (Burtscher, 1992). The physical properties of DPM govern the ability of toxic compounds to adsorb or condense upon the particle surface, it governs a particles ability to deposit in the human respiratory tract (with particle size being a critical parameter), particle number emissions govern the ability of particles to coagulate and therefore grow (according to the Smoluchowski equation), whilst the physical mixing state of particles determines their associated climatic and health impacts. It follows, therefore, that the behaviour of DPM and its climatic and health impacts depend strongly on its physical characteristics.

As the above paragraph suggested, the aerosols literature offers several ways of characterising the physical properties of DPM through the use of various particle metrics. In terms of the physical properties of DPM, common particle metrics employed in the diesel emission literature for characterising DPM include: mass, number, surface and volume. These various metrics are describe below, borrowing heavily from the material presented in chapter 8 (Properties of the Atmospheric Aerosol) from Seinfeld and Pandis (2006).

Particle mass is the simplest, and most commonly used metric in air pollution studies, and is merely the mass of particles emitted per unit volume of air. Particle mass emissions are referred to as Particulate Matter (PM) emissions in the air pollution literature, where it is common for the analyst to collect PM below a specified aerodynamic diameter which acts as a cut-point to provide a size-resolved PM sample. Common cut-points involve 2.5 μm and 10 μm, known as $PM_{2.5}$ (fine particles) and PM_{10} (coarse particles) respectively. Mathematically, PM can be computed in a size dependent manner via:

$$PM = \int_0^\infty \rho(D_p) n_N\left(D_p\right) {D_p}^3 dD_p, \tag{2.1}$$

where: $\rho(D_p)$ denotes a size dependent particle density, $n_N(D_p)$ denotes the number of particles per cm^3 with diameters between D_p and $D_p + dD_p$ and d_p denotes the particle diameter. Integration in (2.1) is required to compute the PM emissions over the full particle size range. Note that if one removes density (ρ) from the integrand in (2.1) we have a working definition for particle volume emissions. Note also from (2.1) that if the particle density is equal to unity, then the PM and particle volume emissions are identical. An important caveat to keep in mind with (2.1) is the fractal-like morphology of DPM. Characterising the morphology of DPM is made possible by simultaneous measurement of the mobility and aerodynamic diameters, with an SMPS-ELPI technique proving to be a common technique (Virtanen et al., 2004; Tzamkiozis et al., 2011); however, other approaches are possible such as simultaneously measuring the vacuum aerodynamic diameter and mobility diameter with a combined Differential Mobility Analyser-Aerosol Mass Spectrometry (AMS) technique (DeCarlo et al., 2004; Slowik et al., 2004).

Similarly, the particle surface area (S) can be computed in a size dependent manner via:

$$S = \int_0^\infty n_N\left(D_p\right) {D_p}^2 dD_p, \tag{2.2}$$

Finally, particle number emissions (N) may be computed by integrating the number of particles across the full size distribution of particles via:

$$N = \int_0^\infty n_N\left(D_p\right) D_p dD_p. \tag{2.3}$$

A very important point to note from the definitions of PM (2.1), particle surface (2.2) and particle number (2.3) is the order of their dependence on particle size. Note that as the order of the dependence on particle diameter increases, the modal value of each parameter shifts to a larger particle diameter. PM and volume (V) possess a cubic dependence on particle diameter ($PM, V \propto D_p^3$), whereas particle surface has a second order dependence on particle diameter ($S \propto D_p^2$), whilst particle number has a zeroth order dependence on particle diameter ($N \propto D_p^0$). It is also possible to measure particle length from diesel engines (Vojtisek-Lom, 2011), which has a first order dependence on particle diameter ($L \propto D_p^1$); however, particle length measurements do not receive as much attention in the diesel emissions literature as other particle metrics.

To summarise the material presented in this sub-section, Figure 2.1 shows particle number, surface and mass distributions plotted with respect to particle diameter on a logarithmic scale. The y-axis has been normalised so that each particle metric is equal to 1 when integrated across all particle diameters. Note very well how the modal value of each parameter shifts to larger particle diameters as the order of the dependence on particle diameter increases. Particle number has a zeroth order dependence on particle diameter and has the smallest modal diameter of about 10 nm. Note that the mode for particle number resides in the nucleation mode (< 30 nm) when nucleation occurs in diesel exhaust. Thus when nucleation occurs practically all the particle number emissions may be defined as nanoparticles (< 50 nm). Particle surface area has a second order dependence on particle diameter and has the next largest modal diameter of around between (100-200 nm). TSP and particle volume both have a cubic dependence on particle diameter, and display the largest mode of over 200 nm.

The location of these modes is very important because if the engine researcher wishes to emphasise different metrics (or aspects of particle behaviour), then this metric is found in a different part of the size distribution. This is of particular importance for the subsequent deposition of diesel exhaust particles in the human lung (for example) because the number of particles deposited has a very strong dependence on particle diameter (Hofmann, 2011) – as can be observed from Figure 2.1.

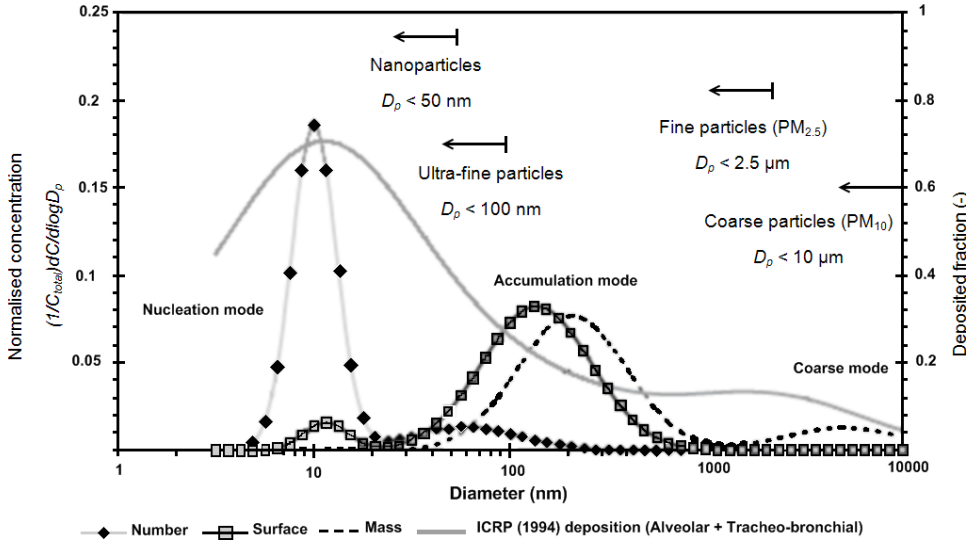

Figure 2.1: A graph showing the relationship between particle number, surface and mass distributions, and the deposition of particles in the tracheo-bronchial region of the human lung upon inhalation (from Kittelson et al. (2004)). Copyright permission license number: 2753471301227.

2.2.3.4 DPM chemical properties

Incomplete combustion of a hydrocarbon fuel containing trace amounts of sulphur, nitrogen, and significant amounts of oxygen (in the case of biofuels), by intuition, will emit a very large number of incomplete combustion products. The presence of sulphur, metals and ash from incomplete combustion of lubricating oil will also contribute to this "cocktail" of chemicals emitted by the internal combustion engine. It has been estimated that diesel exhaust contains about 20 000 different chemical compounds (Sehlstedt et al., 2007) and around 700 have been positively identified in the diesel emissions literature (United States Environmental Protection Agency, 2006). It is therefore the job of the engine researcher to characterise the chemical composition of DPM for the purposes of ascertaining both the health and climate impacts after their subsequent emission into the atmosphere. Characterising the chemical composition of DPM involves investigating the presence of broad classes of particle constituents (such as organics, sulphates, and elemental carbon), investigating the presence of metallic ash and metal oxides (Mayer et al., 2010b), inorganic ions (Cheung et al., 2010), and also the presence of toxic compounds such as polycyclic aromatic hydrocarbons (Burtscher, 1992), reactive oxygen species (Surawski et al., 2010b) and carbonyls (Karavalakis et al., 2010a).

Figure 2.2 provides an engineer's depiction of the structure and composition of DPM (Maricq, 2007). A diesel particle consists of many primary carbonaceous particles that agglomerate together to produce a complex, fractal-like morphology (Eastwood, 2008b). The carbonaceous component of DPM provides a surface for other compounds (like organics, sulphates and metal oxides) to adsorb or condense upon. The organic compounds present in DPM are derived from heavy hydrocarbons (with a high boiling point) that originate from unburnt fuel and lubricating oil. Lighter unburnt hydrocarbons are present in the gas phase, and it should be noted that the organic component of DPM has the ability to partition between the gas and particle phases, dependent upon the level of dilution and cooling employed during DPM sampling (Robinson et al., 2007). The sulphate component of DPM also originates from sulphur present in the fuel and lubricating oil. Metallic ash (such as metal oxides) can also adsorb to the DPM particle surface, with lubricating oil providing a metallic source during combustion.

Besides the composition of DPM, another important feature from Figure 2.2 relates to the physical mixing status of the various DPM constituents. A carbonaceous agglomerate with

other adsorbed or condensed species (such as organics, sulphates or metal oxides) refers to a situation termed internal mixing. In internal mixing, the various DPM constituents mix together to form a single, incorporated particle. The presence of organic droplets (in the nucleation mode) can also be detected from Figure 2.2. When the DPM constituents are physically separated into distinct particle types this situation is referred to as external mixing. The structure, or mixing state, of DPM is an important aspect to consider as it affects the climatic and also health impacts of this pollutant.

In terms of the climatic impacts of the DPM mixing state, internally mixed black carbon (with DPM being such a source) with an adsorbed organic layer has been shown to increase the absorption of light (Shiraiwa et al., 2010) relative to external mixing (Jacobson, 2001). The health effects of DPM are a complicated matter; however, internally mixed DPM enables the particle surface to transport toxic compounds, whilst externally mixed DPM is associated with the formation of volatile organic material that can deposit in the gas exchange region (i.e. alveolar) of the lung (Giechaskiel et al., 2009). A more complete discussion of DPM health effects is reserved for section 2.4 of this chapter.

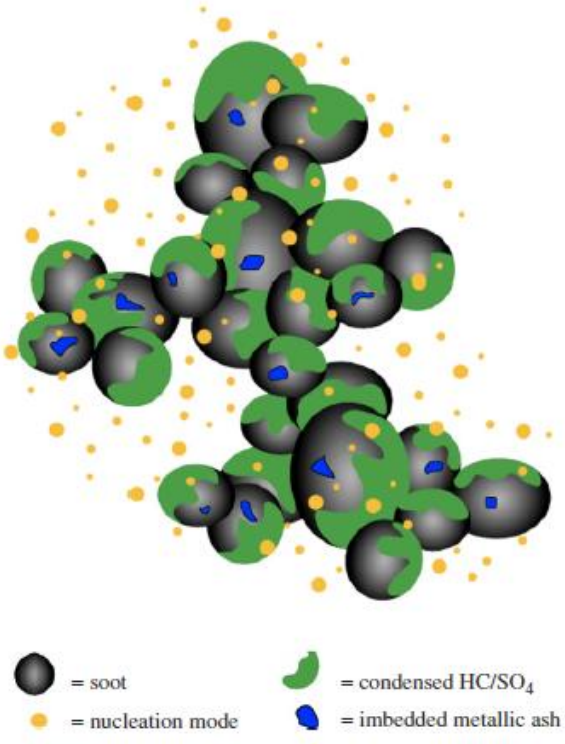

Figure 2.2: An engineer's depiction of DPM (from (Maricq, 2007)). Copyright permission license number: 2753471077279.

2.2.3.5 DPM formation

The preceding discussion has outlined the rather complicated situation related to DPM composition. The formation of DPM emissions is also a highly complicated matter, and depends on the DPM constituents present, as well as the thermodynamic history of the particles (e.g. level of dilution, temperature, rate of mixing etc). Figure 2.3 displays an idealised particle number size distribution for DPM (based on the work of the United States Environmental Protection Agency (2004) and Kittelson (2006a)) and also the physical and chemical processes that are responsible for the characteristic behaviour of each mode. Inspection of Figure 2.3 shows that the DPM particle number size distribution has four modes, namely: the cluster mode, the nucleation mode, the accumulation mode and the coarse mode. The primary demarcation to draw from Figure 2.3 is the distinction between particles that are directly emitted from an internal combustion engine (i.e. accumulation and coarse modes) and those that are formed secondarily after cooling and dilution of the exhaust gas mixture (i.e. cluster and nucleation modes) and hence are not directly emitted from the tailpipe.

Working from larger particle diameters to smaller ones, we firstly have the coarse mode defined as particles emitted which have a particle diameter greater than 500 nm (Kittelson et al., 2006a). The coarse mode consists of mechanically generated particles such as: combustion chamber, exhaust and valve stem wear products (Kittelson et al., 2006a).

The accumulation mode (30-500 nm) is formed in-cylinder via a complex series of reactions involving nucleation, surface growth, agglomeration and adsorption/condensation (Haynes and Wagner, 1981; Amann and Siegla, 1982; Heywood, 1988). This mechanism produces a large number of primarily elemental carbon primary particles which coagulate very quickly (according to the Smoluchowski equation). The rapid in-cylinder coagulation or agglomeration process involving primary particles gives this mode its name (i.e. accumulation). After subsequent exhaust gas cooling and dilution, both in the tailpipe and after being emitted to the atmosphere, enables a number of compounds (such as organics, sulphates and metals) to adsorb or condense on the surface of particles in the accumulation mode producing an internally mixed particle composed mainly of elemental and organic carbon.

The nucleation mode (3-30 nm) consists of particles that have either condensed from the gas phase (i.e. from low-volatility precursors) or have undergone a homogeneous or

heterogeneous nucleation process. In CI engine exhaust, particles in the nucleation mode appear to undergo a two-step nucleation and growth process (Baumgard and Johnson, 1996; Khalek et al., 2000). Nucleation occurs in a size range referred to as the cluster mode (< 3nm). For example, binary homogenous nucleation between water vapour (H_2O) and sulphuric acid (H_2SO_4) occurs from very small stabilised clusters of the binary vapour mixture (1-2 nm) (Baumgard and Johnson, 1996), which then undergo condensational growth from organics (Khalek et al., 2000; Tobias et al., 2001; Sakurai et al., 2003) to reach a particle diameter that can be detected with typical aerosol size measurement equipment (such as an SMPS). Binary nucleation involving water vapour and sulphuric acid is potentially a simplification of what happens in the cluster mode, as a ternary H_2O-H_2SO_4-ammonia (NH_3) nucleation mechanism has been described in the literature (Grose et al., 2006). There is also the possibility of organo-sulphate nucleation, where the interested reader is directed to Meyer and Ristovski (2007) for a discussion of this topic. Also note that particles in a smaller mode may coagulate and hence grow to larger sized particle modes. Figure 2.3 shows, for example, that particles in the nucleation mode can be scavenged by the large particle surface area offered by the accumulation mode, thus enabling nucleation mode particle growth to a larger particle diameter.

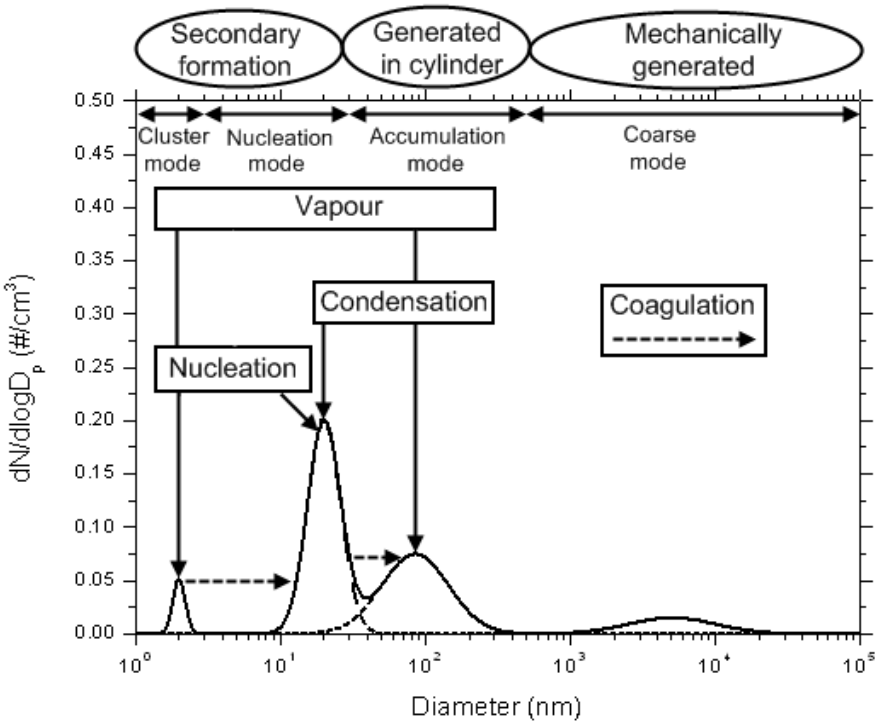

Figure 2.3: Modes and formation mechanisms of the DPM particle number size distribution (Figure adapted from (United States Environmental Protection Agency, 2004; Kittelson et al., 2006a)).

2.2.4 Life cycle greenhouse gas emissions

The gaseous emissions discussed in section 2.2.1 of this review focussed on compounds that primarily affect human health. CI engines are also responsible for emitting greenhouse gases that play a role in global warming, such as carbon dioxide (CO_2), methane (CH_4), and nitrous oxide (N_2O). Whilst technically, N_2O is a nitrogen oxide and CH_4 a hydrocarbon, these compounds are treated separately due to their strong greenhouse forcing potential. To elaborate: relative to carbon dioxide (global warming potential of 1), N_2O has a 100 year global warming potential of 298 and CH_4 has a global warming potential of 25 (Intergovernmental Panel on Climate Change, 2007). N_2O emissions from CI engines are typically quite small (~ 3 ppm) (Havenith and Verbeek, 1997), however, it has been noted that some NOx after-treatment devices (such as SCR catalysis and lean NOx catalysts) are capable of increasing N_2O emissions, thus monitoring this pollutant is quite important in NOx after-treatment design (Majewski, 2010). Overall, monitoring methane and nitrous oxide emissions are two important pollutants (in addition to CO_2) to consider when assessing the life cycle greenhouse gas emissions of transport fuels.

Life cycle analysis (LCA) of a transport fuel (also known as wells-to-wheels emissions) takes into account the total greenhouse gas emissions associated with a given transportation task. A critical point with LCA is that it considers not only tailpipe greenhouse gas emissions (such as CO_2, CH_4, and N_2O), but is also accounts for the pre-combustion greenhouse gas emissions (also known as upstream emissions) associated with extraction, production, transport, processing, conversion and distribution of a given fuel (Beer et al., 2002). The LCA methodology can also be extended to consider the greenhouse gas emissions associated and vehicle manufacturing, maintenance and disposal, and also with road infrastructure – a topic that was considered by Lenzen (1999). To minimise the environmental footprint of transportation fuels, clearly, reductions in both tailpipe and upstream greenhouse gas emissions are desired.

2.2.5 CI engine efficiency

This sub-section of the review has focussed on a range of pollutants that are formed via incomplete combustion of hydrocarbon containing fuel. It is the ultimate objective of the engine researcher to minimise the emission of these harmful pollutants. To achieve this goal, the CI engine researcher wants an efficient internal combustion engine. A metric commonly used in the CI engines literature to assess the efficiency of an engine is to calculate what is properly known as the fuel conversion efficiency (Heywood, 1988), but is a term quite often

referred to as the brake thermal efficiency. The fuel conversion efficiency is calculated according to:

$$\eta_f = \frac{P_b}{\dot{m}_f Q_{HV}},$$

where: P_b is the brake power output of the engine (measured with a dynamometer), $\dot{m}_f$ is the fuel mass flow rate, and Q_{HV} is the heating value of the fuel.

It is standard practice to use the lower heating value of the fuel rather than the higher heating value of the fuel; which takes into account the heat release due to water condensation, as H_2O typically exits the tailpipe of a CI engine as a vapour (Çengel and Boles, 2006).

There are thermodynamic constraints on how efficient a CI engine (a type of heat engine) can be, thus providing theoretical and practical constraints on how efficiently CI engines should be designed. These limits exist as all mechanical devices experience friction, plus the heat release and air induction processes occur at finite temperatures (Heywood, 1988). Modern CI engines typically have brake thermal efficiencies of around 35-38 % (Robert Bosch GmbH, 2007), however, current research and development activities are delivering CI engines with brake thermal efficiencies closer to 50% (Lutz and Modiyani, 2011). High brake thermal efficiency is desired by the engine researcher, and this has implications for the quantity and type of pollutants emitted from the tailpipe.

2.3 DPM mitigation strategies

2.3.1 The case for alternative fuels

2.3.1.1 A historical interlude

The use of alternative fuels in spark ignition and compression ignition engines dates back to the origins of internal combustion engine development. Early spark ignition engines were run on ethanol (Balat, 2009), and Ruldoph Diesel demonstrated that the compression ignition engine could be run on neat (i.e. 100%) peanut oil (Agarwal, 2007). From these promising early beginnings, the discovery of "cheap oil" led to a situation whereby spark ignition engines ran almost exclusively on gasoline (or petrol) and compression ignition engines ran on diesel. The first global energy crisis in 1973 provided an incentive to continue alternative fuels development for internal combustion engines (Hansen et al., 2005; Şahin and Durgun, 2007). Since the global energy crisis in the 1970's, the discovery of new oil reserves has diminished steadily over time (Sorrell et al., 2010). This has lead to a situation referred to as

the “peak oil” scenario, whereby the oil extraction rate will reach a peak, followed thereafter by a terminal decline (Sorrell et al., 2010).

2.3.1.2 Drivers for alternative fuel development and use

In the current economic climate, demand for petroleum products derived from crude oil continues to grow. The Australian economy (for example) has a predicted trade deficit of approximately $30 billion by 2015 (Durie, 2011), with reliance on imported crude oil contributing heavily to this situation. Currently, the world’s energy sector is in a very precarious position whereby demand for oil is beginning to outstrip supply, with new energy resources needing to be found for transportation purposes. Therefore, fuel and energy security issues are a major driver for the development of alternative fuels that can be used in the internal combustion engine - at present (Demirbas, 2007; 2009).

There are, however, other drivers for the use of alternative fuels in internal combustion engines. Alternative fuels also need to play a role in mitigating global warming (Balat et al., 2008). This can be achieved by minimising greenhouse gas emissions (such as CO_2, CH_4 and N_2O) through the whole life cycle of the fuel, including both its pre-combustion and post-combustion emissions (Beer et al., 2002; Beer and Grant, 2007). It has been argued that black and organic carbon emissions from fossil fuel combustion have a similar contribution to global warming as greenhouse gases (Jacobson, 2002a), so alternative fuels also need to deliver reductions in the elemental and organic carbon fraction of DPM as well.

Alternative fuels also need to play a role in improving air quality through reductions in emissions that are deleterious to human health (Liaquat et al., 2010). CO, HCs, NOx, SO_2, DPM and particle number are examples of emissions that should be reduced at the tailpipe to reduce cardiovascular and respiratory mortality and morbidity associated with vehicle emissions. Reduction of NOx and HCs emissions also facilitates mitigation of the urban photochemical smog problem (Wallington et al., 2006).

Overall, the intersection of these three main requirements (energy security, global warming, and urban air quality) provides a very strong motivation to explore the utilisation of alternative fuels in the internal combustion engine (Ahlvik, 2003).

2.3.1.3 Alternative fuel use in the compression ignition engine

Due to the abovementioned drivers for alternative fuels research, naturally, there exists a well developed body of literature applying alternative fuel usage in CI engines. The interested

reader may consult reviews from the CI engines literature by Adelman (1979), Ecklund et al. (1984c) Hansen et al. (2005) and Ribeiro et al. (2007) regarding ethanol usage, Agarwal (2007) and Lapuerta et al. (2008b) for biodiesel utilisation, Sahoo et al. (2009) regarding gaseous fuel applications and Alleman and McCormick (2003a) regarding Fischer-Tropsch diesel fuel. Other topics of research in alternative fuels usage in CI engines have focussed on dimethyl ether (DME) (Ribeiro et al., 2007) and also hydrogen (White et al., 2006); which is a non carbon containing fuel with high energy density and tremendous potential as a renewable fuel provided viable hydrogen production methods are developed (Bika et al., 2008).

The alternative fuels listed in the previous paragraph are a representative sample of those being considered, but does not attempt to provide a comprehensive list. A common feature, however, of these fuels is that there physico-chemical properties are quite different to those of petroleum diesel; a fact which is exploited for reducing emissions from CI engines. The most noticeable difference between biofuels (such as ethanol, methanol and biodiesel) and petroleum diesel is their high oxygen content. Neat methanol has an oxygen content (by mass) of approximately 50 %, neat ethanol has an oxygen content of approximately 35 %, and the oxygen content of neat biodiesel is typically in the 10-12 % range (Graboski and McCormick, 1998), and is dependent on the fatty acid composition of the resulting fuel. The presence of oxygen in a CI engine fuel, whilst lowering its calorific value, offers special emission reduction potential as it produces radicals during combustion that help oxidise CO, HCs and PM to complete combustion products (Kitamura et al., 2001). The impact of biofuels on un-regulated emissions, however, is a topic that has received considerably less attention, although this gap in the literature is being rapidly filled at present (Fontaras et al., 2010a; Karavalakis et al., 2010a).

Another property of alternative fuels that is exploited for regulated emissions reduction is their high cetane number – especially for biodiesel (Lapuerta et al., 2005; Jung et al., 2006b; Bugarski et al., 2010) and also Fischer-Tropsch diesel (Schaberg et al., 2002b; Heikkilä et al., 2009). In direct contrast, alcohol fuels are characterised by a rather low cetane number, with methanol having a cetane number of 4, whilst ethanol has a cetane number of 6 (Zhang et al., 2011). Therefore, a different approach must be taken to permit the use of methanol and ethanol in high quantities in the CI engine, such as dual-injection of alcohol fuel and diesel, or through alcohol fumigation (Ecklund et al., 1984c). The higher cetane number of biodiesel

and Fischer-Tropsch diesel reduces the ignition delay (i.e. the time delay between injection and combustion), where a reduced ignition delay enables inconsistencies in the air-fuel mixing process to be avoided (Schaberg et al., 2002b). Through this mechanism, high cetane fuels can reduce the emissions of regulated pollutants, although the impact on NOx is relatively minor.

2.3.2 The case for alternative injection strategies

Traditionally, fuel injection in CI engines has been handled with a single injection event (Eastwood, 2008b). The quantity of fuel to be injected was determined by the load requirement of the engine, leaving the injector opening and closing times as parameters to be optimised by the engine developer. The advent of electronically controlled common rail injection provides the engine developer with far more control over the injection process. With common rail injection, the engine researcher has full control over the pressure and timing associated with fuel injection, and this approach also permits multiple injections (Guerrassi and Dupraz, 1998). With this greater degree of control over fuel injection (and consequently combustion) the engine researcher is potentially in an improved position to control DPM emissions (Desantes et al., 2011).

A stark difference between mechanical direct injection and common rail injection is that the former typically requires the fuel to be simultaneously pressurised and injected, whereas with common rail injection the fuel injection and pressurisation steps are decoupled (Robert Bosch GmbH, 2007). In common rail injection, fuel pressurisation is achieved with a high pressure pump which is fed into a high pressure fuel rail before injection takes place. Therefore, a primary difference between these two injection technologies is that common rail injection achieves much higher injection pressures – with this feature being heavily exploited for DPM mitigation (Khair and Jääskeläinen, 2010).

A higher injection pressure yields many benefits for the subsequent evolution of the spray pattern from an injector. It enables the spray to penetrate further into the combustion chamber and facilitates the atomisation, vaporisation and dispersion of the injected fuel (Eastwood, 2008b). A combination of these factors facilitates the air-fuel mixing process, where it is noted that in-efficiencies in air-fuel mixing are the primary cause of DPM emissions. Thus, the common rail injection engine coerces the combustion into pre-mixed mode, leaving less fuel to burn in the diffusion flame phase which is typically associated with the production of DPM (Eastwood, 2008b). With the advent of common rail injection, the

engine researcher is left with a greater number of parameters to explore for optimising the fuel injection process, hence potentially playing a role in DPM mitigation.

2.3.3 The case for alternative combustion strategies

As was noted previously, the CI engine combustion process is characterised by a great deal of heterogeneity. Fuel is injected directly into the combustion chamber where it must subsequently mix with air before the combustion process can commence. Locally rich fuel-air mixtures are responsible for DPM formation, and are a consequence of the heterogeneous CI engine combustion process (Heywood, 1988; Majewski and Khair, 2006). Naturally, this raises the question as to whether the CI engine combustion process can be manipulated to avoid these rich fuel-air mixtures from manifesting themselves in the first place? Alternative combustion strategies, such as: homogeneous charge compression ignition (HCCI) (Ryan and Callahan, 1996), pre-mixed compression ignition (PCI) (Chen and Iwashina, 2009), and low temperature combustion (LTC) (Kitamura and Ito, 2010) are tools available to the engine researcher to push combustion away from the envelope responsible for elevated DPM and also NOx emissions.

In this thesis, a type of PCI called fumigation was investigated. The fumigation approach involves injecting a secondary fuel (ethanol) into the intake manifold of a CI engine using low pressure fuel injectors. Intake manifold injection enables the secondary fuel to mix with air before being inducted into the cylinder. Therefore, a pre-mixed charge of secondary fuel and air is inducted into the cylinder whilst the intake valve is open.

There are several benefits of the fumigation approach. Firstly, fumigation is effective at reducing DPM by virtue of preparing a pre-mixed charge. The fumigation approach avoids rich fuel-air mixtures from developing not only for the secondary fuel mixture, but also for the primary diesel spray as less diesel is injected to provide a constant load. A second advantage of fumigation is that if problems are encountered with secondary fuel combustion, the secondary fuel supply can be switched off (Ecklund et al., 1984c). This is a feature not possible for blended secondary fuel-diesel fuel mixtures, as the fuel is injected through a single high pressure diesel injector. The fumigation approach using ethanol as a secondary fuel is advantageous as it enables larger secondary fuel substitutions (Ecklund et al., 1984c). It is difficult to achieve secondary fuel substitutions of over 25% (by energy) with ethanol blended diesel fuel (due to the problem of phase separation); however, fumigation permits secondary fuel substitutions of up to 50% (by energy) before engine knock starts to become a

problem (Abu-Qudais et al., 2000). A more elegant approach to the ethanol substitution problem is to undertake dual injection of diesel and a secondary fuel, however, the cost and complexity of this approach limits its applicability in CI engines.

2.4 Health effects of DPM

2.4.1 Introduction

It has been demonstrated in several human cohort based health effects studies that airborne particulate matter, of which DPM is a major contributor (Robinson et al., 2010), is responsible for causing cardiovascular and respiratory mortality and morbidity (Pope and Dockery, 2006). For example, in their comprehensive synthesis of a range of human based cohort studies, Pope and Dockery (2006) suggest a 0.6-2.2 % increase in respiratory mortality risk for a 10 $\mu g/m^3$ increase in ambient PM. Studies such as the one conducted by Pope and Dockery are useful in establishing a correlation between increased ambient PM exposure and excess cardiovascular and respiratory mortality risk. However, given that ambient PM is a complex mixture of a range of anthropogenic and natural sources (Mejía et al., 2007) a major shortcoming of studies relating "whole" PM exposure to respiratory health outcomes is that studies of this design cannot attribute health outcomes to specific sources, such as CI engines, nor can they attribute health outcomes to specific constituents of DPM, such as elemental and organic carbon. Identifying the DPM constituents responsible for the development of adverse health outcomes is a more beneficial approach as it potentially enables source specific engineering measures to be implemented, consequently improving the ambient PM mixture which CI engines heavily contribute towards (Grahame and Schlesinger, 2007).

In response to the above mentioned limitations of epidemiological research, information relating DPM constituents to adverse health outcomes is tackled in this sub-section via a two-step methodology. Firstly, different DPM constituents are linked to specific cellular level mechanisms (inflammation and oxidative stress) that are precursors to specific health outcomes, and then secondly, these DPM health effects mechanisms are related to specific cardiovascular and respiratory health outcomes.

2.4.2 Inflammation

Inflammation in human body tissues involves a complex set of molecular and cellular responses resulting from exposure to foreign objects such as pathogens or noxious substances (Weiss, 2008) – including particles (Krishnamoorthy and Honn, 2006). The pathways associated with acute inflammation involve a carefully orchestrated sequence of events

mediated by chemotactic molecules called chemokines (Krishnamoorthy and Honn, 2006). Upon deposition of a particle, phagocytic cells such as neutrophils and macrophages are recruited to the foreign particle by chemokines, which after being engulfed, rely on the mucociliary escalator for removal to the gastro-intestinal tract (Donaldson and Tran, 2002). The interaction between particles and cells leads to problems when the normal particle clearance mechanisms are disrupted, thereby leading to: macrophage damage and the release of a variety of inflammatory signalling molecules, such as Interleukin-8 (IL-8) and Tumour Necrosis Factor-alpha (TNF-α) (Stone et al., 2007), from macrophages or epithelial cells (Donaldson and Tran, 2002). This has implications especially for asthmatic individuals, where it is noted that over-expression of the IL-8 and TNF-α chemokines are observed in their broncho-alveolar lavage fluids (Riedl and Diaz-Sanchez, 2005). Whilst the pathways associated with acute inflammation are reasonably well defined and understood, the relationship between chronic inflammation and the progression of cardiovascular and respiratory disease is not (Weiss, 2008).

2.4.3 Oxidative stress

Møller et al. (2010) describe oxidative stress as a situation that develops when there is an imbalance between the production of reactive oxygen species (ROS) and the availability of anti-oxidant defences – a situation which is depicted in Figure 2.4. ROS is a collective term that refers to free radicals such as hydroxyl ($HO^{\cdot}$) and peroxyl ($HOO^{\cdot}$, $ROO^{\cdot}$), ions such as superoxide ($O_2^{-\cdot}$) and peroxynitrite ($ONOO^-$), and molecules such as hydrogen peroxide (H_2O_2) and hydroperoxides (ROOH). Note that the term "reactive" is used to indicate the higher reactivity of ROS relative to molecular oxygen (Mazzoli-Rocha et al., 2010) due to the presence of unpaired electrons (Franco and Panayiotidis, 2009). Precursors of ROS such as carbon-centred radicals can also be considered as ROS. ROS can be generated directly on the surface of DPM via redox cycling processes, or indirectly through interactions between DPM and cells (Li et al., 2010). Oxidative stress initiates redox-sensitive transcription factors, such as the MAPK (mitogen-activated protein kinase) and the NF-κB (nuclear factor kappa-light-chain-enhancer of activated B cells**)**, cascades, which work synergistically to activate the expression of proinflammatory cytokines, such as: Interleukin-4, Interleukin-6, IL-8, and TNF-α as well as chemokines and adhesion receptors (Donaldson et al., 2005; Riedl and Diaz-Sanchez, 2005). Many *in vivo* and *in vitro* studies have reported an increased expression of these transcription factors and proinflammatory genes after exposure to PM (reviewed by (Dreher, 2000; González-Flecha, 2004; Riedl and Diaz-Sanchez, 2005), implying that an increased amount of ROS is generated in cells upon exposure to DPM.

Alveolar macrophages and airway epithelial cells play a central role in the body's defence mechanism against inhaled foreign objects, by generating vigorous, localised inflammatory responses in the respiratory tract. However, excessive inflammation may cause localised tissue damage through apoptosis (Mazzoli-Rocha et al., 2010) and necrosis of cells (Møller et al., 2010); or, if sustained, chronic inflammation may induce progression to a more wide spread cardiovascular or respiratory disease (Pope and Dockery, 2006).

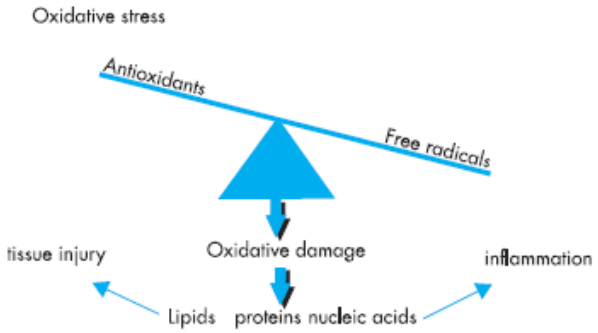

Figure 2.4: An illustration of oxidant/anti-oxidant balance *in vivo* and associated biological responses (from (Kelly, 2003)). Copyright permission license number: 2753470727414.

Considerable research attention has focussed on the formation of *in situ* ROS; formed after particle deposition in the human respiratory tract. *In situ*, or endogenous, ROS production can be formed by chemical species on the particle that have the potential to generate ROS (such as quinones (Grahame and Schlesinger, 2007) – a direct pathway), or by phagocytic processes initiated by the presence of DPM in the lungs (the indirect pathway). However, in addition to the particle-induced generation of ROS, several recent studies have shown that particles may also contain ROS (Hung and Wang, 2001; Huang et al., 2005; Venkatachari et al., 2005; Tousoulis et al., 2006; Venkatachari et al., 2007). Given that they are already present on the particles, they are termed exogenous ROS. Particle bound, exogenous ROS are considered in this thesis.

2.4.4 Physico-chemical properties that drive inflammation and oxidative stress

Oxidative stress and inflammation are a coupled, synergistic phenomenon. Ayres et al. (Ayres et al., 2008) note that oxidative stress is a precursor to inflammation, with the occurrence of inflammation being able to generate more oxidative stress. As such, the physico-chemical properties of DPM that influence these biological processes are presented together in this sub-section.

The first risk factor associated with the development of oxidative stress and associated inflammation is the DPM surface area. Whilst PM mass is a regulated ambient air quality

parameter and is also a regulated pollutant for internal combustion engines, a consistently reported result in the toxicological literature is that particle mass is not a very appropriate metric for describing the ability of particles to induce oxidative stress and inflammation (see (Oberdörster et al., 2005; Oberdörster et al., 2007) and references therein). For example, a rodent particle exposure study by Oberdörster (Oberdörster, 2001), showed that the particle surface area correlated better with the inflammatory response than did particle mass. An increased particle surface area per unit mass dose provides an increase in the availability of adsorbed toxic substances, and provides a locus for which catalytic chemistry can occur, potentially leading to ROS formation. The particle surface area is, also, the physical quantity in contact with the lung lining fluid, so it gives a good measure of the biological activity of particles (Giechaskiel et al., 2009).

Several studies have also demonstrated the importance of the organic fraction in DPM toxicity. As was suggested earlier in the review, the organic fraction of DPM is particularly complex, containing hundreds (or possibly thousands) of compounds, including polycyclic aromatic hydrocarbons (PAHs), which are known human carcinogens (International Agency for Research on Cancer, 1987). Several studies have shown that DPM, as well as its organic extracts are able to induce pro-inflammatory responses and/or induce apoptosis in lung tissue cells, whereas DPM that had its organic constituents extracted was no longer able to induce such responses in cells (Hiura et al., 1999; Li et al., 2000; Bonvallot et al., 2001; Li et al., 2002). Thus the organic component of DPM is implicated in the induction of oxidative stress, which is a viewpoint held by several research groups (Kelly, 2003; Nel, 2005; Ayres et al., 2008; Valavanidis et al., 2008).

2.4.5 Translocation

Whilst the primary route by which DPM causes health effects is via inhalation through the human respiratory system, other particle exposure pathways are possible. Translocation is a route of exposure whereby particles can migrate to a secondary organ (such as the brain, liver or spleen) after inhalation, thereby causing health effects in that secondary organ. In rodent particle exposure studies, a well established link appears to be the translocation of ultra-fine particles to the brain via the olfactory bulb. The work of Oberdörster et al. (2004) and references therein show convincing evidence of translocation of ultra-fine particles to the brain in rats, and also in monkeys (Elder et al., 2006); however, much further work is required to demonstrate similar effects in humans (Schmid et al., 2009). If this route of

exposure is viable in humans, inhalation toxicological studies would need to consider the health effects of DPM that has migrated to secondary organs.

2.4.6 Health effects review conclusion

A clear conclusion to emerge from the previous section is the significant role that adsorbed organic material plays in the adverse health effects of DPM. Therefore, to gain insights into DPM's likely health effects, this component should be monitored by the engine researcher. Systems that are capable of providing the desired information are described in the following section.

2.5 Measurement techniques

Prior to the deployment of DPM measurement instrumentation, a key issue that needs to be taken into account is the potential for physico-chemical transformation of particulates to occur between the sampling point and the point of measurement. The issues associated with DPM sampling are discussed first, followed by the instrumental techniques utilised in this thesis for quantifying DPM emissions.

2.5.1 DPM emissions sampling issues

As was discussed in previous sections of this review (see section 2.2.3.2) one of the complexities of DPM composition and formation was its strong spatio-temporal evolution. Thus, the measurement of DPM needs to take its spatial and temporal dependencies into account when attempting to characterise this pollutant.

One issue to emerge from the literature on DPM sampling relates to the thermodynamic history of particles *en route* from the internal combustion engines exhaust to the particle measurement instrumentation (Kittelson et al., 2002b). The cooling and dilution of the DPM sample is a critical factor to consider when designing laboratory based dilution systems. As CI engines emit a very high number of particles in raw exhaust ($\leq 10^9$ particles/cm^3) at elevated temperature (≤ 600 ^{o} C) it is necessary to dilute the sample to reduce the particle number concentration and to cool it to reduce its temperature. Simultaneous reduction of the number concentration and sample temperature is necessary to enable the use of aerosol instrumentation, and in doing so to attempt a simulation of the atmospheric dilution process (Eastwood, 2008b). How this reduction in concentration (dilution) and temperature (cooling) is achieved is critical to the observed physico-chemical properties of DPM.

In particular, a phenomenon in the aerosol physics literature called nucleation is very sensitive to the level of cooling and dilution. Nucleation is a gas-to-particle conversion

process that depends on the saturation ratio that a nucleating species exhibits. The saturation ratio (S_R) of a nucleating substance can be defined mathematically as:

$$S_R = \frac{p_A}{p_A^S(T)}, \tag{2.4}$$

where p_A is the vapour pressure of substance, and $p_A^S(T)$ is the temperature dependent saturated vapour pressure of substance A. Note that super-saturation occurs for $S > 1$ (Seinfeld and Pandis, 2006).

Each nucleating species has its own threshold S_R at which homogeneous nucleation can occur and for homogeneous nucleation (i.e. nucleation in the absence of a pre-existing particle), saturation ratios in the range of 2 to 10 are typically required (Baron and Willeke, 2001). If S_R exceeds the nucleation threshold, then gas-to-particle conversion will occur forming many nanoparticles (<50 nm) in the nucleation mode.

The dilution ratio can be calculated as the ratio of the total flow divided by the sample flow used by aerosol instrumentation. Mathematically, the dilution ratio (D_R) is computed via (Khalek et al., 1998):

$$D_R = \frac{F_T}{F_S} = \frac{F_D + F_S}{F_S}, \tag{2.5}$$

where F_T, F_s, and F_D are the total flow, sample flow, and dilution air flow, respectively. Whilst the mathematical definition of the dilution ratio is computed based on these 3 flow rates; a more convenient approach for the engine researcher is to use tracer gases such as CO_2 (Ristovski et al., 2005) or NOx (Abdul-Khalek et al., 1998) to enable calculation of the dilution ratio.

Figure 2.5, adapted from the work of Kittelson et al. (1999) shows the Saturation Ratio versus Dilution Ratio. Note that S_R reaches a peak for D_R in the range of 10-20. The S_R peak is reached in this range of D_R due to the competing processes of dilution and cooling. Cooling the exhaust will decrease its temperature and consequently will decrease the saturated vapour pressure of a nucleating substance. The saturation vapour pressure of a nucleating substance exhibits a monotonically increasing exponential relationship versus temperature (Hinds, 1999). Exhaust gas cooling will, therefore, increase S_R. However, as the exhaust gas is cooled it is diluted, which will decrease the vapour pressure of a nucleating substance. Alternatively, dilution will decrease S_R . The interplay between dilution and cooling

produces the S_R versus D_R relationship displayed in Figure 2.5. Note well that intermediate D_R (particularly in the range 10-50) supports nucleation, as the vapour pressure of a nucleating substance is still relatively high, but the exhaust has also cooled sufficiently at intermediate dilution ratios for the saturated vapour pressure to decrease. This is a key factor to take into account when designing laboratory based dilution system. The overall dilution ratio should be achieved with an overall dilution ratio much larger than 100 to avoid the problem of artefactual particle formation, a topic that is discussed by Khalek et al. (1998). Additionally, the residence time at intermediate dilution ratios (between 10-50) should be kept as short as possible to minimise this effect as well.

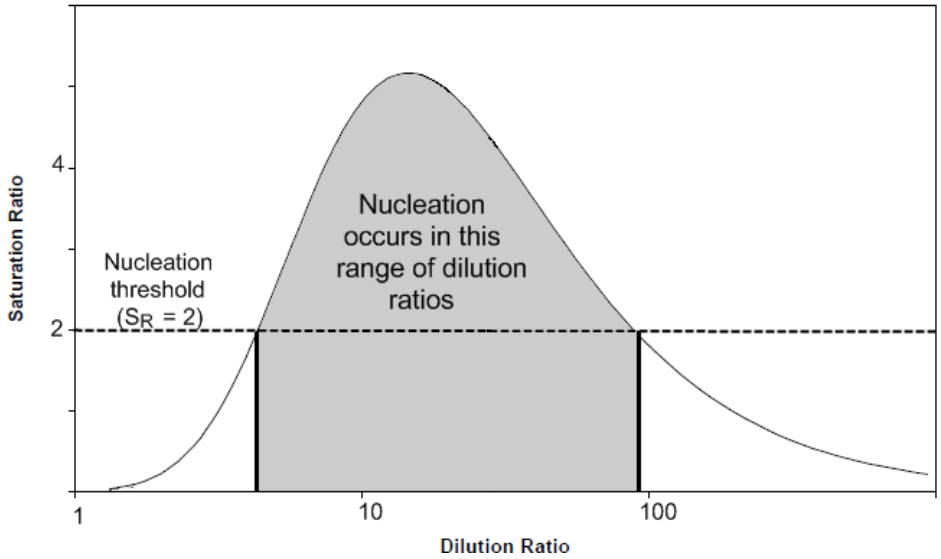

Figure 2.5: A graph showing the dependency of Saturation Ratio on dilution ratio (adapted from (Kittelson et al., 1999)). Note that the saturation ratio threshold has been arbitrarily set to 2.

In summary, the last sub-section serves to illustrate the sensitivity of diesel exhaust particle formation to the cooling and dilution processes which are critical factors for the engine researcher to take into account when designing dilution systems for measurement of DPM composition.

2.5.2 Gaseous emissions measurement

Unlike its particulate counterpart, the measurement of gaseous emissions sampling offers a more mature literature with agreed techniques for measuring these components, as can be seen from consulting various SAE standards (Society of Automotive Engineers, 1993; 2002). According to the SAE standard, J254, hydrocarbons require measurement with a flame ionisation detector, NOx emissions are measured with a chemiluminescence detector, and CO and CO_2 are measured using a non-dispersive infra-red analyser.

2.5.3 DPM emissions measurement

The history of aerosol science has produced a veritable slew of technologies for characterising the physical (Burtscher, 2005) and chemical (Maricq, 2007) properties of DPM. In terms of characterising the physical properties of DPM, electrically based techniques are relied upon heavily, with Flagan (1998) providing a detailed overview of the development of these techniques. In terms of instrument design, it was recognised by Friedlander (1971) that the aerosol scientist ultimately wants an instrument that measures the physico-chemical characteristics of particles in real-time, a situation which is graphically depicted in Figure 2.6. Such an instrument would provide complete information on the temporal and physico-chemical evolution of a particle source.

Figure 2.6: Instrument requirements for instant temporal, physical, and chemical characterisation of particles (from (McMurry, 2000b)). Copyright permission license number: 2753470626692. Same copyright permission license covers Figures 2.7-2.9.

Aerosol instrumentation currently available is not (unfortunately) able to deliver these rather idealised requirements outlined by Friedlander. It thus follows that the development of more advanced instrumentation is a critical requirement in aerosol science. The Aerosol Mass Spectrometer (AMS) is, however, the most suitable instrument available at present for undertaking physico-chemical characterisations of particles (McMurry, 2000b). As was done in Figure 2.6, the time resolution and physio-chemical measurement resolution of this instrument is depicted in Figure 2.7. Note that the AMS provides a vacuum aerodynamic diameter for particles in near real-time (~ 1 second) with the focussing lens achieving good transmission efficiency in the 50-500 nm range (Schneider et al., 2005). The AMS is able to distinguish between a large range of ion fragments based on mass-to-charge ratios, therefore enabling identification of broad classes of particle constituents such as: sulphates, nitrates, and organics (Schneider et al., 2008). It should be noted thought that the ionisation process only works for non-refractory particle components, so refractory components such as elemental carbon are not detected (Slowik et al., 2004). Instrumentation advances in the AMS field are, however, starting to deliver instruments which enable the detection of refractory components (Gao et al., 2007).

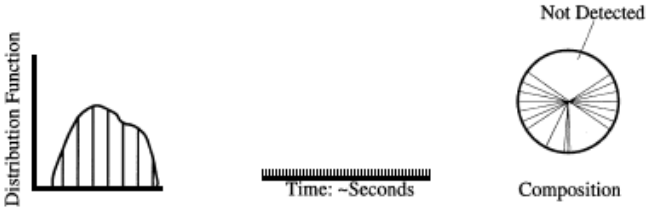

Figure 2.7: The temporal, physical, and chemical resolution of the AMS.

It should be noted that the AMS is an expensive and highly sophisticated instrument, and rather complicated data post-processing is required to obtain useful results using this technique. Without the ability to detect refractory components of particles (such as elemental carbon), and due to the fact that modern CI engines (without advanced after-treatment) do not emit a lot of sulphates or organics, does not make this approach highly suited to DPM physico-chemical characterisations. Clearly, another approach is required.

The approach taken in this thesis is to characterise the volatile and non-volatile components of DPM using an SMPS-TD approach. Whilst this approach does not exhibit the same time resolution as the AMS, due to the limitation of lengthy SMPS scan times (usually 2-3 minutes), nor the same ability to resolve the chemical components of DPM (it will only identify semi-volatile DPM fractions), the SMPS-TD approach greatly simplifies the experimental procedure, and consequent data processing. Considering that the modern CI engine emits (usually) elemental carbon with an adsorbed organic layer makes the SMPS-TD system a highly suited technique for DPM physico-chemical characterisations. The temporal, physical, and chemical resolution of the SMPS-TD technique is depicted in Figure 2.8, which is a compromise between the complexity of the AMS approach, and the time consuming and laborious analytical chemistry techniques required to obtain similar information from filter sampling (see Figure 2.9).

Figure 2.8: The temporal, physical, and chemical resolution of the SMPS-TD approach.

Figure 2.9: The temporal, physical, and chemical resolution of filter based sampling.

The SMPS-TD technique is based around 3 building blocks to characterise the physico-chemical properties of DPM, namely: a classifier, a thermodenuder, and a CPC. A classifier brings the particles to an (approximately) equilibrium Boltzmann charge distribution through beta emission from a ^{85}Kr source (Maricq et al., 2000). The particles are then introduced through a slit between two concentric cylinders; with a voltage being applied between the electrically grounded outer cylinder, and the electrode of the inner cylinder (Maricq et al., 1999). Positively charged particles are deflected towards the inner electrode - a process which is dependent on the electrical mobility of the particle. Due to the applied voltage, only particles within a narrow mobility (and hence size range) can exit the classifier as a mono-disperse flow. By exponentially ramping the applied voltage (Wang and Flagan, 1990), a wide range of mobility diameters can be classified. Monodisperse particles exiting the classifier are subsequently counted with a CPC.

The condensation particle counter (CPC) is used ubiquitously to perform particle number counting, with McMurry (2000a) providing a historical overview of the development of this technique. Particles exiting the classifier are too small to be detected by optical methods. The CPC condenses a saturated vapour of working fluid (typically butanol or water vapour) onto the particles, growing them to sizes of approximately 2-3 µm thus enabling optical particle counting to be achieved with a laser. Selecting the electrical mobility of particles with a classifier, and subsequently counting the particles with a CPC enables a particle number size (electrical mobility) distribution to be obtained.

A TD is a device used in aerosol research to heat particles in a controlled manner. A TD typically consists of a short heating section followed thereafter by an annular bed of activated charcoal that adsorbs any evaporated material. Adsorption of evaporated material is undertaken to prevent the possibility of re-condensation of volatile material downstream of the TD (Burtscher et al., 2001). The TSI 3065 is an example of a TD consisting of both the

heating section, followed by the adsorption region. Some TD's also have an active cooling system to enable reproducible cooling conditions when undertaking measurements (Burtscher et al., 2001).

2.6 Multi-criteria decision analysis techniques

As was discussed in the introduction of this thesis, the modern CI engine must fulfil several criteria to qualify as a viable transportation power source (Ahlvik, 2003). The modern CI engine must be efficient, it must emit very low gaseous and particulate emissions, and it must be powered by fuels that have minimal environmental impact (in terms of life cycle greenhouse gas emissions). The relationship between these various CI engine design constraints yields a multi-faceted optimisation problem that the engine researcher must solve. It is thus the intention of this sub-section of the review to provide a formal methodology enabling the decision maker to obtain a quantitative solution to these various engine design constraints.

A variety of techniques exist in the Operations Research (OR) literature for optimisation problems characterised by a uni-variate (or multi-variate) objective function which requires optimisation subject to several constraints (Winston, 2004). Alternatively, in multi-criteria problems the notion of an "optimal" solution breaks down, meaning that the decision maker is not able to use the standard techniques that populate the OR literature (such as the simplex method and derivative based optimisation techniques) (Brans and Vincke, 1985). A way around this problem is to utilise techniques based on preference rather than "optimal" solutions. There are a variety of multi-criteria decision analysis (MCDA) algorithms which vary in complexity from the elementary (e.g. weighted sum method) to methods which include the notion of outranking (Guitouni and Martel, 1998), such as ELECTRE, PROMETHEE and REGIME. A review of the MCDA literature revealed that the PROMETHEE-GAIA (Preference Ranking Organization Method for Enrichment Evaluations and Geometrical Analysis for Interactive Aid) approach proved quite useful in environmental applications (Behzadian et al., 2010). A significant advantage of the PROMETHEE-GAIA algorithm (compared to other MCDA methods) is that it facilitates a rational decision making process. This is achieved by virtue of a decision vector that directs the decision maker towards "preferred" solutions (Brans and Mareschal, 1994).

The theory of the PROMETHEE-GAIA algorithm provided below draws heavily on material presented by the developers in: Brans and Vincke (1985), Brans et al. (1986), Mareschal and

Brans (1988), Brans and Mareschal (1994), where the absence of references in the ensuing section denotes that the discussion of the algorithm follows that presented in these papers. The reader is directed to Behzadian et al. (2010) for a review of the history and the fields of application for this algorithm.

The PROMETHEE-GAIA algorithm permits solution of MCDA problems of the following form:

$$\text{Max}\{f_1(a), \cdots, f_{1k}(a) | \text{a} \in \text{A}\},$$

where: A is a set of n alternatives which are evaluated through k criteria $(f_1, \cdots, f_k)$.

In the field of engine research, alternatives would entail different techniques to mitigate the impacts of a CI engine, such as alternative fuels, injection technologies and combustion strategies. Alternatively, the criteria against which alternatives are assessed would involve factors such as low gaseous and particulate emissions, low life cycle greenhouse gas emissions with each chosen fuel, whilst also making sure that the engine efficiency is maximised.

PROMETHEE-GAIA accepts a real valued evaluation table ($f_i \in \mathbb{R}, \forall i$, see Table 2.1) as a numerical input to the algorithm in the following form (i.e. categorical data cannot be analysed):

Table 2.1: The PROMETHEE-GAIA evaluation table.

	$f_1(.)$	⋯	$f_{k(.)}$
a_1	$f_1(a_1)$	⋯	$f_k(a_1)$
…	…	…	…
a_n	$f_1(a_n)$	⋯	$f_k(a_n)$

If we take a particular criterion (say f_i) that has to be maximised, pairwise comparison between alternatives lead to the following preference structure ($\forall a, b \in A$):

$$\begin{cases} f_i(a) > f_i(b) \Leftrightarrow a\ P\ b, \\ f_i(a) = f_i(b) \Leftrightarrow a\ I\ b, \end{cases}$$

where: P and I denote preference and indifference, respectively.

To take into account the relative scale of the criteria, a generalised criterion must be applied to each criterion. This is achieved with the preference function $P(a,b)$ which takes into account the preference of a over b for criterion f_i. The preference function $P(a,b)$ is usually expressed in terms of the relative difference $d = f_i(a) - f_i(b)$, and is a normalised quantity such that $0 \leq P(a,b) \leq 1$. The preference function offers the following structure:

$$\begin{cases} P(a,b) = 0, \ if \ d \leq 0, & \text{no preference or indifference} \\ P(a,b) \approx 0, if \ d > 0, & \text{weak preference} \\ P(a,b) \approx 1, if \ d \gg 0, & \text{strong preference} \\ P(a,b) = 1, if \ d \ggg 0, & \text{strict preference.} \end{cases}$$

The preference function $P(a,b)$ is required to be a strictly monotonically increasing function of d, being similar in form to that presented in Figure 2.10.

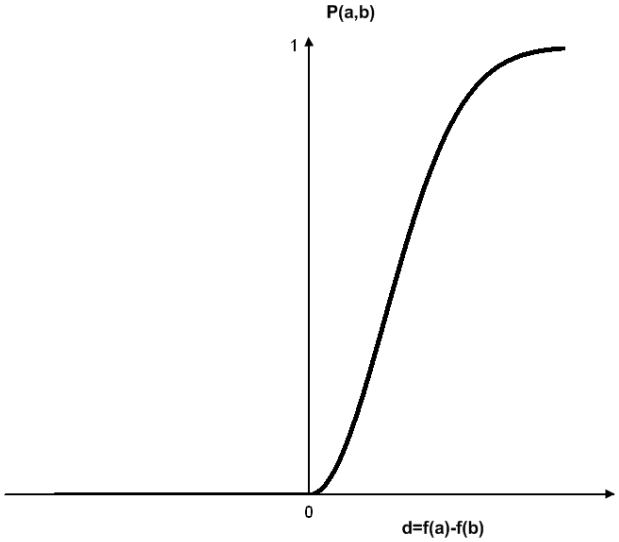

Figure 2.10: PROMETHEE-GAIA preference function.

A total of 6 preference functions are available to the PROMETHEE-GAIA user, and include functions such as: linear, V-shaped, Gaussian and other preference functions with varying thresholds.

Once a generalised criterion (through the preference function) has been applied to each criterion (f_i), a multi-criteria preference index $\pi(a,b)$ for a compared to b (for all criteria) can be computed via:

$$\pi(a,b) = \sum_{j=1}^{k} w_j P_j\,(a,b), \quad \sum_{j=1}^{k} w_j = 1,$$

where: $w_j > 0\ \forall j$, are the weights assigned to each criterion with $w_j \in \mathbb{R}$, noting well that the weights sum to unity.

Under the assumption of equal weights the preference index simplifies to:

$$\pi(a,b) = \frac{1}{k}\sum_{j=1}^{k} P_j\,(a,b),$$

however, it is possible to undertake a sensitivity analysis with a un-equal weights applied to each criterion (Dağdeviren, 2008).

To aid in the decision making process, the algorithm then computes the positive outranking flow:

$$\phi^{+}(a) = \frac{1}{n-1}\sum_{x\in A} \pi(a,x),$$

and also the negative outranking flow:

$$\phi^{-}(a) = \frac{1}{n-1}\sum_{x\in A} \pi(x,a).$$

The positive outranking flow quantifies how much a given alternative outranks the others, with a higher value of $\phi^{+}(a)$ indicating a more preferred alternative. Conversely, the negative outranking flow quantifies how a given alternative is outranked by other alternatives. A smaller value of $\phi^{-}(a)$ is preferred.

A ranking of alternatives is available to the PROMETHEE-GAIA decision maker by considering the difference between the positive and negative outranking flows by considering the net outranking flow given by:

$$\phi(a) = \phi^{+}(a) - \phi^{-}(\text{a}).$$

A higher value of the net outranking flow indicates a more preferable alternative.

It should be noted that the net outranking flow in the PROMETHEE-GAIA algorithm can also be solved subject to constraints, which are handled by a 0-1 linear program in the software.

Most MCDA problems involve several criteria. As a result, the solution to the problem exists in a multi-dimensional space. The GAIA component of the PROMETHEE-GAIA algorithm

then performs Principal Component Analysis (PCA) to reduce the dimensionality of the problem to 2 spatial dimensions (called the GAIA plane) for visual interpretation of the problem. The projection error associated with PCA is governed by the 2 dominant eigenvalues (λ_1, λ_2) of the variance-covariance matrix (C) associated with the uni-criterion (ϕ_j) net flows. The proportion of information retained after PCA (δ) is given by:

$$\delta = (\lambda_1 + \lambda_2) \Big/ \sum_{j=1}^{k} \lambda_{j,}$$

where: λ_k are the k eigenvalues of C. Typically, δ is greater than 60%, but often exceeds 80% for MCDA problems, so the GAIA plane retains a reasonable fraction of useful information.

Unlike PCA, PROMETHEE-GAIA has the critical difference that it provides a decision vector for the analyst. This enables the decision maker to view different alternatives in the GAIA plane, and to be directed towards preferred solutions by the decision vector. The decision vector is computed by calculating the projection of the different alternatives (α_i) onto the weights of the problem (w) which is achieved via:

$$(\alpha_i, w) = \sum_{j=1}^{k} w_i \phi_j\,(a_i) = \phi(a_i).$$

A decision vector that is long, and not orthogonal to the GAIA plane is preferred for strong decision making power.

2.7 Research needs addressed by this thesis

2.7.1 DPM physico-chemistry

Whilst a considerable amount of research has addressed gaseous emissions with alternative fuels, injection technologies, and combustion strategies, there is a vast absence of information in existence describing the relationship between these technologies and the physico-chemical properties of their resulting DPM emissions. Broadly, it is this primary knowledge gap that is addressed by this thesis. Through the literature research conducted in this thesis, there exist many publications exploiting the high oxygen content of biofuels such as methanol (Yao et al., 2007; Cheng et al., 2008a; Cheng et al., 2008b; Cheung et al., 2008; Yao et al., 2008; Cheung et al., 2009a; Zhang et al., 2009; 2010b; Zhang et al., 2010a), ethanol (Ajav et al., 1998; 1999; Abu-Qudais et al., 2000; Corkwell et al., 2003; He et al., 2003a; He et al., 2003b; He et al., 2004; Nord et al., 2004; Di et al., 2009d; Zhang et al., 2011), biodiesel (Durbin et al., 2000; Turrio-Baldassarri et al., 2004; Szybist et al., 2007; Cheung et al., 2009b; Di et al.,

2009c; Di et al., 2009b; Di et al., 2009a; Karavalakis et al., 2009b; Fontaras et al., 2010a; Karavalakis et al., 2010c; Zhu et al., 2010) and other oxygenates (Liotta and MontaIvo, 1993; Maricq et al., 1998; Miyamoto et al., 1998; Shi et al., 2005; Wang et al., 2009; Di et al., 2010b) for reducing regulated emissions. A literature is also beginning to emerge on the impact of oxygenated biofuels on un-regulated pollutants such as carbonyls (Corrêa and Arbilla, 2008; Fontaras et al., 2009; Karavalakis et al., 2009a; Fontaras et al., 2010a; Karavalakis et al., 2010a) and polycyclic aromatic hydrocarbons (Corrêa and Arbilla, 2006; Ballesteros et al., 2010; Karavalakis et al., 2010b); however, much of the research is not focussed on the direct causative agent of CI engine health impacts.

There is evidence beginning to emerge that the precursor to a range of cardiovascular and respiratory disease is oxidative stress (and associated inflammation) (Pope and Dockery, 2006), and that oxidative stress is heavily influenced by the presence of organics on the DPM particle surface (Kelly, 2003; Li et al., 2003; Nel, 2005; Ayres et al., 2008; Valavanidis et al., 2008; Grahame and Schlesinger, 2010). The organic fraction of DPM has traditionally been characterised in an off-line manner using techniques from analytical chemistry; which is a time consuming and laborious process. An emerging technique for characterising the organic material present in DPM is to explore the volatility properties of particles (Maricq, 2007). This technique has been used to investigate the organic fraction of DPM in a much more limited set of research studies (Burtscher et al., 2001; Sakurai et al., 2003; Meyer and Ristovski, 2007). This technique offers near real-time information (limited by the SMPS scan time) on both the volatile (organic carbon) and non-volatile (elemental carbon) fraction of DPM, and perhaps most importantly, could provide evidence of toxic compounds (such as reactive oxygen species and PAHs) adsorbed or condensed on the DPM particle surface. The potential for a correlation to exist between the organic fraction of DPM (utilising an SMPS-TD approach) with compounds involved in the oxidative stress pathway is a specific research need addressed by this thesis.

2.7.2 Particle size reduction with alternative fuels

The particle number size distribution measurements conducted in this thesis demonstrated a significant reduction in median particle diameter for most alternative fuel types. Whilst a considerable amount of recent research has addressed the morphological restructuring of combustion generated soot particles upon exposure to organic and water vapours (Saathoff et al., 2003; Lu et al., 2008; Zhang et al., 2008b; Pagels et al., 2009a), a discussion of possible mechanisms explaining this effect remain limited. A possible mechanism cited in the

literature implicates surface tension as the driving force for soot particle restructuring (Kütz and Schmidt-Ott, 1992b; Cross et al., 2010); however, other mechanisms should be investigated. As a result, another specific research need addressed by this thesis is to investigate hypotheses related to combustion generated particle structuring, such as the role of surface tension, wetting of the particle surface, and the role of organics in flocculating elemental carbon containing primary particles.

2.7.3 Multi-criteria decision analysis

A plethora of literature is devoted to the impact of various CI engine emission reduction strategies, such as: alternative fuels, injection technologies, and combustion strategies on the resulting emissions profile. Consultation of the reference list in a recent text published by Eastwood (2008b) gives an indication as to how much work has been done on this topic. There is, however, a lack of research taking a holistic approach to the CI engine emissions problem. As was noted in the introduction to this thesis, the primary constraints that the engine researcher must work with entail; minimising gaseous, particulate and life cycle greenhouse gas emissions, whilst making sure that engine efficiency is not compromised in the process of meeting emissions requirements. As a result, this thesis applies a well known MCDA algorithm (PROMETHEE-GAIA) to investigate how well different CI engine emissions mitigation strategies satisfy these 3 constraints. PROMEHTEE-GAIA has been applied as a decision making tool in several environmental applications (Behzadian et al., 2010); however, apart from a study by Lim et al. (2007a) (which investigated the impact of diesel fuel sulphur reduction on the elemental composition of CI engine emissions) the author is not aware of any other studies applying an MCDA tool (like PROMETHEE-GAIA) to a CI engine emissions dataset. Application of this algorithm provides the user with a rationale basis for decision making which potentially enables viable emissions mitigation strategies to be identified for CI engines subject to the constraints imposed by the user. This research activity is another specific research need addressed by this thesis.

2.8 References

Abdul-Khalek, I.S., Kittelson, D.B., Brear, F., 1998. Diesel trap performance: particle size measurements and trends. Society of Automotive Engineers, SAE Paper No. 982599.

Abu-Qudais, M., Haddad, O., Qudaisat, M., 2000. The effect of alcohol fumigation on diesel engine performance and emissions. Energy Conversion and Management 41(4), 389-399.

Adelman, H., 1979. Alcohols in diesel engines - a review. Society of Automotive Engineers, SAE Paper No. 790956.

Agarwal, A.K., 2007. Biofuels (alcohols and biodiesel) applications as fuels for internal combustion engines. Progress in Energy and Combustion Science 33(3), 233-271.

Ahlvik, P., 2003. Alternative diesel fuels. Dieselnet Technology Guide, Ecopoint Inc, http://www.dieselnet.com/tech/fuel_alt.html, last accessed 16th September 2011.

Ajav, E.A., Singh, B., Bhattacharya, T.K., 1998. Performance of a stationary diesel engine using vapourized ethanol as supplementary fuel. Biomass & Bioenergy 15(6), 493-502.

Ajav, E.A., Singh, B., Bhattacharya, T.K., 1999. Experimental study of some performance parameters of a constant speed stationary diesel engine using ethanol-diesel blends as fuel. Biomass & Bioenergy 17(4), 357-365.

Alleman, T.L., McCormick, R.L., 2003. Fischer-Tropsch diesel fuels - properties and exhaust emissions: a literature review. Society of Automotive Engineers, SAE Paper No. 2003-01-0763.

Amann, C.A., Siegla, D.C., 1982. Diesel particulates-what they are and why. Aerosol Science and Technology 1(1), 73-101.

Atkins, R.D., 2009. An introduction to engine testing and development. SAE International, Warrendale, pp. 1-289.

Ayres, J.G., Borm, P., Cassee, F.R., Castranova, V., Donaldson, K., Ghio, A., Harrison, R.M., Hider, R., Kelly, F., Kooter, I.M., Marano, F., Maynard, R.L., Mudway, I., Nel, A., Sioutas, C., Smith, S., Baeza-Squiban, A., Cho, A., Duggan, S., Froines, J., 2008. Evaluating the toxicity of airborne particulate matter and nanoparticles by measuring oxidative stress potential - A workshop report and consensus statement. Inhalation Toxicology 20(1), 75-99.

Balat, M., 2009. Bioethanol as a vehicular fuel: a critical review. Energy Sources Part a-Recovery Utilization and Environmental Effects 31(14), 1242-1255.

Balat, M., Balat, H., Öz, C., 2008. Progress in bioethanol processing. Progress in Energy and Combustion Science 34(5), 551-573.

Ballesteros, R., Hernández, J.J., Lyons, L.L., 2010. An experimental study of the influence of biofuel origin on particle-associated PAH emissions. Atmospheric Environment 44(7), 930-938.

Baron, P.A., Willeke, K., 2001. Aerosol measurement: principles, techniques and applications. John Wiley & Sons, Inc., New York, pp. 1-1131.

Baumgard, K.J., Johnson, J.H., 1996. The effect of fuel and engine design on Diesel exhaust particle size distributions. Society of Automotive Engineers, SAE Paper No. 960131.

Beer, T., Grant, T., 2007. Life-cycle analysis of emissions from fuel ethanol and blends in Australian heavy and light vehicles. Journal of Cleaner Production 15(8-9), 833-837.

Beer, T., Grant, T., Williams, D., Watson, H., 2002. Fuel-cycle greenhouse gas emissions from alternative fuels in Australian heavy vehicles. Atmospheric Environment 36(4), 753-763.

Behzadian, M., Kazemadeh, R.B., Albadvi, A., Aghdasi, M., 2010. PROMETHEE: a comprehensive literature review on methodologies and applications. European Journal of Operational Research 200(1), 198-215.

Bika, A.S., Franklin, L.M., Kittelson, D.B., 2008. Emissions effects of hydrogen as a supplementary fuel with diesel and biodiesel. Society of Automotive Engineers, SAE Paper No. 2008-01-0648.

Bonvallot, V., Baeza-Squiban, A., Baulig, A., Brulant, S., Boland, S., Muzeau, F., Barouki, R., Marano, F., 2001. Organic compounds from diesel exhaust particles elicit a proinflammatory response in human airway epithelial cells and induce cytochrome p450 1A1 expression. American Journal of Respiratory Cell and Molecular Biology 25(4), 515-521.

Brans, J.P., Mareschal, B., 1994. The PROMCALC & GAIA decision-support system for multicriteria decision aid. Decision Support Systems 12(4-5), 297-310.

Brans, J.P., Vincke, P.H., 1985. A preference ranking organization method - (The PROMETHEE method for multiple criteria decision-making) Management Science 31(6), 647-656.

Brans, J.P., Vincke, P.H., Mareschal, B., 1986. How to select and how to rank projects - the PROMETHEE method. European Journal of Operational Research 24(2), 228-238.

Bugarski, A.D., Cauda, E.G., Janisko, S.J., Hummer, J.A., Patts, L.D., 2010. Aerosols Emitted in Underground Mine Air by Diesel Engine Fueled with Biodiesel. Journal of the Air & Waste Management Association 60(2), 237-244.

Burtscher, H., 1992. Measurement and characteristics of combustion aerosols with special consideration of photoelectric charging and charging by flame ions. Journal of Aerosol Science 23(6), 549-595.

Burtscher, H., 2005. Physical characterization of particulate emissions from diesel engines: a review. Journal of Aerosol Science 36(7), 896-932.

Burtscher, H., Baltensperger, U., Bukowiecki, N., Cohn, P., Hüglin, C., Mohr, M., Matter, U., Nyeki, S., Schmatloch, V., Streit, N., Weingartner, E., 2001. Separation of volatile and non-volatile aerosol fractions by thermodesorption: instrumental development and applications. Journal of Aerosol Science 32(4), 427-442.

Çengel, Y.A., Boles, M.A., 2006. Thermodynamics: an engineering approach, 5th edition. McGraw-Hill, New York, pp. 1-988.

Chen, Z., Iwashina, T., 2009. HC and CO formation factors in a PCI engine. Society of Automotive Engineers, SAE Paper No. 2009-01-1889.

Cheng, C.H., Cheung, C.S., Chan, T.L., Lee, S.C., Yao, C.D., 2008a. Experimental investigation on the performance, gaseous and particulate emissions of a methanol fumigated diesel engine. Science of the Total Environment 389(1), 115-124.

Cheng, C.H., Cheung, C.S., Chan, T.L., Lee, S.C., Yao, C.D., Tsang, K.S., 2008b. Comparison of emissions of a direct injection diesel engine operating on biodiesel with emulsified and fumigated methanol. Fuel 87(10-11), 1870-1879.

Cheung, C.S., Cheng, C.H., Chan, T.L., Lee, S.C., Yao, C.D., Tsang, K.S., 2008. Emissions characteristics of a diesel engine fueled with biodiesel and fumigation methanol. Energy & Fuels 22(2), 906-914.

Cheung, C.S., Zhang, Z.H., Chan, T.L., Yao, C.D., 2009a. Investigation on the effect of port-injected methanol on the performance and emissions of a Diesel engine at different engine speeds. Energy & Fuels 23(11), 5684-5694.

Cheung, C.S., Zhu, L., Huang, Z., 2009b. Regulated and unregulated emissions from a diesel engine fueled with biodiesel and biodiesel blended with methanol. Atmospheric Environment 43(32), 4865-4872.

Cheung, K.L., Ntziachristos, L., Tzamkiozis, T., Schauer, J.J., Samaras, Z., Moore, K.F., Sioutas, C., 2010. Emissions of particulate trace elements, metals and organic species from gasoline, Diesel, and biodiesel passenger vehicles and their relation to oxidative potential. Aerosol Science and Technology 44(7), 500-513.

Corkwell, K.C., Jackson, M.M., Daly, D.T., 2003. Review of exhaust emissions of compression ignition engines operating on E diesel fuel blends. Society of Automotive Engineers, SAE Paper No. 2003-01-3283.

Corrêa, S.M., Arbilla, G., 2006. Aromatic hydrocarbons emissions in diesel and biodiesel exhaust. Atmospheric Environment 40(35), 6821-6826.

Corrêa, S.M., Arbilla, G., 2008. Carbonyl emissions in diesel and biodiesel exhaust. Atmospheric Environment 42(4), 769-775.

Cross, E.S., Onasch, T.B., Ahern, A., Wrobel, W., Slowik, J.G., Olfert, J., Lack, D.A., Massoli, P., Cappa, C.D., Schwarz, J.P., Spackman, J.R., Fahey, D.W., Sedlacek, A., Trimborn, A., Jayne, J.T., Freedman, A., Williams, L.R., Ng, N.L., Mazzoleni, C., Dubey, M., Brem, B., Kok, G., Subramanian, R., Freitag, S., Clarke, A., Thornhill, D., Marr, L.C., Kolb, C.E., Worsnop, D.R., Davidovits, P., 2010. Soot particle studies-instrument inter-comparison-project overview. Aerosol Science and Technology 44(8), 592-611.

Dağdeviren, M., 2008. Decision making in equipment selection: an integrated approach with AHP and PROMETHEE. Journal of Intelligent Manufacturing 19(4), 397-406.

Davies, B., 2002. Diesel particulate control strategies at some Australian underground coal mines. Aiha Journal 63(5), 554-558.

DeCarlo, P.F., Slowik, J.G., Worsnop, D.R., Davidovits, P., Jimenez, J.L., 2004. Particle morphology and density characterization by combined mobility and aerodynamic diameter measurements. Part 1: Theory. Aerosol Science and Technology 38(12), 1185-1205.

Demirbas, A., 2007. Progress and recent trends in biofuels. Progress in Energy and Combustion Science 33(1), 1-18.

Demirbas, A., 2009. Political, economic and environmental impacts of biofuels: a review. Applied Energy 86(Supplement 1), S108-S117.

Desantes, J.M., Bermúdez, V., García, A., Linares, W.G., 2011. A comprehensive study of particle size distributions with the use of postinjection strategies in DI Diesel engines. Aerosol Science and Technology 45(10), 1161-1175.

Di, Y.G., Cheung, C.S., Huang, Z.H., 2009a. Comparison of the effect of biodiesel-diesel and ethanol-diesel on the gaseous emission of a direct-injection diesel engine. Atmospheric Environment 43(17), 2721-2730.

Di, Y.G., Cheung, C.S., Huang, Z.H., 2009b. Comparison of the effect of biodiesel-diesel and ethanol-diesel on the particulate emissions of a direct injection diesel engine. Aerosol Science and Technology 43(5), 455-465.

Di, Y.G., Cheung, C.S., Huang, Z.H., 2009c. Experimental investigation on regulated and unregulated emissions of a diesel engine fueled with ultra-low sulfur diesel fuel blended with biodiesel from waste cooking oil. Science of the Total Environment 407(2), 835-846.

Di, Y.G., Cheung, C.S., Huang, Z.H., 2009d. Experimental study on particulate emission of a diesel engine fueled with blended ethanol-dodecanol-diesel. Journal of Aerosol Science 40(2), 101-112.

Di, Y.G., Cheung, C.S., Huang, Z.H., 2010. Experimental investigation of particulate emissions from a diesel engine fueled with ultralow-sulfur diesel fuel blended with diglyme. Atmospheric Environment 44(1), 55-63.

Dieselnet, 2006. Fuel regulations, Australia. Ecopoint Inc, http://www.dieselnet.com/standards/au/fuel.php, last accessed 16th September 2011.

Donaldson, K., Tran, C.L., 2002. Inflammation caused by particles and fibers. Inhalation Toxicology 14(1), 5-27.

Donaldson, K., Tran, L., Jimenez, L.A., Duffin, R., Newby, D.E., Mills, N., MacNee, W., Stone, V., 2005. Combustion-derived nanoparticles: a review of their toxicology following inhalation exposure. Particle and fibre toxicology 2, Article Number 10.

Dreher, K.L., 2000. Particulate matter physicochemistry and toxicology: in search of causality - a critical perspective. Inhalation Toxicology 12(Supplement 3), 45-57.

Durbin, T.D., Collins, J.R., Norbeck, J.M., Smith, M.R., 2000. Effects of biodiesel, biodiesel blends, and a synthetic diesel on emissions from light heavy-duty diesel vehicles. Environmental Science & Technology 34(3), 349-355.

Durie, J., 2011. Shell shutdown a rational move, but it will cost jobs, The Australian.

Eastwood, P., 2008. Particulate emissions from vehicles. John Wiley & Sons, Ltd, Chichester, pp. 1-493.

Ecklund, E.E., Bechtold, R.L., Timbario, T.J., McCallum, P.W., 1984. State-of-the-art report on the use of alcohols in diesel engines. Society of Automotive Engineers, SAE Paper NO. 840118.

Elder, A., Gelein, R., Silva, V., Feikert, T., Opanashuk, L., Carter, J., Potter, R., Maynard, A., Ito, Y., Finkelstein, J., Oberdörster, G., 2006. Translocation of inhaled ultrafine manganese oxide particles to the central nervous system. Environmental Health Perspectives 114(8), 1172-1178.

Flagan, R.C., 1998. History of electrical aerosol measurements. Aerosol Science and Technology 28(4), 301-380.

Fontaras, G., Karavalakis, G., Kousoulidou, M., Ntziachristos, L., Bakeas, E., Stournas, S., Samaras, Z., 2010. Effects of low concentration biodiesel blends application on modern passenger cars. Part 2: Impact on carbonyl compound emissions. Environmental Pollution 158(7), 2496-2503.

Fontaras, G., Karavalakis, G., Kousoulidou, M., Tzamkiozis, T., Ntziachristos, L., Bakeas, E., Stournas, S., Samaras, Z., 2009. Effects of biodiesel on passenger car fuel consumption, regulated and non-regulated pollutant emissions over legislated and real-world driving cycles. Fuel 88(9), 1608-1617.

Franco, R., Panayiotidis, M.I., 2009. Environmental toxicity, oxidative stress, human disease and the "black box" of their synergism: How much have we revealed? Mutation Research-Genetic Toxicology and Environmental Mutagenesis 674(1-2), 1-2.

Friedlander, S.K., 1971. The characterization of aerosols distributed with respect to size and chemical composition - II. Classification and design of aerosol measuring devices. Journal of Aerosol Science 2(3), 331-340.

Gao, R.S., Schwarz, J.P., Kelly, K.K., Fahey, D.W., Watts, L.A., Thompson, T.L., Spackman, J.R., Slowik, J.G., Cross, E.S., Han, J.H., Davidovits, P., Onasch, T.B., Worsnop, D.R., 2007. A novel method for estimating light-scattering properties of soot aerosols using a modified single-particle soot photometer. Aerosol Science and Technology 41(2), 125-135.

Giechaskiel, B., Alföldy, B., Drossinos, Y., 2009. A metric for health effects studies of diesel exhaust particles. Journal of Aerosol Science 40(8), 639-651.

González-Flecha, B., 2004. Oxidant mechanisms in response to ambient air particles. Molecular Aspects of Medicine 25(1-2), 169-182.

Graboski, M.S., McCormick, R.L., 1998. Combustion of fat and vegetable oil derived fuels in diesel engines. Progress in Energy and Combustion Science 24(2), 125-164.

Grahame, T.J., Schlesinger, R.B., 2007. Health effects of airborne particulate matter: Do we know enough to consider regulating specific particle types or sources? Inhalation Toxicology 19(6-7), 457-481.

Grahame, T.J., Schlesinger, R.B., 2010. Cardiovascular health and particulate vehicular emissions: a critical evaluation of the evidence. Air Quality, Atmosphere and Health 3(1), 3-27.

Grose, M., Sakurai, H., Savstrom, J., Stolzenburg, M.R., Watts, W.F., Jr., Morgan, C.G., Murray, I.P., Twigg, M.V., Kittelson, D.B., McMurry, P.H., 2006. Chemical and physical properties of ultrafine diesel exhaust particles sampled downstream of a catalytic trap. Environmental Science & Technology 40(17), 5502-5507.

Guerrassi, N., Dupraz, P., 1998. A common rail injection system for high speed direct injection diesel engines. Society of Automotive Engineers, SAE Paper No. 980803.

Guitouni, A., Martel, J.M., 1998. Tentative guidelines to help choosing an appropriate MCDA method. European Journal of Operational Research 109(2), 501-521.

Hansen, A.C., Zhang, Q., Lyne, P.W.L., 2005. Ethanol-diesel fuel blends - a review. Bioresource Technology 96(3), 277-285.

Harris, G.W., Mackay, G.I., Iguchi, T., Schiff, H.I., Schuetzle, D., 1987. Measurement of NO_2 and HNO_3 in diesel exhaust gas by tunable diode laser absorption spectroscopy. Environmental Science & Technology 21(3), 299-304.

Havenith, C., Verbeek, R.P., 1997. Transient performance of a urea deNOx catalyst for low emissions heavy-duty diesel engines. Society of Automotive Engineers, SAE Paper No. 970185.

Haynes, B.S., Wagner, H.G., 1981. Soot formation. Progress in Energy and Combustion Science 7(4), 229-273.

He, B.Q., Shuai, S.J., Wang, J.X., He, H., 2003a. The effect of ethanol blended diesel fuels on emissions from a diesel engine. Atmospheric Environment 37(35), 4965-4971.

He, B.Q., Wang, J.X., Shuai, S.J., Yan, X.G., 2004. Homogeneous charge combustion and emissions of ethanol ignited by pilot diesel on diesel engines. Society of Automotive Engineers, SAE Paper No. 2004-01-0094.

He, B.Q., Wang, J.X., Yan, X.G., Tian, X., Chen, H., 2003b. Study on combustion and emission characteristics of diesel engines using ethanol blended diesel fuels. Society of Automotive Engineers, SAE Paper No. 2003-01-0762.

Heikkilä, J., Virtanen, A., Rönkkö, T., Keskinen, J., Aakko-Saksa, P., Murtonen, T., 2009. Nanoparticle emissions from a heavy-duty engine running on alternative diesel fuels. Environmental Science & Technology 43(24), 9501-9506.

Hesterberg, T.W., Long, C.M., Bunn, W.B., Sax, S.N., Lapin, C.A., Valberg, P.A., 2009. Non-cancer health effects of diesel exhaust: a critical assessment of recent human and animal toxicological literature. Critical Reviews in Toxicology 39(3), 195-227.

Heywood, J.B., 1988. Internal combustion engine fundamentals. McGraw-Hill, Inc, New York, pp. 1-930.

Hinds, W.C., 1999. Aerosol technology: properties, behavior, and measurement of airborne particles, 2nd edition. John Wiley & Sons, Inc., New York, pp. 1-483.

Hiura, T.S., Kaszubowski, M.P., Li, N., Nel, A.E., 1999. Chemicals in diesel exhaust particles generate reactive oxygen radicals and induce apoptosis in macrophages. Journal of Immunology 163(10), 5582-5591.

Hofmann, W., 2011. Modelling inhaled particle deposition in the human lung - a review. Journal of Aerosol Science 42(10), 693-724.

Huang, M.F., Lin, W.L., Ma, Y.C., 2005. A study of reactive oxygen species in mainstream of cigarette. Indoor Air 15(2), 135-140.

Hung, H.F., Wang, C.S., 2001. Experimental determination of reactive oxygen species in Taipei aerosols. Journal of Aerosol Science 32(10), 1201-1211.

Intergovernmental Panel on Climate Change, 2007. Climate change 2007: the physical science basis, contribution of Working Group I to the Fourth Assessment Report of the Intergovernmental Panel on Climate Change, IPCC Fourth Assessment Report (AR4), in: Solomon, S., Qin, D., Manning, M., Chen, Z., Marquis, M., Averyt, K.B., Tignor, M., Miller, H.L. (Eds.). IPCC, Cambridge, United Kingdom, pp. 1-996.

International Agency for Research on Cancer, 1987. Overall Evaluations of Carcinogenicity: An updating of IARC Monographs Volumes 1–42. IARC Monographs Evaluation of Carcinogenic Risks to Humans Supplement 7, pp. 1-440 http://www.iarc.fr/ last accessed, September 22nd 2011.

Jacobson, M.Z., 2001. Strong radiative heating due to the mixing state of black carbon in atmospheric aerosols. Nature 409(6821), 695-697.

Jacobson, M.Z., 2002. Control of fossil-fuel particulate black carbon and organic matter, possibly the most effective method of slowing global warming. Journal of Geophysical Research-Atmospheres 107(D19), Article Number 4410.

Jung, H., Kittelson, D.B., Zachariah, M.R., 2006. Characteristics of SME biodiesel-fueled diesel particle emissions and the kinetics of oxidation. Environmental Science & Technology 40(16), 4949-4955.

Karavalakis, G., Alvanou, F., Stournas, S., Bakeas, E., 2009a. Regulated and unregulated emissions of a light duty vehicle operated on diesel/palm-based methyl ester blends over NEDC and a non-legislated driving cycle. Fuel 88(6), 1078-1085.

Karavalakis, G., Bakeas, E., Stournas, S., 2010a. Influence of Oxidized Biodiesel Blends on Regulated and Unregulated Emissions from a Diesel Passenger Car. Environmental Science & Technology 44(13), 5306-5312.

Karavalakis, G., Fontaras, G., Ampatzoglou, D., Kousoulidou, M., Stournas, S., Samaras, Z., Bakeas, E., 2010b. Effects of low concentration biodiesel blends application on modern passenger cars. Part 3: Impact on PAH, nitro-PAH, and oxy-PAH emissions. Environmental Pollution 158(5), 1584-1594.

Karavalakis, G., Stournas, S., Bakeas, E., 2009b. Effects of diesel/biodiesel blends on regulated and unregulated pollutants from a passenger vehicle operated over the European and the Athens driving cycles. Atmospheric Environment 43(10), 1745-1752.

Karavalakis, G., Tzirakis, E., Stournas, S., Zannikos, F., Karonis, D., 2010c. Biodiesel emissions from a Diesel vehicle operated on a non-legislative driving cycle. Energy Sources Part A-Recovery Utilization and Environmental Effects 32(4), 376-383.

Kelly, F.J., 2003. Oxidative stress: its role in air pollution and adverse health effects. Occupational and Environmental Medicine 60(8), 612-616.

Keskinen, J., Rönkkö, T., 2010. Can Real-World Diesel Exhaust Particle Size Distribution be Reproduced in the Laboratory? A Critical Review. Journal of the Air & Waste Management Association 60(10), 1245-1255.

Khair, M.K., Jääskeläinen, H., 2010. Common Rail Fuel Injection, Dieselnet technology guide, Ecopoint Inc, http://www.dieselnet.com/tech/diesel_fi_cr.html, last accessed 19th October 2011.

Khalek, I.A., Bougher, T.L., Merritt, P.M., 2009. Phase 1 of the advanced collaborative emissions study, CRC Report: ACES Phase 1, pp. 1-158.

Khalek, I.A., Kittelson, D., Graskow, B., Brear, F., 1998. Diesel exhaust particle size: measurement issues and trends. Society of Automotive Engineers, SAE Paper No. 980525.

Khalek, I.A., Kittelson, D.B., Brear, F., 2000. Nanoparticle growth during dilution and cooling of diesel exhaust: experimental investigation and theoretical assessment. Society of Automotive Engineers, SAE Paper No. 2000-01-0515.

Kitamura, T., Ito, T., 2010. Mixing-controlled, low temperature diesel combustion with pressure modulated multiple-injection for HSDI Diesel engine. Society of Automotive Engineers, SAE Paper No. 2010-01-0609.

Kitamura, T., Ito, T., Senda, J., Fujimoto, H., 2001. Extraction of the supression effects of oxygenated fuels on soot formation using a detailed chemical kinetic model, Society of Automotive Engineers of Japan, pp. 139-145.

Kittelson, D., Watts, W., Johnson, J., 2002. Diesel aerosol sampling methodology - CRC E-43. Final report. University of Minnesota, Department of Mechanical Engineering. Report for the Coordinating Research Council, pp. 1-181.

Kittelson, D.B., 1998. Engines and nanoparticles: a review. Journal of Aerosol Science 29(5/6), 575-588.

Kittelson, D.B., Arnold, M., Watts, W.F., Jr., 1999. Review of diesel particulate matter sampling methods. Final report. University of Minnesota, Department of Mechanical Engineering, Center for Diesel Research., Minneapolis, Minnesota, pp. 1-64.

Kittelson, D.B., Watts, W.F., Johnson, J.P., 2004. Nanoparticle emissions on Minnesota highways. Atmospheric Environment 38(1), 9-19.

Kittelson, D.B., Watts, W.F., Johnson, J.P., Rowntree, C., Payne, M., Goodier, S., Warrens, C., Preston, H., Zink, U., Ortiz, M., Goersmann, C., Twigg, M.V., Walker, A.P., Caldow, R., 2006. On-road evaluation of two Diesel exhaust aftertreatment devices. Journal of Aerosol Science 37(9), 1140-1151.

Klimstra, J., Westing, J.E., 1995. NO_2 from lean burn engines - on its lower sensitivity to leaning than NO. Society of Automotive Engineers, SAE Paper No. 950158.

Konstandopoulos, A.G., Zarvalis, D., Dolios, I., 2007. Multi-instrumental assessment of diesel particulate filters. Society of Automotive Engineers SAE Paper No. 2007-01-0313.

Krishnamoorthy, S., Honn, K.V., 2006. Inflammation and disease progression. Cancer and Metastasis Reviews 25(3), 481-491.

Kütz, S., Schmidt-Ott, A., 1992. Characterization of agglomerates by condensation-induced restructuring. Journal of Aerosol Science 23(S1), 357-360.

Lapuerta, M., Armas, O., Ballesteros, R., Fernández, J., 2005. Diesel emissions from biofuels derived from Spanish potential vegetable oils. Fuel 84(6), 773-780.

Lapuerta, M., Armas, O., Rodríguez-Fernández, J., 2008. Effect of biodiesel fuels on diesel engine emissions. Progress in Energy and Combustion Science 34(2), 198-223.

Lenzen, M., 1999. Total requirements of energy and greenhouse gases for Australian transport. Transportation Research Part D-Transport and Environment 4(4), 265-290.

Li, J.J., Muralikrishnan, S., Ng, C.T., Yung, L.Y.L., Bay, B.H., 2010. Nanoparticle-induced pulmonary toxicity. Experimental Biology and Medicine 235(9), 1025-1033.

Li, N., Sioutas, C., Cho, A., Schmitz, D., Misra, C., Sempf, J., Wang, M.Y., Oberley, T., Froines, J., Nel, A., 2003. Ultrafine particulate pollutants induce oxidative stress and mitochondrial damage. Environmental Health Perspectives 111(4), 455-460.

Li, N., Venkatesan, M.I., Miguel, A., Kaplan, R., Gujuluva, C., Alam, J., Nel, A., 2000. Induction of heme oxygenase-1 expression in macrophages by diesel exhaust particle chemicals and quinones via the antioxidant-responsive element. Journal of Immunology 165(6), 3393-3401.

Li, N., Wang, M.Y., Oberley, T.D., Sempf, J.M., Nel, A.E., 2002. Comparison of the pro-oxidative and proinflammatory effects of organic diesel exhaust particle chemicals in bronchial epithelial cells and macrophages. Journal of Immunology 169(8), 4531-4541.

Liaquat, A.M., Kalam, M.A., Masjuki, H.H., Jayed, M.H., 2010. Potential emissions reduction in road transport sector using biofuel in developing countries. Atmospheric Environment 44(32), 3869-3877.

Lim, M.C.H., Ayoko, G.A., Morawska, L., Ristovski, Z.D., Jayaratne, E.R., 2007. The effects of fuel characteristics and engine operating conditions on the elemental composition of emissions from heavy duty diesel buses. Fuel 86(12-13), 1831-1839.

Liotta, F.J., Jr., MontaIvo, D.M., 1993. The effect of oxygenated fuels on emissions from a modern heavy-duty diesel engine. Society of Automotive Engineers, SAE Paper No. 932734.

Lu, Z.F., Hao, J.M., Hu, L.H., Takekawa, H., 2008. The compaction of soot particles generated by spark discharge in the propene ozonolysis system. Journal of Aerosol Science 39(10), 897-903.

Lutz, T., Modiyani, R., 2011. Brake thermal efficiency improvements of a commercially based diesel engine modified for operation on JP 8 fuel. Society of Automotive Engineers, SAE Paper No. 2011-01-0120.

Majewski, W.A., 1999. Health effects of gas phase components. Dieselnet Technology Guide, Ecopoint Inc, http://www.dieselnet.com/tech/health_gas.html, last accessed 16th September 2011.

Majewski, W.A., 2007. Diesel emission control. Dieselnet Technology Guide, Ecopoint Inc, http://www.dieselnet.com/tech/engine_control.html, last accessed 16th September 2011.

Majewski, W.A., 2010. Gaseous emissions. Dieselnet Technology Guide, Ecopoint Inc, http://www.dieselnet.com/tech/emi_gas.html, last accessed 16th September 2011.

Majewski, W.A., Jääskeläinen, H., 2008. Emission Formation in Diesel Engines. Dieselnet Technology Guide, Ecopoint Inc, http://www.dieselnet.com/tech/diesel_emiform.html, last accessed 16th September 2011.

Majewski, W.A., Khair, M.K., 2006. Diesel emissions and their control. SAE International, Warrendale, pp. 1-561.

Mareschal, B., Brans, J.P., 1988. Geometrical representations for MCDA European Journal of Operational Research 34(1), 69-77.

Maricq, M.M., 2007. Chemical characterization of particulate emissions from diesel engines: a review. Journal of Aerosol Science 38(11), 1079-1118.

Maricq, M.M., Chase, R.E., Podsiadlik, D.H., Siegl, W.O., Kaiser, E.W., 1998. The effect of dimethoxy methane additive on Diesel vehicle particulate emissions. Society of Automotive Engineers, SAE Paper No. 982572.

Maricq, M.M., Chase, R.E., Podsiadlik, D.H., Vogt, R., 1999. Vehicle exhaust particle size distributions: a comparison of tailpipe and dilution tunnel measurements. Society of Automotive Engineers, SAE Paper No. 1999-01-1461.

Maricq, M.M., Podsiadlik, D.H., Chase, R.E., 2000. Size distributions of motor vehicle exhaust PM: a comparison between ELPI and SMPS measurements. Aerosol Science and Technology 33(3), 239-260.

Mayer, A., Czerwinski, J., Ulrich, A., Wichser, A., Kasper, M., Mooney, J., 2010. Metal-oxide particles in combustion engine exhaust. Society of Automotive Engineers, SAE Paper No. 2010-01-0792.

Mazzoli-Rocha, F., Fernandes, S., Einicker-Lamas, M., Zin, W.A., 2010. Roles of oxidative stress in signaling and inflammation induced by particulate matter. Cell Biology and Toxicology 26(5), 481-498.

McCormick, R.L., 2007. The impact of biodiesel on pollutant emissions and public health. Inhalation Toxicology 19(12), 1033-1039.

McMurry, P.H., 2000a. The history of condensation nucleus counters. Aerosol Science and Technology 33(4), 297-322.

McMurry, P.H., 2000b. A review of atmospheric aerosol measurements. Atmospheric Environment 34(12-14), 1959-1999.

Mejía, J.F., Wraith, D., Mengersen, K., Morawska, L., 2007. Trends in size classified particle number concentration in subtropical Brisbane, Australia, based on a 5 year study. Atmospheric Environment 41(5), 1064-1079.

Meyer, N.K., Ristovski, Z.D., 2007. Ternary nucleation as a mechanism for the production of diesel nanoparticles: experimental analysis of the volatile and hygroscopic properties of diesel exhaust using the volatilization and humifidication tandem differential mobility analyzer. Environmental Science & Technology 41(21), 7309-7314.

Miyamoto, N., Ogawa, H., Nurun, N.M., Obata, K., Arima, T., 1998. Smokeless, low NOx, high thermal efficiency, and low noise diesel combustion with oxygenated agents as main fuel. Society of Automotive Engineers, SAE Paper No. 980506.

Møller, P., Jacobsen, N.R., Folkmann, J.K., Danielsen, P.H., Mikkelsen, L., Hemmingsen, J.G., Vesterdal, L.K., Forchhammer, L., Wallin, H., Loft, S., 2010. Role of oxidative damage in toxicity of particulates. Free Radical Research 44(1), 1-46.

Nel, A., 2005. Air pollution-related illness: effects of particles. Science 308(5723), 804-806.

Nord, K., Haupt, D., Ahlvik, P., Egebäck, K.E., 2004. Particulate emissions from an ethanol fueled heavy-duty diesel engine equipped with EGR, catalyst and DPF, Society of Automotive Engineers, SAE Paper No. 2004-01-1987.

Oberdörster, G., 2001. Pulmonary effects of inhaled ultrafine particles. International Archives of Occupational and Environmental Health 74(1), 1-8.

Oberdörster, G., Oberdörster, E., Oberdörster, J., 2005. Nanotoxicology: an emerging discipline evolving from studies of ultrafine particles. Environmental Health Perspectives 113(7), 823-839.

Oberdörster, G., Sharp, Z., Atudorei, V., Elder, A., Gelein, R., Kreyling, W., Cox, C., 2004. Translocation of inhaled ultrafine particles to the brain. Inhalation Toxicology 16(6-7), 437-445.

Oberdörster, G., Stone, V., Donaldson, K., 2007. Toxicology of nanoparticles: a historical perspective. Nanotoxicology 1(1), 2-25.

Pagels, J., Khalizov, A.F., McMurry, P.H., Zhang, R.Y., 2009. Processing of soot by controlled sulphuric acid and water condensation-mass and mobility relationship. Aerosol Science and Technology 43(7), 629-640.

Pope, C.A., III, Dockery, D.W., 2006. Health effects of fine particulate air pollution: lines that connect. Journal of the Air & Waste Management Association 56(6), 709-742.

Ribeiro, N.M., Pinto, A.C., Quintella, C.M., da Rocha, G.O., Teixeira, L.S.G., Guarieiro, L.L.N., Rangel, M.D.C., Veloso, M.C.C., Rezende, M.J.C., da Cruz, R.S., de Oliveira, A.M., Torres, E.A., de Andrade, J.B., 2007. The role of additives for diesel and diesel blended (ethanol or biodiesel) fuels: a review. Energy & Fuels 21(4), 2433-2445.

Riedl, M., Diaz-Sanchez, D., 2005. Biology of diesel exhaust effects on respiratory function. Journal of Allergy and Clinical Immunology 115(2), 221-228.

Ristovski, Z.D., Jayaratne, E.R., Morawska, L., Ayoko, G.A., Lim, M., 2005. Particle and carbon dioxide emissions from passenger vehicles operating on unleaded petrol and LPG fuel. Science of the Total Environment 345(1-3), 93-98.

Robert Bosch GmbH, 2007. Automotive handbook, 7th edition. John Wiley Inc, Chichester, pp. 1-1192.

Robinson, A.L., Donahue, N.M., Shrivastava, M.K., Weitkamp, E.A., Sage, A.M., Grieshop, A.P., Lane, T.E., Pierce, J.R., Pandis, S.N., 2007. Rethinking organic aerosols: semivolatile emissions and photochemical aging. Science 315(5816), 1259-1262.

Robinson, A.L., Grieshop, A.P., Donahue, N.M., Hunt, S.W., 2010. Updating the conceptual model for fine particle mass emissions from combustion systems. Journal of the Air & Waste Management Association 60(10), 1204-1222.

Ryan, T.W., III., Callahan, T.J., 1996. Homogeneous charge compression ignition of diesel fuel. Society of Automotive Engineers, SAE Paper No. 961160.

Saathoff, H., Naumann, K.H., Schnaiter, M., Schöck, W., Möhler, O., Schurath, U., Weingartner, E., Gysel, M., Baltensperger, U., 2003. Coating of soot and $(NH4)_2SO_4$ particles by ozonolysis products of α-pinene. Journal of Aerosol Science 34(10), 1297-1321.

Şahin, Z., Durgun, O., 2007. Theoretical investigation of effects of light fuel fumigation on diesel engine performance and emissions. Energy Conversion and Management 48(7), 1952-1964.

Sahoo, B.B., Sahoo, N., Saha, U.K., 2009. Effect of engine parameters and type of gaseous fuel on the performance of dual-fuel gas diesel engines-a critical review. Renewable & Sustainable Energy Reviews 13(6-7), 1151-1184.

Sakurai, H., Tobias, H.J., Park, K., Zarling, D., Docherty, K.S., Kittelson, D.B., McMurry, P.H., Ziemann, P.J., 2003. On-line measurements of diesel nanoparticle composition and volatility. Atmospheric Environment 37(9-10), 1199-1210.

Samy, S., Zielinska, B., 2010. Secondary organic aerosol production from modern diesel engine emissions. Atmospheric Chemistry and Physics 10(2), 609-625.

Schaberg, P.W., Zarling, D.D., Waytulonis, R.W., Kittelson, D.B., 2002. Exhaust particle number and size distributions with conventional and Fischer-Tropsch diesel fuels, Society of Automotive Engineers, SAE Paper No. 2002-01-2727.

Schmid, O., Möller, W., Semmler-Behnke, M., Ferron, G.A., Karg, E., Lipka, J., Schulz, H., Kreyling, W.G., Stoeger, T., 2009. Dosimetry and toxicology of inhaled ultrafine particles. Biomarkers 14(S1), 67-73.

Schneider, J., Hock, N., Weimer, S., Borrmann, S., Kirchner, U., Vogt, R., Scheer, V., 2005. Nucleation particles in diesel exhaust: composition inferred from in situ mass spectrometric analysis. Environmental Science & Technology 39(16), 6153-6161.

Schneider, J., Kirchner, U., Borrmann, S., Vogt, R., Scheer, V., 2008. In situ measurements of particle number concentration, chemically resolved size distributions and black carbon content of traffic-related emissions on German motorways, rural roads and in city traffic. Atmospheric Environment 42(18), 4257-4268.

Sehlstedt, M., Forsberg, B., Westerholm, R., Boman, C., Sandström, T., 2007. The role of particle size and chemical composition for health risks of exposure to traffic related aerosols - a review of the current literature.

Seinfeld, J.H., Pandis, S.N., 2006. Atmospheric Chemistry and Physics - From Air Pollution to Climate Change, 2nd Edition. John Wiley & Sons, pp. 1-1225.

Shi, X., Yu, Y., He, H., Shuai, S., Wang, J., Li, R., 2005. Emission characteristics using methyl soyate-ethanol-diesel fuel blends on a diesel engine. Fuel 84(12-13), 1543-1549.

Shiraiwa, M., Kondo, Y., Iwamoto, T., Kita, K., 2010. Amplification of light absorption of black carbon by organic coating. Aerosol Science and Technology 44(1), 46-54.

Slowik, J.G., Stainken, K., Davidovits, P., Williams, L.R., Jayne, J.T., Kolb, C.E., Worsnop, D.R., Rudich, Y., DeCarlo, P.F., Jimenez, J.L., 2004. Particle morphology and density characterization by combined mobility and aerodynamic diameter measurements. Part 2: Application to combustion-generated soot aerosols as a function of fuel equivalence ratio. Aerosol Science and Technology 38(12), 1206-1222.

Society of Automotive Engineers, 1993. Instrumentation and techniques for exhaust gas emissions measurement, SAE standard J254.

Society of Automotive Engineers, 2002. Measurement of carbon dioxide, carbon monoxide, and oxides of nitrogen in diesel exhaust, SAE standard J177.

Sorrell, S., Speirs, J., Bentley, R., Brandt, A., Miller, R., 2010. Global oil depletion: a review of the evidence. Energy Policy 38(9), 5290-5295.

Stone, V., Johnston, H., Clift, M.J.D., 2007. Air pollution, ultrafine and nanoparticle toxicology: Cellular and molecular interactions. IEEE Transactions on Nanobioscience 6(4), 331-340.

Surawski, N.C., Miljevic, B., Roberts, B.A., Modini, R.L., Situ, R., Brown, R.J., Bottle, S.E., Ristovski, Z.D., 2010. Particle emissions, volatility, and toxicity from an ethanol fumigated compression ignition engine. Environmental Science & Technology 44(1), 229-235.

Szybist, J.P., Song, J., Alam, M., Boehman, A.L., 2007. Biodiesel combustion, emissions and emission control. Fuel Processing Technology 88(7), 679-691.

Tobias, H.J., Beving, D.E., Ziemann, P.J., Sakurai, H., Zuk, M., McMurry, P.H., Zarling, D., Waytulonis, R., Kittelson, D.B., 2001. Chemical analysis of diesel engine nanoparticles using a nano-DMA/thermal desorption particle beam mass spectrometer. Environmental Science & Technology 35(11), 2233-2243.

Tousoulis, D., Antoniades, C., Koumallos, N., Stefanadis, C., 2006. Pro-inflammatory cytokines in acute coronary syndromes: from bench to bedside. Cytokine and Growth Factor Reviews 17(4), 225-233.

Turrio-Baldassarri, L., Battistelli, C.L., Conti, L., Crebelli, R., De Berardis, B., Iamiceli, A.L., Gambino, M., Iannaccone, S., 2004. Emisssion comparison of urban bus engine fueled with diesel oil and 'biodiesel' blend. Science of the Total Environment 327(1-3), 147-162.

Tzamkiozis, T., Ntziachristos, L., Mamakos, A., Fontaras, G., Samaras, Z., 2011. Aerodynamic and Mobility Size Distribution Measurements to Reveal Biodiesel Effects on Diesel Exhaust Aerosol. Aerosol Science and Technology 45(5), 587-595.

United States Environmental Protection Agency, 2002. Health assessment document for diesel exhaust, Washington DC, pp. 1-669.

United States Environmental Protection Agency, 2004. Air quality criteria for particulate matter. USEPA, Research Triangle Park, North Carolina, pp. 1-900.

United States Environmental Protection Agency, 2006. Expanding and updating the master list of compounds emitted by mobile sources - phase III, Novato, California, pp. 1-58.

Vaaraslahti, K., Ristimäki, J., Virtanen, A., Keskinen, J., Giechaskiel, B., Solla, A., 2006. Effect of oxidation catalysts on diesel soot particles. Environmental Science & Technology 40(15), 4776-4781.

Valavanidis, A., Fiotakis, K., Vlachogianni, T., 2008. Airborne Particulate Matter and Human Health: Toxicological Assessment and Importance of Size and Composition of Particles for Oxidative Damage and Carcinogenic Mechanisms. Journal of Environmental Science and Health Part C-Environmental Carcinogenesis & Ecotoxicology Reviews 26(4), 339-362.

Venkatachari, P., Hopke, P.K., Brune, W.H., Ren, X.R., Lesher, R., Mao, J.Q., Mitchel, M., 2007. Characterization of wintertime reactive oxygen species concentrations in Flushing, New York. Aerosol Science and Technology 41(2), 97-111.

Venkatachari, P., Hopke, P.K., Grover, B.D., Eatough, D.J., 2005. Measurement of particle-bound reactive oxygen species in Rubidoux aerosols. Journal of Atmospheric Chemistry 50(1), 49-58.

Virtanen, A.K.K., Ristimäki, J.M., Vaaraslahti, K.M., Keskinen, J., 2004. Effect of engine load on diesel soot particles. Environmental Science & Technology 38(9), 2551-2556.

Vojtisek-Lom, M., 2011. Total Diesel Exhaust Particulate Length Measurements Using a Modified Household Smoke Alarm Ionization Chamber. Journal of the Air & Waste Management Association 61(2), 126-134.

Wallington, T.J., Kaiser, E.W., Farrell, J.T., 2006. Automotive fuels and internal combustion engines: a chemical perspective. Chemical Society Reviews 35(4), 335-347.

Wang, J.X., Wu, F.J., Xiao, J.H., Shuai, S.J., 2009. Oxygenated blend design and its effects on reducing diesel particulate emissions. Fuel 88(10), 2037-2045.

Wang, S.C., Flagan, R.C., 1990. Scanning electrical mobility spectrometer Aerosol Science and Technology 13(2), 230-240.

Weiss, U., 2008. Inflammation. Nature 454(7203), 427-427.

White, C.M., Steeper, R.R., Lutz, A.E., 2006. The hydrogen-fueled internal combustion engine: a technical review. International Journal of Hydrogen Energy 31(10), 1292-1305.

Wilt, G.A., 2007. Growth of diesel exhaust particulate matter in a ventilated tunnel mine, College of Engineering and Mineral Resources. West Virginia University, Morgantown, pp. 1-196.

Winston, W.L., 2004. Operations research: applications and algorithms, fourth edition. Brooks/Cole - Thomson Learning, Toronto, pp. 1-1418.

World Health Organization, 2005. WHO air quality guidelines for particulate matter, ozone, nitrogen dioxide and sulfur dioxide: global update 2005, summary of risk assessment. World Health Organization, Geneva, pp. 1-20.

Yao, C.D., Cheung, C.S., Cheng, C.H., Wang, Y.S., 2007. Reduction of smoke and NOx from diesel engines using a diesel/methanol compound combustion system. Energy & Fuels 21(2), 686-691.

Yao, C.D., Cheung, C.S., Cheng, C.H., Wang, Y.S., Chan, T.L., Lee, S.C., 2008. Effect of Diesel/methanol compound combustion on Diesel engine combustion and emissions. Energy Conversion and Management 49(6), 1696-1704.

Yao, M.F., Zheng, Z.L., Liu, H.F., 2009. Progress and recent trends in homogeneous charge compression ignition (HCCI) engines. Progress in Energy and Combustion Science 35(5), 398-437.

Zhan, R., Eakle, S.T., Weber, P., 2010. Simultaneous reduction of PM, HC, CO and NOx emissions from a GDI engine. Society of Automotive Engineers, SAE Paper No. 2010-01-0365.

Zhang, R.Y., Khalizov, A.F., Pagels, J., Zhang, D., Xue, H.X., McMurry, P.H., 2008. Variability in morphology, hygroscopicity, and optical properties of soot aerosols during atmospheric processing. Proceedings of the National Academy of Sciences of the United States of America 105(30), 10291-10296.

Zhang, Z.H., Cheung, C.S., Chan, T.L., Yao, C.D., 2009. Emission reduction from diesel engine using fumigation methanol and diesel oxidation catalyst. Science of the Total Environment 407(15), 4497-4505.

Zhang, Z.H., Cheung, C.S., Chan, T.L., Yao, C.D., 2010a. Experimental investigation of regulated and unregulated emissions from a diesel engine fueled with Euro V diesel fuel and fumigation methanol. Atmospheric Environment 44(8), 1054-1061.

Zhang, Z.H., Cheung, C.S., Chan, T.L., Yao, C.D., 2010b. Experimental investigation on regulated and unregulated emissions of a diesel/methanol compound combustion engine with and without diesel oxidation catalyst. Science of the Total Environment 408(4), 865-872.

Zhang, Z.H., Tsang, K.S., Cheung, C.S., Chan, T.L., Yao, C.D., 2011. Effect of fumigation methanol and ethanol on the gaseous and particulate emissions of a direct-injection diesel engine. Atmospheric Environment 45(11), 2001-2008.

Zhu, L., Cheung, C.S., Zhang, W.G., Huang, Z., 2010. Emissions characteristics of a diesel engine operating on biodiesel and biodiesel blended with ethanol and methanol. Science of the Total Environment 408(4), 914-921.

Zielinska, B., Samy, S., McDonald, J.D., Seagrave, J.C., 2010. Atmospheric transformations of diesel emissions. Health Effects Institute, pp. 5-60.

Chapter 3: Gaseous and particle emissions from an ethanol fumigated compression ignition engine

Nicholas C. Surawski[a,b], Zoran D. Ristovski[a*], Richard J. Brown[b], Rong Situ[b,1]

[a]International Laboratory for Air Quality and Health, Queensland University of Technology, 2 George St, Brisbane QLD 4001, Australia

[b]School of Engineering Systems, Queensland University of Technology, 2 George St, Brisbane QLD 4001, Australia

[1]Current address: School of Engineering and Physical Sciences, James Cook University, Townsville QLD, 4811

Publication: Accepted for publication Energy Conversion and Management, 2011.

Contributor	Statement of contribution
Nicholas C. Surawski Signature Date 21/10/11	Contributed to the ethanol fumigation system set-up, design of the experimental program, conducted the emissions measurements, performed data analysis, and wrote the manuscript.
Zoran D. Ristovski	Contributed to the overall study design, data analysis, and reviewed the manuscript.
Richard J. Brown	Involved with the ethanol fumigation system installation, reviewed the manuscript.
Rong Situ	Assisted with the ethanol fumigation set-up, and experiments.

Principal Supervisor Confirmation

I have sighted email or other correspondence from all Co-authors confirming their certifying authorship.

Associate Professor Zoran Ristovski		21/10/11
Name	**Signature**	**Date**

Abstract

A 4-cylinder Ford 2701C test engine was used in this study to explore the impact of ethanol fumigation on gaseous and particle emission concentrations. The fumigation technique delivered vaporised ethanol into the intake manifold of the engine, using an injector, a pump and pressure regulator, a heat exchanger for vaporising ethanol and a separate fuel tank and lines. Gaseous (Nitric oxide (NO), Carbon monoxide (CO) and hydrocarbons (HC)) and particulate emissions (particle mass ($PM_{2.5}$) and particle number) testing was conducted at intermediate speed (1700 rpm) using 4 load settings with ethanol substitution percentages ranging from 10-40 % (by energy). With ethanol fumigation, NO and $PM_{2.5}$ emissions were reduced, whereas CO and HC emissions increased considerably and particle number emissions increased at most test settings. It was found that ethanol fumigation reduced the excess air factor for the engine and this led to increased emissions of CO and HC, but decreased emissions of NO. $PM_{2.5}$ emissions were reduced with ethanol fumigation, as ethanol has a very low "sooting" tendency. This is due to the higher hydrogen-to-carbon ratio of this fuel, and also because ethanol does not contain aromatics, both of which are known soot precursors. The use of a diesel oxidation catalyst (as an after-treatment device) is recommended to achieve a reduction in the four pollutants that are currently regulated for compression ignition engines. The increase in particle number emissions with ethanol fumigation was due to the formation of volatile (organic) particles; consequently, using a diesel oxidation catalyst will also assist in reducing particle number emissions.

3.1 Introduction

Globally, the transportation sector contributes approximately 26% of greenhouse gas emissions, and due to the growing demand for transport (and hence increased vehicle kilometres travelled), global warming mitigation in this sector is proving difficult (Chapman, 2007). A recent report by the International Energy Agency has highlighted that biofuels could be a key technology in reducing transport related CO_2 emissions by 50 % by 2050 (relative to 2005 emission levels) (International Energy Agency, 2011). To achieve this outcome, biofuels would achieve 27% of the world's transport energy share by 2050, with advanced biofuels, such as ligno-cellulosic ethanol and algal biodiesel, playing a prominent role. As such, a primary motivation for exploring the usage of biofuels in the transportation sector is for energy security reasons (Ahlvik, 2003; Demirbas, 2007). The use of renewable bio-fuels plays a role in energy security issues by reducing dependence on imported petroleum products, which as a non-renewable energy resource, are being depleted rapidly (Demirbas, 2007). Despite this, other factors are having an influence of the uptake of

biofuels such as the need to mitigate global warming, and also to reduce exhaust emissions (Ahlvik, 2003; Agarwal, 2007; Lapuerta et al., 2008b). Of the bio-fuels available, ethanol is one example that is being explored as a substitute for diesel in the transportation sector (Jääskeläinen, 2006).

There are two advantages of ethanol (from an emissions perspective) that have led to it being pursued as a compression ignition (CI) fuel. Firstly, ethanol provides significant full load particle mass emission reductions (Heisey and Lestz, 1981; Abu-Qudais et al., 2000). Jacobson (2002b) showed through simulations that reducing the black-carbon (i.e. soot) emissions from the combustion of petroleum fossil fuels is a very effective strategy for mitigating global warming. Ramanathan et al. (2007) note that fossil fuel combustion is involved in the formation of atmospheric brown clouds, which due to light absorption by primarily carbonaceous aerosol, contribute as much to anthropogenic warming trends as greenhouse gases. A second advantage of ethanol is that it offers significant life-cycle greenhouse gas savings (Beer et al., 2002; Beer and Grant, 2007), especially if waste wood is used as a feedstock for ethanol production. Also, second-generation bio-fuels that are based on renewable, non-agricultural feedstocks do not interfere with food production, unlike some first generation feedstocks (Ahlvik, 2003).

In this study, the test engine was fitted with a fumigation system which delivered ethanol vapor to the intake manifold of the engine using low pressure fuel injectors. The ethanol fumigation approach can be contrasted with the ethanol blending approach, which involves injecting an ethanol-diesel blend through high pressure diesel injectors into the combustion chamber, where it is noted that the ethanol blending approach has received considerable research attention recently (Lapuerta et al., 2008a; Rakopoulos et al., 2008; Di et al., 2009d; Sayin and Canakci, 2009). One advantage of the fumigation approach is that it is capable of delivering more ethanol on an energy basis (~50%) than ethanol blending (~25%) (Ecklund et al., 1984a). The ethanol blending approach is limited by the relativity poor miscibility of ethanol in diesel, which leads to the problem of the two fluid phases separating. To overcome the problem of phase separation, it is common to use an alcoholic co-solvent (such as propanol (Can et al., 2004) or dodecanol (Di et al., 2009d)), or a mixer (Sayin and Canakci, 2009) to improve the stability of the blend. Thus, the amount of energy which can be delivered by the secondary fuel (i.e. ethanol) is a major difference between the ethanol blending and fumigation approaches. An added benefit of the fumigation approach is that

engine operation can be reverted to neat diesel operation (if problems are encountered with ethanol combustion) since separate fuel tanks or systems are used (Ecklund et al., 1984a). This option is not available for the ethanol blending approach, as a dual-fuel blend is injected through a single high pressure fuel injector. The reader is directed to an excellent review paper by Ecklund et al. (1984a) which discusses other technologies enabling the usage of ethanol in compression ignition engines, such as dual-injection, spark assisted compression ignition, the cetane number improvement approach, and emulsions.

A critical factor influencing the uptake of ethanol as a supplementary fuel for compression ignition engines is its performance from an emissions perspective. As a result, this study aims to characterise the performance of an ethanol fumigated compression ignition engine in terms of both its gaseous and particle emissions. A noted advantage of this study is the both the mass and number of particles emitted by the test engine are measured, whereas in previous ethanol fumigation emissions studies, only the mass of particulates emitted by the test engine has been considered (such as Abu-Qudais et al. (2000)). Research from the health effects literature have shown that the respiratory health effects (in particular asthma) from particle emissions correlate better with particle number, rather than particle mass emissions (Peters et al., 1997), which provides a strong motivation to measure the number of particles emitted as has been done in this study. In a related development, the number of particles emitted by compression ignition engines (in addition to a particle mass limit) will be regulated at the Euro VI stage, which demonstrates that considering particle number emissions is set to become more important in vehicle emissions studies (Dieselnet Technology Guide, 2009).

3.2 Methodology

3.2.1 Engine and fuel specifications

The experimental set-up and design used in this study follows very closely the description provided in Surawski et al. (Surawski et al., 2010a). The reader is directed to this paper for a more complete description of the engine, test modes, fuel settings and test protocol, which were identical to those used in the present investigation. In the present study, gaseous and particle number emission factors are presented, whereas more detailed results regarding the particle physical properties (including the issue of particle size distributions) and particle chemistry were presented in Surawski et al. (Surawski et al., 2010a). Particle number emission factors involve the number of particles emitted by the engine per unit of work

delivered by the engine (#/kWh), and are therefore reported on a brake-specific basis as is done for the other pollutants presented in this paper.

In terms of the experimental design used in this study, each load setting involved one ethanol substitution (in addition to the neat diesel test at each load), except for half load operation which employed three ethanol substitutions. The experiments were designed this way as ethanol fumigation is more likely to be implemented under partial loading conditions, rather than at full or light load (Ecklund et al., 1984a). As a result, a more detailed examination of ethanol fumigation at half load is undertaken in this study.

Figure 3.1 provides an illustration of the experimental set-up employed in this study. The ethanol was injected upstream of a heat exchanger that was used to vaporise ethanol, as intake manifolds are not designed to handle two-phase flows. Delivering vaporised ethanol was a critical requirement, since un-vaporised ethanol would lead to an uneven distribution of supplementary fuel to each cylinder – which is not desirable. After the heat exchanger, the injected ethanol passed through a vortex creator (Kruger, 2006), which consists of a number of swirling vanes that create a low pressure core which thoroughly mixes air with supplementary fuel before being inducted into each cylinder. The ethanol fumigation system had its own fuel tank, fuel lines and pump for delivering supplementary fuel to the engine. In this paper, the term "EX" refers to how X% of the total fuel energy was supplied by ethanol. At full and intermediate loads, up to 40% ethanol substitutions (E40) were employed in this study.

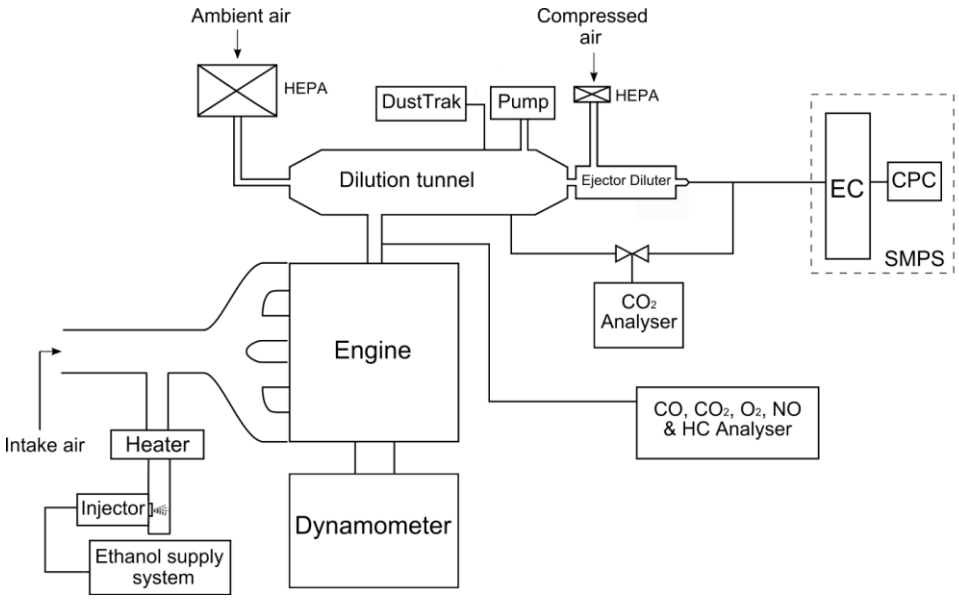

Figure 3.1: Schematic representation of the experimental set-up used in this study.

3.2.2 Emissions measurement methodology

Gaseous emissions were measured with an Andros 6600/6800 Gas Bench. CO_2, NO, CO, HC and O_2 emissions were measured directly from the exhaust, whereas $PM_{2.5}$ emissions were sampled from the dilution tunnel using a TSI 8520 Dust-Trak. An iso-kinetic sampling port was used to sample PM emissions.

Particle number distributions were measured with a Scanning Mobility Particle Sizer (SMPS) consisting of a TSI 3071A classifier, which pre-selects particles within a narrow mobility (and hence size) range, and a TSI 3782 condensation particle counter (CPC) which grows particles (via condensation) to optically detectable sizes. The SMPS software increases the classifier voltage in a pre-determined manner so that particles within a 10-400 nm size range are pre-selected and subsequently counted using the CPC. The software also integrated the particle number distribution to enable calculation of the total number of particles emitted by the engine (on a brake-specific basis) at each test mode.

A two-stage unheated dilution system consisting of a dilution tunnel (first) and an ejector diluter (second) was used to dilute the exhaust gas before particulate size sampling. A 3-way valve was placed on the dilution tunnel to periodically switch the exhaust flow from the tunnel to after the ejector diluter, enabling either the primary or total dilution ratio to be computed. In order to calculate dilution ratios, CO_2 was used as a tracer gas. CO_2 was measured either from the dilution tunnel or after the Dekati diluter (as indicated in Figure 3.1), with dilution ratios being calculated using the following equation:

$$Dilution\ ratio = \frac{CO_{2,Exhaust} - CO_{2,Background}}{CO_{2,Sample} - CO_{2,Background}},$$

where: $CO_{2,Exhaust}$ was measured with an Andros 6600/6800 Gas Bench (± 3% relative error), and $CO_{2,Sample}$ and $CO_{2,Background}$ were measured with a Sable Systems CA-10A Carbon Dioxide Analyser (± 1% relative error). Laboratory background CO_2 measurements were made before the commencement of each test session. Both CO_2 measurements were performed with a sampling frequency of 1 Hz. Velocity and temperature were monitored within the dilution tunnel to ensure that turbulent conditions were achieved, hence enabling particulate matter to be fully mixed before sampling occurred.

For internal combustion engines, the excess air factor (λ) (or relative air-fuel ratio) is defined as the ratio of the actual air-fuel ratio to the stoichiometric air-fuel ratio (Heywood, 1988).

The following chemical equation describes complete combustion for a hydrocarbon and ethanol:

$$C_xH_y + \alpha C_2H_5OH + \beta(O_2 + 3.773N_2) \rightarrow (x + 2\alpha)CO_2 + {}^{1}/_{2}\,(y + 6\alpha)H_2O + 3.773\beta N_2, \quad (3.1)$$

where:

α is the number of moles of ethanol consumed per mole of diesel, and $\beta = \left(\frac{y+4x+12\alpha}{4}\right)$ is a co-efficient that makes (3.1) balance.

From (3.1), the excess air factor for dual-fuel combustion of diesel and ethanol can be calculated via:

$$\lambda = \frac{\left({}^{A}/_{F}\right)_{actual}}{\left({}^{A}/_{F}\right)_{stoichiometric}} = \left({}^{A}/_{F}\right)_{actual}\left(\frac{34.56 \times [y + 4x + 12\alpha]}{\alpha(2 \times 12.011 + 6 \times 1.008 + 16) + 12.011x + 1.008y}\right).$$

3.3 Results and discussion

Engine performance data for the experimental campaign appears in Table 3.1 and includes data on fuel consumption, excess air factors, brake thermal efficiencies, brake mean effective pressures (BMEP) and the count median diameter of the particle emissions for each test.

Table 3.1: Engine performance data for the ethanol fumigation experiments conducted at 1700 rpm.

Engine load BMEP (MPa)	Engine load (%)	Ethanol fumigation percentage (%)	$\dot{m}_{Diesel}$ (kg/h)	$\dot{m}_{Ethanol}$ (kg/h)	Excess air factor (λ)	Brake thermal efficiency (%)	Count median diameter (nm)
0.624	100	0	8.4	0.0	1.36	34.5	83.4
	100	40	5.1	5.2	1.00	34.5	25.8
0.325	50	0	5.0	0.0	2.43	30.4	31.6
	50	10	4.5	0.8	2.23	29.4	34.0
	50	20	4.0	1.5	1.98	29.0	33.8
	50	40	3.0	2.9	1.64	26.2	34.9
0.163	25	0	3.3	0.0	3.78	22.8	29.4

	25	20	2.7	1.0	2.96	18.4	32.3
0.030	Idle	0	2.1	0.0	5.20	6.8	27.0
	Idle	10	1.9	0.3	4.16	7.2	32.8

Figure 3.2 presents brake-specific $PM_{2.5}$ and particle number emissions. The $PM_{2.5}$ data in Figure 3.2 was previously published in (Surawski et al., 2010a), but has been augmented in this study by particle number emission factors. Error bars present in figures denote ± one standard deviation of the data collected for each emissions parameter.

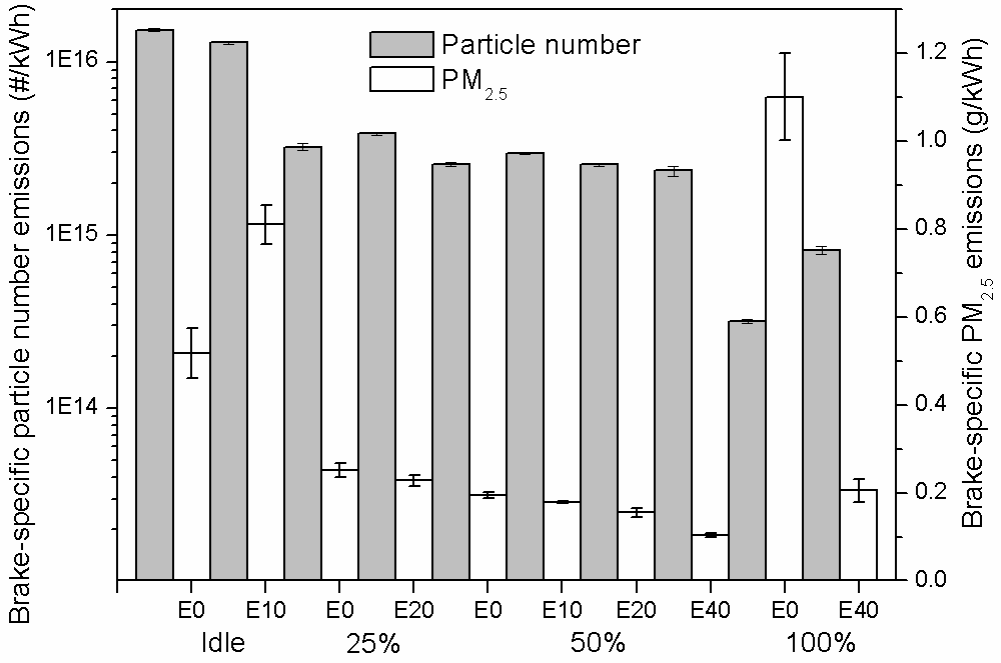

Figure 3.2: Brake-specific $PM_{2.5}$ and particle number emissions at intermediate speed (1700 rpm) with various load settings and ethanol substitutions.

Brake-specific particle mass emissions decreased for all ethanol fumigation substitutions, except for the E10 test at idle mode. The most significant particle mass reductions were evident at full load, where a 40% ethanol substitution provided a five-fold reduction in particle mass. Particle mass reductions at other loads were not as substantial; however, particle mass was reduced by approximately 50% at half load with a 40% ethanol substitution. Slight particle mass reductions were achieved at quarter load (~ 10%), whilst a modest particle mass increase occurred at idle mode (~ 55%). The count median diameter of particles emitted for the E10 idle mode test (see Table 3.1) are about 20% bigger that those for E0 idle. So assuming spherical particles with unit density, and taking into account that fewer particles are emitted for the E10 idle test, a 55% increase in particle mass could be considered reasonable. The particle mass results are in qualitative agreement with Heisey and Lestz (1981) who observed that reductions in particle mass increased with increasing

engine load. Full load particle mass reductions of up to 65% were achieved in the study by Heisey and Lestz (1981) (using a 40% ethanol substitution), whereas Abu-Qudais et al. (2000) reported full load particle mass reductions in the 33-51% range (using a 20% ethanol substitution). Consequently, the particle mass reductions achieved in this study (at full load) were greater than those encountered in other fumigation studies. A possible explanation for this behaviour is that ethanol was passed through a low pressure region in a vortex creator. This meant that the supplementary fuel would have been mixed more thoroughly (compared to other fumigation studies) before entering the cylinder. Since fuel-rich regions are known to produce increased PM emissions (Khair and Jääskeläinen, 2008), a thoroughly mixed charge may have assisted in suppressing the formation of particulate matter.

A number of factors have contributed to the significant particle mass reductions achieved at quarter, half and full load with ethanol fumigation. The first observation is that the fumigant (ethanol) has a very low sooting tendency, as it is free from aromatics and has a much lower carbon-to-hydrogen (C/H) ratio than diesel. Both the aromatics content and the C/H ratio of a fuel are indicators of its sooting tendency (Eastwood, 2008a). The combustion of fumigated ethanol will also produce more OH radicals (Surawski et al., 2010a), which will assist in the oxidation of soot, leading to lower PM emissions (Eastwood, 2008a). Additionally, the secondary fuel introduced via fumigation is pre-mixed and is therefore less likely to form particulates, leaving the fuel-rich diesel spray as the primary source of particle mass emissions. Interestingly, the above mentioned factors contribute to lower particle mass emissions even though combustion is more fuel-rich with ethanol fumigation (see Figure 3.6). Figure 3.2 shows that whilst particle mass reductions were observed with ethanol fumigation (except at idle mode operation), particle number emissions generally increased. At full load, the number of particles emitted by the engine more than doubled, since the E40 fuel setting produced a nucleation mode which formed a large number of nanoparticles with a diameter < 50 nm (see Surawski et al. (2010a) for size distribution information). No such nucleation mode was evident with neat diesel operation at full load. At half load, more particles are emitted for the E10 test but fewer particles were emitted for the E20 and E40 tests. At quarter load, the number of particles emitted increased by about 20% and decreased by 15% at the idle mode. Generally, ethanol fumigation increased the number of particles emitted by the engine. This is a fundamentally different result to that reported by Zhang et al. (2011) who found particle number reductions for E10-E20 fumigation. Unlike the results of Zhang et al., the increase in particle number emissions in this study occurred due to the phenomenon of

homogeneous nucleation (as outlined in Surawski et al. (2010a)), which in an engine's exhaust, is a gas-to-particle conversion process driven by super-saturated volatile (i.e. organic) vapors. A reduction in particle mass emissions can exacerbate the particle number emissions (as has occurred in this study), since instead of volatile vapors condensing on a particle, they are more likely to remain in the gas phase (hence increasing their saturation ratio) and become involved in nucleation. Overall, the particle emissions results show that whilst significant reductions can occur in particle mass, particle number emissions increases can occur, which is not an advantageous result from a human respiratory health perspective.

Ethanol fumigation reduced brake-specific NO emissions at all loads (see Figure 3.3) with reductions ranging from 20% (idle mode) to approximately 70% (half load). Whilst only NO measurements were made in this study and not NOx (NO and NO_2), comparing NO results with NOx results is valid for older engines as their NO_2/NOx ratio is around 5% (Dieselnet Technology Guide, 2010).

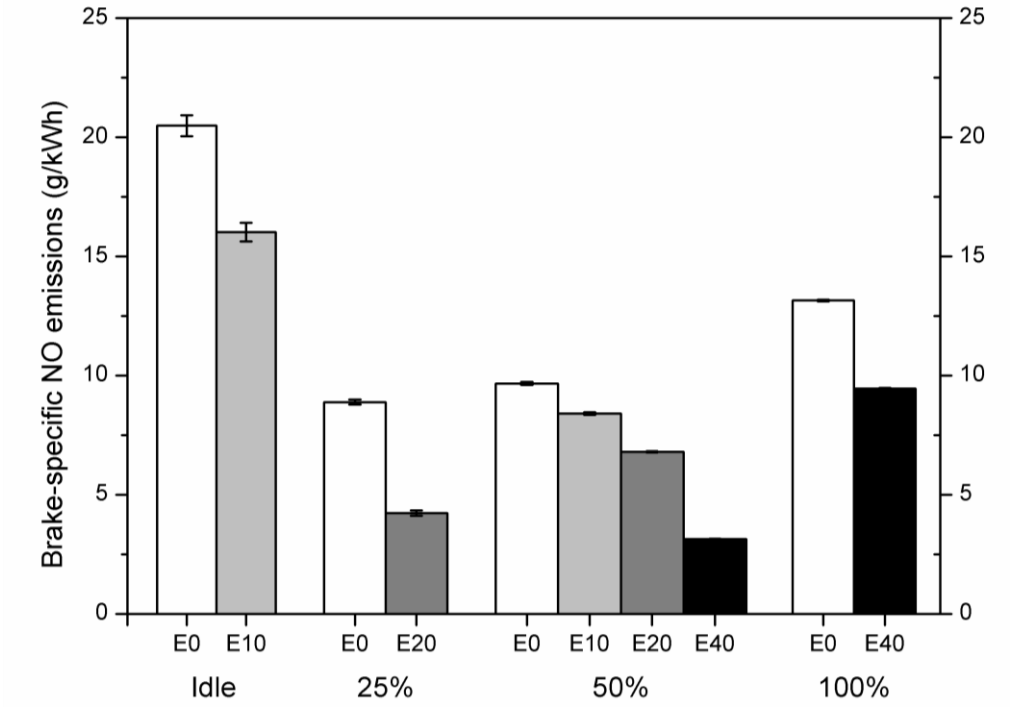

Figure 3.3: Brake-specific NO emissions at intermediate speed (1700 rpm) with various load settings and ethanol substitutions.

The NO reductions exhibited by this engine were generally higher than those reported in other fumigation studies (which report a NOx decrease), although Heisey and Lestz (1981) did report a 50% NOx reduction at 2400 rpm, with a 40% (by energy) ethanol substitution and a 1/3 rack setting . In a rack and pinion system for fuel injection, linear motion of the

rack imparts circular motion to a control sleeve which varies the stroke of the delivery plunger. As a result, varying the rack position is analogous to controlling the load of an engine.

To shed light on the NO results, a discussion of the extended Zeldovich mechanism is required, which consists of the following three chemical equations (Heywood, 1988; Khair and Jääskeläinen, 2008):

$$N_2 + O \rightleftarrows NO + N, \quad (3.2)$$

$$N + O_2 \rightleftarrows NO + O, \quad (3.3)$$

$$N + OH \rightleftarrows NO + H. \quad (3.4)$$

The performance data in Table 3.1 shows that at each load setting, ethanol fumigation reduces the excess air factor, making the combustion more fuel rich. The reduced excess air factor implies that less molecular Oxygen (O_2) and Nitrogen (N_2) is available for combustion in fumigation mode. With a reduction in O_2 and N_2 availability, equations (3.2-3.3) of the Zeldovich mechanism are less likely to proceed, therefore limiting the production of NO. Figure 3.6 shows that the NO emissions at half load operation are correlated quite well with the excess air factor (R^2=0.97).

Brake-specific CO emissions (see Figure 3.4) increased at all loads tested, except idle mode. The thermal efficiency of the engine was slightly higher under idle mode operation with E10, leading to lower CO and HC emissions. A 40% ethanol substitution at half load approximately tripled CO emissions, whereas the same ethanol substitution at full load nearly doubled CO emissions. CO emissions approximately doubled at quarter load, however, only a 20% ethanol substitution was used in this case. Idle mode CO emissions were reduced by about 15% using a 10% ethanol substitution. At half and quarter loads these results were in good agreement qualitatively with Heisey and Lestz (1981), who observed large increases in CO emissions at the 1/3 and 2/3 rack settings at 2400 rpm. These results differ from those of Heisey and Lestz (1981) in that large CO increases (~ 80%) were also observed at full load.

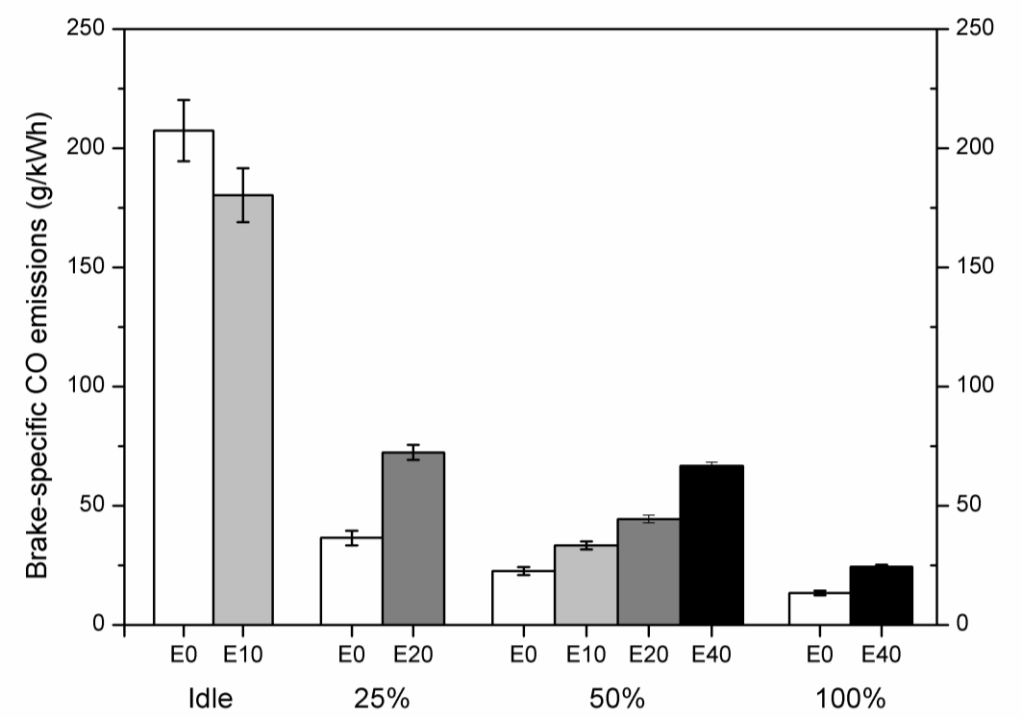

Figure 3.4: Brake-specific CO emissions at intermediate speed (1700 rpm) with various load settings and ethanol substitutions.

Brake-specific HC emissions appear in Figure 3.5. HC emissions increased at all loads, as ethanol fumigation increased, except at idle mode and also for the E20 test at half load. The most significant HC increases were achieved at half load, where a 40% ethanol substitution more than doubled HC emissions. At full load, the same ethanol substitution led to a doubling of HC emissions. Idle mode HC emissions were reduced by approximately 30% using a 10% ethanol substitution, whereas HC emissions increased by about 30% at quarter load using a 20% ethanol substitution. These results are in agreement with Jiang et al. (1990), who reported very significant HC emission increases at full load but more moderate HC increases at lower load.

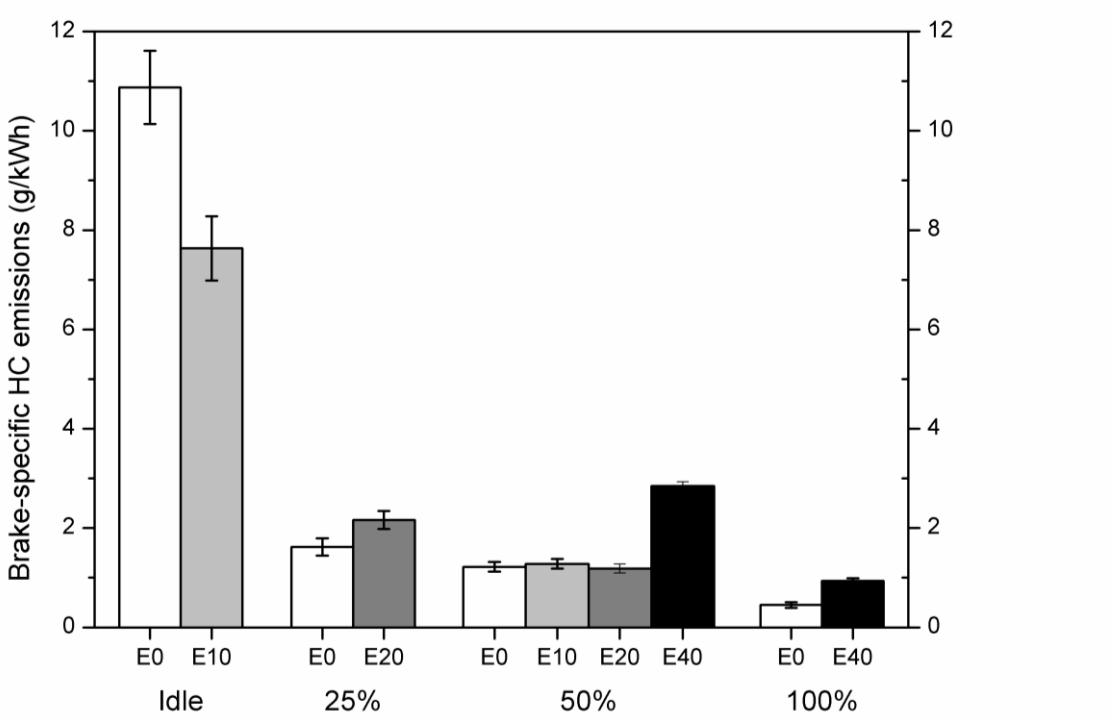

Figure 3.5: Brake-specific HC emissions at intermediate speed (1700 rpm) with various load settings and ethanol substitutions.

The excess air factor (λ) (or its inverse, the equivalence ratio) is an engine parameter that has a strong influence on the composition of diesel exhaust (Chase et al., 2007). To explore this effect, the CO, HC, NO and $PM_{2.5}$ emissions at half load half been plotted versus the excess air factor (see Figure 3.6). With a higher excess air factor, CO and HC should be more readily oxidised to complete combustion products, yielding lower CO and HC emissions (Heywood, 1988). This general trend is evident in the dataset, with CO emissions correlating very well (R^2=0.99) with the excess air factor, but this correlation does not perform as well for HC emissions (R^2=0.54). The difference in the strength of these two correlations suggests that factors other than the excess air factor govern HC emissions, such as flame quenching (Heywood, 1988).

It can be observed that ethanol fumigation leads to rather large increases in both CO and HC emissions. Two main factors contribute to this. Firstly, a reduction in the excess air factor with ethanol fumigation leads to more fuel-rich combustion (see Figure 3.6). Secondly, the fact that supplementary fuel is inducted during the intake stroke, and not delivered to the combustion chamber in a controlled manner (as would be the case if ethanol were injected), can lead to ethanol impinging on the cylinder wall and combustion chamber. This will lead

to incomplete combustion (and consequently increased CO and HC emissions) if the diesel flame is extinguished before reaching the cylinder and combustion chamber wall.

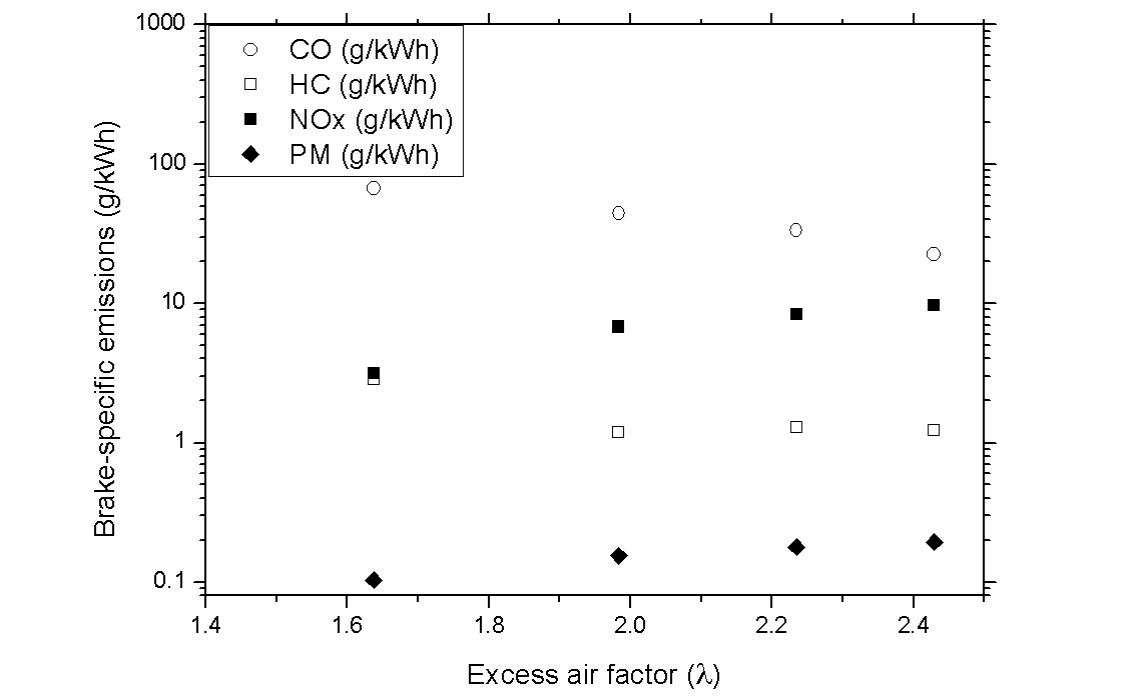

Figure 3.6: Correlation of CO, HC, NO and $PM_{2.5}$ emissions versus excess air factor (λ) at half load operation. Note the logarithmic scale on the ordinate.

As for the other pollutants, a reduction in excess air factor reduces the availability of molecular oxygen (O_2) and nitrogen (N_2) which inhibits the formation of NO in the extended Zeldovich mechanism (R^2=0.97). Even though particulate matter emissions are a by-product of a fuel-rich diesel spray, $PM_{2.5}$ emissions are reduced with a lower excess air factor.

3.4 Conclusions

The results from this investigation showed that $PM_{2.5}$ and NO emissions (two major CI engine pollutants) were significantly reduced by ethanol fumigation. Conversely, HC and CO emissions increased substantially. To achieve a reduction in the four pollutants currently regulated, the use of a diesel oxidation catalyst (as an after-treatment device) should be investigated, as it will assist in oxidising hydrocarbons and CO to complete combustion products. There was an increase in the number of particles emitted at most test modes, and it is quite likely that these particles are primarily volatile (organic) droplets. Therefore, using a diesel oxidation catalyst could also assist in reducing particle number emissions from this test engine in future studies. Alternatively, the amount of ethanol that is fumigated at a particular load may need to be limited by the injection control system.

A noted limitation of the gaseous emission measurements is that only NO results are presented. NO_2 emission increases would be expected with ethanol fumigation, as NO_2 increases with methanol fumigation (Cheng et al., 2008b; Zhang et al., 2010a) and ethanol has similar physico-chemical properties to methanol. There would also be a load dependency for NO_2 emissions, with lower loads producing higher brake-specific NO_2 emissions.

Acknowledgements

We gratefully acknowledge donations of fuel ethanol from Freedom Fuels and Rocky Point Sugar Refinery. The authors thank Alternative Engine Technologies Pty Ltd for providing equipment and software enabling the dual-fuel installation on the test engine. The authors thank the following undergraduate students for dynamometer operation during the two experimental campaigns: Mr Adrian Schmidt, Mr Peter Clark, Mr Yoann Despiau and Mr Steven Herdy. We thank Mr Tony Morris for assisting with the design of the experimental campaigns. We also thank Mr Jonathan James and Mr Glenn Geary for enabling an undergraduate teaching engine to be used for research purposes. Proofreading assistance from Mr Timothy Bodisco is greatly appreciated. This work was undertaken under an Australian Research Council Linkage Grant (LP0775178).

3.5 References

Abu-Qudais, M., Haddad, O., Qudaisat, M., 2000. The effect of alcohol fumigation on diesel engine performance and emissions. Energy Conversion and Management 41(4), 389-399.

Agarwal, A.K., 2007. Biofuels (alcohols and biodiesel) applications as fuels for internal combustion engines. Progress in Energy and Combustion Science 33(3), 233-271.

Ahlvik, P., 2003. Alternative diesel fuels. Dieselnet Technology Guide, Ecopoint Inc, http://www.dieselnet.com/tech/fuel_alt.html, last accessed 16th September 2011.

Beer, T., Grant, T., 2007. Life-cycle analysis of emissions from fuel ethanol and blends in Australian heavy and light vehicles. Journal of Cleaner Production 15(8-9), 833-837.

Beer, T., Grant, T., Williams, D., Watson, H., 2002. Fuel-cycle greenhouse gas emissions from alternative fuels in Australian heavy vehicles. Atmospheric Environment 36(4), 753-763.

Can, Ö., Çelikten, İ., Usta, N., 2004. Effects of ethanol addition on performance and emissions of a turbocharged indirect injection Diesel engine running at different injection pressures. Energy Conversion and Management 45(15-16), 2429-2440.

Chapman, L., 2007. Transport and climate change: a review. Journal of Transport Geography 15(5), 354-367.

Chase, S., Nevin, R., Winsor, R., Baumgard, K., 2007. Stoichiometric compression ignition (SCI) engine. Society of Automotive Engineers SAE Paper No. 2007-01-4224.

Cheng, C.H., Cheung, C.S., Chan, T.L., Lee, S.C., Yao, C.D., Tsang, K.S., 2008. Comparison of emissions of a direct injection diesel engine operating on biodiesel with emulsified and fumigated methanol. Fuel 87(10-11), 1870-1879.

Demirbas, A., 2007. Progress and recent trends in biofuels. Progress in Energy and Combustion Science 33(1), 1-18.

Di, Y.G., Cheung, C.S., Huang, Z.H., 2009. Experimental study on particulate emission of a diesel engine fueled with blended ethanol-dodecanol-diesel. Journal of Aerosol Science 40(2), 101-112.

Dieselnet Technology Guide, 2009. Emissions Standards, European Union, Heavy-Duty Diesel Truck and Bus Engines. Ecopoint Inc, http://www.dieselnet.com/standards/eu/hd.php,last accessed 16th September 2011.

Dieselnet Technology Guide, 2010. Gaseous emissions. Ecopoint Inc, http://www.dieselnet.com/tech/emi_gas.html, last accessed 16th September 2011.

Eastwood, P., 2008. Particulate emissions from vehicles. John Wiley & Sons, Ltd, Chichester.

Ecklund, E., Bechtold, R., Timbario, T., McCallum, P., 1984. State-of-the-art report on the use of alcohols in diesel engines. Society of Automotive Engineers SAE Paper No. 840118.

Heisey, J.B., Lestz, S.S., 1981. Aqueous alcohol fumigation of a single-cylinder DI diesel engine. Society of Automotive Engineers, SAE Paper No. 811208.

Heywood, J.B., 1988. Internal combustion engine fundamentals. McGraw-Hill, Inc, New York, pp. 1-930.

International Energy Agency, 2011. Technology roadmap: biofuels for transport. International Energy Agency, Paris, pp. 1-52.

Jääskeläinen, H., 2006. Ethanol-diesel blends. Dieselnet technology guide, Ecopoint Inc, http://www.dieselnet.com/tech/fuel_ediesel.html, last accessed 16th September 2011.

Jacobson, M.Z., 2002. Control of fossil-fuel particulate black carbon and organic matter, possibly the most effective method of slowing global warming. Journal of Geophysical Research-Atmospheres 107(D19).

Jiang, Q., Ottikkutti, P., VanGerpen, J., VanMeter, D., 1990. The effect of alcohol fumigation on diesel flame temperature and emissions. Society of Automotive Engineers SAE Paper No. 900386.

Khair, M.K., Jääskeläinen, H., 2008. Emission formation in diesel engines. Dieselnet technology guide, Ecopoint Inc, http://www.dieselnet.com/tech/diesel_emiform.html#nox, last accessed 16th September 2011.

Kruger, U., 2006. Compression ignition engines, United States Patent Number 7000573, in: United States Patent Office, pp. 1-9.

Lapuerta, M., Armas, O., Herreros, J.M., 2008a. Emissions from a diesel-bioethanol blend in an automotive diesel engine. Fuel 87(1), 25-31.

Lapuerta, M., Armas, O., Rodríguez-Fernández, J., 2008b. Effect of biodiesel fuels on diesel engine emissions. Progress in Energy and Combustion Science 34(2), 198-223.

Peters, A., Wichmann, H.E., Tuch, T., Heinrich, J., Heyder, J., 1997. Respiratory effects are associated with the number of ultrafine particles. American Journal of Respiratory and Critical Care Medicine 155(4), 1376-1383.

Rakopoulos, D.C., Rakopoulos, C.D., Kakaras, E.C., Giakoumis, E.G., 2008. Effects of ethanol-diesel fuel blends on the performance and exhaust emissions of heavy duty DI diesel engine. Energy Conversion and Management 49(11), 3155-3162.

Ramanathan, V., Ramana, M.V., Roberts, G., Kim, D., Corrigan, C., Chung, C., Winker, D., 2007. Warming trends in Asia amplified by brown cloud solar absorption. Nature 448(7153), 575-579.

Sayin, C., Canakci, M., 2009. Effects of injection timing on the engine performance and exhaust emissions of a dual-fuel diesel engine. Energy Conversion and Management 50(1), 203-213.

Surawski, N.C., Miljevic, B., Roberts, B.A., Modini, R.L., Situ, R., Brown, R.J., Bottle, S.E., Ristovski, Z.D., 2010. Particle emissions, volatility and toxicity from an ethanol fumigated compression ignition engine. Environmental Science & Technology 44(1), 229-235.

Zhang, Z.H., Cheung, C.S., Chan, T.L., Yao, C.D., 2010. Experimental investigation of regulated and unregulated emissions from a diesel engine fueled with Euro V diesel fuel and fumigation methanol. Atmospheric Environment 44(8), 1054-1061.

Zhang, Z.H., Tsang, K.S., Cheung, C.S., Chan, T.L., Yao, C.D., 2011. Effect of fumigation methanol and ethanol on the gaseous and particulate emissions of a direct-injection diesel engine. Atmospheric Environment 45(11), 2001-2008.

Chapter 4: Particle emissions, volatility and toxicity from an ethanol fumigated compression ignition engine

Nicholas C. Surawski[1,2], Branka Miljevic[1], Boyd A. Roberts[1], Robin L. Modini[1], Rong Situ[2], Richard J. Brown[2], Steven E. Bottle[3], Zoran D. Ristovski[1*]

[1]International Laboratory for Air Quality and Health, Queensland University of Technology, GPO Box 2434, Brisbane QLD 4001, Australia

[2]School of Engineering Systems, Queensland University of Technology, GPO Box 2434, Brisbane QLD 4001, Australia

[3]ARC Centre of Excellence for Free Radical Chemistry and Biotechnology, Queensland University of Technology, GPO Box 2434, Brisbane QLD 4001, Australia

Publication: Environmental Science & Technology, 2010, 44(1), 229-235.

Contributor	Statement of contribution
Nicholas C. Surawski Signature Date 21/10/11	Contributed to the ethanol fumigation system set-up, design of the experimental program, conducted particle number size distribution and mass measurements, performed data analysis, wrote most of the manuscript.
Branka Miljevic	Performed the experiments, data analysis, and manuscript writing related to the BPEAnit assay, reviewed manuscript.
Boyd A. Roberts	Performed the V-TDMA measurements and data analysis.

Rong Situ	Assisted with the ethanol fumigation set-up.
Richard J. Brown	Involved with the ethanol fumigation system installation, reviewed the manuscript.
Robin L. Modini	Assisted with the V-TDMA experimental set-up, data analysis and laboratory based calibrations, reviewed the manuscript.
Steven E. Bottle	Reviewed the manuscript.
Zoran D. Ristovski	Contributed to the overall study design, data analysis, and writing of the manuscript

Principal Supervisor Confirmation

I have sighted email or other correspondence from all Co-authors confirming their certifying authorship.

Associate Professor Zoran Ristovski		21/10/11
Name	**Signature**	**Date**

Abstract

Particle emissions, volatility and the concentration of reactive oxygen species (ROS) were investigated for a pre-Euro I compression ignition engine to study the potential health impacts of employing ethanol fumigation technology. Engine testing was performed in two separate experimental campaigns, with most testing performed at intermediate speed with four different load settings and various ethanol substitutions. A Scanning Mobility Particle Sizer (SMPS) was used to determine particle size distributions, a Volatilisation Tandem Differential Mobility Analyser (V-TDMA) was used to explore particle volatility and a new profluorescent nitroxide probe, BPEAnit, was used to investigate the potential toxicity of particles. The greatest particulate mass reduction was achieved with ethanol fumigation at full load, which contributed to the formation of a nucleation mode. Ethanol fumigation increased the volatility of particles by coating the particles with organic material or by making extra organic material available as an external mixture. In addition, the particle related ROS concentrations increased with ethanol fumigation and was associated with the formation of a nucleation mode. The smaller particles, increased volatility and the increase in potential particle toxicity with ethanol fumigation may provide a substantial barrier for the uptake of fumigation technology using ethanol as a supplementary fuel.

4.1 Introduction

The transportation sector is in urgent need of alternative fuels due to the peak-oil scenario and the growing global demand for transport, and the accompanying increase in greenhouse gas emissions (Ahlvik, 2007). Biofuels are being pursued as a replacement for diesel in the transportation sector to facilitate global warming mitigation, to reduce exhaust emissions and also for energy security reasons (Demirbas, 2007; Balat et al., 2008). Ethanol is one example of an oxygenated biofuel that is being explored as a potential replacement for diesel in heavy-duty compression ignition (CI) engines (He et al., 2003a; Nord et al., 2004).

Several ethanol substitution technologies are available for use in CI engines and include the use of ethanol blends, ethanol emulsions, a spark ignition approach, ignition assisting additives, dual injection of diesel and ethanol, and ethanol fumigation (Ecklund et al., 1984b; Abu-Qudais et al., 2000). The ethanol fumigation approach involves delivering ethanol vapour to the intake manifold of an engine (Ecklund et al., 1984b) and complements the existing literature on methanol fumigation (Cheng et al., 2008a; Zhang et al., 2009). Up to 50% of the total fuel energy at full load can be provided through ethanol fumigation, which lies between the energy substitutions achievable by blends (~25%) and dual-injection (~90%)

(Abu-Qudais et al., 2000). The European Union is committed to a 10% substitution (by energy) of transportation fuel by renewable sources by 2020 (Wiesenthal et al., 2009), so it is possible that fumigation technology may play a vital role in achieving this outcome.

A well documented advantage of ethanol usage in CI engines is the significant reduction in particulate mass emissions, especially at full load operation (Abu-Qudais et al., 2000; Di et al., 2009d). Despite this, a reduction in the mass of particulates emitted by an engine may not be the most appropriate metric for assessing the potential health effects of diesel particulate matter. For example, a study by Peters et al. (Peters et al., 1997) showed that respiratory health effects in asthma sufferers were related more strongly to the number of ambient ultrafine particles, rather than to the mass (measured as PM_{10}) of ambient particulates. In light of these observations, the measurement of particle number distributions from ethanol combustion in CI engines is an emerging area of research interest, with several recent papers having been published on this topic (Kim and Choi, 2008; Lapuerta et al., 2008a; Di et al., 2009d; 2009b). This study represents the first attempt to address the issue of particle number distributions from CI engines that employ ethanol fumigation.

Previous research has addressed the issue of regulated emissions from ethanol fumigation (Ecklund et al., 1984b; Abu-Qudais et al., 2000). Little work, however, has focused on the health-related properties of these emissions. Particle related health effects are still not understood entirely, but a widely accepted hypothesis for the many adverse health effects induced by particles is that the particles contain and/or are able to generate reactive oxygen species (ROS) and, thus, induce oxidative stress at the sites of deposition (Dellinger et al., 2001; Li et al., 2003). In addition to the particle-induced generation of ROS, several studies have shown that particles may also contain ROS (Hung and Wang, 2001; Venkatachari et al., 2007). As a result, knowledge of the amount of particulate matter (PM) related ROS would assist in assessing the potential toxicological impact of particle emissions from engines that employ ethanol fumigation technology.

To address the lack of data on the emissions of ROS from CI engines, a novel profluorescent nitroxide probe, BPEAnit, was used to detect and quantify the amount of ROS and free radicals generated from neat diesel and ethanol fumigated particle emissions. BPEAnit is a weakly fluorescent compound, but it exhibits strong fluorescence upon radical trapping or redox activity (Fairfull-Smith and Bottle, 2008). This makes it a powerful optical sensor for

radicals and redox active compounds. The collection of other data involved using a V-TDMA system to explore the volatile properties of particles, along with a Dust-Trak to measure $PM_{2.5}$ emissions.

4.2 Methodology

4.2.1 Engine, fuel and testing specifications

Emissions testing was performed on a pre-Euro I, 4 cylinder, Ford 2701C engine. Studying pre-Euro I engines (from an Australian perspective) continues to have relevance due to the large percentage of the truck fleet (~40 %) that belongs to this emissions class (Australian Bureau of Statistics, 2008). Detailed specifications for the test engine are documented in the supporting information for this paper. The engine was coupled to a Froude hydraulic dynamometer to provide a brake load to the engine. The major components of the dual-fuel system fitted to this engine include an electronically controlled ethanol injector, a pump and pressure regulator, a heat exchanger for vapourising ethanol, and a separate fuel tank and fuel lines. A 1 kW heater positioned downstream of the ethanol injector was required to fully vapourise ethanol for higher ethanol substitutions.

Testing was performed with commercially available 10 ppm sulphur diesel. The ethanol used in testing had a moisture content of 0.55% (by mass) and was denatured with 1% unleaded petrol (by volume) in accordance with the fuel supplier's legal requirements. Two experimental campaigns were conducted. The first was conducted at 2000 rpm, full load, and the second at intermediate speed (1700 rpm) using four different load settings. Table 4.1 documents the speed, load and fuel settings used in both experimental campaigns. Note that "EX" denotes that X% of the total fuel energy was provided by ethanol. Consequently, E0 indicates a test that was conducted with neat diesel.

Table 4.1: Speed, load and fuel settings used for both experimental campaigns.

Campaign number	Speed (rpm)	Load (%)	Fuels used
1	2000	100%	E0, E10.6, E16.3, E22.9
2	1700	100%	E0, E40
2	1700	50%	E0, E10, E20, E40
2	1700	25%	E0, E20
2	1700	Idle	E0, E10

Apart from the different speed settings used, the biggest difference between the two experimental campaigns involved the ability to control ethanol fumigation percentages. Full percentage ethanol substitutions (such as 20%) could not be achieved in the first experimental campaign due to using an oversized injector that could not provide the required flow rate. This problem was rectified in time for the second experimental campaign.

For each load setting, all tests were conducted at the brake load associated with neat diesel operation. Tests were designed this way so that any change in the emissions was due to the change in fuel and not due to the different power output of the engine. Data collection did not commence until the exhaust, cooling water and lubricant temperatures and the gaseous emissions had stabilised. In order to prevent the results from being affected, another test procedure involved flushing the fuel lines of ethanol, and leaving the engine to stabilise for approximately half an hour before further tests were conducted.

4.2.2 Particle measurement methodology

A two-stage, unheated dilution system was used to condition exhaust gas before particulate sampling. The first stage of dilution was performed with a dilution tunnel and the second stage with a Dekati ejector diluter (Dekati, Tampere, Finland). Dilution air was passed through a large HEPA filter to provide particle free air for the primary dilution. Filtered compressed air at 2 bar gauge pressure was fed to the ejector diluter for the second stage of dilution. Particulate mass emissions were measured with a Dust-Trak using a specially designed isokinetic sampling port on the dilution tunnel. CO_2 was used as a tracer gas to calculate dilution ratios.

After the ejector diluter, the aerosol stream was split into three flows for particle size, volatility and ROS measurements. Figure 4.1 displays a schematic of the experimental set-up used in this study. The methodology for each type of measurement is described below.

Particle number distributions were measured with a SMPS consisting of a TSI 3071A Classifier (EC) and a TSI 3782 Condensation Particle Counter (CPC). Particles within a 10-400 nm size range were measured. For the neat diesel tests, 15 SMPS scans were taken and at least 5 scans were taken for tests involving ethanol.

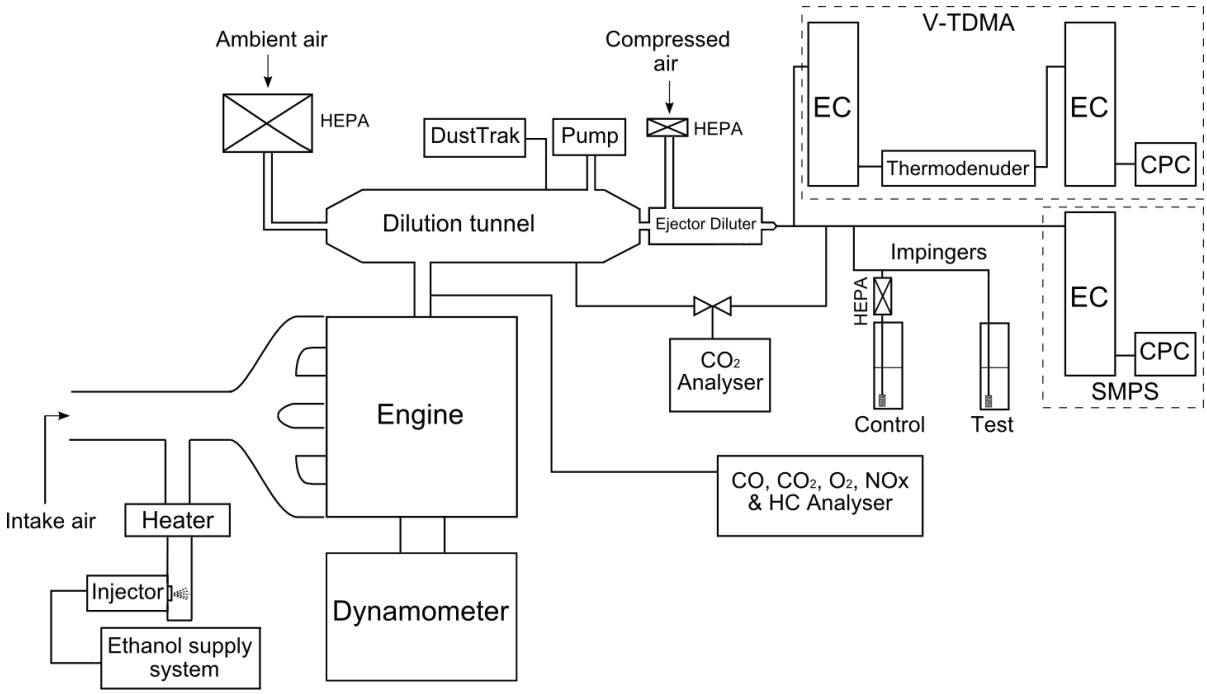

Figure 4.1: Schematic representation of the experimental configuration used in this study.

4.2.3 Particle volatility methodology

A Volatilisation Tandem Differential Mobility Analyser (V-TDMA) was used to investigate the volatility of particles (Johnson et al., 2004; Meyer and Ristovski, 2007). The system is composed of an electrostatic classifier that pre-selects particles of a set size, followed by a thermodenuder that heats the pre-selected particles (see Figure 4.1) to a set temperature. Once particles are heated, the change in particle size is measured with an SMPS. The SMPS consists of an identical classifier to the one that pre-selects the particles and also consists of a TSI 3010 CPC. The temperature difference between the saturator and condenser of the CPC was increased to 21 °C to improve the particle detection efficiency down to 8 nm. The thermodenuder temperature was increased in discrete steps and the change in the particle diameter was recorded as the volatile components evaporated.

Accumulation mode particles with a diameter of 80 nm were pre-selected for V-TDMA analysis. Pre-selecting this particle size was based on the mode of the neat diesel particle size distribution as derived by the SMPS system at full load. Scan times of 90 seconds were chosen for the SMPS system downstream of the thermodenuder and measured particles within an 8-109.1 nm size range. The thermodenuder was set up to scan temperatures in an approximate range of 30 to 320 ^{o}C, with temperature increments of 25 to 30 ^{o}C between scans. All testing with the V-TDMA system was performed at intermediate speed. The thermodenuder temperatures were calibrated in the laboratory after testing.

Particle volatilisation is presented through the volume fraction remaining (VFR),

$VFR = (D_v/D_{v0})^3$, where D_{v0} is the particle diameter before heating, and D_v is the particle diameter after heating in the thermodenuder to a temperature T_d. The dependence of the VFR on thermodenuder temperature provides a volatility signature for particles that enables basic hypotheses regarding the chemical composition and formation mechanisms of particles to be tested. For example, using a V-TDMA system, Sakurai et al. (Sakurai et al., 2003) demonstrated that diesel nanoparticles had a volatility signature consistent with heavy hydrocarbons (C24-C32) that are prominent constituents of lubricating oil.

In diesel particles, it is common to observe particles of the same size but significantly different composition and therefore volatility (Sakurai et al., 2003). Particles such as this are known as external mixtures. As a measure of external mixing, we have quantified the percentage of volatile particles (PVP) according to the following equation:

$$PVP\ (\%) = 100\left(\frac{N_{PRE-VOLATILISATION} - N_{POST-VOLATILISATION}}{N_{PRE-VOLATILISATION}}\right), \quad (4.1)$$

where:

$N_{PRE-VOLATILISATION}$ is the total particle concentration measured by the V-TDMA before the thermodenuder temperature is increased, and $N_{POST-VOLATILISATION}$ is the total concentration of the non-volatile peak at the highest temperature applied by the thermodenuder.

4.2.4 ROS concentration measurement – BPEAnit assay

Samples were collected by bubbling aerosol for 15 to 20 minutes through an impinger containing 20 mL of 4 µM BPEAnit solution, after which fluorescence was measured. Impingers were placed after the two-stage dilution system. For each fuel type and test mode, fluorescence measurements from both the test sample and a HEPA filtered control sample were measured.

The new profluorescent nitroxide probe BPEAnit and its methyl adduct (BPEAnit-Me), which was used for the calibration curve, were synthesised in our laboratory. The details of the synthesis are presented in Fairfull-Smith and Bottle (Fairfull-Smith and Bottle, 2008) and details of the evaluation of the probe for applications in particle bound ROS quantification are presented in Miljevic et al. (Miljevic et al., 2009a). The solvent used in all experiments was AR grade dimethyl sulfoxide (DMSO). Impingers used in this study were custom made and consisted of a Quickfit Dreschel bottle head, they were sintered (porosity grade 1: pore

size of 100-160 µm) and were modified to fit a Quickfit 75 mL test tube (Barloworld Scientific, Staffordshire, UK).

Fluorescence spectra were recorded using a USB2000 fibre-optic spectrometer combined with a cuvette holder and a pulsed Xenon lamp (both Ocean Optics, Dunedin FL, USA) which used a narrow bandpass filter at 430 nm (Edmund Optics, Barrington, NJ, USA). In all of the fluorescence measurements a 10 mm quartz cuvette (Starna Pty Ltd, Hainault, UK) was used.

In order to conduct quantitative chemical analysis on the particles collected by the impingers, it was important to know the collection efficiency of the impinger. This was determined as described in Miljevic et al. (Miljevic et al., 2009b).

The amount of BPEAnit that reacted when exposed to engine exhaust was calculated from a standard curve obtained by plotting known concentrations of methyl adduct of BPEAnit (BPEAnit-Me; fluorescent) against fluorescence intensity at 485 nm. Based on the difference in the fluorescence signal between the test and the control sample, the amount of ROS for each test mode was calculated and normalised to the PM mass calculated from the SMPS data. The portion of particles remaining in the impinger upon bubbling was calculated by multiplying the size distribution by the impinger collection efficiency curve.

4.3 Results

4.3.1 Particle size distributions

Full load size distribution data from the SMPS is shown for the neat diesel (E0) and E40 test in Figure 4.2. Full load size distributions are shown since a clear difference was exhibited for the E0 and E40 tests. Size distributions, at all other loads, for the neat diesel and ethanol tests were quite similar, since nucleation occurred in each size distribution.

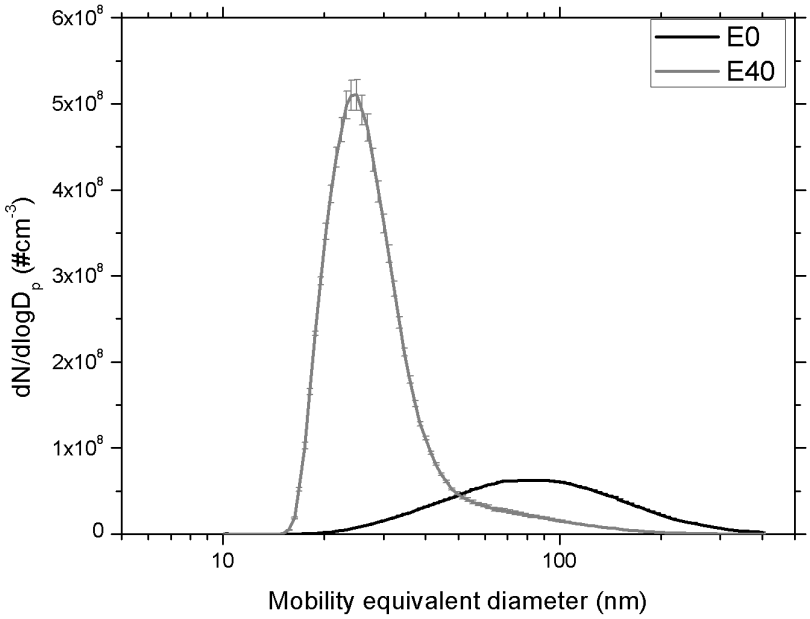

Figure 4.2: SMPS derived particle number distributions at intermediate speed (1700 rpm), full load, for neat diesel (E0) and 40% ethanol (E40) engine operation. Error bars denote ± one standard error.

The mode for the diesel size distribution was about 90 nm, which was in very good agreement with that expected for diesel particulate matter (Harris and Maricq, 2001). A 40% ethanol substitution (on an energy basis) markedly changed the neat diesel size distribution. The ethanol size distribution had a large peak in the nucleation mode, and it also had a reduced particle mode diameter and reduced accumulation mode particle concentrations.

A correlation between particle size and ethanol substitution is shown in Figure 4.3, for tests conducted in the first experimental campaign at 2000 rpm, full load. The count median diameter (CMD) of the SMPS-derived particle size distribution was used as a metric for the size of particles. Relative to the neat diesel case (E0), the E22.9 test reduced the CMD by approximately 20%, from 81 nm to 63 nm. It can be seen that the CMD is anti-correlated with the ethanol substitution percentage (r=-0.939), where r is the Pearson correlation co-efficient.

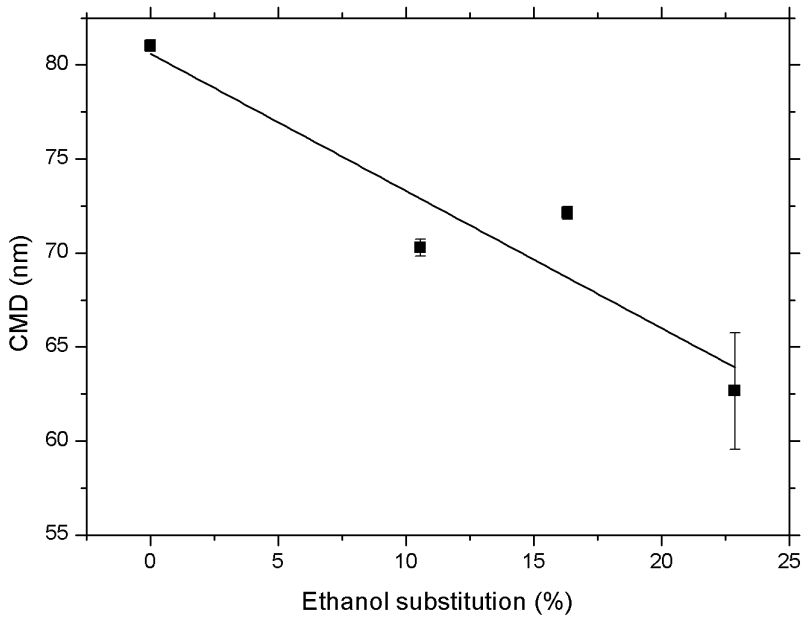

Figure 4.3: Correlation of particle size (CMD) with the ethanol substitution percentage for tests conducted at 2000 rpm, full load (r=-0.939). Error bars denote ± one standard error.

Brake-specific particulate matter ($PM_{2.5}$) emissions, for tests conducted at intermediate speed (1700 rpm) and various loads settings during the second experimental campaign, are shown in Figure 4.4. In general, the addition of ethanol significantly reduced PM emissions, especially at full load operation during the E40 test. The results at idle mode were not consistent with the general trend, since E10 led to an increase in PM emissions, relative to E0. No explanation can be provided for this result. Full-load PM reductions from ethanol were significantly greater than those observed at half or quarter load.

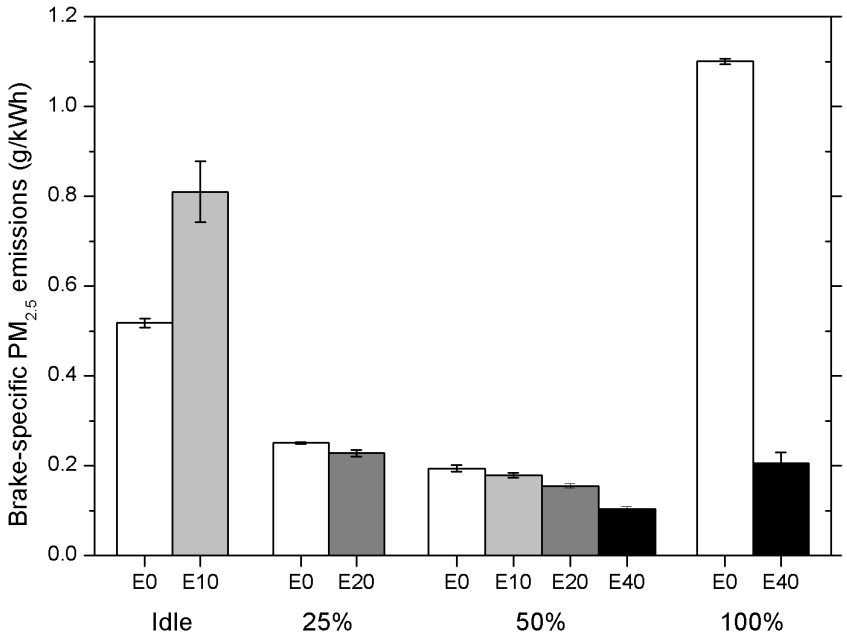

Figure 4.4: Brake-specific $PM_{2.5}$ emissions at intermediate speed (1700 rpm) with various load settings and ethanol substitutions. Error bars denote ± one standard error.

4.3.2 Particle volatility

The volume fraction remaining (VFR) curves are displayed in Figure 4.5a and 4.5b. It can be observed that for neat diesel at full load (Figure 4.5a), heating the particles results in a very small reduction in particle volume, whilst for the E40 test at the same load there was a significant reduction in particle volume. For loads other than full load, heating of particles introduces a second, far more volatile peak in the size distributions. This more volatile peak separates from the initial distribution of particles pre-selected for V-TDMA analysis, and consequently has to be analysed separately to the less volatile peak for volatilisation information (see Figure 4.5b). Further, it should be noted that significant volatilisation occurred between 50 and 100 ^{o}C, suggesting the presence of fuel or lubricating oil derived organic material (Sakurai et al., 2003; Meyer and Ristovski, 2007). Size distribution information for the V-TDMA scans can be found in the Supporting Information of this paper.

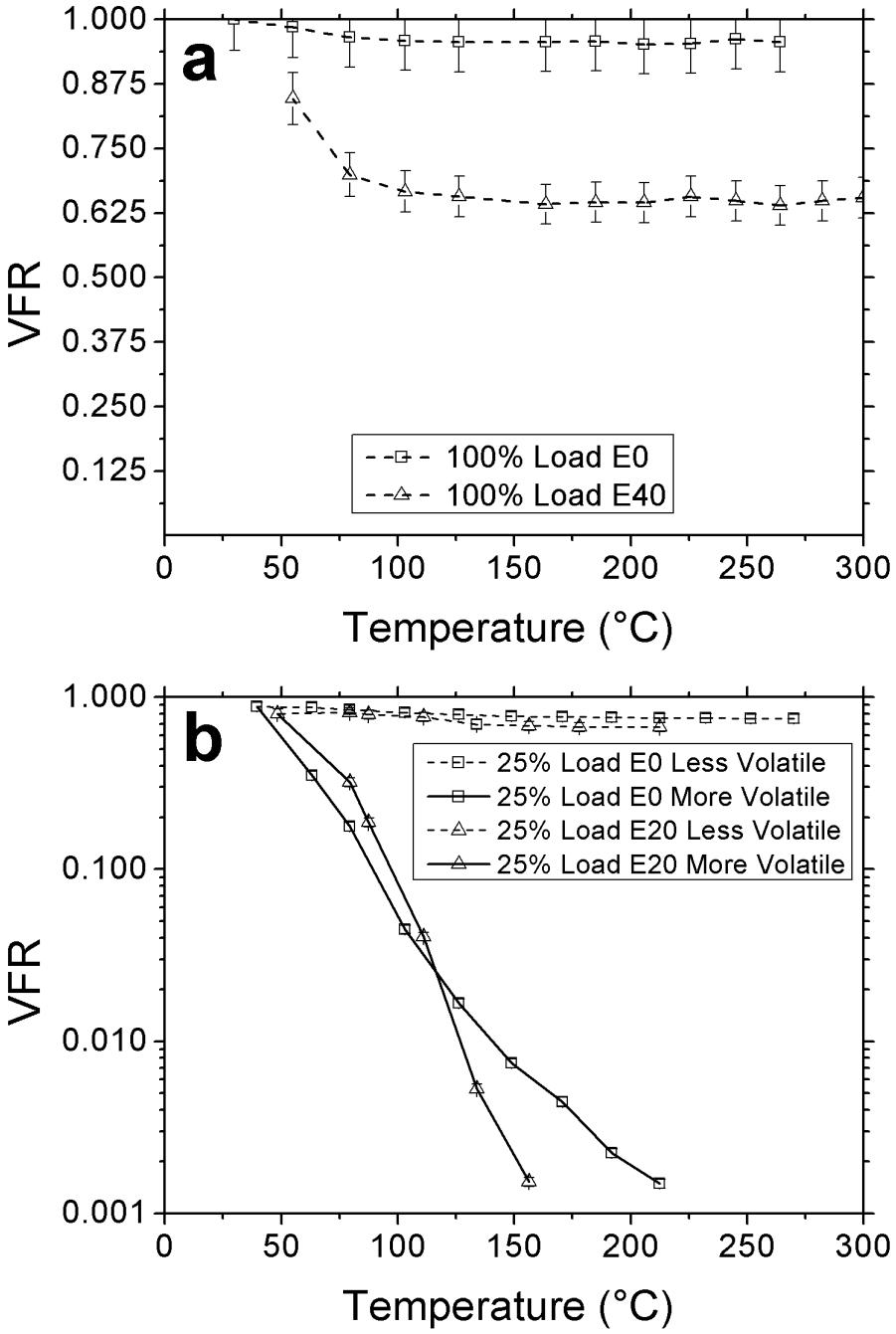

Figure 4.5: Volume fraction remaining (VFR) versus thermodenuder temperature at intermediate speed (1700 rpm). (a) 100% load E0 and E40. (b) 25% load E0 and E20. Note well the linear scale on the ordinate for (a) and the logarithmic scale on the ordinate for (b). Error bars are calculated using the uncertainties in the diameter measurement.

The volatility results require external and internal mixtures to be defined. An external mixture in automotive exhaust entails carbon and other aerosol particles (such as volatile droplets) existing as distinct, or separate, particles. Alternatively, internally mixed particles have the various components incorporated together and could consist of a carbon core coated

with other aerosol particles (Jacobson, 2001). The level of external mixture can be presented through the percentage of volatile particles (PVP). Figure 4.6 presents the PVP as a function of ethanol substitution for three load conditions, namely: idle, 25% and 50% load. The PVP at full load is not shown as the particles were not externally mixed and consequently the PVP was zero. For all three loads, an increase in the percentage of volatile particles was observed with ethanol. For the half load case, where several ethanol substitutions were measured, a clear increasing trend in PVP can be observed with higher ethanol substitutions. The volume fraction of organic material coating the non-volatile particles increased with increasing ethanol substitutions at all loads, with results appearing in the Supporting Information of this paper (see Figure S 4.2).

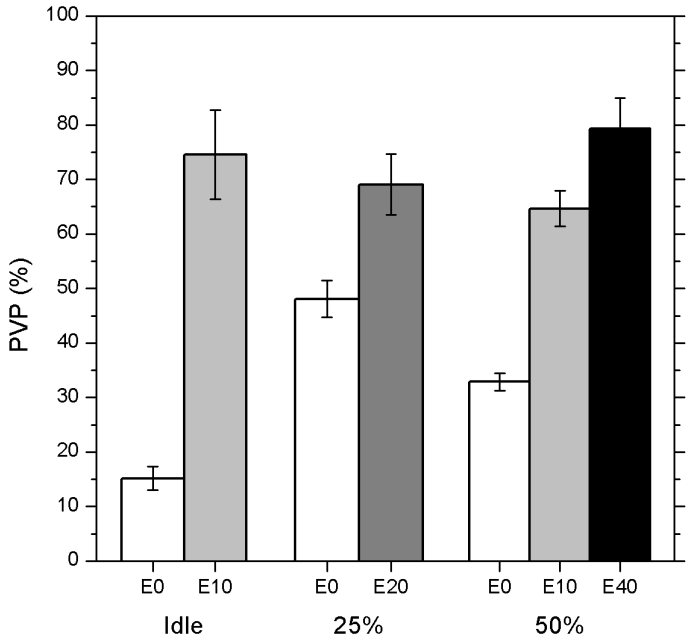

Figure 4.6: Percentage of volatile particles at intermediate speed (1700 rpm) and 50%, 25% load and idle mode for various ethanol substitutions. Error bars have been calculated using the statistical uncertainty in the counts ($\boldsymbol{\sigma = 1/\sqrt{n}}$).

4.3.3 ROS concentration results

Figure 4.7 shows fluorescence emissions for the BPEAnit solution when exposed to diesel exhaust, and also for the HEPA-filtered control samples, at intermediate speed (1700 rpm) and full load for the neat diesel (E0) and 40% ethanol (E40) tests. There was an increase in the fluorescence signal for BPEAnit when exposed to the engines exhaust, with the fluorescence signal for E40 being significantly higher than for E0. An increase in fluorescence for the HEPA-filtered control samples (grey curves in Figure 4.7) is due to gaseous reactive species, whereas the fluorescence of test samples (black curves in Figure

4.7) represents the response due to aerosol being bubbled through the impinger. The difference between the black and the grey curves is, therefore, the fluorescence induced by particles. A small increase in fluorescence was observed for PM emissions from neat diesel testing. On the contrary, PM emissions from the E40 test led to a 4.5-fold increase in fluorescence, relative to the neat diesel case.

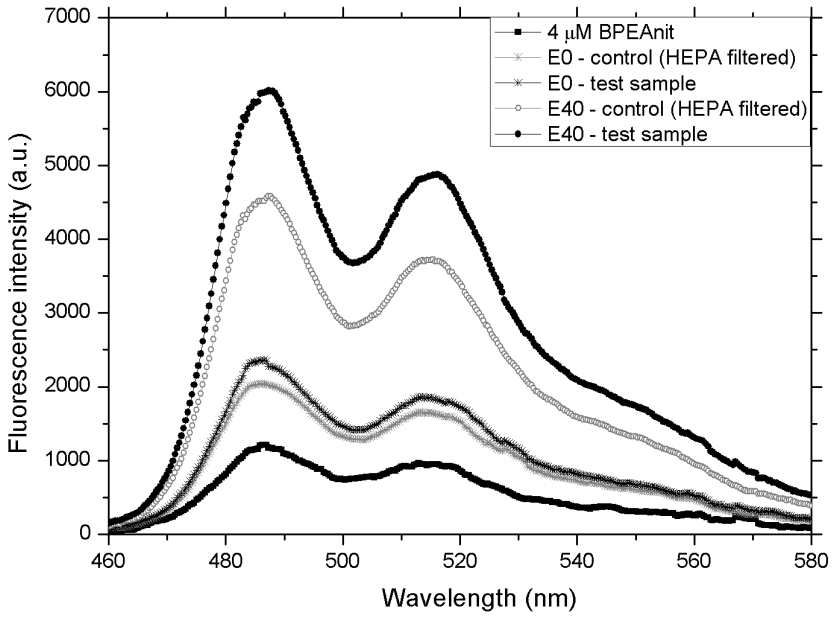

Figure 4.7: Fluorescence spectra of BPEAnit control (HEPA filtered) and test samples for neat diesel (E0) and 40% ethanol (E40) at intermediate speed (1700 rpm) and full load.

Normalisation of the amount of BPEAnit being converted to fluorescent product, with respect to the PM mass, represents a measure of ROS concentration. Figure 4.8 displays ROS concentrations calculated for PM emissions at intermediate speed with various load settings and ethanol substitutions. ROS concentrations for neat diesel emissions at 0% (idle), 25%, 50% and 100% load show a significant increase with decreasing engine load. ROS concentrations for 10%, 20% and 40% ethanol tend to exhibit the same increasing trend as the load is decreased, similar to the neat diesel emissions. At a particular load setting, the ROS concentrations for the E10 and E20 tests, relative to E0, do not differ by any more than 20%. At half load, however, the E40 test resulted in approximately double the ROS concentration relative to E0, and for full load, the E40 test resulted in a ROS concentration almost 40 times higher than for neat diesel.

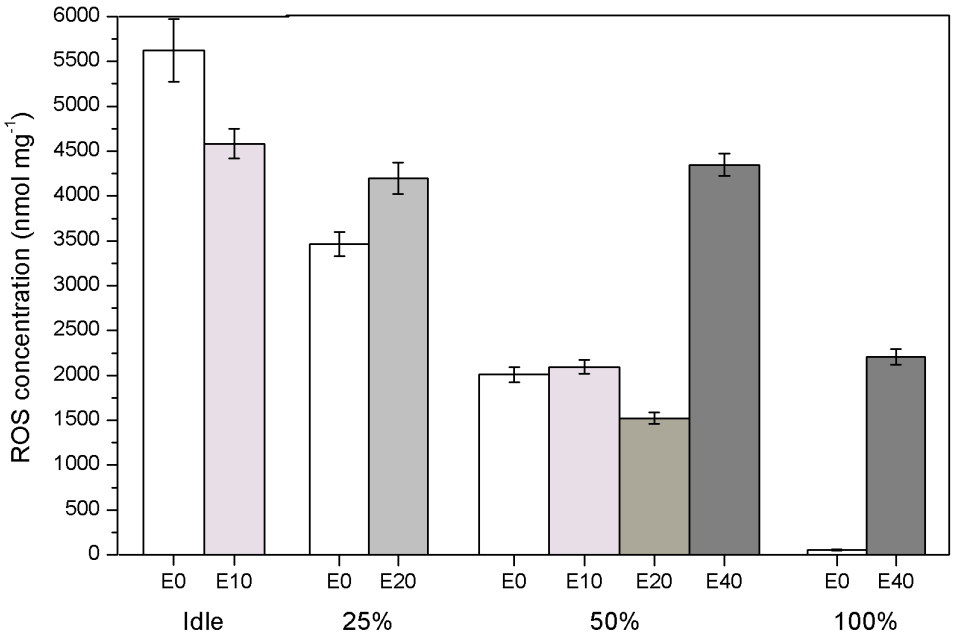

Figure 4.8: ROS concentrations at intermediate speed (1700 rpm) with various load settings and ethanol substitutions. Error bars denote ± one standard error.

4.4 Discussion

Several recent papers have addressed the issue of particle number distributions emanating from CI engines using the ethanol blending approach (Kim and Choi, 2008; Lapuerta et al., 2008a; Di et al., 2009d; 2009b). Although measurements were taken at different speeds, and different loads and ethanol blend percentages, a common feature of the work of Di et al. (Di et al., 2009d; 2009b) and Lapuerta et al. (Lapuerta et al., 2008a) is that ethanol reduces the peak particle concentration and shifts the CMD of the size distribution to a smaller particle diameter. As a result, ethanol blending technology produces a higher percentage of particles that reside in the ultrafine (<100 nm) size range, but the overall number concentration with ethanol blends is lower relative to the neat diesel case. Using fumigation technology, the result presented in this study (see Figure 4.2) is different. The reduction in particle concentration in the accumulation mode (>50 nm) is still evident, but the concentration in the nucleation mode (<50 nm) is higher by a factor of approximately 8.

The mechanism responsible for nucleation in this case appears to be consistent with a theory developed by Kittelson et al. (Kittelson et al., 2002a). The accumulation mode is very effective at absorbing organic material, due to the large surface area available. With the high ethanol substitutions achieved with fumigation, the accumulation mode surface area is reduced to a level such that organic material has very little particle surface area upon which

to condense. So instead of the accumulation mode acting as a "sponge", absorbing organic material and hence reducing its vapour pressure, the organic material resides in the vapour phase with an increased vapour concentration. Under conditions where the vapour pressure of a nucleating species is high and exhaust gas dilution cools the organic material, thereby decreasing its saturation vapour pressure, the saturation ratio of organic material is significantly increased and nucleation can occur instead (Kittelson et al., 2002a). In this case, nucleation occurred solely due to the change in fuel and was not related to some artefact of the dilution process, such as having different dilution ratios or tunnel temperatures during each test. This study provides the first experimental evidence that high ethanol substitutions are capable of inducing nucleation in particle size distributions, in addition to decreasing the concentration of particles in the accumulation mode.

Results from the V-TDMA analysis suggest the presence of an organic substance, either derived from fuel or lubricating oil, which coats particles and potentially leaves a sufficient concentration in the vapour phase for nucleation to occur. The amount of volatile material available for nucleation is proportional to the percentage of volatile particles (PVP) and increases with ethanol substitution (see Figure 4.6). Ethanol fumigation increased the volatility of particulates, either through coating particles with volatile, organic material or through making organic material available for nucleation to occur, producing an external mixture of purely volatile and partially volatile particles.

Ethanol fumigation increased the particle related ROS concentration, especially at full load operation, although the ROS concentration was reduced at idle mode operation with E10. The lowest ROS concentration occurred with the full load E0 test, which was the only size distribution measured which did not exhibit a nucleation mode. For all the other tests (involving a nucleation mode), at least a 30 fold increase in ROS emissions occurred, relative to the E40 full load test. Therefore, significantly higher ROS concentrations are associated with the formation of nucleation mode particles. An explanation for the mechanism governing the formation of ROS due to ethanol fumigation and its relationship to the formation of a nucleation mode is not possible with the data collected in this study; therefore, further investigation is recommended. The significant increase in potential particle toxicity with ethanol fumigation may provide a substantial barrier for the uptake of fumigation technology using ethanol as a supplementary fuel. Other supplementary fuels should be investigated with fumigation technology to explore the potential toxicological impacts.

The reduction in particle size was also strongly anti-correlated with the percentage of ethanol fumigated (see Figure 4.3). A possible mechanism for this observation is the oxidation of particulate matter by OH radicals. It has been suggested that OH radicals are much more effective at oxidising the soot surface than other oxidants such as O_2 (Xu et al., 2003), which are decreased by ethanol fumigation (see calculation in the Supporting Information for this paper) since the intake air is being replaced by fumigated mixture. At temperatures relevant for combustion (1200-2200 K), Daly and Nag (Daly and Nag, 2001) showed through kinetic modelling that the peak concentration of OH radicals during combustion were approximately doubled for a 10% ethanol blend. The concentration of OH radicals tends to peak at the onset of soot depletion (Hasse et al., 2000); therefore, ethanol combustion potentially involves more available oxidant to attack the particle surface and hence reduce its size. An increase in OH radicals with increasing ethanol fumigation percentages is also confirmed by an AVL Boost simulation conducted as part of this study. The Boost program solves the one-dimensional Euler equations for in-viscid, compressible flow and is coupled to a zero-dimensional combustion model. A detailed chemistry module is available in the program for performing emissions simulations (AVL LIST GmbH, 2008b). Results for this simulation appear in the Supporting Information for this paper.

A modelling study conducted by Benvenutti et al. (*27*) demonstrated that the methyl radical (CH_3) is an important precursor for the formation of excited species such as OH radicals. That fact that the nitroxide probe traps radicals and that, in general, radical concentrations were greater with ethanol fumigation, suggests that ethanol combustion provides a pathway capable of significant CH_3, and subsequently, OH radical production. This could also be one of the reasons for a significant increase in the ROS concentration observed with ethanol substitution.

A detailed characterisation of particle emission properties has been undertaken for a pre-Euro I engine without after-treatment. Newer engine technologies, with after-treatment devices, should be investigated to ascertain if the same qualitative trends are evident.

Acknowledgements

The authors wish to thank Alternative Engines Technologies Pty Ltd for providing equipment and software enabling the dual fuel installation on the test engine to take place. Proof reading assistance from Mr Timothy Bodisco was greatly appreciated. This work was undertaken under an Australian Research Council Linkage Grant (LP0775178).

Supporting Information Available

The supporting information includes one table and four figures that augment the results presented in the manuscript. This information is available free of charge via the Internet at http://pubs.acs.org/

4.5 References

Abu-Qudais, M., Haddad, O., Qudaisat, M., 2000. The effect of alcohol fumigation on diesel engine performance and emissions. Energy Conversion and Management 41(4), 389-399.

Ahlvik, P., 2007. Alternative diesel fuels. Dieselnet Technology Guide, Ecopoint Inc, http://www.dieselnet.com/tech/fuel_alt.html, last accessed 16th September 2011.

Australian Bureau of Statistics, 2008. Motor vehicle census, pp. 1-28.

AVL LIST GmbH, 2008. AVL Boost, Version 5.1, Users Guide, Graz, Austria.

Balat, M., Balat, H., Öz, C., 2008. Progress in bioethanol processing. Progress in Energy and Combustion Science 34(5), 551-573.

Cheng, C.H., Cheung, C.S., Chan, T.L., Lee, S.C., Yao, C.D., 2008. Experimental investigation on the performance, gaseous and particulate emissions of a methanol fumigated diesel engine. Science of the Total Environment 389(1), 115-124.

Daly, D.T., Nag, P., 2001. Combustion modeling of soot reduction in Diesel and Alternate Fuels using Chemkin. Society of Automotive Engineers SAE Paper No. 2001-01-1239.

Dellinger, B., Pryor, W.A., Cueto, R., Squadrito, G.L., Hegde, V., Deutsch, W.A., 2001. Role of free radicals in the toxicity of airborne fine particulate matter. Chemical Research in Toxicology 14(10), 1371-1377.

Demirbas, A., 2007. Progress and recent trends in biofuels. Progress in Energy and Combustion Science 33(1), 1-18.

Di, Y.G., Cheung, C.S., Huang, Z.H., 2009a. Comparison of the Effect of Biodiesel-Diesel and Ethanol-Diesel on the Particulate Emissions of a Direct Injection Diesel Engine. Aerosol Science and Technology 43(5), 455-465.

Di, Y.G., Cheung, C.S., Huang, Z.H., 2009b. Experimental study on particulate emission of a diesel engine fueled with blended ethanol-dodecanol-diesel. Journal of Aerosol Science 40(2), 101-112.

Ecklund, E.E., Bechtold, R.L., Timbario, T.J., McCallum, P.W., 1984. State-of-the-art report on the use of alcohols in diesel engines. Society of Automotive Engineers SAE Paper No. 840118.

Fairfull-Smith, K.E., Bottle, S.E., 2008. The Synthesis and Physical Properties of Novel Polyaromatic Profluorescent Isoindoline Nitroxide Probes. European Journal of Organic Chemistry32), 5391-5400.

Harris, S.J., Maricq, M.M., 2001. Signature size distributions for diesel and gasoline engine exhaust particulate matter. Journal of Aerosol Science 32(6), 749-764.

Hasse, C., Bikas, G., Peters, N., 2000. Modeling DI-diesel combustion using the eulerian particle flamelet model (EPFM). Society of Automotive Engineers SAE Paper No. 2000-01-2934.

He, B.Q., Shuai, S.J., Wang, J.X., He, H., 2003. The effect of ethanol blended diesel fuels on emissions from a diesel engine. Atmospheric Environment 37(35), 4965-4971.

Hung, H.F., Wang, C.S., 2001. Experimental determination of reactive oxygen species in Taipei aerosols. Journal of Aerosol Science 32(10), 1201-1211.

Jacobson, M.Z., 2001. Strong radiative heating due to the mixing state of black carbon in atmospheric aerosols. Nature 409(6821), 695-697.

Johnson, G.R., Ristovski, Z., Morawska, L., 2004. Method for measuring the hygroscopic behaviour of lower volatility fractions in an internally mixed aerosol. Journal of Aerosol Science 35(4), 443-455.

Kim, H., Choi, B., 2008. Effect of ethanol-diesel blend fuels on emission and particle size distribution in a common-rail direct injection diesel engine with warm-up catalytic converter. Renewable Energy 33(10), 2222-2228.

Kittelson, D., Watts, W., Johnson, J., 2002. Diesel aerosol sampling methodology CRC E-43, Final Report, pp1-181, University of Minnesota, Minneapolis.

Lapuerta, M., Armas, O., Herreros, J.M., 2008. Emissions from a diesel-bioethanol blend in an automotive diesel engine. Fuel 87(1), 25-31.

Li, N., Sioutas, C., Cho, A., Schmitz, D., Misra, C., Sempf, J., Wang, M.Y., Oberley, T., Froines, J., Nel, A., 2003. Ultrafine particulate pollutants induce oxidative stress and mitochondrial damage. Environmental Health Perspectives 111(4), 455-460.

Meyer, N.K., Ristovski, Z.D., 2007. Ternary nucleation as a mechanism for the production of diesel nanoparticles: experimental analysis of the volatile and hygroscopic properties of diesel exhaust using the volatilization and humifidication tandem differential mobility analyzer. Environmental Science & Technology 41(21), 7309-7314.

Miljevic, B., Fairfull-Smith, K.E., Bottle, S.E., Ristovski, Z.D., 2009a. The application of profluorescent nitroxides to detect reactive oxygen species derived from combustion generated particulate matter: Cigarette smoke - a case study. Submitted to Journal of Aerosol Science.

Miljevic, B., Modini, R.L., Bottle, S.E., Ristovski, Z.D., 2009b. On the efficiency of impingers with fritted nozzle tip for collection of ultrafine particles. Atmospheric Environment 43(6), 1372-1376.

Nord, K., Haupt, D., Ahlvik, P., Egebäck, K.E., 2004. Particulate emissions from an ethanol fueled heavy-duty diesel engine equipped with EGR, catalyst and DPF, Society of Automotive Engineers, SAE Paper No. 2004-01-1987.

Peters, A., Wichmann, H.E., Tuch, T., Heinrich, J., Heyder, J., 1997. Respiratory effects are associated with the number of ultrafine particles. American Journal of Respiratory and Critical Care Medicine 155(4), 1376-1383.

Sakurai, H., Tobias, H.J., Park, K., Zarling, D., Docherty, K.S., Kittelson, D.B., McMurry, P.H., Ziemann, P.J., 2003. On-line measurements of diesel nanoparticle composition and volatility. Atmospheric Environment 37(9-10), 1199-1210.

Venkatachari, P., Hopke, P.K., Brune, W.H., Ren, X.R., Lesher, R., Mao, J.Q., Mitchel, M., 2007. Characterization of wintertime reactive oxygen species concentrations in Flushing, New York. Aerosol Science and Technology 41(2), 97-111.

Wiesenthal, T., Leduc, G., Christidis, P., Schade, B., Pelkmans, L., Govaerts, L., Georgopoulos, P., 2009. Biofuel support policies in Europe: Lessons learnt for the long way ahead. Renewable & Sustainable Energy Reviews 13(4), 789-800.

Xu, F., El-Leathy, A.M., Kim, C.H., Faeth, G.M., 2003. Soot surface oxidation in hydrocarbon/air diffusion flames at atmospheric pressure. Combustion and Flame 132(1-2), 43-57.

Zhang, Z.H., Cheung, C.S., Chan, T.L., Yao, C.D., 2009. Emission reduction from diesel engine using fumigation methanol and diesel oxidation catalyst. Science of the Total Environment 407(15), 4497-4505.

4.6 Supporting information

Table S 4.1: Test engine specifications.

Item	Specification
Model	Ford 2701C
Cylinders	4 in line
Capacity (L)	4.152
Bore × stroke (mm)	108.2 × 115
Maximum power (kW/rpm)	48/2500
Maximum torque (Nm/rpm)	207/1700
Compression ratio	15.5
Aspiration	Naturally aspirated
Emissions certification	Pre-Euro I

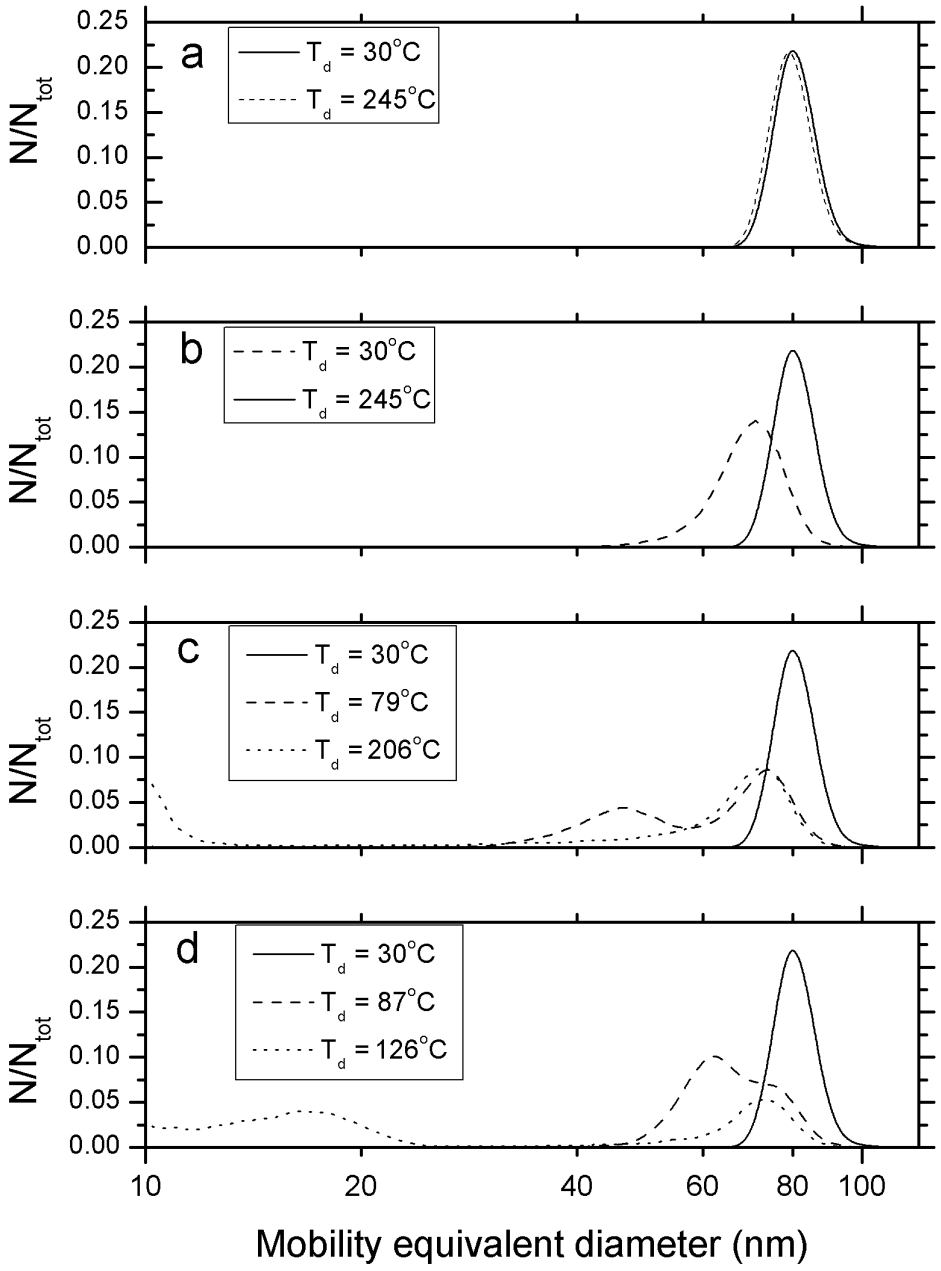

Figure S 4.1: Particle size distribution for different thermodenuder temperatures ($\boldsymbol{T_d}$). (a) 100% load E0. (b) 100% load E40. (c) 50% load E0. (d) 50% load E40.

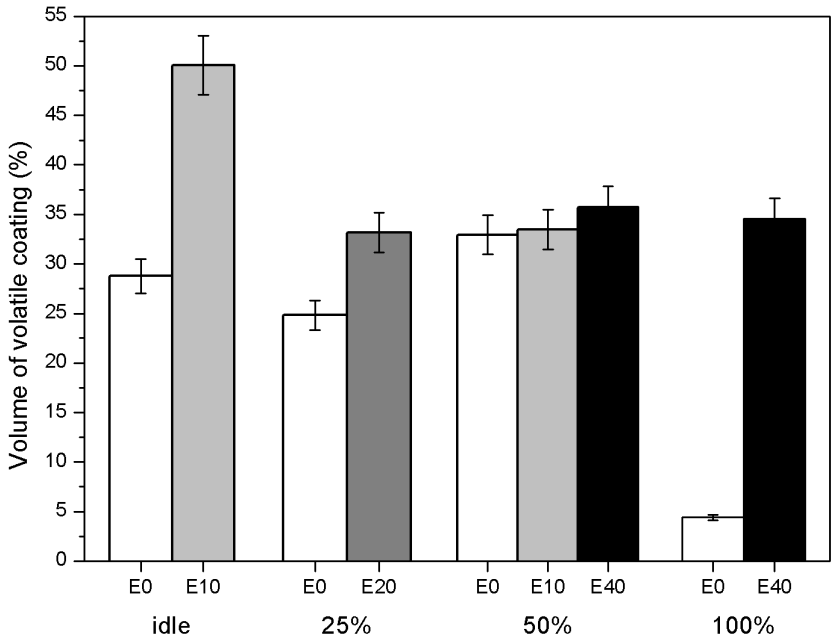

Figure S 4.2: The volume percentage of volatile material that coats non-volatile particles at intermediate speed (1700 rpm) and for various load settings and ethanol substitutions. Error bars are calculated using the uncertainties in the diameter measurement.

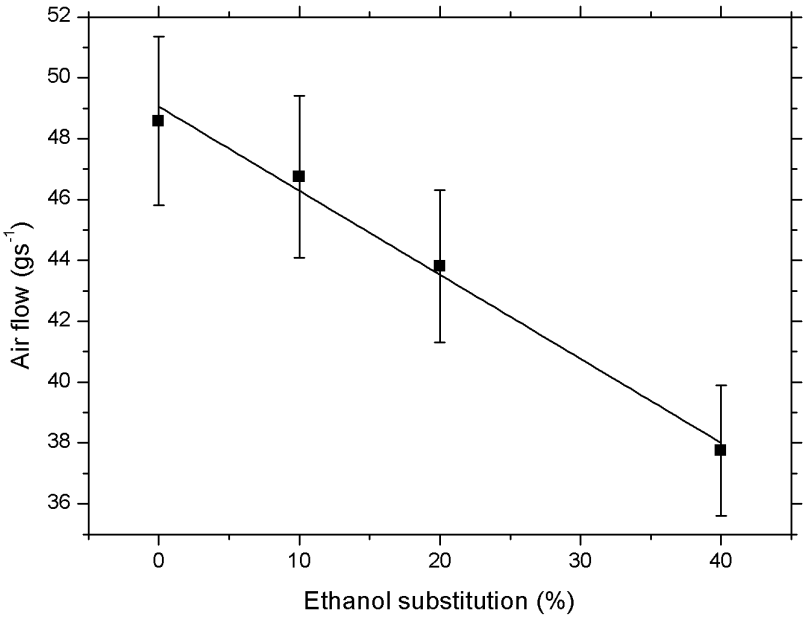

Figure S 4.3: A calculation of air available for combustion at intermediate speed (1700 rpm), half load, for various ethanol substitutions. Error bars are calculated based using the uncertainties in the fuel consumption and gaseous emissions measurements.

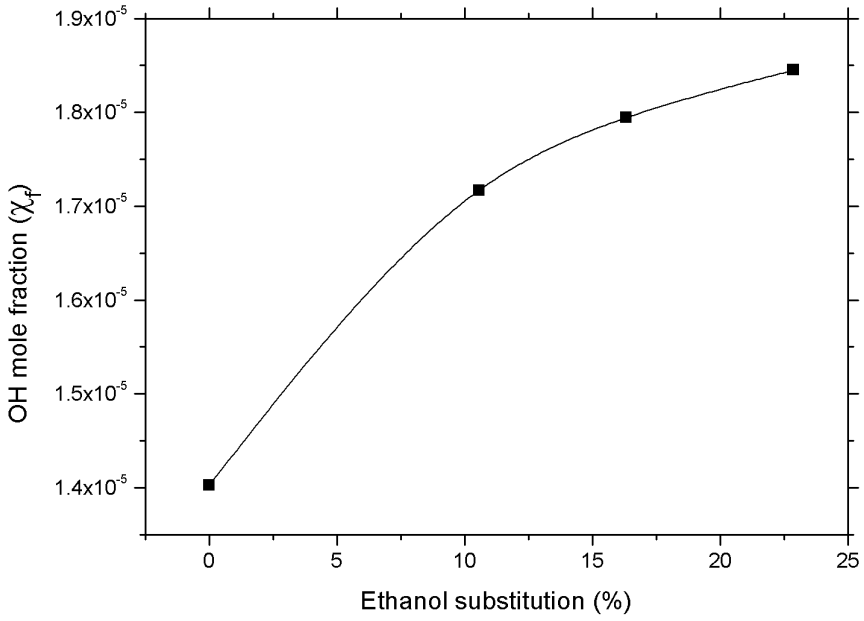

Figure S 4.4: OH radical emissions from an AVL Boost simulation conducted at 2000 rpm, full load.

Chapter 5: A physico-chemical characterisation of particulate emissions from a compression ignition engine employing two injection technologies and three fuels

N.C. Surawski[a,b], B. Miljevic[a,d], G.A. Ayoko[c], B.A. Roberts[a,1], S. Elbagir[c], K.E. Fairfull-Smith[d], S.E. Bottle[d], Z.D. Ristovski[a*]

[a]International Laboratory for Air Quality and Health, Queensland University of Technology, 2 George St, Brisbane QLD 4001, Australia

[b]School of Engineering Systems, Queensland University of Technology, 2 George St, Brisbane QLD 4001, Australia

[c]Discipline of Chemistry, Faculty of Science and Technology, Queensland University of Technology, 2 George St, Brisbane QLD 4001, Australia

[1]Current address: School of Mechanical and Mining Engineering, University of Queensland, St Lucia, QLD 4067, Australia

[d]ARC Centre of Excellence for Free Radical Chemistry and Biotechnology, Queensland University of Technology, 2 George St, 4001 Brisbane, Australia

Publication: Environmental Science & Technology, 2011, 45(13), 5498-5505.

Contributor	Statement of contribution
Nicholas C. Surawski	Contributed to the experimental design, conducted particle number size distribution and mass measurements, performed data analysis, wrote most of the manuscript.
Signature	
Date	

21/10/11	
Branka Miljevic	Contributed to the experimental design, conducted measurements, data analysis, and manuscript writing related to the BPEAnit assay.
Boyd A. Roberts	Assisted with particle number size distribution and mass measurements plus data analysis.
Godwin A. Ayoko	Involved with the PAH measurement experimental design, data analysis and manuscript writing.
Sohair Elbagir	Involved with the PAH extraction and quantification, and also data analysis.
K.E. Fairfull-Smith	Reviewed manuscript.
Steven E. Bottle	Reviewed the manuscript.
Zoran D. Ristovski	Contributed to the experimental design, data analysis, and manuscript writing.

Principal Supervisor Confirmation

I have sighted email or other correspondence from all Co-authors confirming their certifying authorship.

Associate Professor Zoran Ristovski		21/10/11
Name	**Signature**	**Date**

Abstract

Alternative fuels and injection technologies are a necessary component of particulate emission reduction strategies for compression ignition engines. Consequently, this study undertakes a physico-chemical characterisation of diesel particulate matter (DPM) for engines equipped with alternative injection technologies (direct injection and common rail) and alternative fuels (ultra low sulphur diesel, a 20% biodiesel blend and a synthetic diesel). Particle physical properties were addressed by measuring particle number size distributions and particle chemical properties were addressed by measuring polycyclic aromatic hydrocarbons (PAHs) and reactive oxygen species (ROS). Particle volatility was determined by passing the poly-disperse size distribution through a thermodenuder set to 300 ^{o}C. The results from this study, conducted over a four point test cycle, showed that both fuel type and injection technology have an impact on particle emissions, but injection technology was the more important factor. Significant particle number emission (54% - 84%) reductions were achieved at half load operation (1% increase - 43% decrease at full load) with the common rail injection system, however, the particles had a significantly higher PAH fraction (by a factor of 2 to 4) and ROS concentrations (by a factor of 6 to 16) both expressed on a test-cycle averaged basis. The results of this study have significant implications for the health effects of DPM emissions from both direct injection and common rail engines utilising various alternative fuels.

5.1 Introduction

Long term exposure to diesel particulate matter (DPM) is associated with a range of adverse health effects including lung cancer and cardiopulmonary mortality (Pope et al., 2002), therefore strategies need to be invoked to minimise their impact on human health. A range of strategies exist for mitigating DPM emissions in on-road and off-road environments, such as using diesel particulate filters (DPF's), but alternative fuels and injection technologies are also used. The DPF filtration strategy is one that has been employed with some success in on-road vehicle emissions studies, especially if a catalysed DPF system is used (Kittelson et al., 2006c). Indeed, some studies have shown an almost 3 orders of magnitude reduction in particle number emissions factors using this approach (Mayer et al., 2010a), along with a significant reduction in carcinogenic and mutagenic PAH emissions (Heeb et al., 2010). There have been, however, studies reporting the formation of nucleation mode particles downstream of a DPF (Vaaraslahti et al., 2004; Grose et al., 2006), so this technique should be applied with some caution.

Other than particulate after-treatment, alternative fuels and injection technologies potentially offer some improvement to DPM emissions (Majewski, 2007). Biodiesel and synthetic diesel have been investigated as a DPM reduction strategy in several emissions studies owing to their high cetane number, smooth combustion characteristics along with their sulphur free composition (Schaberg et al., 2002a; Heikkilä et al., 2009). It is for these reasons that these two alternative fuels were chosen for this study. Alternative injection technologies are also investigated to reduce DPM emissions, and compared to mechanical direct injection, common rail injection offers a higher injection pressure across a wide range of an engines operating map (Robert Bosch GmbH, 2007), and with this potentially comes a concomitant reduction in particle number emissions due to improved fuel atomisation and fuel-air mixing (Jääskeläinen, 2010).

Considering that DPM health effects involve both physical and chemical factors (Giechaskiel et al., 2009), this study focuses on a physico-chemical characterisation of particulate emissions from compression ignition engines equipped with two alternative fuels and alternative injection technologies for the purpose of gaining insights into their health impacts. In particular, the organic component of DPM would include compounds deleterious to human health such as PAHs and ROS (Sklorz et al., 2007). ROS are known to cause oxidative stress at the sites of deposition, which has been proposed as a mechanism for many of the adverse health outcomes associated with exposure to DPM (Dellinger et al., 2001; Li et al., 2003). In this study, particle physical properties are addressed by measuring particle number size distributions and chemical properties are addressed by measuring the emissions of PAHs and ROS.

5.2 Methodology

5.2.1 Engine, injection system and fuel specifications

Particulate emissions testing was performed on a 4 cylinder Perkins 1104C-44 engine which is representative of compression ignition engines used in underground coal mines in Australia. The engine is naturally aspirated and has a Euro II (off-road) emissions certification. According to the nomenclature of Hesterberg et al. (Hesterberg et al., 2009), this engine technology can be classed as “transitional” diesel exhaust, and still has relevance as the transition to “new technology diesel exhaust” (equipped with DPF’s) is not yet complete. More detailed information on the engine investigated in this study can be found in Table S 5.1.

In this study, the engine was tested with two different injection configurations. The engine was originally tested with a retro-fitted electronically controlled common rail injection system (denoted CR in figures), whilst for the second phase of testing; the engine was restored to its default mechanical direct injection system (denoted DI in figures). With the common rail injection configuration, the engine was tuned to provide the same gaseous emissions output compared to the mechanical injection system. Keeping the gaseous emissions output fixed was the method chosen to compare the two injection technologies, however, in reality an electronically controlled injection system would be "tuned" to optimise both its gaseous and particulate emissions.

Engine testing was performed using four speed and load settings taken from the AS3584 test cycle, with these 4 test modes also forming part of the ECE R49 and ISO8178 test cycles. The speed and load settings investigated in the study can be found in Table S 5.2 and enabled a range of engine exhaust conditions to be tested. The four modes were tested in the same order (as listed in Table S 5.2) for all three fuels and for both injection technologies. Testing took approximately half an hour at each mode, and each test cycle was repeated in the afternoon after a complete engine shutdown. At the commencement of each test session, the engine was run initially under light load and then ramped to full load at intermediate speed (once the oil temperature reached 60 ^{o} C) until the water and lubricating oil temperatures stabilised. The engine was then taken to the first test mode (1400 rpm 50% load), whereby testing did not commence until the exhaust temperature and CO_2 emissions reached steady-state. The warm up period lasted for approximately 15 minutes before sampling in the first test mode commenced. To enable a load to be provided to the engine, it was coupled to a water-brake dynamometer.

For both injection configurations, three fuel types were investigated. The base fuel was an ultra low sulphur diesel (< 10 ppm sulphur), whilst a 20 % biodiesel blend (trans-esterified waste cooking oil) and a gas-to-liquids synthetic diesel blend (using Fischer-Tropsch synthesis) were also investigated. The three fuels are denoted in the manuscript by ULSD (ultra low sulphur diesel), B20 (20% biodiesel blend), and Synthetic (for the Fischer-Tropsch synthetic diesel). Detailed properties for the fuels used in this study and their test methods can be located in Table S 5.3. After completion of testing with a particular fuel, the fuel tank and lines were flushed and a new fuel filter was installed. After the fuel flushing procedure, the oil sump was drained and replenished with new oil (Penrite HPR Diesel 15) and a new oil

filter was installed. After each oil change, the engine was run under moderate load for approximately two hours to pre-condition the new lubricating oil.

5.2.2 Particulate emissions measurement methodology

A two-stage unheated dilution system with a dilution tunnel followed by a Dekati ejector diluter was used to dilute exhaust gas before particulate sampling. The partial flow dilution system used in this study is based on the design of Ristovski et al. (2006) and is discussed in further detail in Surawski et al. (2010b) and Surawski et al. (2010c). CO_2 was used as a tracer gas to calculate dilution ratios. $PM_{2.5}$ emissions were also measured with a TSI 8520 DustTrak. To convert the DustTrak readings into a gravimetric measurement, the tapered element oscillating microbalance to DustTrak correlation for diesel particles published by Jamriska et al. (Jamriska et al., 2004) was used. The experimental configuration employed in this study is shown in Figure S 5.1.

The measurements conducted in this study consisted of: the measurement of particle number size distributions, measurement of PAHs, as well as measurement of the oxidative potential of DPM with a cell-free BPEAnit (9-(1,1,3,3-tetramethylisoindolin-2-yloxyl-5-ethynyl)-10-(phenylethynyl) anthracene) assay, hereafter referred to as ROS (i.e. Reactive Oxygen Species) concentrations. Particle number size distributions were measured with a Scanning Mobility Particle Sizer (SMPS) consisting of a TSI 3071A classifier and a TSI 3782 water based condensation particle counter. Particles within a 10-400 nm size range were measured with the SMPS using a scan time of two minutes. Particle volatility was also investigated by passing the diesel aerosol through a TSI 3065 thermodenuder (TD), which consists of a short heated section followed by an annular bed of activated charcoal to adsorb evaporated material from the particles. The residence time for aerosol in the TD is approximately 20 seconds. Size distributions of diesel aerosols obtained using a TD have been corrected for diffusional losses using diesel particles passed through the TD at 25 ^{o} C. The difference in particle number concentrations upstream and downstream of the TD (switched using a 3-way valve) was used to enable a size-dependent loss correction function to be obtained.

Particle phase PAHs were collected on filters and vapour phase PAHs were collected in tubes with XAD-2 adsorbent prior to their subsequent quantification using a Gas-Chromatography Mass-Spectrometry (GC-MS) system. The PAH emission factors presented in this study are the sum of both the particle and vapour phase PAH emission factors. The methodology for quantification of PAH emissions following DPM collection onto filters and tubes follows

guidelines from Lim et al. (2007b). Prior to chromatographic analysis, 0.5 µg of semi-volatile internal standard supplied by Supelco and containing naphthalene - D8, acenaphthene - D10, phenanthrene - D14, chrysene - D12 and perylene - D12 was added to all extracts for quantification purposes. The QTM PAH standard used for the analyses was purchased from Supelco and contained 2-bromo-naphthalene and the following US EPA priority PAHs in dichloromethane: Naphthalene, Acenaphthylene, Acenaphthene, Fluorene, Phenanthrene, Anthracene, Fluoranthene, Pyrene, Benzo(a) anthracene, Chrysene, Benzo(b)fluoranthene, Benzo(a)pyrene, Indeno(1,2,3-cd)pyrene, Dibenzo(a,h)anthracene, and Benzo(g,h,i)perylene. The PAH analysis was performed on an Agilent 6890 GC (fitted with an auto-sampler) coupled to an Agilent 5973 MS (30.0 m × 0.32 mm × 0.25 µm). Helium with a purity of 99.99% was used as the carrier gas at a constant flow of 1 ml/min. The following oven temperature program was used: first the initial temperature was set to 100 °C for 2 min, and then increased to 170 °C at a rate of 10°C/min and then raised to 320 °C at a rate of 10°C/min and then kept at 320 °C for 18 min. The MS was operated in single ion monitoring mode. Identification was based on the GC retention times relative to those of related internal standards, and the relative abundance of the ions monitored. PAH emissions are expressed as emission factors (mg/kWh) and are based on summing the concentrations of the 15 PAHs that were measured successfully, as problems were encountered with the quantification of 2-bromo-naphthalene during analysis.

A profluorescent nitroxide probe, BPEAnit, was used to detect and quantify ROS associated with DPM emissions. Profluorescent nitroxides are weakly fluorescent compounds, but become strongly fluorescent upon radical trapping or redox activity (Micallef et al., 2005; Fairfull-Smith and Bottle, 2008; Jia et al., 2009). BPEAnit has been applied previously to assess the *in vitro* oxidative potential of cigarette smoke (Miljevic et al., 2010a), DPM (Surawski et al., 2010b) and wood smoke (Miljevic et al., 2010b). The amount of BPEAnit converted to a fluorescent product represents a measure of the oxidative potential of DPM.

Samples were collected by bubbling aerosol through an impinger containing 20 mL of 4 µm BPEAnit solution (using AR grade dimethylsulphoxide as a solvent) followed by fluorescence measurements with a spectrofluorometer (Ocean Optics). BPEAnit has a fluorescence excitation maximum at 430 nm and a fluorescence emission maximum at 485 nm The amount of BPEAnit reacting with the engine's exhaust was calculated from a standard curve obtained by plotting known concentrations of the methyl adduct of BPEAnit

(BPEAnit-Me; fluorescent) against the fluorescence intensity at 485 nm. Based on the difference in fluorescence signals at 485 nm between the test and HEPA-filtered control sample, the amount of ROS emitted for each test sample was calculated and normalised to the DPM mass measured by a TSI 8520 DustTrak to give ROS concentrations (nmol/mg). Sampling for PAHs and ROS was performed via sampling ports located on the dilution tunnel (rather than after secondary dilution) so that sufficient particle concentrations were present for analysis.

5.2.3 Data analysis

Raw data from this experimental campaign for both injection configurations and all three fuels can be found in Table S 5.4. The PAH emission factors, ROS concentrations and benzo(a)pyrene toxic equivalency factors (BaP_{eq}) emission factors rely on a test cycle average to facilitate observation of the important trends in the data. The data is presented this way as the effects of injection technology and fuel type have more influence on the variability of PAH and BaP_{eq} emission factors and ROS concentrations rather than the effect due to engine speed and load.

The test cycle averaging was performed using weighting factors derived from the ECE R49 steady-state test cycle which was used for type approval of heavy duty engines (on-road) at the Euro II stage (Dieselnet, 2000). The emissions results at a particular speed and load setting are multiplied by the appropriate weighting factor allowing an emissions parameter to be calculated for the complete test cycle. Because the 4 mode points used for testing emissions in this study are a subset of the 13 mode ECE R49 cycle, the weights have been multiplied by a constant factor (20/9) so that the weights sum to unity (see Table S 5.5).

A further calculation arising from the PAH measurements involved computing benzo(a)pyrene toxic equivalency factors (BaP_{eq}) using the set of co-efficients published by Nisbet and LaGoy (1992). A monograph published by the International Agency for Research on Cancer (1987) categorised Benzo(a) anthracene, Benzo(a)pyrene, and Dibenzo(a,h)anthracene as probable (2A) human carcinogens, whereas; Naphthalene, Benzo(b)fluoranthene, benzo(k)fluoranthene, and Indeno(1,2,3-cd)pyrene were categorised as possible (2B) human carcinogens. There is a tendency for “heavier” PAHs with a greater number of aromatic rings to be categorised as carcinogenic (i.e. type 2A/2B), although Naphthalene is a notable exception. The set of toxic equivalency factors for PAHs applied in this study represent well the true carcinogenic potency of PAHs (Nisbet and LaGoy, 1992),

and consequently have been used in several investigations for assessing the potency of complex PAH mixtures (Petry et al., 1996; Mi et al., 2001; Lim et al., 2007b). BaP_{eq} emission factors are calculated by multiplying PAH emission factors (for individual PAHs) by its Nisbet and LaGoy (1992) toxic equivalency factor, and then summing this result over all PAHs measured.

5.3 Results and discussion

5.3.1 Particle number size distributions

Figures 5.1 and 5.2 display particle number size distributions for all the four test modes considered using all three fuels and both injection technologies. In addition, particle number size distributions are presented whereby the poly-disperse size distribution was passed through a TD set to 300 ^{o}C. Particle number size distributions passed through the TD for the other two fuel settings (ie ULSD and the Synthetic fuel) are not shown to avoid cluttering the figures, however, the results for these two fuels show the same conceptual volatility behaviour (i.e. a reduction in particle size and a load dependent reduction in particle number) as biodiesel. Figure 5.1 presents particle number size distributions at intermediate speed (i.e. 1400 rpm), whilst Figure 5.2 presents results at rated speed (i.e. 2400 rpm).

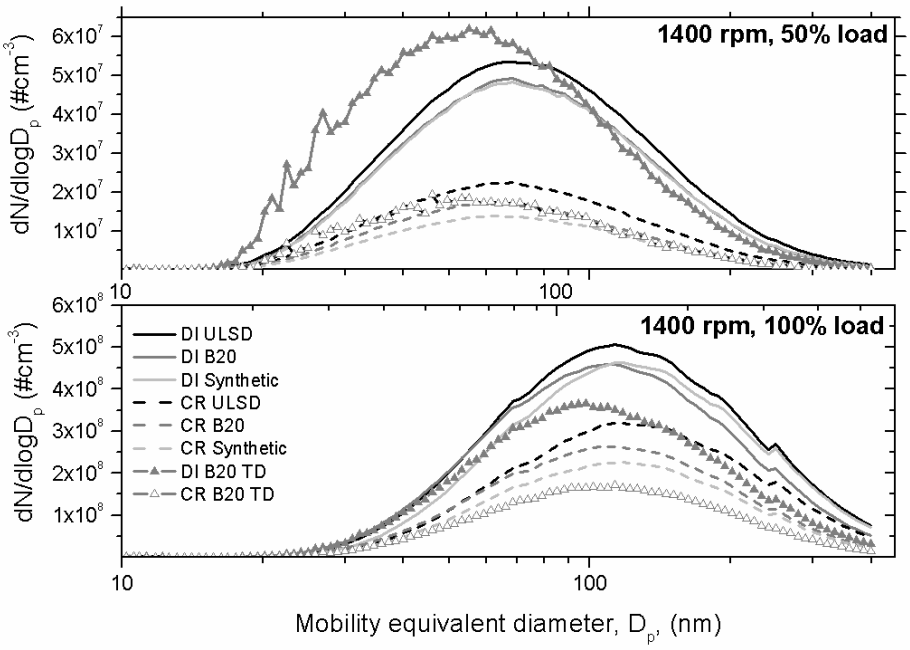

Figure 5.1: Particle number size distribution comparison for both injection technologies and all 3 fuels at 1400 rpm 50% load and 1400 rpm 100% load. Note well that particle number size distributions are also presented for B20 with the aerosol passed through a TD set to 300 ^{o}C.

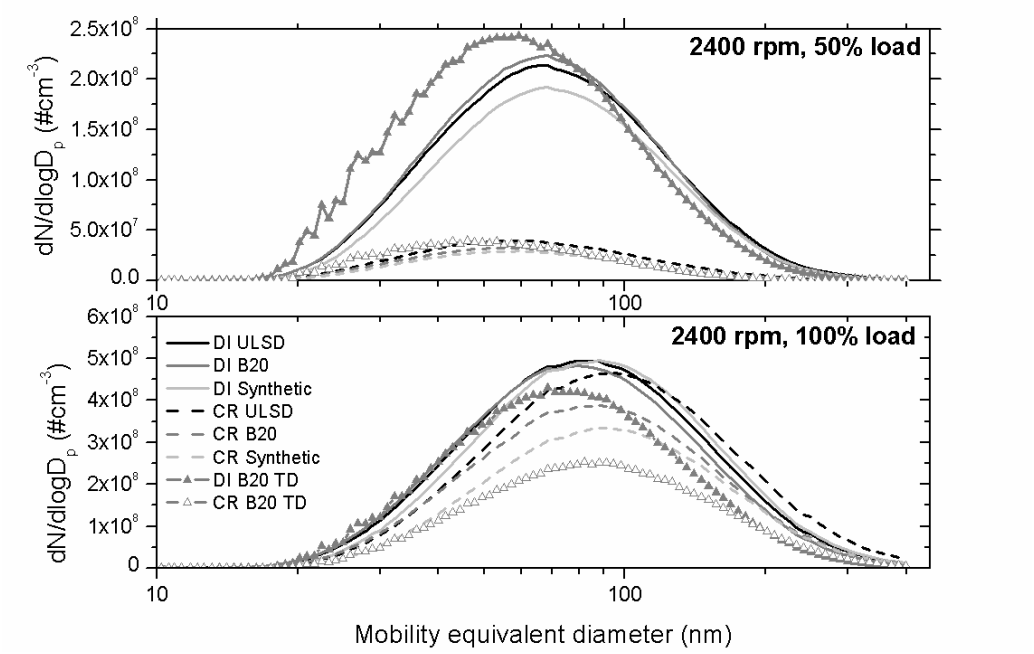

Figure 5.2: Particle number size distribution comparison for both injection technologies and all 3 fuels at 2400 rpm 50% load and 2400 rpm 100% load. Note well that particle number size distributions are also presented for B20 with the aerosol passed through a TD set to 300 ^{o}C.

The most striking observation from Figures 5.1 and 5.2 is that the number of particles emitted was lower when the engine was equipped with the common rail injection system – especially at half load conditions. At the intermediate speed and half load setting, the particle number emissions reductions achieved with common rail injection (relative to direct injection) are approximately 54% for the ULSD fuel setting and 60% and 66% respectively for the B20 and the Synthetic fuel. At rated speed and full load (see Figure 5.2) particle number reductions are less noticeable, with B20 providing a 12% reduction, the Synthetic fuel, a 24% reduction and ULSD yielding a 1% increase in particle number emissions.

Another feature evident from Figures 5.1 and 5.2 is that when comparing particle number emissions for a fixed injection set-up (either common rail or direct injection) both alternative fuels reduce particle number emissions; however, the reductions are larger for common rail injection than for direct injection. At intermediate speed and half load, the use of B20 (with common rail injection) reduces particle number emissions by 24% whilst the Synthetic fuel reduces particle number emissions by 34%, whereas with direct injection the reductions are 12% with B20 and 9% with the Synthetic fuel. At rated speed and full load, the use of B20 with common rail injection reduces particle number emissions by 16% and the Synthetic fuel

reduces them by 28%. With direct injection, the reductions are 4% with B20 and 3% with the Synthetic fuel.

The results at intermediate speed and full load plus rated speed and half load, whilst not discussed in full detail, are conceptually similar to the results discussed at length previously. Particle number reductions at intermediate speed and full load are similar to the rated speed and full load results, as particle number reductions are less evident at this load setting, however, particle number reductions range from 31% for ULSD, to 36% for B20 and 43% for the Synthetic fuel when comparing the common rail particle emissions to those for direct injection. At the half load setting at rated speed considerable particle number reductions are exhibited, as was the case at intermediate speed. Particle number reductions range from 80% for ULSD to 84% for B20 with an 82% reduction being observed for the Synthetic fuel when comparing the particle number reductions for common rail injection technology to direct injection. When comparing the impact of alternative fuels for a fixed injection technology, particle number reductions are evident with both alternative fuels at intermediate speed full load and also rated speed half load.

Common rail injection has several advantages compared to direct injection, and these benefits are evident from the particle number reductions demonstrated in this study - especially at half load operation. Common rail injection is characterised by an injection pressure that is largely independent of the speed and load of the engine (Khair and Jääskeläinen, 2010), as the fuel pressurisation and injection processes are decoupled from one another, whereas for direct injection fuel pressurisation and injection occur simultaneously (Robert Bosch GmbH, 2007). An increased injection pressure has many benefits for reducing particulate emissions such as improving spray penetration and subsequent mixing of fuel and air (Khair and Jääskeläinen, 2010). Another feature of common rail injection is that it permits multiple injections (Khair and Jääskeläinen, 2010) (such as pre and post injections) which can improve the thermal efficiency of the engine and can assist the DPM oxidation process (Jääskeläinen, 2010).

Substantial reductions in particle number emissions were observed with B20 and the Synthetic fuel, but the reductions were more evident with common rail injection. Both alternative fuels were less compatible with direct injection technology, but an explanation for this effect cannot be provided at this stage. In terms of fuel properties, the higher cetane number for both alternative fuels (see Table S 5.3) should reduce DPM emissions –especially

for the Synthetic fuel (Alleman and McCormick, 2003b). In addition, the higher oxygen content of B20 is also a factor in reducing particle emissions (Graboski et al., 2003) as it enables the diffusion flame phase of combustion to be completed more fully (Lapuerta et al., 2008b).

The presence of uni-modality is a common feature of all the size distributions measured in this study. Recent studies have reported the presence of a nucleation mode when using alternative fuels in compression ignition engines similar to those used in the current investigation. Heikkilä et al. (2009) report the presence of a non-volatile nucleation mode when running the engine on a gas-to-liquids synthetic diesel and also a rapeseed methyl ester. Fontaras et al. (2010b) report the formation of a volatile nucleation mode when running a diesel passenger car on ten percent blends of rapeseed and palm oil methyl esters. In this study, the absence of nucleation mode particles can be partially attributed to the large accumulation mode surface area adsorbing a lot of volatile material upon exhaust gas cooling and dilution therefore preventing the occurrence of nucleation. Moreover, the hydrocarbon emissions from this engine are low and do not provide precursors for the formation of nucleation mode particles.

5.3.2 PAH emission factors and ROS concentrations

Figures 5.3 displays the test cycle averaged PAH emission factors (mg/kWh) and also the ROS concentrations (nmol/mg). Error bars on Figures 5.3 denote ± one standard error of the mean. Figure 5.3 shows that both fuel choice and injection technology have an impact of PAH emissions, but it is clearly injection technology that has a larger impact on the overall emissions profile. When comparing the common rail PAH emission factors with those of direct injection, the ULSD and B20 PAH emission factors are higher by a factor of approximately four, whilst they are higher by a factor of approximately two for the Synthetic fuel. Relative to the ULSD PAH emission factors for common rail injection, B20 provides a 10% increase in PAH emission factors, whilst for the Synthetic fuel a 5% increase is achieved. Alternatively, for direct injection B20 yields a 4% decrease in PAH emission factors and the Synthetic fuel PAH emission factors are approximately twice those of low sulphur diesel.

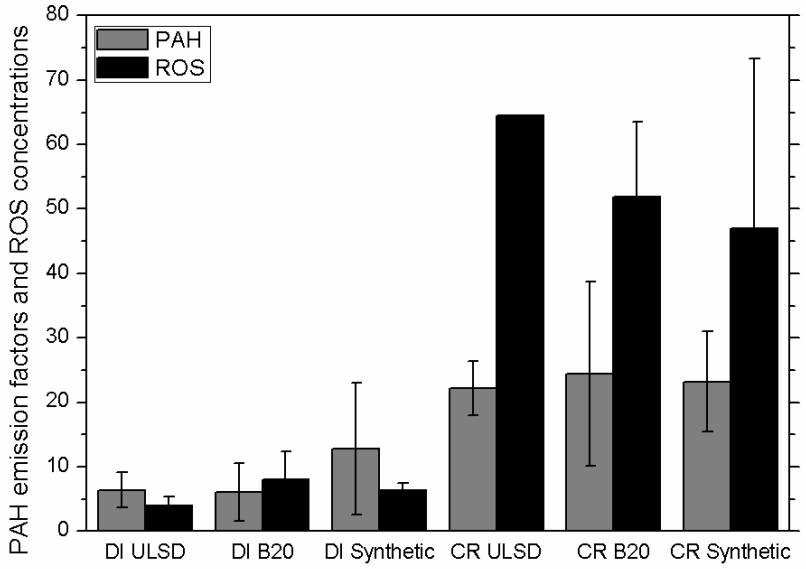

Figure 5.3: Test cycle averaged PAH (mg/kWh) emission factors and ROS concentrations (nmol/mg) for both injection technologies and all three fuels.

Similar to the PAH emission factors, the impact of injection technology on ROS concentrations is evident. When comparing the two injection technologies, common rail injection leads to a sixteen fold increase in ROS concentrations with ULSD, whilst for B20 and the Synthetic fuel the ROS concentrations increase by a factor of approximately seven relative to direct injection. When comparing the effect of the alternative fuel applied (with common rail injection), B20 reduces ROS concentrations by approximately 20% and the Synthetic fuel reduces ROS concentrations by about 27%. For direct injection, B20 doubles ROS concentrations and the Synthetic fuel leads to an increase of approximately 60% in ROS concentrations.

A recent study by Cheung et al. (Cheung et al., 2010) showed a strong correlation between PAH emission factors and the oxidative potential of particles measured with a DTT assay. Similarly, the results from this investigation (see Figure S 5.2) show that the test-cycle averaged PAH and ROS emissions are strongly correlated (Pearson's correlation co-efficient 0.913). This is a promising result considering that cell-free assays for assessing the oxidative potential of DPM are a rather new analytical technique in diesel emissions testing.

Figure 5.4 displays the BaP_{eq} emission factors (mg/kWh) for both injection technologies and all three fuels. Qualitatively, the trends obtained by considering the toxicity equivalent factor

of each PAH are similar, as the common rail BaP_{eq} emission factors are much higher than those for direct injection. Quantitatively, however, the PAH results are changed by considering the carcinogenic potency of individual PAHs. After calculating BaP_{eq} emission factors, the Synthetic fuel with common rail injection emits the most potent PAHs, whereas, the B20 fuel setting with common rail injection originally had the highest PAH emission factors. The BaP_{eq} emission factors calculation also shows that with common rail injection relative to direct injection, that both alternative fuels (B20 and the Synthetic fuel) emit more potent PAHs when compared to the original PAH emission factors. Relative to direct injection, the common rail B20 and the Synthetic fuel PAHs are more potent by a factor of approximately 12, whereas based on the raw PAH emission factors (comparing common rail to direct injection) B20 was higher by a factor of four and the Synthetic fuel was higher by a factor of approximately two. For ULSD, the common rail BaP_{eq} emission factors relative to direct injection are more potent by a factor of approximately 6, whereas based on the raw PAH emission factors they were different by a factor of three and a half. To summarise, consideration of the BaP_{eq} emission factors elicited a 3 fold increase in the carcinogenic potency of B20 PAH emissions and a 6 fold increase in carcinogenic potency for the Synthetic fuel (both for common rail injection compared to direct injection), whereas for ULSD a increase by a factor of approximately 1.5 observed. This result highlights the importance of considering BaP_{eq} toxic equivalency factors when assessing the carcinogenic potency of complex PAH mixtures in diesel exhaust.

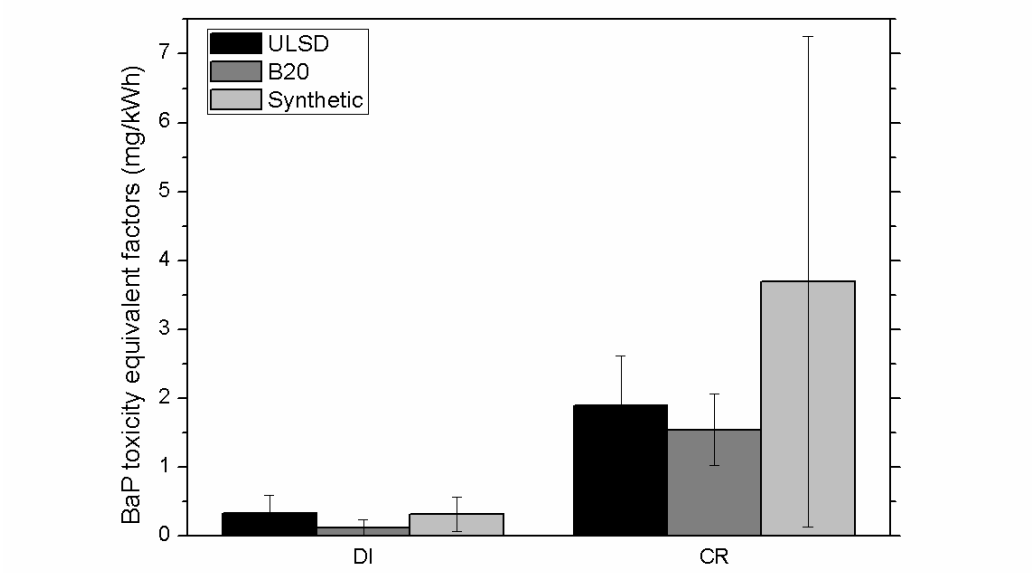

Figure 5.4: Test cycle averaged BaP_{eq} emission factors (mg/kWh) for PAHs for both injection technologies and all three fuels.

5.3.3 Particle volatility

Particle number size distributions for the bio-diesel fuel setting were shown where the aerosol was passed through a TD set to 300 ^{o}C as shown in Figures 5.1 and 5.2. It can be noted from Figures 5.1 and 5.2 that both the raw and TD size distributions were uni-modal, and that heating the particles decreased the median diameter without introducing a second peak in the size distribution. For all measurements at 50% load, there was no significant decrease in particle number concentration. With direct injection at half load, an increase in particle number concentration was observed for smaller particles (< 100 nm), which is an artefact of the diffusional loss correction procedure. This indicates that at 50% load, the particles are internally mixed, with volatile components (such as PAHs and ROS) condensed on the surface of particles for both injection technologies and all fuels. Alternatively, at 100% load, there was a decrease in the particle number concentration after volatilisation in addition to a reduction in particle size. At 100% load there is, therefore, the possibility that purely volatile particles have evaporated after heating in the TD. Increased volatility under high load is an uncommon result, but was observed previously by Meyer and Ristovski (2007).

The volatile (i.e. material which evaporated in the TD) volume percentage of particles (V_{ORG}) has been calculated to explore the relationship between the volatility of particles with both injection technologies and all three fuels on a test cycle averaged basis (see Figure S 5.3). V_{ORG} was calculated from the integrated raw (V_{raw} , i.e. unheated) and TD (V_{TD} , i.e. heated) particle volume size distributions assuming spherical particles with unit density via:

$$V_{ORG}(\%) = 100\left(\frac{V_{raw} - V_{TD}}{V_{raw}}\right), \tag{5.1}$$

It is clear from Figure S 5.3 that the common rail injection particles are more volatile (and hence have a higher semi-volatile organic fraction) than those with direct injection - especially for the Synthetic fuel. This finding sheds light on the observed increases in the PAH and ROS emissions with common rail injection, as correlations between ROS emissions and semi-volatile organic species have been observed previously (Biswas et al., 2009; Miljevic et al., 2010b).

Given that rather large increases in ROS and PAH emissions occurred with the common rail injection configuration, (in some cases a more than 10 fold increase was observed) this has significant implications for the overall toxicological properties of the emitted particles. Limbach et al. (2007) describe a mechanism whereby the catalytic action of metal oxides adsorbed on the surface of nanoparticles induce oxidative stress in exposed human lung epithelial cells, a phenomenon referred to as a the "Trojan horse" mechanism. Heeb et al. (2010) refer to the same mechanism when describing the transport of genotoxic compounds (such as PAHs) across the alveolar membrane. In the current investigation, sub-micron combustion generated particles act as a "transport vector" for genotoxic PAHs and potentially oxidative ROS substances adsorbed on the particles. The somewhat disturbing overall conclusion from this study is that the injection technology which produces fewer particles (i.e. common rail injection) has significantly more oxidative and genotoxic material available on the surface of the particle, potentially causing health effects that are not captured by considering only particle number, or particle mass based emissions. Clearly, the size resolved chemistry of particulate emissions needs to be taken further into account to elucidate the potential health impacts of DPM.

Acknowledgements

The authors acknowledge the support and funding provided by SkillPro Services Pty Ltd and the Australian Coal Association Research Program for funding project C18014. Special thanks go to Mr. Julian Greenwood and Mr. Dale Howard, from SkillPro Services, for their invaluable and friendly assistance throughout the testing period in operating the dynamometer and providing the gaseous emissions and diagnostic test data.

Supporting Information Available

Tables S 5.1-S 5.5 and Figures S 5.1-S 5.3 constitute the supporting information for this manuscript.

5.4 References

Alleman, T.L., McCormick, R.L., 2003. Fischer-Tropsch Diesel Fuels – Properties and Exhaust Emissions: A Literature Review. Society of Automotive Engineers SAE Paper No. 2003-01-0763.

Biswas, S., Verma, V., Schauer, J.J., Cassee, F.R., Cho, A.K., Sioutas, C., 2009. Oxidative Potential of Semi-Volatile and Non Volatile Particulate Matter (PM) from Heavy-Duty Vehicles Retrofitted with Emission Control Technologies. Environmental Science & Technology 43(10), 3905-3912.

Cheung, K.L., Ntziachristos, L., Tzamkiozis, T., Schauer, J.J., Samaras, Z., Moore, K.F., Sioutas, C., 2010. Emissions of Particulate Trace Elements, Metals and Organic Species from

Gasoline, Diesel, and Biodiesel Passenger Vehicles and Their Relation to Oxidative Potential. Aerosol Science and Technology 44(7), 500-513.

Dellinger, B., Pryor, W.A., Cueto, R., Squadrito, G.L., Hegde, V., Deutsch, W.A., 2001. Role of free radicals in the toxicity of airborne fine particulate matter. Chemical Research in Toxicology 14(10), 1371-1377.

Dieselnet, 2000. Emission Test Cycles: ECE R49. Dieselnet technology guide, Ecopoint Inc, http://www.dieselnet.com/standards/cycles/ece_r49.html, last accessed 16th May 2011.

Fairfull-Smith, K.E., Bottle, S.E., 2008. The Synthesis and Physical Properties of Novel Polyaromatic Profluorescent Isoindoline Nitroxide Probes. European Journal of Organic Chemistry32), 5391-5400.

Fontaras, G., Kousoulidou, M., Karavalakis, G., Tzamkiozis, T., Pistikopoulos, P., Ntziachristos, L., Bakeas, E., Stournas, S., Samaras, Z., 2010. Effects of low concentration biodiesel blend application on modern passenger cars. Part 1: Feedstock impact on regulated pollutants, fuel consumption and particle emissions. Environmental Pollution 158(5), 1451-1460.

Giechaskiel, B., Alföldy, B., Drossinos, Y., 2009. A metric for health effects studies of diesel exhaust particles. Journal of Aerosol Science 40(8), 639-651.

Graboski, M.S., McCormick, R.L., Alleman, T.L., Herring, A.M., 2003. The Effect of Biodiesel Composition on Engine Emissions from a DDC Series 60 Diesel Engine. National Renewable Energy Laboratory, Golden, Colorado, pp. 1-91.

Grose, M., Sakurai, H., Savstrom, J., Stolzenburg, M.R., Watts, W.F., Jr., Morgan, C.G., Murray, I.P., Twigg, M.V., Kittelson, D.B., McMurry, P.H., 2006. Chemical and physical properties of ultrafine diesel exhaust particles sampled downstream of a catalytic trap. Environmental Science & Technology 40(17), 5502-5507.

Heeb, N.V., Schmid, P., Kohler, M., Gujer, E., Zennegg, M., Wenger, D., Wichser, A., Ulrich, A., Gfeller, U., Honegger, P., Zeyer, K., Emmenegger, L., Petermann, J.L., Czerwinski, J., Mosimann, T., Kasper, M., Mayer, A., 2010. Impact of Low- and High-Oxidation Diesel Particulate Filters on Genotoxic Exhaust Constituents. Environmental Science & Technology 44(3), 1078-1084.

Heikkilä, J., Virtanen, A., Rönkkö, T., Keskinen, J., Aakko-Saksa, P., Murtonen, T., 2009. Nanoparticle Emissions from a Heavy-Duty Engine Running on Alternative Diesel Fuels. Environmental Science & Technology 43(24), 9501-9506.

Hesterberg, T.W., Long, C.M., Bunn, W.B., Sax, S.N., Lapin, C.A., Valberg, P.A., 2009. Non-cancer health effects of diesel exhaust: A critical assessment of recent human and animal toxicological literature. Critical Reviews in Toxicology 39(3), 195-227.

International Agency for Research on Cancer, 1987. Overall Evaluations of Carcinogenicity: An updating of IARC Monographs Volumes 1–42. IARC Monographs Evaluation of Carcinogenic Risks to Humans Supplement 7, pp. 1-440 http://www.iarc.fr/ accessed, December 22nd 2010.

Jääskeläinen, H., 2010. Fuel Injection for Clean Diesel Engines. Dieselnet technology guide, Ecopoint Inc, http://www.dieselnet.com/tech/engine_fi.html.

Jamriska, M., Morawska, L., Thomas, S., He, C., 2004. Diesel bus emissions measured in a tunnel study. Environmental Science & Technology 38(24), 6701-6709.

Jia, M., Tang, Y., Lam, Y.F., Green, S.A., Blough, N.V., 2009. Prefluorescent Nitroxide Probe for the Highly Sensitive Determination of Peroxyl and Other Radical Oxidants. Analytical Chemistry 81(19), 8033-8040.

Khair, M.K., Jääskeläinen, H., 2010. Common Rail Fuel Injection, Dieselnet technology guide, Ecopoint Inc, http://www.dieselnet.com/tech/diesel_fi_cr.html, last accessed 13th May 2011.

Kittelson, D.B., Watts, W.F., Johnson, J.P., Rowntree, C.J., Goodier, S.P., Payne, M.J., Preston, W.H., Warrens, C.P., Ortiz, M., Zink, U., Goersmann, C., Twigg, M.V., Walker, A.P., 2006. Driving down on-highway particulate emissions. Society of Automotive Engineers SAE Paper No. 2006-01-0916.

Lapuerta, M., Armas, O., Rodríguez-Fernández, J., 2008. Effect of biodiesel fuels on diesel engine emissions. Progress in Energy and Combustion Science 34(2), 198-223.

Li, N., Sioutas, C., Cho, A., Schmitz, D., Misra, C., Sempf, J., Wang, M.Y., Oberley, T., Froines, J., Nel, A., 2003. Ultrafine particulate pollutants induce oxidative stress and mitochondrial damage. Environmental Health Perspectives 111(4), 455-460.

Lim, M.C.H., Ayoko, G.A., Morawska, L., Ristovski, Z.D., Jayaratne, E.R., 2007. Influence of fuel composition on polycyclic aromatic hydrocarbon emissions from a fleet of in-service passenger cars. Atmospheric Environment 41(1), 150-160.

Limbach, L.K., Wick, P., Manser, P., Grass, R.N., Bruinink, A., Stark, W.J., 2007. Exposure of engineered nanoparticles to human lung epithelial cells: Influence of chemical composition and catalytic activity on oxidative stress. Environmental Science & Technology 41(11), 4158-4163.

Majewski, W.A., 2007. Diesel Emission Control. Dieselnet technology guide, Ecopoint Inc, http://www.dieselnet.com/tech/engine_control.html, last accessed 3rd May 2011.

Mayer, A., Czerwinski, J., Ulrich, A., Wichser, A., Kasper, M., Mooney, J., 2010. Metal-oxide particles in combustion engine exhaust. Society of Automotive Engineers SAE Paper No. 2010-01-0792.

Meyer, N.K., Ristovski, Z.D., 2007. Ternary nucleation as a mechanism for the production of diesel nanoparticles: experimental analysis of the volatile and hygroscopic properties of diesel exhaust using the volatilization and humifidication tandem differential mobility analyzer. Environmental Science & Technology 41(21), 7309-7314.

Mi, H.H., Lee, W.J., Tsai, P.J., Chen, C.B., 2001. A comparison on the emission of polycyclic aromatic hydrocarbons and their corresponding carcinogenic potencies from a

vehicle engine using leaded and lead-free gasoline. Environmental Health Perspectives 109(12), 1285-1290.

Micallef, A.S., Blinco, J.P., George, G.A., Reid, D.A., Rizzardo, E., Thang, S.H., Bottle, S.E., 2005. The application of a novel profluorescent nitroxide to monitor thermo-oxidative degradation of polypropylene. Polymer Degradation and Stability 89(3), 427-435.

Miljevic, B., Fairfull-Smith, K.E., Bottle, S.E., Ristovski, Z.D., 2010a. The application of profluorescent nitroxides to detect reactive oxygen species derived from combustion-generated particulate matter: Cigarette smoke - A case study. Atmospheric Environment 44(18), 2224-2230.

Miljevic, B., Heringa, M.F., Keller, A., Meyer, N.K., Good, J., Lauber, A., Decarlo, P.F., Fairfull-Smith, K.E., Nussbaumer, T., Burtscher, H., Prevot, A.S.H., Baltensperger, U., Bottle, S.E., Ristovski, Z.D., 2010b. Oxidative Potential of Logwood and Pellet Burning Particles Assessed by a Novel Profluorescent Nitroxide Probe. Environmental Science & Technology 44(17), 6601-6607.

Nisbet, I.C.T., LaGoy, P.K., 1992. Toxic equivalency factors (TEFS) for polycyclic aromatic-hydrocarbons (PAHS) Regulatory Toxicology and Pharmacology 16(3), 290-300.

Petry, T., Schmid, P., Schlatter, C., 1996. The use of toxic equivalency factors in assessing occupational and environmental health risk associated with exposure to airborne mixtures of polycyclic aromatic hydrocarbons (PAHs). Chemosphere 32(4), 639-648.

Pope, C.A., III, Burnett, R.T., Thun, M.J., Calle, E.E., Krewski, D., Ito, K., Thurston, G.D., 2002. Lung cancer, cardiopulmonary mortality, and long-term exposure to fine particulate air pollution. JAMA-Journal of the American Medical Association 287(9), 1132-1141.

Ristovski, Z.D., Jayaratne, E.R., Lim, M., Ayoko, G.A., Morawska, L., 2006. Influence of diesel fuel sulfur on nanoparticle emissions from city buses. Environmental Science & Technology 40(4), 1314-1320.

Robert Bosch GmbH, 2007. Automotive handbook, 7th edition. John Wiley Inc, Chichester, pp. 1-1192.

Schaberg, P.W., Zarling, D.D., Waytulonis, R.W., Kittelson, D.B., 2002. Exhaust particle number and size distributions with conventional and Fischer-Tropsch diesel fuels. Society of Automotive Engineers SAE Paper No. 2002-01-2727.

Sklorz, M., Briedé, J.J., Schnelle-Kreis, J., Liu, Y., Cyrys, J., de Kok, T.M., Zimmermann, R., 2007. Concentration of oxygenated polycyclic aromatic hydrocarbons and oxygen free radical formation from urban particulate matter. Journal of Toxicology and Environmental Health-Part A-Current Issues 70(21), 1866-1869.

Surawski, N.C., Miljevic, B., Roberts, B.A., Modini, R.L., Situ, R., Brown, R.J., Bottle, S.E., Ristovski, Z.D., 2010a. Particle Emissions, Volatility, and Toxicity from an Ethanol Fumigated Compression Ignition Engine. Environmental Science & Technology 44(1), 229-235.

Surawski, N.C., Ristovski, Z.D., Brown, R.J., Situ, R., 2010b. Gaseous and particle emissions from an ethanol fumigated compression ignition engine. Submitted to Energy Conversion and Management.

Vaaraslahti, K., Virtanen, A., Ristimäki, J., Keskinen, J., 2004. Nucleation mode formation in heavy-duty diesel exhaust with and without a particulate filter. Environmental Science & Technology 38(18), 4884-4890.

5.5 Supporting information

Table S 5.1: Engine specifications.

Item	Specification
Model	Perkins 1104C-44
Cylinders	4 in-line
Capacity (L)	4.41
Bore × stroke (mm)	105 × 127
Maximum power (kW/rpm)	64/2400
Maximum torque (Nm/rpm)	302/1400
Compression ratio	19.25:1
Aspiration	Naturally aspirated
Emissions certification	EU Stage II non-road

Table S 5.2: Speed and load settings investigated in this study.

Mode number	Speed (rpm)	Load (%)
1	1400 (Intermediate)	50
2	1400 (Intermediate)	100
3	2400 (Rated)	50
4	2400 (Rated)	100

Table S 5.3: Fuel specifications.

Property	ULSD	B20	Synthetic
Density (kg/L) ASTM D4052	0.8354	0.8393	0.8308
Kinematic viscosity (mm^2/s) @ 40 ^oC ASTM D445	2.7189	3.1228	3.2195
Flash point (^oC) ASTM D93	66.5	71.5	73.5
Distillation (^oC) ASTM D86			
10%	205	220	225
50%	266	289	277
90%	327	335	335
95%	340	344	344
Calculated cetane index ASTM D4737	51.6	55.2	57.4
Sulphur content (mg/kg) ASTM D 5453	4.5	5.9	5.0
Carbon (% mass) ASTM D5291	84.6	85.4	84.2
Hydrogen (% mass) ASTM D5291	14.2	13.4	14.4
Water and sediment (% volume) ASTM D2709	< 0.01	< 0.01	< 0.01
Polycyclic aromatic hydrocarbons (% mass) IP 391	1.2	0.96	1.5
Fatty Acid Methyl Ester content (% volume) EN 14078	-	19.6	-
Acid number ASTM D664 (mg KOH/g)	-	0.07	-

Table S 5.4: Tabulated results for all emissions parameters reported in this study. Uncertainties are calculated as ± one standard error of the mean. NC denotes that the standard error was not computed as the measurement was not replicated.

Fuel	Speed/load (rpm/%)	Injection configuration	Primary Dilution Ratio	Secondary Dilution Ratio	Total Dilution Ratio	$PM_{2.5}$ (g/kWh)	Particle number concentration (#/cm^3)	CMD (nm)	ROS (nmol/mg)	PAHs (mg/kWh)	Organic volume percentage (%)
ULSD	1400/50	Direct Injection	26.7	10.2	270.6	0.20 ± 0.003	2.6E+14 ± 2.0E+13	72.3 ±1.6	14.2 ± 5.3	10.8 ± 7.4	0.004
ULSD	1400/100	Direct Injection	26.8	10.0	266.6	3.03 ± 0.18	1.2E+15 ± 1.3E+13	115.6 ± 0.4	0.1 ± 0.1	4.7 ± 1.8	20.2
ULSD	2400/50	Direct Injection	20.4	9.8	163.7	0.25 ± 0.01	1.0E+15 ± 2.3E+13	68.3 ± 0.3	12.1 ± 2.7	5.8 ± 0.5	0.2
ULSD	2400/100	Direct Injection	14.2	10.7	151.6	0.68 ± 0.01	1.3E+15 ± 8.0E+13	82.0 ± 0.3	3.8 ± 0.9	7.0 ± 1.8	0.8
B20	1400/50	Direct Injection	30.1	9.6	288.6	0.16 ± 0.02	2.3E+14 ± 1.7E+12	71.7 ±2.2	32.8 ± 17.8	9.1 ± 8.2	17.6
B20	1400/100	Direct Injection	30.0	9.7	290.9	2.16 ± 0.11	1.1E+15 ± 1.4E+13	109.9 ± 1.7	2.1 ± 1.0	5.1 ± 4.6	14.1
B20	2400/50	Direct Injection	17.3	11.4	197.0	0.22 ± 0.01	1.1E+15 ± 4.3E+13	67.5 ± 1.4	18.6 ± 8.3	21.5 ± 9.7	20.1

B20	2400/100	Direct Injection	16.7	10.5	175.0	0.55 ± 0.002	1.3E+15 ± 9.5E+12	79.0 ± 0.7	0.9 ± 0.9	3.2 ± 0.3	31.4
Synthetic	1400/50	Direct Injection	38.1	8.2	313.6	0.20 ±0.01	2.4E+14 ± 1.5E+13	71.9 ±0.6	27.8±3.3	10.2 ± 7.5	1.0
Synthetic	1400/100	Direct Injection	41.2	7.9	326.3	3.38 ± 0.07	1.1E+15 ± 3.3E+13	120.0 ± 0.4	1.1± 0.3	6.6 ± 3.8	10.9
Synthetic	2400/50	Direct Injection	21.1	9.2	192.5	0.29 ± 0.01	9.1E+14 ± 4.3E+13	69.9 ± 0.3	8.4 ± 2.1	20.9 ± 9.6	0.4
Synthetic	2400/100	Direct Injection	21.3	9.2	196.2	0.81 ± 0.005	1.3E+15 ± 6.4E+13	86.0 ± 0.4	2.1 ± 0.9	28.7 ± 28.3	6.1
ULSD	1400/50	Common Rail	24.5	8.1	198.2	0.048 ± 0.03	1.2E+14 ± 2.8E+12	68.1 ± 0.6	284.1 ± NC	28.6 ± NC	3.2
ULSD	1400/100	Common Rail	26.6	8.8	234.4	1.59 ± 0.17	8.6E+14 ± 5.2E+13	120.8 ± 2.8	7.9 ± NC	26.8 ± 5.8	10.7
ULSD	2400/50	Common Rail	15.8	9.9	155.4	0.36 ± 0.03	2.1E+14 ± 6.6E+12	60.9 ± 0.9	149.0 ± NC	16.9 ± 9.5	0.8
ULSD	2400/100	Common Rail	16.2	9.2	148.5	0.805 ± 0.12	1.3E+15 ± 4.7E+13	91.9 ± 1.3	13.2 ± NC	6.4 ± 2.6	12.5
B20	1400/50	Common Rail	19.9	10.9	215.1	0.029 ± 0.05	9.1E+13 ± 9.4E+12	65.8 ± 1.2	202.2 ± 43.4	7.5 ± 0.6	7.9
B20	1400/100	Common	24.5	10.3	251.4	0.972 ±	7.2E+14 ±	110.4 ±	8.1 ± 4.5	34.6 ±	38.4

		Rail				0.14	5.9E+13	0.3		20.8	
B20	2400/50	Common Rail	16.9	10.7	180.7	0.028 ± 0.04	1.7E+14 ± 2.4E+13	58.3 ± 0.03	233.0 ± 8.7	14.0 ± NC	11.7
B20	2400/100	Common Rail	17.5	9.63	168.6	0.538 ± 0.10	1.1E+15 ± 5.2E+13	84.8 ± 0.5	5.1 ± 2.9	14.7 ± 11.7	36.3
Synthetic	1400/50	Common Rail	28.8	6.9	200.1	0.035 ±0.03	7.9E+13 ± 1.2E+13	66.9 ±1.2	139.9 ±139.9	10.5 ±NC	35.7
Synthetic	1400/100	Common Rail	32.5	8.4	272.4	0.954 ± 0.11	6.3E+14 ± 2.6E+13	113.2 ± 0.4	6.2 ± 0.1	29.7 ± NC	56.9
Synthetic	2400/50	Common Rail	18.3	9.5	175.2	0.030 ± 0.03	1.6E+14 ± 2.0E+12	60.2 ± 0.7	358.4 ± 21.1	80.4 ± NC	30.5
Synthetic	2400/100	Common Rail	20.2	9.3	188.8	0.522 ± 0.03	9.7E+14 ± 2.2E+13	89.9 ± 1.0	12.7 ± 2.1	5.9 ± NC	54.3

Table S 5.5: Weighting factors for the 4 mode test cycle adopted in this study.

Mode number	Speed (rpm)	Load (%)	ECE R49 weighting	Test cycle averaging (this study)
1	1400	50	0.08	0.178
2	1400	100	0.25	0.556
3	2400	50	0.02	0.044
4	2400	100	0.10	0.222

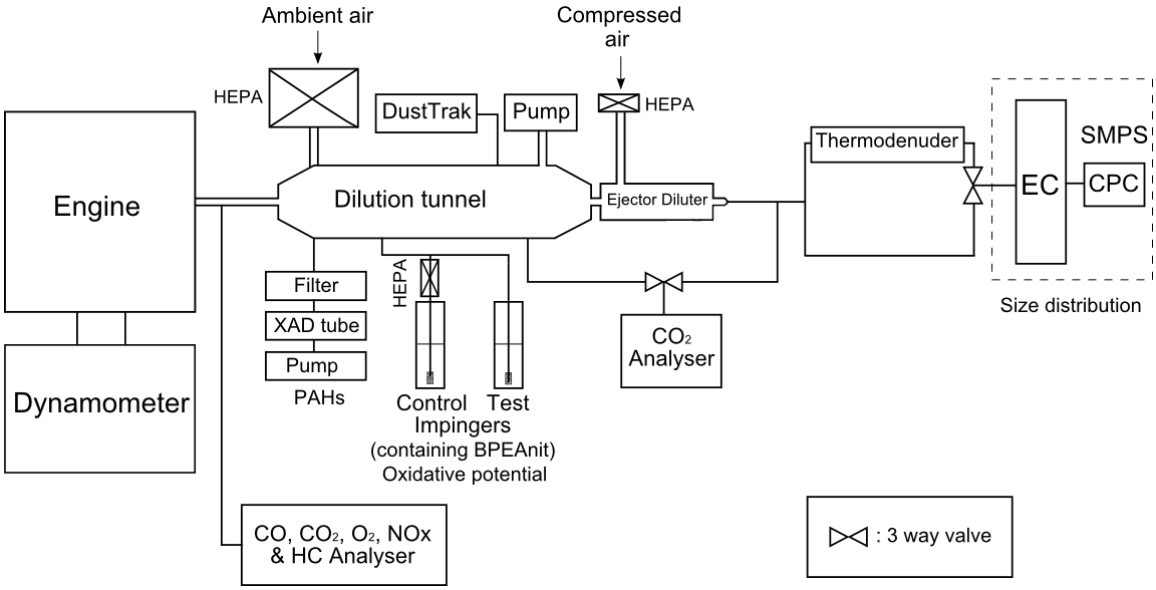

Figure S 5.1: A schematic of the experimental set-up utilised in this study.

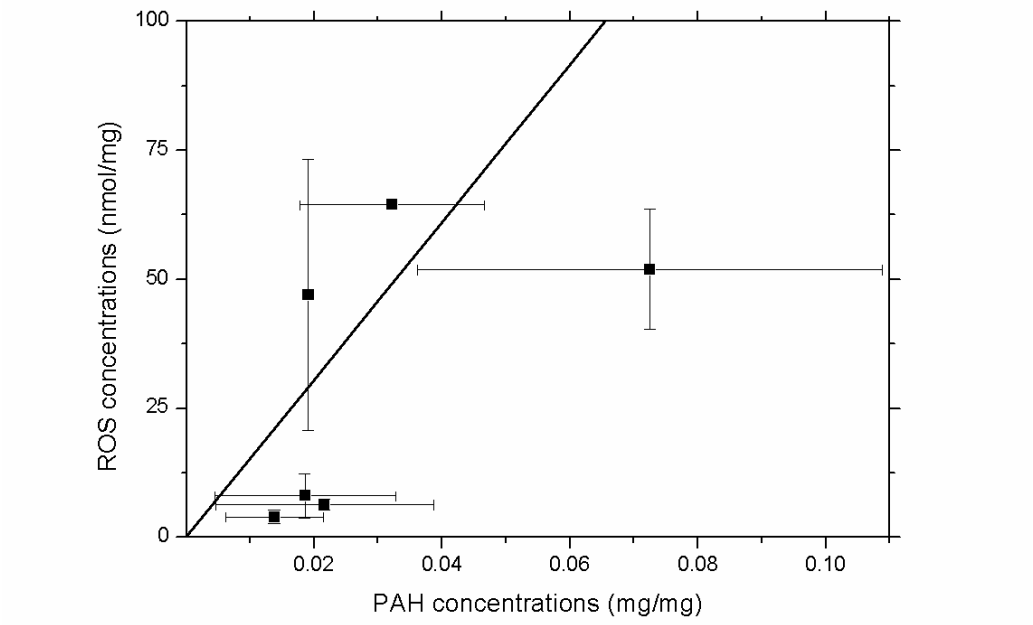

Figure S 5.2: A graph demonstrating correlation between the ROS and PAH measurements. Note: both the PAHs and ROS are expressed on a per unit mg of DPM basis. The Pearson correlation co-efficient, $\boldsymbol{r}$, is 0.913.

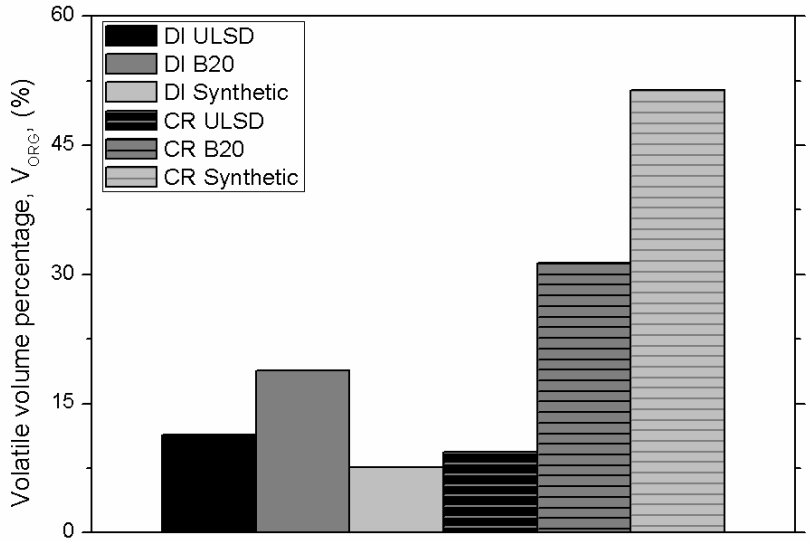

Figure S 5.3: Test cycle averaged volatile volume percentage of particles for both injection technologies, and all three fuels.

Chapter 6: A physico-chemical characterisation of particulate emissions from a compression ignition engine: the influence of biodiesel feedstock

N.C. Surawski[a,b], B. Miljevic[a,d], G.A. Ayoko[c], S. Elbagir[c], S. Stevanovic[a,d], K.E. Fairfull-Smith[d], S.E. Bottle[d], Z.D. Ristovski[a]

[a]International Laboratory for Air Quality and Health, Queensland University of Technology, 2 George St, Brisbane QLD 4001, Australia

[b]School of Engineering Systems, Queensland University of Technology, 2 George St, Brisbane QLD 4001, Australia

[c]Discipline of Chemistry, Queensland University of Technology, 2 George St, Brisbane QLD 4001, Australia

[d]ARC Centre of Excellence for Free Radical Chemistry and Biotechnology, Queensland University of Technology, 2 George St, 4001 Brisbane, Australia

Publication: Under review with Environmental Science & Technology, 2011.

Contributor	Statement of contribution
Nicholas C. Surawski Signature Date 21/10/11	Contributed to the experimental design, conducted particle number size distribution and mass measurements, performed data analysis, wrote most of the manuscript.
Branka Miljevic	Contributed to the experimental design, conducted measurements, data analysis, and manuscript writing related to the BPEAnit assay.

Godwin A. Ayoko	Involved with the PAH measurement experimental design, data analysis and manuscript writing.
Sohair Elbagir	Involved with the PAH extraction and quantification, and also data analysis.
Svetlana Stevanovic	Assisted with ROS measurements, and data analysis.
K.E. Fairfull-Smith	Reviewed manuscript.
Steven E. Bottle	Reviewed the manuscript.
Zoran D. Ristovski	Contributed to the experimental design, data analysis, and manuscript writing.

Principal Supervisor Confirmation

I have sighted email or other correspondence from all Co-authors confirming their certifying authorship.

Associate Professor Zoran Ristovski		21/10/11
Name	**Signature**	**Date**

Abstract

This study undertook a physico-chemical characterisation of particle emissions from a single compression ignition engine operated at one test mode with 3 biodiesel fuels made from 3 different feedstocks (i.e. soy, tallow and canola) at 4 different blend percentages (20%, 40%, 60% and 80%) to gain insights into their particle-related health effects. Particle physical properties were inferred by measuring particle number size distributions both with and without heating within a thermodenuder (TD) and also by measuring particulate matter (PM) emission factors with an aerodynamic diameter less than 10 μm (PM_{10}). The chemical properties of particulates were investigated by measuring particle and vapour phase Polycyclic Aromatic Hydrocarbons (PAHs) and also Reactive Oxygen Species (ROS) concentrations. The particle number size distributions showed strong dependency on feedstock and blend percentage with some fuel types showing increased particle number emissions, whilst others showed particle number reductions. In addition, the median particle diameter decreased as the blend percentage was increased. Particle and vapour phase PAHs were generally reduced with biodiesel, with the results being relatively independent of the blend percentage. The ROS concentrations increased monotonically with biodiesel blend percentage, but did not exhibit strong feedstock variability. Furthermore, the ROS concentrations correlated quite well with the organic volume percentage of particles – a quantity which increased with increasing blend percentage. At higher blend percentages, the particle surface area was significantly reduced, but the particles were internally mixed with a greater organic volume percentage (containing ROS) which has implications for using surface area as a regulatory metric for diesel particulate matter (DPM) emissions.

6.1 Introduction

Alternative fuels, such as biodiesel, are currently being investigated not only to address global warming (Agarwal, 2007) but also to reduce DPM emissions (McCormick, 2007). Whilst a considerable database exists describing the impact of different transesterified biodiesel fuel types on regulated emissions (i.e. PM, NOx, CO and HCs) (United States Environmental Protection Agency, 2002a; Lapuerta et al., 2008b), limited information is available addressing the impact of different biodiesel fuel types on other particle emission properties, such as particle number and size. Regulated emissions from compression ignition engines typically exhibit strong dependencies on both feedstock and blend percentage. With PM emissions (for example), animal fat based biodiesel gives greater PM reductions than soy based biodiesel, and the PM reductions exhibit a non-linear reduction with respect to blend percentage (United States Environmental Protection Agency, 2002a). Given these results, it

is quite likely that particle emissions will display similar dependencies. At present, a detailed database is not in existence characterising the unregulated physico-chemical characteristics of DPM such as: particle number emission factors, particle size distributions, surface area as well as PAHs and ROS with different biodiesel feedstocks and blend percentages. Consequently, a primary objective of this study was to explore the physico-chemical properties of particle emissions from 3 biodiesel feedstocks tested at 4 different blend percentages to shed light on their potential health impacts.

A combination of physical and chemical factors influences the health effects of DPM (Giechaskiel et al., 2009), where it is noted with biodiesel combustion that the particles have a much higher organic fraction (Knothe et al., 2006). The organic fraction of DPM includes many compounds that are deleterious to human health such as PAHs and ROS (Sklorz et al., 2007). Previous research has demonstrated a correlation between the semi-volatile organic component (i.e. they partition between the gas and particle phase) of particles and their oxidative potential for DPM (Biswas et al., 2009), and also for wood smoke particles (Miljevic et al., 2010b). Furthermore, a correlation has been demonstrated between the oxidative potential of particles and also PAH emission factors (Cheung et al., 2010; Surawski et al., 2011b). Typically, the chemical properties of particulate emissions, such as PAHs and ROS are detected using off-line analytical chemistry techniques. The development of a near real-time technique enabling the detection of semi-volatile organic compounds would be quite useful, given their importance in assessing the health effects of DPM. As PAHs and ROS are both classed as semi-volatile organic compounds, it is therefore possible that heating diluted exhaust within a TD will provide near real-time qualitative information on the presence of these components. As a result, a secondary objective of this work was to assess whether on-line measurements of the organic volume percentage (V_{ORG}) of DPM can provide information on genotoxic compounds on the surface of the particle that are usually measured using off-line analytical chemistry techniques. To achieve this objective, the relationship between V_{ORG} and ROS concentrations is explored.

Historically, the regulation of DPM emissions has been achieved using a mass-based emissions standard (Dieselnet, 2009), however, a particle number standard for heavy duty diesel engines will be introduced in the European Union at the Euro VI stage (Dieselnet, 2009). Whilst there have been studies suggesting that particle number emissions correlate with respiratory (Peters et al., 1997) and cardio-vascular (Pekkanen et al., 2002) morbidity

from DPM more adequately than particle mass; toxicological studies have shown a strong inflammatory response from inert ultrafine particles in a size-dependent manner (Brown et al., 2001; Oberdörster, 2001). Consequently, the toxicological literature suggests that particle surface area could be a relevant metric for assessing DPM health effects. Given that DPM is quite often composed of a solid elemental carbon core with internally mixed semi-volatile organics (Maricq, 2007), a surface area based metric would provide information on the ability of toxic organic compounds to adsorb or condense on the surface of the particle. Consequently, a third objective of this work was to critically examine whether regulation of the DPM surface area emitted by a compression ignition engine has merit. All of the research objectives have been undertaken by investigating particle emissions from a non-road diesel engine operated with various biodiesel feedstocks and blend percentages.

6.2 Methodology

6.2.1 Engine and fuel specifications

Particulate emissions testing was performed on a naturally aspirated 4 cylinder Perkins 1104C-44 engine with a Euro II (off-road) emissions certification. The engine investigated is typical of those used in underground mines in Australia, and is the same engine used in Surawski et al. (*11*). The engine was coupled to a Heenan & Froude water brake dynamometer (DPX 4) to provide a load to the engine.

Ultra-low sulfur diesel (denoted ULSD hereafter, < 10 ppm sulfur) was used as the baseline fuel in this experiment, along with 13 biodiesel blends from 3 different feedstocks, all of which were commercially available in Australia. All blends were prepared using calibrated graduated cylinders using a single batch of ULSD. The 3 biodiesel feedstocks investigated were soy, tallow and canola, with each feedstock being investigated at 4 different blend percentages, namely: 20%, 40%, 60% and 80%. The opportunity arose during testing to undertake particle physical measurements with neat (i.e. 100%) soy biodiesel. The notation "BX" denotes that X% is the percentage (by volume) of the total blend made from biodiesel. In total, 14 different fuel types were investigated in this study, all of which were undertaken at intermediate (i.e. 1400 rpm) speed full load. This test mode has the highest weighting in the ECE R49 test cycle introduced for Euro II engines, and hence was selected for investigation in this study as it is the most representative mode from this test cycle (Dieselnet, 2006a) . Particle physical measurements were made with all 14 fuel types, whereas particle chemical measurements were only made for ULSD, B20, and B80 blends made with each

biodiesel feedstock. Further details on the engine specifications, the daily warm-up and oil changing procedure can be found in Surawski et al. (Surawski et al., 2011b).

6.2.2 Particulate emissions measurement methodology

The methodology used for diluting the exhaust sample follows that of Surawski et al. (Surawski et al., 2010b), and consists of a partial flow dilution tunnel followed by a Dekati ejector diluter. The methodology for measuring particle number size distributions follows that of Surawski et al. (Surawski et al., 2010b), however a TSI 3010 condensation particle counter (CPC) was used instead of a TSI 3782 CPC. The methodology for measuring ROS is identical to that used in Surawski et al. (Surawski et al., 2010b). Particle volatility was explored by passing the poly-disperse size distribution through a TSI 3065 TD set to 300 ^{o}C. A correction for TD diffusional losses was performed using dried sodium chloride (NaCl) particles produced by an atomiser. The TD loss curve was obtained by measuring the NaCl particle number size distribution upstream and downstream of the TD (set to 300 ^{o} C) by switching the flow with a 3-way valve, and then calculating the proportion of particles lost (η_{loss}) via: $\eta_{loss} = (1 - \frac{PN_{downstream}}{PN_{upstream}})$, where PN denotes particle number concentration. PM_{10} measurements were obtained with a TSI 8520 DustTrak and were converted to a gravimetric measurement using the tapered element oscillating microbalance to DustTrak correlation for DPM obtained by Jamriska et al. (Jamriska et al., 2004). The particle mass and number size distributions were all measured after the second stage of dilution.

Measurements of particle phase and vapour phase PAHs were also performed. 2-bromo-naphthalene and the following US EPA priority PAHs in dichloromethane were quantified with a Gas-Chromatography Mass-Spectrometry (GC-MS) system: Naphthalene, Acenaphthylene, Acenaphthene, Fluorene, Phenanthrene, Anthracene, Fluoranthene, Pyrene, Benzo(a) anthracene, Chrysene, Benzo(b)fluoranthene, Benzo(a)pyrene, Indeno(1,2,3-cd)pyrene, Dibenzo(a,h)anthracene, and Benzo(g,h,i)perylene. The methodology for sampling and quantification following guidelines presented in Lim et al. (2007b), and further information on the extraction procedure and the GC-MS system can be found in (Surawski et al., 2011b). Particle phase PAHs were collected on filters and vapour phase PAHs were collected in tubes containing XAD-2 adsorbent prior to their quantification using the GC-MS system.

An *in vitro* cell-free assay was used to determine the oxidative capacity of particles, hereafter, referred to as ROS concentrations (inferred from fluorescence measurements) (Miljevic et al., 2010a). For the ROS measurements, particles were bubbled through impingers (a test impinger, and a HEPA filtered control impinger) containing 20 ml of 4 μM BPEAnit solution, using dimethylsulphoxide (DMSO) as a solvent. More details on the ROS sampling and quantification methodology such as: the impinger collection efficiency, nitroxide probe theory and its application to various combustion sources can be found in Miljevic et al. (Miljevic et al., 2009b; Miljevic et al., 2010a; Miljevic et al., 2010b). All the ROS results were normalised to the gravimetric PM_{10} mass to give ROS concentrations in units of nmol/mg.

Measurements of particle and vapour phase PAHs and ROS were made from the dilution to enable sufficiently high concentrations for analysis. For the chemical measurements (i.e. PAHs and ROS) five replicates were used for ULSD and B80 soy, whereas for the other fuel types (B20 and B80 tallow and canola and B20 soy) three replicates were obtained. A diagram of the complete experimental set-up can be found in the supplementary information from Surawski et al. (Surawski et al., 2011b).

6.2.3 Data analysis

Particles from biodiesel combustion usually exhibit a higher semi-volatile organic fraction (Knothe et al., 2006). As a result, heating biodiesel combustion particles with a TD should lead to a greater reduction in particle size compared with heating DPM. To quantify the volume reduction of particles upon heating with a TD, V_{ORG} (see Figure 6.7) was calculated from integrated particle volume size distributions obtained with a Scanning Mobility Particle Sizer (SMPS) via:

$$V_{ORG}\,(\%) = 100\left(\frac{V_{raw} - V_{TD}}{V_{raw}}\right), \tag{6.1}$$

where: V_{raw} is the particle volume for unheated particles, V_{TD} is the particle volume for particles passed through a TD set to 300 ^{o}C. The assumption of spherical particles was made when performing calculations with equation (6.1).

Raw results reporting the physico-chemistry of DPM for all 14 fuel types along with dilution ratios can be found in Table S 6.1.

6.3 Results and discussion

6.3.1 PM_{10} emission factors

Figure 6.1 displays the brake-specific PM10 emission factors for all 14 fuel types investigated in this study. This figure shows that PM_{10} emission factors decrease in a monotonic fashion with respect to biodiesel blend percentage, and that the PM_{10} emissions are also strongly dependent on biodiesel feedstock. For the soy feedstock, PM_{10} reductions range from 43% with B20 to 92% with B100, reductions in PM10 range from 58% for B20 to 88% for B80 for the tallow feedstock, whereas for the canola feedstock, the reductions range from 65% with B20 to 88% for B80. The observation of very large reductions in particulate matter emissions with biodiesel is a very commonly reported result in the biodiesel literature (United States Environmental Protection Agency, 2002a; Lapuerta et al., 2008b), with the results from this study confirming this general trend.

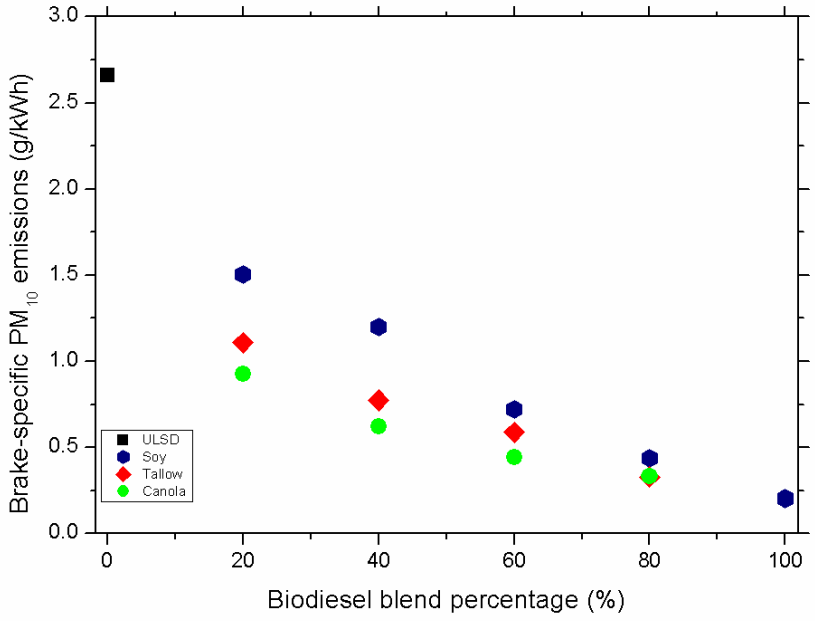

Figure 6.1: Brake specific PM_{10} emission factors (g/kWh) for the 14 fuel types investigated in this study.

6.3.2 Particle number emission factors

Figure 6.2 shows brake-specific particle number emission factors (#/kWh) for all 14 fuel types. The results show a strong dependency on both biodiesel feedstock and blend percentage. For the soy feedstock, particle number reductions range from 4% (B40) to 53% (B100), whilst for B20 a 12% particle number increase occurs. Particle number increases range from 71% (B20) to 44% (B80) for the canola feedstock. For the tallow feedstock, particle number increases range from 7% (B20) to 25% (B40), whilst a particle number reduction of 14% occurs for B80.

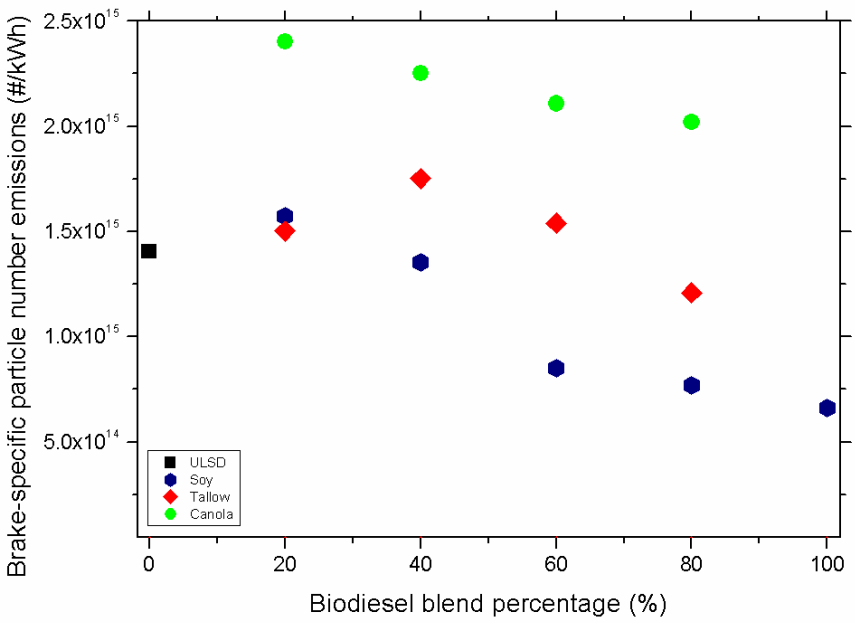

Figure 6.2: Brake-specific particle number emissions (#/kWh) for the 14 fuel types investigated in this study.

A puzzling result to emerge from this study was the non-monotonic trends in particle number emissions with respect to blend percentage. For all 3 feedstocks, a 20% blend increased particle number emissions, and for subsequent increases in blend percentage, the particle number emissions decreased. An exception to this trend was the tallow feedstock, which produced increased particle number emission for both 20% and 40% blends followed by subsequent decreases in particle number emissions with further increases in blend percentage. Non-monotonic particle number emissions (relative to ULSD) with increasing blend percentages were observed by Di et al. (2010b), where the particle number increases were reduced as the diethylene glycol dimethyl ether blend (an oxygenated alternative fuel) percentage was increased. Di et al. (Di et al., 2010a) suggested that particle oxidation kinetics were responsible for this result, with oxidation being suppressed at low blend percentages (giving particle number increases) and oxidation being promoted at high blend percentages (giving particle number reductions). This is a finding that should be investigated further with other biofuels. Given the absence of combustion-related diagnostic data, it is quite difficult to provide a detailed mechanistic description of this result at this stage.

Variability in regulated emissions from compression ignition engines (i.e. PM, NOx, CO and HCs) employing various biodiesel feedstocks is a topic that has been addressed fairly comprehensively in the diesel emissions literature (Durbin et al., 2000; Wang et al., 2000; United States Environmental Protection Agency, 2002a). The variability of particle number

emissions with different biodiesel feedstocks, however, is a topic that has only been addressed recently (Fontaras et al., 2010b). Fontaras et al. (Fontaras et al., 2010b) found that particle number emissions could be higher for biodiesel (by up to a factor of 3) due to the occurrence of nucleation with soy blends, however, reductions in particle number were achieved with other biodiesel feedstocks (such as palm and used frying oil methyl esters). The observation of variability in particle number emissions with different biodiesel feedstocks has implications for conducting future biodiesel studies as this suggests that measurements should be conducted on an individual basis, rather than assuming generalisable trends with different feedstocks.

6.3.3 Particle number size distributions

Particle number size distributions for all 14 fuel types are shown in Figure 6.3; with all size distributions showing uni-modality with a peak only in the accumulation mode. It can be seen from this graph that fuel type and blend percentage have varying effects on the observed particle number size distribution. Whilst all fuel types display a shift to smaller particle diameters; the number of particles emitted is greater than that emitted by ULSD for all 4 canola blends, it is greater than ULSD for 2 tallow blends (less than ULSD for 2 blends), and it is greater than ULSD for only one soy blend (less than ULSD for the other 4 blends). Another feature evident from the particle number size distributions is that all biodiesel fuel types are particularly effective at reducing particle number concentrations at larger mobility diameters (> 200 nm); however, for smaller mobility diameters (< 50 nm) the number concentration of nanoparticles emitted is increased – especially for the canola and tallow fuel types. Overall, the size distribution results presented here are quite different to those that are commonly reported, since increases in the accumulation mode particle concentrations are observed without the occurrence of nucleation. This effect is particularly evident for the canola blends, but also for the lower percentage tallow blends (B20-B60), and also for one soy blend (B20).

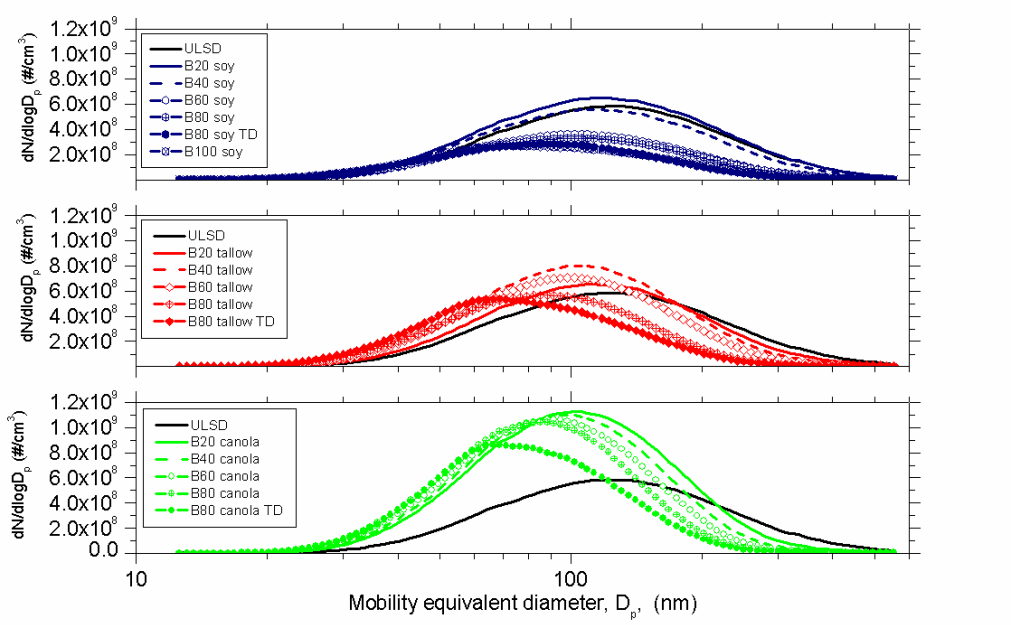

Figure 6.3: Particle number size distributions (corrected for dilution) for all fourteen fuel types (top panel: soy feedstock, middle panel: tallow feedstock, bottom panel: canola feedstock). TD denotes tests where diesel aerosol was passed through a TD set to 300 ^{o}C.

A significant reduction in the count median diameter (CMD) of particles occurs as the biodiesel blend percentage is increased, which is a result that is commonly reported (but is certainly not a universal trend) in the biodiesel literature (Lapuerta et al., 2008b). Canola blends (B20-B80) exhibit the largest reduction in CMD (19-33 %), followed by tallow (10-30 %); with soy blends showing the smallest reduction in CMD (6-19 %) (see Figure 6.4). Factors that could contribute to a reduced CMD with biodiesel include: the relative ease with which the biodiesel particle surface can be oxidised (Jung et al., 2006a) and also structural compaction of the particles (Smekens et al., 2007). Structural compaction of particles (characterised by particles having a higher fractal dimension) would reduce the drag force on particles in a differential mobility analyser which could reduce a particle's transit time hence providing a reduction in the particle's electrical mobility diameter.

The particle number size distributions whereby diesel aerosol was passed through a TD (shown in Figure 6.3 for the B80 blends) can also offer information on the mixing state of particles. Heating the particles with a TD led to a reduction in the median size of particles without a reduction in particle number for all feedstocks (except canola), which suggests that the semi-volatile organic component of particles for the soy and tallow feedstocks are present as an internal mixture. Alternatively, for the canola feedstock, a reduction in particle number occurred in addition to a reduction in particle size which suggests that the presence of an

external mixture of some purely volatile particles, in addition to some partially volatile particles for this fuel type. The presence of an external mixture containing some fully volatile organic compounds for the canola blends has implications for DPM health effects, as inflammation and oxidative stress (precursors to some cardiovascular and respiratory diseases) are more heavily driven by the presence of organic compounds, rather than inert substances, such as soot (Nel, 2005; Ayres et al., 2008).

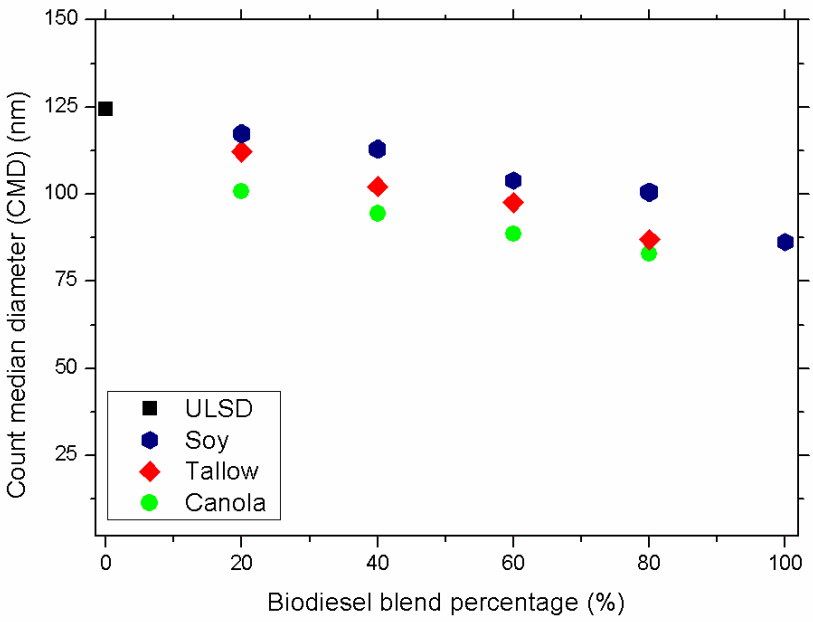

Figure 6.4: Count median diameter of particles (derived from a particle number size distribution) for all fourteen fuel types.

6.3.4 PAH emission factors and ROS concentrations

Figure 6.5 displays the particle phase and vapour phase PAH emission factors. It can be observed that both particle and vapour phase PAHs are reduced for all 6 biodiesel fuel types (relative to the ULSD results), except for the B80 soy particle phase result. Particle phase PAH reductions range from a 3.5% increase for B80 soy to a decrease of about 60% for B80 canola. Vapour phase PAH reductions range from 33% for B80 soy to 84% for B20 tallow. Overall, very strong feedstock dependency can be observed for the PAH emissions factors, with the tallow feedstock generally providing the greatest reduction in particle and vapour phase PAHs (16-84 %), followed by the canola feedstock (no change – 62 % decrease), with the soy feedstock generally providing the smallest particle and vapour phase PAH reductions (4 % increase – 59 % decrease). These results are consistent with the findings of Karavalakis et al. (Karavalakis et al., 2010a) and Ballesteros et al. (2010) who both found vastly different PAH emission profiles when the biodiesel feedstock was changed.

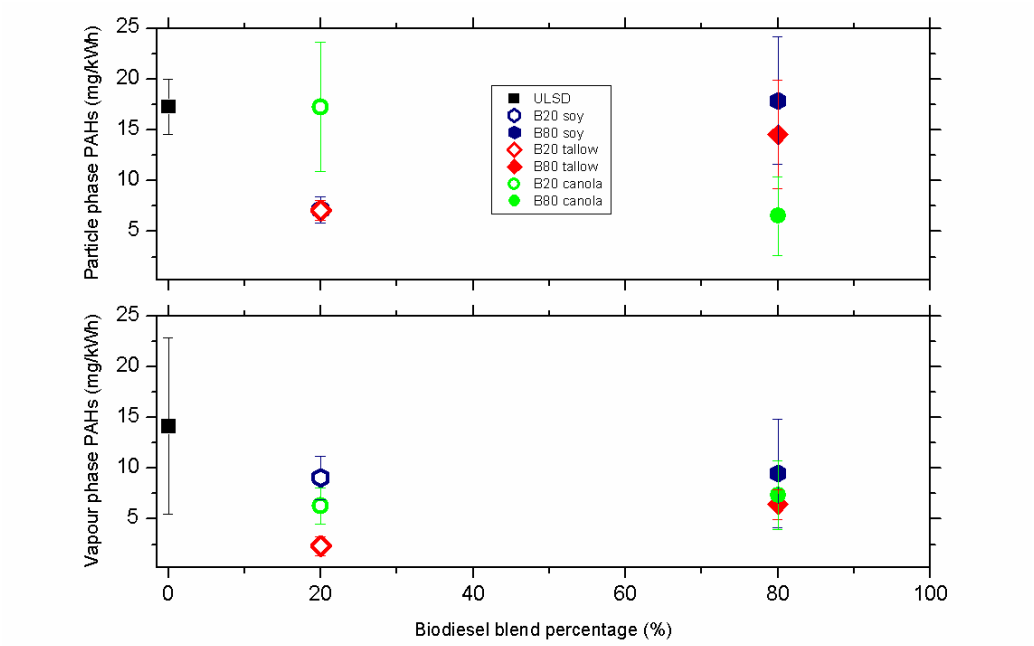

Figure 6.5: Brake-specific particle phase (top panel) and vapour phase (bottom panel) PAH emissions for the 7 fuel types where chemical analysis was performed. Error bars denote ± one standard error of the mean.

In terms of the PAH reductions with biodiesel, the USEPA (United States Environmental Protection Agency, 2002a) states that the emissions of toxics (such as PAHs) should decrease with biodiesel. This is due to the correlation between emissions of toxics and emissions of hydrocarbons - which are generally reduced with biodiesel (Lapuerta et al., 2008b). Despite the reduction in particle and vapour phase PAHs with biodiesel, a concerning result is the phase distribution of the PAHs. PAHs with a greater number of aromatic rings (and hence higher molecular weight) exist in the particle phase and have a greater carcinogenicity than lower molecular weight, gas phase PAHs (International Agency for Research on Cancer, 1987). The percentage of PAHs that are in the particle phase range from 44-75%, a result that is substantially higher than that reported by He et al. (He et al., 2010), who reported particle phase PAH percentages (i.e. of the total PAH emissions) ranging from 19 to 31% for a range of soy biodiesel blends.

Another feature that may be observed from the PAH vapour phase results is how the emissions are independent of, or do not vary significantly with, biodiesel blend percentage for the soy and canola fuel types. This experimental result was also observed by Ballesteros et al. (2010), who noted that PAH reductions with rapeseed and waste cooking oil methyl esters did not exhibit a linear reduction with biodiesel blend percentage.

ROS concentrations for the 6 fuel types where a fluorescence signal was obtained (i.e. no data for B20 soy) are shown in Figure 6.6. From Figure 6.6, it can be observed that the ROS concentrations increase with biodiesel blend percentage, although there is not strong feedstock dependency, unlike some of the particle physical measurements presented thus far (e.g. particle number emission factors). Relative to neat diesel, ROS concentrations are reduced by 21% for B20 tallow and are increased by 16% for B20 canola. For the B80 tests, the tallow feedstock increased ROS concentrations by a factor of just over 9, for the soy feedstock an almost 10-fold increase was observed, whilst the B80 canola test increased ROS concentrations by a factor of approximately 7.

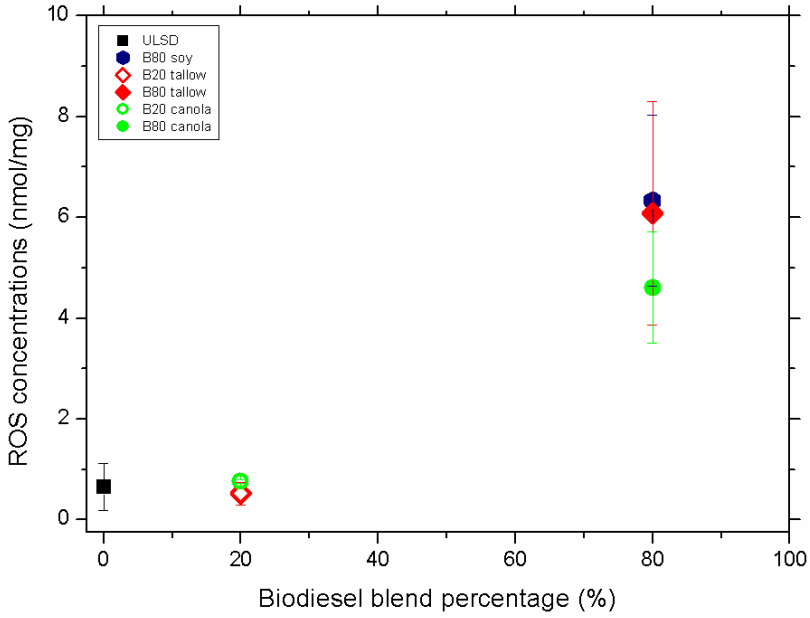

Figure 6.6: ROS concentrations (nmol/mg) for the 6 fuel types where a fluorescence signal was obtained.

6.3.5 Particle volatility and ROS correlation

ROS are generally classed as "semi-volatile" organic compounds that evaporate when exposed to thermal treatment with a TD (Miljevic et al., 2010b). Therefore, it is possible that qualitative information on ROS concentrations can be gained by investigating the volatility of particles. Equation (6.1) demonstrated how V_{ORG} could be calculated from the integrated raw (i.e. non TD) and heated (i.e. with TD) particle volumes. Figure 6.7 represents an attempt to establish a correlation between V_{ORG}, or the volatility of particles, and their associated ROS concentrations. It can be observed from this graph that as the biodiesel blend percentage is increased; particles are internally mixed with more ROS (i.e. internal mixing present for soy and tallow feedstocks but not canola) and also have a higher V_{ORG}. Despite the presence of considerable scatter in the relationship, the Pearson correlation co-efficient is quite strong (~

0.91). Consideration of the volatility of particles with a TD is, therefore, able to provide potentially useful information on ROS concentrations.

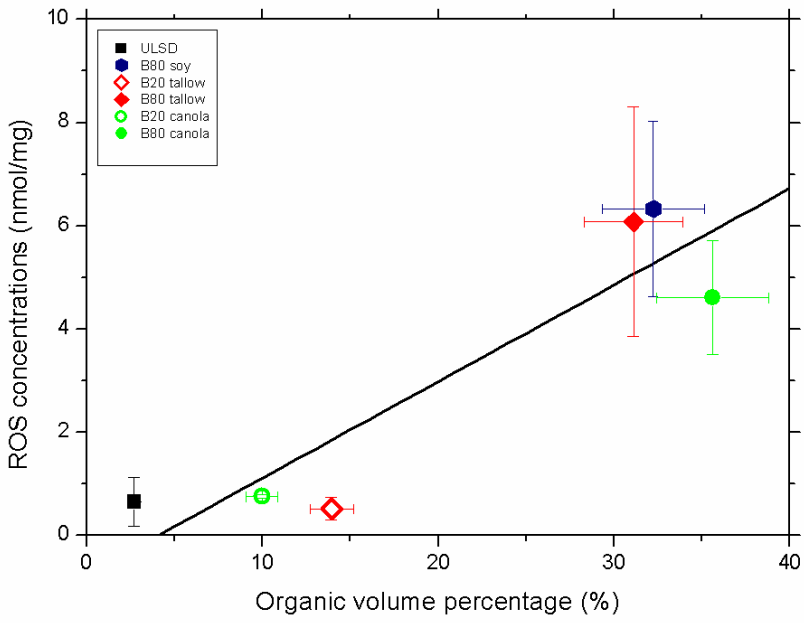

Figure 6.7: A correlation between ROS concentrations and $\boldsymbol{V_{ORG}}$ for particles.

6.3.6 Particle surface area and organic volume percentage of particles

Toxicological studies, such as (Oberdörster, 2001), have pointed to the particle surface area as a potential metric for assessing the health effects of DPM. The surface area of a particle provides a measure of the ability of toxic compounds (such as PAHs or ROS) to adsorb or condense upon it. Therefore, a particle's surface area can be viewed as a "transport vector" for many compounds deleterious to human health. Figure 6.8 shows a relationship between the heated particle surface area (i.e. heated with a TD and assuming spherical particles) and V_{ORG}, plotted with respect to biodiesel blend percentage for all fuel types investigated. The heated particle surface area is employed in Figure 6.8 as this provides a good estimate of the total surface area that is available for adsorption or condensation. With increasing biodiesel blend percentage the heated particle surface area is reduced, with reductions ranging from no change to 74 % with the soy fuel types, reductions of 14-65 % were achieved with tallow, and reductions of 15-55 % were achieved with canola fuel blends. Alternatively, as the biodiesel blend percentage is increased, the particles are composed of a greater V_{ORG}. Changes in V_{ORG} range from a 50 % reduction to a 160 % increase for soy fuel types, whilst for tallow; V_{ORG} increases are between 13-150 %, whilst for canola fuel types, V_{ORG} ranges from a 19 % decrease to a 190% increase. As was demonstrated in Figure 6.7, particles which contain a greater V_{ORG} display a concomitant increase in their ROS concentrations and

hence the ability of these particles to induce oxidative stress. This is a particularly important result, as for alternative fuels to be a viable alternative to ULSD they must be able to deliver not only a reduction in the surface area of particles emitted (without a reduction in particle size) but also a reduction of semi-volatile organics internally mixed within the particle surface.

The results presented in Figures 6.7 and 6.8 naturally have implications for the regulation of DPM exhaust emissions using a surface area based metric. Regulating only the raw particle surface area emitted by a compression ignition engine would not be able to provide meaningful information on results such as those presented in Figure 6.8, as the surface chemistry of particles is not explicitly considered. Therefore, not only the raw surface area of particles but also the surface chemistry of particles is important for assessing the health impacts of DPM. These results suggest that the development of instrumentation (and standards) that enable the internal mixing status of particles to be determined (within a surface area framework) are potentially required.

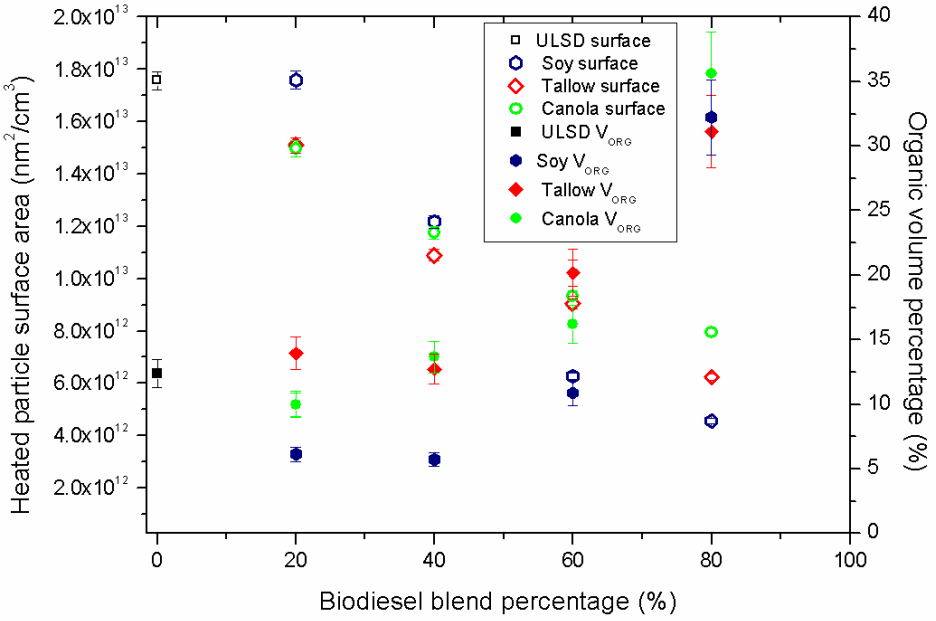

Figure 6.8: A graph showing the relationship between the heated particle surface area of DPM, and $\boldsymbol{V_{ORG}}$ for all fuel types investigated.

Acknowledgements

The authors wish to acknowledge support and funding provided by SkillPro Services Pty Ltd and the Australian Coal Association Research Program for funding project C18014. Special thanks go to Mr Julian Greenwood and Mr Dale Howard, from SkillPro Services, for their

technical expertise throughout testing, and also for operating the dynamometer and providing the gaseous emissions and diagnostic test data.

Supporting Information Available

One table constitutes the supplementary material for this manuscript.

6.4 References

Agarwal, A.K., 2007. Biofuels (alcohols and biodiesel) applications as fuels for internal combustion engines. Progress in Energy and Combustion Science 33(3), 233-271.

Ayres, J.G., Borm, P., Cassee, F.R., Castranova, V., Donaldson, K., Ghio, A., Harrison, R.M., Hider, R., Kelly, F., Kooter, I.M., Marano, F., Maynard, R.L., Mudway, I., Nel, A., Sioutas, C., Smith, S., Baeza-Squiban, A., Cho, A., Duggan, S., Froines, J., 2008. Evaluating the toxicity of airborne particulate matter and nanoparticles by measuring oxidative stress potential - a workshop report and consensus statement. Inhalation Toxicology 20(1), 75-99.

Ballesteros, R., Hernández, J.J., Lyons, L.L., 2010. An experimental study of the influence of biofuel origin on particle-associated PAH emissions. Atmospheric Environment 44(7), 930-938.

Biswas, S., Verma, V., Schauer, J.J., Cassee, F.R., Cho, A.K., Sioutas, C., 2009. Oxidative Potential of Semi-Volatile and Non Volatile Particulate Matter (PM) from Heavy-Duty Vehicles Retrofitted with Emission Control Technologies. Environmental Science & Technology 43(10), 3905-3912.

Brown, D.M., Wilson, M.R., MacNee, W., Stone, V., Donaldson, K., 2001. Size-dependent proinflammatory effects of ultrafine polystyrene particles: a role for surface area and oxidative stress in the enhanced activity of ultrafines. Toxicology and Applied Pharmacology 175(3), 191-199.

Cheung, K.L., Ntziachristos, L., Tzamkiozis, T., Schauer, J.J., Samaras, Z., Moore, K.F., Sioutas, C., 2010. Emissions of Particulate Trace Elements, Metals and Organic Species from Gasoline, Diesel, and Biodiesel Passenger Vehicles and Their Relation to Oxidative Potential. Aerosol Science and Technology 44(7), 500-513.

Di, Y., Cheung, C.S., Huang, Z.H., 2010a. Experimental investigation of particulate emissions from a diesel engine fueled with ultralow-sulfur diesel fuel blended with diglyme. Atmospheric Environment 44(1), 55-63.

Di, Y.G., Cheung, C.S., Huang, Z.H., 2010b. Experimental investigation of particulate emissions from a diesel engine fueled with ultralow-sulfur diesel fuel blended with diglyme. Atmospheric Environment 44(1), 55-63.

Dieselnet, 2006. Emission test cycles ECE R49, Ecopoint Inc, http://www.dieselnet.com/standards/cycles/ece_r49.html, last accessed 18th August 2011.

Dieselnet, 2009. Emissions standards, European Union, heavy-duty truck and bus engines, Ecopoint Inc , http://www.dieselnet.com/standards/eu/hd.php, last accessed 17th August 2011.

Durbin, T.D., Collins, J.R., Norbeck, J.M., Smith, M.R., 2000. Effects of biodiesel, biodiesel blends, and a synthetic diesel on emissions from light heavy-duty diesel vehicles. Environmental Science & Technology 34(3), 349-355.

Fontaras, G., Kousoulidou, M., Karavalakis, G., Tzamkiozis, T., Pistikopoulos, P., Ntziachristos, L., Bakeas, E., Stournas, S., Samaras, Z., 2010. Effects of low concentration biodiesel blend application on modern passenger cars. Part 1: feedstock impact on regulated pollutants, fuel consumption and particle emissions. Environmental Pollution 158(5), 1451-1460.

Giechaskiel, B., Alföldy, B., Drossinos, Y., 2009. A metric for health effects studies of diesel exhaust particles. Journal of Aerosol Science 40(8), 639-651.

He, C., Ge, Y.S., Tan, J.W., You, K.W., Han, X.K., Wang, J.F., 2010. Characteristics of polycyclic aromatic hydrocarbons emissions of diesel engine fueled with biodiesel and diesel. Fuel 89(8), 2040-2046.

International Agency for Research on Cancer, 1987. Overall Evaluations of Carcinogenicity: An updating of IARC Monographs Volumes 1–42. IARC Monographs Evaluation of Carcinogenic Risks to Humans Supplement 7, pp. 1-440 http://www.iarc.fr/ accessed, December 22nd 2010.

Jamriska, M., Morawska, L., Thomas, S., He, C., 2004. Diesel bus emissions measured in a tunnel study. Environmental Science & Technology 38(24), 6701-6709.

Jung, H., Kittelson, D., Zachariah, M., 2006. Characteristics of SME biodiesel-fueled diesel particle emissions and the kinetics of oxidation. Environmental Science & Technology 40(16), 4949-4955.

Karavalakis, G., Bakeas, E., Stournas, S., 2010. Influence of Oxidized Biodiesel Blends on Regulated and Unregulated Emissions from a Diesel Passenger Car. Environmental Science & Technology 44(13), 5306-5312.

Knothe, G., Sharp, C.A., Ryan, T.W., III., 2006. Exhaust emissions of biodiesel, petrodiesel, neat methyl esters, and alkanes in a new technology engine. Energy & Fuels 20(1), 403-408.

Lapuerta, M., Armas, O., Rodríguez-Fernández, J., 2008. Effect of biodiesel fuels on diesel engine emissions. Progress in Energy and Combustion Science 34(2), 198-223.

Lim, M.C.H., Ayoko, G.A., Morawska, L., Ristovski, Z.D., Jayaratne, E.R., 2007. Influence of fuel composition on polycyclic aromatic hydrocarbon emissions from a fleet of in-service passenger cars. Atmospheric Environment 41(1), 150-160.

Maricq, M.M., 2007. Chemical characterization of particulate emissions from diesel engines: A review. Journal of Aerosol Science 38(11), 1079-1118.

McCormick, R.L., 2007. The impact of biodiesel on pollutant emissions and public health. Inhalation Toxicology 19(12), 1033-1039.

Miljevic, B., Fairfull-Smith, K.E., Bottle, S.E., Ristovski, Z.D., 2010a. The application of profluorescent nitroxides to detect reactive oxygen species derived from combustion-generated particulate matter: cigarette smoke - a case study. Atmospheric Environment 44(18), 2224-2230.

Miljevic, B., Heringa, M.F., Keller, A., Meyer, N.K., Good, J., Lauber, A., Decarlo, P.F., Fairfull-Smith, K.E., Nussbaumer, T., Burtscher, H., Prevot, A.S.H., Baltensperger, U., Bottle, S.E., Ristovski, Z.D., 2010b. Oxidative Potential of Logwood and Pellet Burning Particles Assessed by a Novel Profluorescent Nitroxide Probe. Environmental Science & Technology 44(17), 6601-6607.

Miljevic, B., Modini, R.L., Bottle, S.E., Ristovski, Z.D., 2009. On the efficiency of impingers with fritted nozzle tip for collection of ultrafine particles. Atmospheric Environment 43(6), 1372-1376.

Nel, A., 2005. Air pollution-related illness: effects of particles. Science 308(5723), 804-806.

Oberdörster, G., 2001. Pulmonary effects of inhaled ultrafine particles. International Archives of Occupational and Environmental Health 74(1), 1-8.

Pekkanen, J., Peters, A., Hoek, G., Tiittanen, P., Brunekreef, B., de Hartog, J., Heinrich, J., Ibald-Mulli, A., Kreyling, W.G., Lanki, T., Timonen, K.L., Vanninen, E., 2002. Particulate air pollution and risk of ST-segment depression during repeated submaximal exercise tests among subjects with coronary heart disease - The exposure and risk assessment for fine and ultrafine particles in ambient air (ULTRA) study. Circulation 106(8), 933-938.

Peters, A., Wichmann, H.E., Tuch, T., Heinrich, J., Heyder, J., 1997. Respiratory effects are associated with the number of ultrafine particles. American Journal of Respiratory and Critical Care Medicine 155(4), 1376-1383.

Sklorz, M., Briedé, J.J., Schnelle-Kreis, J., Liu, Y., Cyrys, J., de Kok, T.M., Zimmermann, R., 2007. Concentration of oxygenated polycyclic aromatic hydrocarbons and oxygen free radical formation from urban particulate matter. Journal of Toxicology and Environmental Health-Part a-Current Issues 70(21), 1866-1869.

Smekens, A., Godoi, R.H.M., Vervoort, M., Van Espen, P., Potgieter-Vermaak, S.S., Van Grieken, R., 2007. Characterization of individual soot aggregates from different sources using image analysis. Journal of Atmospheric Chemistry 56(3), 211-223.

Surawski, N.C., Miljevic, B., Ayoko, G.A., Roberts, B.A., Elbagir, S., Fairfull-Smith, K.E., Bottle, S.E., Ristovski, Z.D., 2011. A physico-chemical characterisation of particulate emissions from a compression ignition engine employing two injection technologies and three fuels. Accepted Environmental Science & Technology.

Surawski, N.C., Miljevic, B., Roberts, B.A., Modini, R.L., Situ, R., Brown, R.J., Bottle, S.E., Ristovski, Z.D., 2010. Particle Emissions, Volatility, and Toxicity from an Ethanol Fumigated Compression Ignition Engine. Environmental Science & Technology 44(1), 229-235.

United States Environmental Protection Agency, 2002. A comprehensive analysis of biodiesel impacts on exhaust emissions. Draft technical report., pp. 1-126.

Wang, W.G., Lyons, D.W., Clark, N.N., Gautam, M., Norton, P.M., 2000. Emissions from nine heavy trucks fueled by diesel and biodiesel blend without engine modification. Environmental Science & Technology 34(6), 933-939.

6.5 Supporting information

Table S 6.1: A tabulation of raw results for this study. Uncertainties related to measurement precision (i.e. not measurement accuracy) are calculated as ± one standard error of the mean ($\sigma_{\bar{x}} = \frac{\sigma}{\sqrt{n}}$), where σ is the standard deviation and n is the sample size (i.e. number of data points). NA denotes that the quantity was not available (i.e. chemical measurements for B40 and B60). * Indicates that the control fluorescence was greater than the test sample fluorescence, implying that an ROS concentration could not be calculated.

Fuel	Primary dilution ratio	Secondary dilution ratio	Total dilution ratio	PM_{10} (g/kWh)	Particle number emission factors (#/kWh)	CMD (nm)	TD particle surface area (nm^2/cm^3)	Particle phase PAHs (mg/kWh)	Vapour phase PAHs (mg/kWh)	ROS concentrations (nmol/mg)	Organic volume percentage V_{ORG} (%)
ULSD	30.8	9.2	283.7	$2.66 \pm 3.0 \times 10^{-2}$	$1.4 \times 10^{15} \pm 2.2 \times 10^{13}$	124.4 ± 0.8	$1.8 \times 10^{13} \pm 3.5 \times 10^{11}$	17.3 ± 2.7	14.1 ± 8.7	0.7 ± 0.5	12.4
B20 soy	25.4	7.7	195.1	$1.50 \pm 1.2 \times 10^{-1}$	$1.6 \times 10^{15} \pm 1.4 \times 10^{13}$	117.4 ± 0.2	$1.8 \times 10^{13} \pm 3.5 \times 10^{11}$	7.1 ± 1.3	9.0 ± 2.1	*	6.1
B40 soy	21.6	8.2	176.6	$1.20 \pm 3.5 \times 10^{-3}$	$1.4 \times 10^{15} \pm 9.9 \times 10^{12}$	113.0 ± 0.3	$1.2 \times 10^{13} \pm 2.4 \times 10^{11}$	NA	NA	NA	5.7
B60 soy	22.0	7.3	160.2	$0.72 \pm 5.7 \times 10^{-3}$	$8.5 \times 10^{14} \pm 4.3 \times 10^{12}$	103.9 ± 0.04	$6.3 \times 10^{12} \pm 1.3 \times 10^{11}$	NA	NA	NA	10.9

B80 soy	24.5	6.0	148.0	0.44 ± 8.1×10^{-3}	7.7×10^{14} ± 6.6×10^{12}	100.7 ± 0.4	5.7×10^{12} ± 1.1×10^{11}	17.9 ± 6.3	9.5 ± 5.3	6.3 ± 1.7	32.2
B100 soy	27.2	6.4	172.9	0.20 ± 1.1×10^{-3}	6.6×10^{14} ± 5.0×10^{12}	86.2 ± 0.9	NA	NA	NA	NA	NA
B20 tallow	26.3	7.2	188.4	1.11 ± 3.2×10^{-2}	1.5×10^{15} ± 2.1×10^{13}	112.2 ± 0.6	1.5×10^{13} ± 3.0×10^{11}	7.1 ± 1.0	2.3 ± 0.9	0.5 ± 0.2	13.9
B40 tallow	21.1	8.9	187.3	0.77 ± 1.4×10^{-2}	1.8×10^{15} ± 1.8×10^{13}	102.2 ± 0.3	1.1×10^{13} ± 2.2×10^{11}	NA	NA	NA	12.7
B60 tallow	20.5	8.3	170.8	0.59 ± 3.3×10^{-3}	1.5×10^{15} ± 1.4×10^{13}	97.6 ± 1.1	9.0×10^{12} ± 1.8×10^{11}	NA	NA	NA	20.2
B80 tallow	25.9	6.4	165.7	0.33 ± 3.2×10^{-3}	1.2×10^{15} ± 1.2×10^{13}	87.0 ± 0.3	6.2×10^{12} ± 1.2×10^{11}	14.5 ± 5.3	6.4 ± 1.4	6.1 ± 2.2	31.1
B20 canola	25.3	7.1	180.6	0.92 ± 8.0×10^{-3}	2.4×10^{15} ± 1.4×10^{13}	100.9 ± 0.9	1.5×10^{13} ± 3.0×10^{11}	17.3 ± 6.4	6.3 ± 1.8	0.8 ± 0.03	10.0

B40 canola	25.7	7.1	183.1	0.62 ± 1.9×10^{-3}	2.3×10^{15} ± 1.1×10^{13}	94.5 ± 1.7	1.2×10^{13} ± 2.3×10^{11}	NA	NA	NA	13.7
B60 canola	26.3	7.4	194.3	0.44 ± 1.5×10^{-3}	2.1×10^{15} ± 1.2×10^{13}	88.6 ± 0.8	9.3×10^{12} ± 1.9×10^{11}	NA	NA	NA	16.2
B80 canola	26.1	6.4	165.7	0.33 ± 3.7×10^{-3}	2.0×10^{15} ± 1.1×10^{13}	82.9 ± 0.8	8.0×10^{12} ± 1.6×10^{11}	6.5± 3.9	7.4± 3.4	4.6± 1.1	35.6

Chapter 7: Restructuring of carbonaceous particles upon exposure to organic vapours

Miljevic, Branka[a], Surawski, Nicholas C.[a,b], Bostrom, Thor[a] and Ristovski, Zoran D.[a,*]

[a]International Laboratory for Air Quality and Health, Queensland University of Technology, GPO Box 2434, 4001, Brisbane, Australia

[b]School of Engineering Systems, Queensland University of Technology, GPO Box 2434, 4001, Brisbane, Australia

Publication: Submitted to the Journal of Aerosol Science, 2011.

Contributor	Statement of contribution
Nicholas C. Surawski Signature Date 21/10/11	Assisted with the experimental set-up, and the electron microscopy sampling for diesel measurements.
Branka Miljevic	Contributed to the experimental design, undertook measurements, performed data analysis, and wrote the manuscript.
Thor Bostrom	Undertook the microscopy work, and reviewed the manuscript.
Zoran D. Ristovski	Contributed to the experimental design, assisted with the experimental set-up and reviewed the manuscript.

Principal Supervisor Confirmation

I have sighted email or other correspondence from all Co-authors confirming their certifying authorship.

Associate Professor Zoran Ristovski		21/10/11
Name	**Signature**	**Date**

Abstract

Recent research has described the restructuring of particles upon exposure to organic vapours; however, as yet hypotheses able to explain this phenomenon are limited. In this study, a range of experiments were performed to explore different hypotheses related to carbonaceous particle restructuring upon exposure to organic and water vapours, such as: the effect of surface tension, the role of organics in flocculating primary particles, as well as the ability of vapours to "wet" the particle surface. The change in mobility diameter (d_m) was investigated for a range carbonaceous particle types (diesel exhaust, petrol exhaust, cigarette smoke, candle smoke, particles generated in a heptane/toluene flame, and wood smoke particles) exposed to different organic (heptane, ethanol, and dimethyl sulfoxide/water (1:1 vol%) mixture) and water vapours. Particles were first size-selected and then bubbled through an impinger (bubbler) containing either an organic solvent or water, where particles trapped inside rising bubbles were exposed to saturated vapours of the solvent in the impinger. The size distribution of particles was simultaneously measured upstream and downstream from the impinger. A size-dependent reduction in d_m was observed when bubbling diesel exhaust, particles generated in a heptane/toluene flame, and candle smoke particles through heptane, ethanol and a dimethyl sulfoxide/water (1:1 vol %) mixture. In addition, the size distributions of particles bubbled through an impinger were broader. Moreover, an increase of the geometric standard deviation (σ) of the size distributions of particles bubbled through an impinger was also found to be size-dependent. Size-dependent reduction in d_m and an increase of σ indicate that particles undergo restructuring to a more compact form, which was confirmed by TEM analysis. However, bubbling of these particles through water did not result in a size-dependent reduction in d_m, nor in an increase of σ. Cigarette smoke, petrol exhaust, and wood smoke particles did not result in any substantial change in d_m, or σ, when bubbled through organic solvents or water. Therefore, size-dependent reduction in the d_m upon bubbling through organic solvents was observed only for particles that had a fractal-like structure, whilst particles that were liquid or were assumed to be spherical did not exhibit any reduction in d_m. Compaction of fractal-like particles was attributed to the ability of condensing vapours to efficiently wet the particles. Our results also show that the presence of an organic layer on the surface of fractal-like particles, or the surface tension of the condensed liquid do not influence the extent of compaction.

7.1 Introduction

The majority of fine PM in urban atmosphere comes from combustion sources. A dominant component in combustion-generated particles is black carbon or soot. Soot particles affect

regional climate by modifying cloud condensation and contributing to Earth's radiative forcing through scattering and absorbing solar light (Jacobson, 2001; Menon et al., 2002). These effects, as well as the lifetime in the atmosphere, strongly depend on soot's physicochemical properties, such as their composition, hygroscopicity and morphology. However, ageing in the atmosphere alters these properties, influencing in that way climate effects of soot. Freshly generated soot particles exist in the form of fractal-like aggregates consisting of hydrophobic, mainly spherical primary particles with diameters in the range of 15 -40 nm (Wentzel et al., 2003; Hu and Koylu, 2004; Burtscher, 2005). Atmospheric ageing can result in condensation of H_2SO_4 and other low volatility compounds on soot particles, which increases their hygroscopicity and, subsequently, their ability to act as a cloud condensation nuclei (Saathoff et al., 2003; Zhang et al., 2008b). Condensation of H_2SO_4 and subsequent exposure to high humidity (~90%) was found to increase light scattering and absorption of soot particles (Zhang et al., 2008a). Similarly, Saathof et al. (2003) have found that condensation of the ozonolysis products of α-pinene onto soot particles results in increased light scattering and absorption. Xue et al. (2009b) have observed the same effects on the optical properties of soot particles when coating them with glutaric acid and then exposing them to 90% relative humidity and subsequently drying them. In all these studies, the observed enhancement in optical properties of soot was explained by restructuring of soot particles to a more compact form. Compaction of soot particles upon coating with H_2SO_4 or organic compounds was confirmed by electron microscopy analysis (Saathoff et al., 2003; Lu et al., 2008; Zhang et al., 2008b; Pagels et al., 2009a), as well as by measurements of the change in mobility diameter and mass - mobility relationship of soot particles (Slowik et al., 2007; Zhang et al., 2008a; Pagels et al., 2009b; Xue et al., 2009a). It was shown that the mobility diameter decreases after coating soot particles with H_2SO_4 (Zhang et al., 2008a; Pagels et al., 2009b) or glutaric acid (Xue et al., 2009a) and subsequently heating them to 200^{o}C, with the size reduction being more pronounced for particles with larger initial mobility diameter. On the other hand, effective density and fractal dimension, which were obtained from the relationship between mass and mobility diameters, were found to increase after the aforementioned processing with H_2SO_4 or glutaric acid. In addition, the effective density of processed soot particles was found not to have such a large reduction in its value with an increase of mobility diameter as was the case for fresh soot particles.

Kütz and Schmidt-Ott (1992a) exposed butane-air flame soot particles to subsaturated vapours of n-hexane, 2-propanol and water, and measured their electrical mobility using a

Tandem Differential Mobility Analyser (TDMA) arrangement. A decrease in mobility diameter was observed when particles were exposed to n-hexane and 2-propanol, while exposure to water vapour did not result in any significant change in mobility diameter. However, under supersaturated conditions, all three compounds lead to a similar degree of reduction in mobility diameter. For subsaturated conditions, the reduction in mobility diameter was explained by the ability of n-hexane and 2-propanol to wet the hydrophobic surface of soot and to dissolve substances condensed onto primary particles of agglomerates, consequently enabling restructuring to a more compact form. During supersaturated conditions, liquid condenses onto particles to form a droplet which during evaporation tends to retain the form of a sphere and in that way leads to restructuring of particles to a more compact form.

In this study, a TDMA technique in combination with Transmission Electron Microscopy (TEM) measurements was used to examine the effects of various solvents on the morphology of particles generated from different combustion sources. Whilst several studies have reported morphological restructuring of soot agglomerates due to condensation of various compounds (such as sulphuric acid and glutaric acid), information on a mechanistic explanation of this phenomenon is very limited. Consequently, an objective of this study is to provide a conceptual mechanism explaining structural compaction of soot agglomerates exposed to saturated organic and water vapours.

7.2 Materials and methods

7.2.1 Particle sources

To study how various solvents influence particles with different structures, several different combustion sources were investigated. Namely, these were: a diesel engine, a petrol powered generator, a cigarette, a candle, wood and burning of a heptane/toluene mixture. Diesel exhaust particles were generated using a Euro 3 common rail diesel engine operating at intermediate speed (1500 rpm) and 25% load. A two stage, unheated dilution system was used to reduce the concentration of particles before their detection with the sampling equipment. Aerosol generated by all other sources was introduced into a particle-free 1 m^3 chamber from where it was delivered to the instruments. A cigarette and a small piece of wood were lit outside the chamber and placed inside the chamber for around 1 min to smoulder. A candle and a heptane/toluene mixture were lit outside the chamber and placed inside it for around 1 min to burn in a steady flame. A petrol generator was first turned on and

then connected directly to the chamber for about 2 s in order to deliver aerosol into the chamber.

7.2.2 Experimental set-up

A schematic diagram of the experimental set-up employed in this study is shown in Figure 7.1. To generate monodisperse aerosol, the particles were first passed through a Kr-85 bipolar charger and were then size-selected according to their electrical mobility diameter (d_m), using a Differential Mobility Analyser (pre-DMA; custom made). The sheath air flow rate in the pre-DMA was 13 L min^{-1} and the aerosol flow rate was 2 L min^{-1}. Measurements were performed for various particle sizes in the size range 30 – 200 nm. Monodisperse aerosol was then bubbled through an impinger (bubbler) containing 20 ml of various solvents and the size distribution of the particles was measured upstream and downstream from the impinger by using two Scanning Mobility Particle Sizers (SMPS) operating simultaneously. Both of the SMPS systems consisted of a custom-made DMA and a TSI 3010 Condensation Particle Counter (CPC). The sheath air flow rate in the two DMAs was 7.5 L min^{-1} and the aerosol flow rate was 1 L min^{-1}. The flowrate through the impinger was 1 L min^{-1} and the residence time of aerosol in a bubble (the time from bubble formation till bubble bursting) was around 1 s. The impinger used in this study had a fritted nozzle tip (porosity grade 1: 100 – 160 μm) in order to increase the contact surface between the aerosol and the liquid and thus to increase the formation of bubbles. When bubbling aerosol through the impinger, a certain portion of particles gets trapped in the sampling liquid (Miljevic et al., 2009b), whereas the rest of particles stays in the bubble and gets released upon bubble bursting at the liquid-air interface. In this study, we are investigating the particles that do not get trapped in the sampling liquid upon bubbling. As mentioned previously, these particles, while travelling in a bubble, are exposed to saturated vapour of a liquid that surrounds the bubble. Under these conditions, condensation of vapour onto particles will occur. Upon bubble bursting and further transport of particles through the sampling lines, the saturation of solvent vapour in the surrounding air decreases and leads to evaporation of condensed liquid off the particles.

To investigate the role that solvents with different polarity and surface tension have on particle morphological changes upon exposure to their vapours we have used heptane, ethanol, water and a dimethyl sulfoxide (DMSO)/water mixture (1:1 vol%). Heptane is a non-polar solvent, while ethanol, water and DMSO/water mixture are polar. The surface tension (at 20^{o}C) of heptane, ethanol and water are 20.1 mN m^{-1}, 22.4 mN m^{-1} and 72.9 mN m^{-1},

respectively, while the surface tension of the DMSO/ water mixture (1:1 vol%) is ~ 56 mN m^{-1} (Markarian and Terzyan, 2007).

7.2.3 TEM sampling and analysis

To get more insight into the changes in the structure of the particles upon exposure to solvent vapours we have performed TEM analysis for diesel exhaust particles. Particles of 80 nm d_m were preselected using an Electrostatic Classifier (TSI 3071) and after that collected onto copper TEM grids (200 mesh with carbon film; ProSciTech) using a Nanometer Aerosol Sampler (NAS; TSI 3089) operating at 1 L min^{-1} and -7 kV. The size of 80 nm was chosen as this was near the mode of the accumulation mode particles for our engine/load conditions. The aerosol to sheath ratio was set to 1:5 to assure that there was a sufficient amount of particles collected on the grids. To investigate the influence of solvent vapours on particle morphology two TEM samples were collected – one without an impinger placed in front of the NAS, and one with the impinger placed before the NAS. A transmission electron microscope (Philips CM200) was operating at an accelerating voltage of 115 kV to obtain images of particles collected on TEM grids.

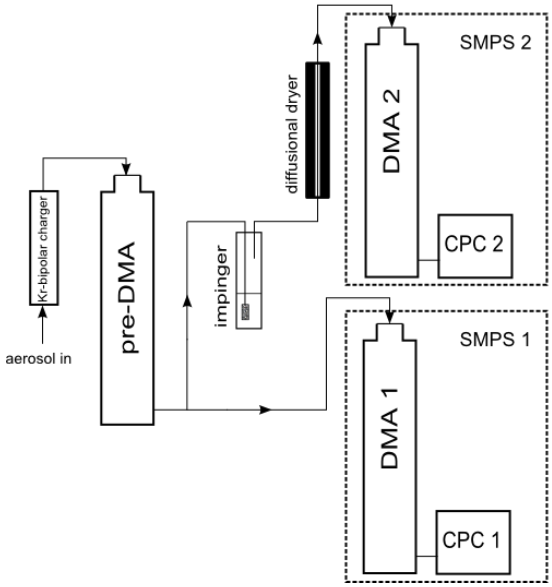

Figure 7.1: A schematic of the experimental set-up used for measurements of mobility diameter of combustion-generated particles upon exposure to organic and water vapours.

7.3 Results

7.3.1 TDMA measurements

Bubbling monodisperse diesel exhaust, candle smoke and particles produced by burning heptane/toluene mixture through an impinger containing an organic solvent resulted in a reduction of their d_m. An example of this is shown in Figure 7.2 for the case where the

solvent used in the impinger was heptane. It can be observed that this reduction in mobility diameter (Δd_m) was found to be size-dependent – it is first observed at 40 nm (burnt heptane/toluene mixture) to 70 nm (diesel exhaust and candle smoke) and from there it grows exponentially with respect to d_m. The effect was most pronounced for particles generated in a premixed heptane/toluene flame, reaching a 30 nm reduction in d_m when bubbling 187 nm pre-selected particles through heptane. This was followed by candle smoke, for which 189 nm pre-selected particles resulted in 24 nm reduction in d_m, and then diesel exhaust, for which 187 nm pre-selected particles resulted in 20 nm reduction in d_m.

Figure 7.2 also shows changes in d_m when cigarette smoke, wood smoke and petrol exhaust particles of different initial d_m are bubbled through heptane. As can be seen, for particles produced by these sources, a size-dependent reduction in d_m upon exposure to heptane vapours was not observed, although there was a small reduction of up to 3 nm throughout the whole sampling size range.

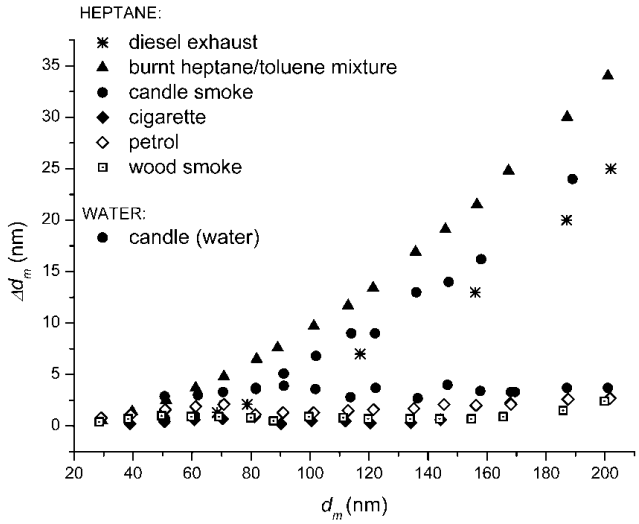

Figure 7.2: The difference between the initial mobility diameter and the mobility diameter after bubbling (Δd_m) for particles originating from different combustion sources and bubbled through either heptane or water.

Candle smoke particles, which resulted in a size-dependent reduction in initial d_m when bubbled through heptane, did not show the same behaviour when bubbled through an impinger containing water. However, they did result in a small reduction in d_m, which was up to 4 nm throughout the whole sampling size range (Figure 7.2). The same behaviour was observed when bubbling diesel exhaust particles through water, as well as for particles generated in heptane/toluene flame (not shown on the graph). The summary of all particle

sources used in this study, solvents and their effect on size-dependent reduction in d_m is shown in Table 7.1.

Table 7.1: A summary of the experiments.

Aerosol	Solvent	Size-dependent reduction in d_m
Candle smoke	Water	No
	Heptane	*Yes*
	Ethanol	*Yes*
	DMSO/water	*Yes*
Petrol exhaust	Water	No
	Heptane	No
	DMSO/water	No
Cigarette smoke	Water	No
	Heptane	No
Heptane/toluene flame soot	Water	No
	Heptane	*Yes*
Diesel exhaust	Heptane	*Yes*
Wood smoke (smouldering)	Heptane	No

To illustrate the influence of different solvents on the restructuring of particles, size distributions of 200 nm pre-selected candle smoke particles prior to bubbling and after bubbling through an impinger containing different solvents are presented (Figure 7.3). Both ethanol and DMSO/water (1:1 vol%) have a similar effect on 200 nm candle smoke particles as heptane, i.e. a reduction in d_m occurs, although the reduction in size is slightly larger (21% for both solvents, compared to 18% for particles exposed to heptane vapours). For all three solvents (heptane, ethanol, DMSO/water) it can also be seen that, in addition to the reduction in d_m, the geometric standard deviation (σ) of the particle size distribution is substantially increased upon bubbling. This widening of the size distribution is observed not only for candle smoke, but also for every particle source where size-dependent reduction in d_m occurred. A dependence of σ of the size distribution with pre-selected particles bubbled through heptane on initial d_m is shown in Figure 7.4. The geometric standard deviation of the size distributions of diesel exhaust, candle smoke particles and particles generated in heptane/toluene flame bubbled through heptane are compared with σ of their size

distributions prior to bubbling. It is evident from Figure 7.4 that in all three cases σ of particles bubbled through heptane increases linearly with respect to the particles' initial d_m. However, the slope of the linear fit is not the same for all three particle sources. The smallest slope was found to be for diesel exhaust particles (2.39×10^{-4}), followed by particles generated in heptane/toluene flame (3.36×10^{-4}) and then candle smoke particles (4.77×10^{-4}). As can be seen from Figure 7.3, bubbling of candle smoke particles through water results in only a slight reduction in d_m and no obvious widening in the size distribution of treated particles.

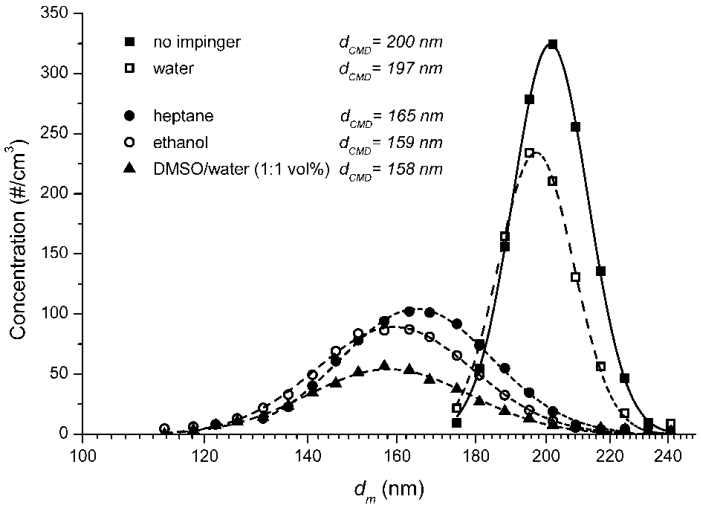

Figure 7.3: 200 nm pre-selected candle smoke particles (black solid line) after bubbling through water, heptane, ethanol and DMSO/water (1:1 vol%). Note: The total number concentration of particles upon bubbling is smaller due to partial trapping of particles in the liquid.

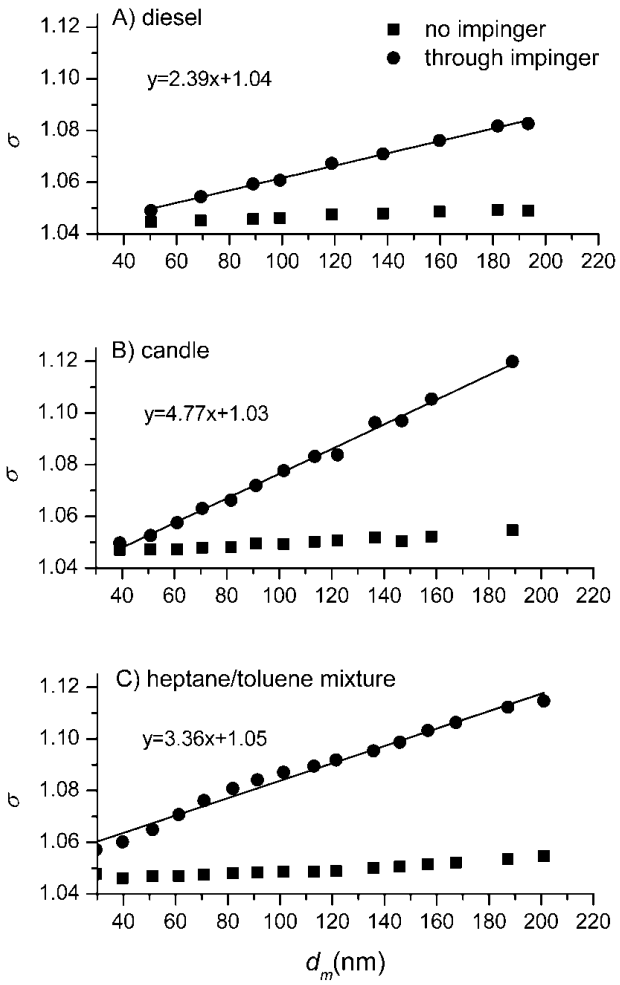

Figure 7.4: A dependence of the geometric standard deviation (σ) of the size distribution with pre-selected particles bubbled through heptane on the initial d_m. Squares present σ of particles' size distributions prior to bubbling and circles present σ after bubbling.

7.3.2 TEM images

An example of TEM images of pre-selected 80 nm diesel exhaust particles before and after bubbling through an impinger containing heptane is shown in Figure 7.5. Heptane was chosen as a solvent as it was found that exposure to its vapours resulted in reduction of d_m, and diesel exhaust was chosen as it had exhibited reduction in d_m upon exposure to heptane vapours. The first three images (Figure 7.5: a, b, c) are an example of diesel exhaust particles prior to bubbling and the following three images (Figure 7.5: d, e, f) show particles after bubbling. It is clear from the images that 80 nm pre-selected particles bubbled through heptane are generally not as branched as non-treated 80 nm pre-selected particles indicating that diesel exhaust particles, when exposed to saturated heptane vapours, undergo morphological changes that make them more compact.

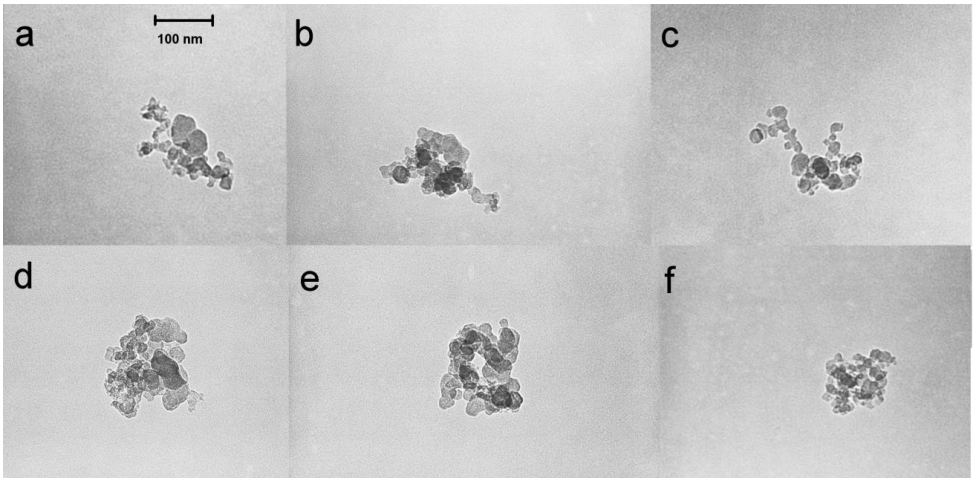

Figure 7.5: TEM images of 80 nm preselected diesel exhaust particles prior to bubbling through heptane (a, b, c) and after bubbling through heptane (d, e, f).

7.4 Discussion

The results presented in this study show that some combustion particles, namely, diesel exhaust, candle smoke and particles generated in the heptane/toluene flame, exhibit size-dependent reduction in their initial d_m upon exposure to saturated vapours of heptane, ethanol and DMSO/water mixture that are experienced during bubbling through an impinger containing these solvents. Particles from these sources are known to have fractal, chain-like structure (e.g. Tumolva et al. (2010)). The shift in d_m upon exposure to saturated solvent vapours indicates that the particles have restructured to a more compact form which resulted in a decrease in the drag force exerted on the particles and thus, a decrease in their electrical mobility diameter. Although only on a qualitative level, the TEM images complement the TDMA measurements and confirm that diesel exhaust particles exhibited restructuring to a more compact form. TEM images were not obtained for candle smoke particles and particles from the heptane/toluene flame, but it is expected that structural change to a more compact, regular shape would be observed for such analysis if undertaken.

Size-dependence of the d_m reduction means that the compaction was more pronounced for larger particles. In the case of fractal aggregates, such as diesel soot, particles with larger diameters have smaller effective densities (Olfert et al., 2007) and therefore can exhibit larger compaction than smaller particles. It is evident from Figure 7.2 that the size-dependent reduction in d_m was the strongest for particles generated in the heptane/toluene flame (followed by candle smoke and then diesel exhaust particles), suggesting that these particles had either the lowest fractal dimension (i.e. were highly branched) or the "degree of compaction" was the highest (i.e. the restructured particles were closer to a spherical shape).

In addition to the size-dependent reduction in d_m, compaction also resulted in widening of the size distribution (increase in σ) of pre-selected particles. Similar to the reduction in d_m, the widening of the size-distribution was also shown to be size-dependent, i.e. to increase with the increase of initial d_m. Considering their chain-like structure, particles of different shapes will have the same mobility in an electric field (Sorensen, 2011). Restructuring of particles with a different shape to a more compact structure will result in particles with a number of different near-spherical sizes, with each having a slightly different d_m. The drag force on the restructured, near-spherical particles is always smaller comparing to the drag force than non-treated particles experience, so, in addition to reduction in d_m, the widening of the size distribution is observed only leftwards from the initial size distribution (Figure 7.3). Statistically, the bigger the particles are the more particles of different shape will have the same mobility diameter. Restructuring of bigger particles, thus, leads to compacted particles that are spread over a bigger mobility range and results in the size-dependent widening of the narrow size distribution of pre-selected particles (as observed). In Figure 7.4, the biggest slope of the linear fit is obtained for candle smoke particles, suggesting that these particles were the most branched (i.e. had the greatest number of particles with different shape having the same d_m). This was followed by particles produced in heptane/toluene flame and then by diesel exhaust particles.

Whereas diesel exhaust, candle smoke and particles generated in the heptane/toluene flame exhibit size-dependent reduction in their initial d_m upon bubbling through heptane, ethanol and DMSO/water mixture, this effect was not observed when bubbling these particles through water. Similarly, Kütz and Schmidt-Ott (1992a) have found that, under subsaturated conditions, water does not induce reduction in d_m, whereas n-hexane and 2-propanol do. This was explained by the ability of n-hexane and 2-propanol to wet the soot surface and to dissolve substances condensed onto primary particles of agglomerates, allowing in that way restructuring to a more compact form. The reason why heptane, ethanol and DMSO/water mixture cause size-dependent compaction of particles whilst water does not might be due to the stronger adhesion forces between these solvents and primary spheres of fractal particles. Stronger adhesion forces result in stronger capillary action and, thus more efficient wetting of the particles, which enables movement of primary particles and rearrangement to a more compact structure. Considering that the surface of combustion-generated particles is mainly hydrophobic, cohesion forces between molecules of water would be stronger than adhesion forces between water and particles' surface and, thus, water would not be able to efficiently

wet these kinds of particles. This might be a reason why the compaction was not observed. On the other hand, heptane is a non-polar, hydrophobic solvent and therefore, it is expected to efficiently wet hydrophobic soot particles. However, ethanol and DMSO/water mixture are polar, hydrophilic solvents and yet, are still able to wet the particles and cause compaction. Considering that soot particles are not pure elemental carbon, but contain a thin layer of organic compounds condensed on the carbonaceous surface of primary particles, ethanol and DMSO/water mixture (as well as heptane) might dissolve (fully or partially) the condensate coating and by "liquidifying" the contact area between primary particles, enable them to collapse to a more compact form. It has been suggested by Kütz and Schmidt-Ott (1992a) that the organic layer already present on the surface could play a role in a condensing liquid-induced particle compaction. Therefore, the ability of condensing vapour to dissolve substances adsorbed on the surface of fractal agglomerates might be the main factor influencing compaction of these particles. If this was the case then passing the particles through a thermodenuder would remove this layer and reduce the compaction. To investigate the role of organic condensates on compaction of fractal agglomerates, a thermodenuder, consisting of a heated tube set to 300^{o}C, followed by an activated charcoal section, was placed after the pre-DMA and upon passing through the thermodenuder candle smoke particles were bubbled through heptane. Figure 7.6 shows the reduction in the initial d_m for candle smoke particles sampled with and without thermodenuder placed after the pre-DMA. As can be seen, there is no difference in the reduction of d_m between thermodenuded (i.e. without organic layer) and non-thermodenuded (i.e. with organic layer) particles. This suggests that the organic layer does not play a role in restructuring of fractal particles induced by a condensing liquid. If the organic layer had been distributed in-between the primary particles of the agglomerates and played any role in keeping the particle together then the compaction of particles with this layer present had to be different than compaction of particles with this layer removed. The only role that the organic layer could play is then enhancing condensation of the organic solvent through the absorption process. This mechanism would be important for subsaturated, but not that important for saturated or supersaturated conditions.

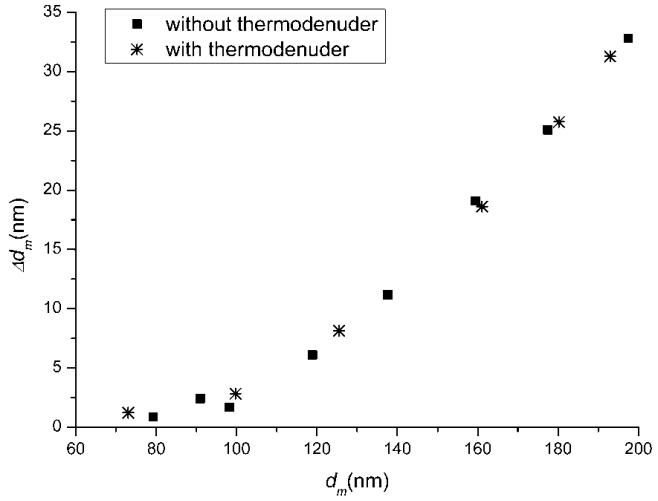

Figure 7.6: The difference between the initial mobility diameter and the mobility diameter after bubbling (Δd_m) of candle smoke particles bubbled through heptane and sampled without and with thermodenuder placed after the pre-DMA.

Considering that water, as a solvent that has the highest surface tension (with respect to air), did not cause compaction of fractal-like agglomerates, this study shows that at non-supersaturated conditions surface tension of the condensing liquid does not play a role in particle restructuring. This is further supported by the fact that 200 nm pre-selected candle smoke particles exposed to ethanol and DMSO/water vapours have experienced the same degree of compaction (Figure 7.3) although the surface tension of ethanol (22 mN m^{-1}) is 2.5 times lower than the surface tension of DMSO/water (56 mN m^{-1}) (Markarian and Terzyan, 2007). In addition, ethanol and heptane, which both have virtually the same surface tension, have resulted in slightly different degree of reduction in d_m of 200 nm pre-selected particles (21% and 18%, respectively).

Cigarette smoke, wood smoke and petrol exhaust mobility-selected particles did not exhibit size-dependent compaction and widening of their size distribution when exposed to saturated heptane vapours. It is suggested that this is due to a more compact, near-spherical structure of these types of particles. Indeed, wood smoke particles produced during a smouldering phase were found to have a spherical, tar-like structure (Kocbach et al., 2005; Tumolva et al., 2010). Although petrol exhaust particles were reported to have fractal structure (Colbeck et al., 1997), we believe that, due to a cold start (i.e. low combustion temperature), it is valid to assume that petrol exhaust particles in this study were dominated by volatile species (Philip et al., 2007) and, thus, had a near-spherical structure.

As already mentioned, candle smoke particles were found to undergo size-dependent restructuring to a more compact form when exposed to heptane vapours. However, one experiment with candle smoke performed during this study was found to be inconsistent with the rest of the results obtained for candle smoke particles. During that experiment, pre-selected candle smoke particles were bubbled through heptane, but size-dependent reduction in d_m was not observed. Figure 7.7A shows 200 nm pre-selected candle smoke particles before and after exposing them to heptane vapours. As can be seen, after bubbling, pre-selected particles had a bimodal size distribution with one peak being at approximately the same size as particles prior to bubbling (200 nm) and another peak being at smaller sizes (d_{CMD} = 165 nm) and substantially wider. This indicates that candle smoke particles sampled from the chamber were an external mixture consisting of irregular, fractal-like particles that compacted upon bubbling and near-spherical particles that did not experience compaction upon bubbling. This was confirmed by placing the thermodenuder set at 300^{o}C in front of the pre-DMA. Size distributions of 200 nm pre-selected particles before and after bubbling through heptane and with thermodenuder placed in front of the sampling inlet are presented in Figure 7.7B. The figure shows that particles that had passed through the thermodenuder before pre-selection had an unimodal size distribution after bubbling through heptane. The shape and position of the size distribution of particles upon bubbling through heptane was almost the same as the one shown in Figure 7.3, i.e. its d_{CMD} was at 165 nm and it was substantially wider than the initial size distribution (prior to bubbling). Absence of the peak at the pre-selected size of 200 nm (as the peak in Figure 7.7A) means that those particles were fully volatile (organic) and evaporated upon passing through the thermodenuder. Organic particles are known to have near-spherical shape (Zelenyuk et al., 2008), what explains why there was no reduction in d_m upon bubbling through heptane. For this specific experiment it is reasonable to assume that the particles in the chamber were an external mixture as, in addition to candle burning in a steady flame, there was also a smouldering phase created upon extinction of the candle when white smoke was emitted. Pagels et al. (2009c) reported that smouldering particles generated upon extinction of candles were found to be liquid and volatile. The reduction in d_m for thermodenuded, 200 nm pre-selected particles (Figure 7.7B) was the same as presented in Figure 7.2 and Figure 7.3, what also points out that the presence of organic layers on the surface of fractal particles does not have any significant influence on the degree of compaction.

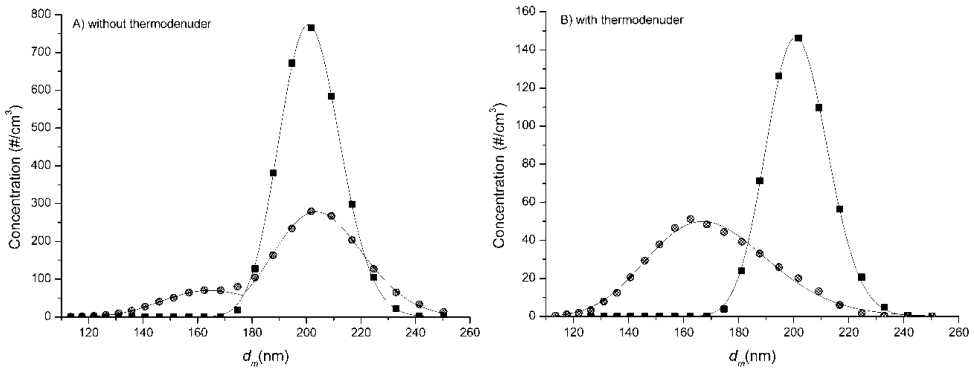

Figure 7.7: 200 nm pre-selected candle smoke particles before (squares) and after (circles) bubbling through heptane sampled without (A) and with (B) thermodenuder placed in front of the pre-DMA.

7.5 Conclusions

We have analysed the change in the particle d_m of combustion generated aerosols after exposure to organic and water vapours. Size-dependent reduction in the particle diameter was observed for all particles that had a soot or fractal like structure, while particles that were liquid or assumed to be spherical did not exhibit any reduction in d_m. The reduction in d_m was caused by the restructuring of particles making them more compact. This was confirmed by TEM analysis which showed that the particles were much less branched. Larger particles exhibit larger compaction as they have a smaller effective density and therefore are less compact before exposure to the organic vapours. Considering that size-dependent compaction is observable only for fractal-like particles, the methodology presented in this study could serve as a quick test to determine whether the particles are fractal or not and whether the particles being tested present internal or external mixture.

While previous work has suggested that the presence of an organic layer on the surface of fractal-like particles might enhance the degree of compaction, our results clearly show that this is not the case, as removing the organic surface layer did not change the degree of compaction. In addition, the degree of compaction was neither influenced by the surface tension of the condensing liquid. This implies that as long as the liquid is able to wet the particles then compaction will occur, with the degree of compaction depending on the fractal structure of the particles. This further implies that other atmospherically relevant vapours, as long as they are capable of wetting the particles, will have similar effects.

7.6 References

Burtscher, H., 2005. Physical characterization of particulate emissions from diesel engines: a review. Journal of Aerosol Science 36(7), 896-932.

Colbeck, I., Atkinson, B., Johar, Y., 1997. The morphology and optical properties of soot produced by different fuels. Journal of Aerosol Science 28(5), 715-723.

Hu, B., Koylu, U., 2004. Size and Morphology of Soot Particulates Sampled from a Turbulent Nonpremixed Acetylene Flame. Aerosol Science and Technology 38(10), 1009 - 1018.

Jacobson, M.Z., 2001. Strong radiative heating due to the mixing state of black carbon in atmospheric aerosols. Nature 409(6821), 695-697.

Kocbach, A., Johansen, B.V., Schwarze, P.E., Namork, E., 2005. Analytical electron microscopy of combustion particles: a comparison of vehicle exhaust and residential wood smoke. Science of The Total Environment 346(1-3), 231 - 243.

Kütz, S., Schmidt-Ott, A., 1992. Characterization of agglomerates by condensation-induced restructuring. Journal of Aerosol Science 23(Supplement 1), 357-360.

Lu, Z.F., Hao, J.M., Hu, L.H., Takekawa, H., 2008. The compaction of soot particles generated by spark discharge in the propene ozonolysis system. Journal of Aerosol Science 39(10), 897-903.

Markarian, S.A., Terzyan, A.M., 2007. Surface Tension and Refractive Index of Dialkylsulfoxide + Water Mixtures at Several Temperatures. Journal of Chemical & Engineering Data 52(5), 1704-1709.

Menon, S., Hansen, J., Nazarenko, L., Luo, Y., 2002. Climate Effects of Black Carbon Aerosols in China and India. Science 297(5590), 2250-2253.

Miljevic, B., Modini, R.L., Bottle, S.E., Ristovski, Z.D., 2009. On the efficiency of impingers with fritted nozzle tip for collection of ultrafine particles. Atmospheric Environment 43(6), 1372-1376.

Olfert, J.S., Symonds, J.P.R., Collings, N., 2007. The effective density and fractal dimension of particles emitted from a light-duty diesel vehicle with a diesel oxidation catalyst. Journal of Aerosol Science 38(1), 69-82.

Pagels, J., Khalizov, A.F., McMurry, P.H., Zhang, R.Y., 2009a. Processing of soot by controlled sulphuric acid and water condensation-mass and mobility relationship. Aerosol Science and Technology 43(7), 629-640.

Pagels, J., Wierbicka, A., Nilsson, E., Isaxon, C., Dahl, A., Gudmundsson, A., Swietlicki, E., Bohgard, M., 2009b. Chemical composition and mass emission factors of candle smoke particles. Journal of Aerosol Science 40(3), 193-208.

Philip, P., Richard, S., Dave, O., Xiangdong, C., 2007. Cold Start Particulate Emissions from a Second Generation DI Gasoline Engine. SAE technical paper 2007-01-1931.

Saathoff, H., Naumann, K.H., Schnaiter, M., Schöck, W., Möhler, O., Schurath, U., Weingartner, E., Gysel, M., Baltensperger, U., 2003. Coating of soot and $(NH4)_2SO_4$ particles by ozonolysis products of a-pinene. Journal of Aerosol Science 34(10), 1297-1321.

Slowik, J.G., Cross, E.S., Han, J.-H., Kolucki, J., Davidovits, P., Williams, L.R., Onasch, T.B., Jayne, J.T., Kolb, C.E., Worsnop, D.R., 2007. Measurements of Morphology Changes of Fractal Soot Particles using Coating and Denuding Experiments: Implications for Optical Absorption and Atmospheric Lifetime. Aerosol Science and Technology 41(8), 734 - 750.

Sorensen, C.M., 2011. The Mobility of Fractal Aggregates: A Review. Aerosol Science and Technology 45(7), 755 - 769.

Tumolva, L., Park, J.Y., Kim, J.S., Miller, A.L., Chow, J.C., Watson, J.G., Park, K., 2010. Morphological and elemental classification of freshly emitted soot particles and atmospheric ultrafine particles using the TEM/EDS. Aerosol Science and Technology 44(3), 202-215.

Wentzel, M., Gorzawski, H., Naumann, K.H., Saathoff, H., Weinbruch, S., 2003. Transmission electron microscopical and aerosol dynamical characterization of soot aerosols. Journal of Aerosol Science 34(10), 1347-1370.

Xue, H.X., Khalizov, A.F., Wang, L., Zheng, J., Zhang, R.Y., 2009a. Effects of Coating of Dicarboxylic Acids on the Mass-Mobility Relationship of Soot Particles. Environmental Science & Technology 43(8), 2787-2792.

Xue, H.X., Khalizov, A.F., Wang, L., Zheng, J., Zhang, R.Y., 2009b. Effects of dicarboxylic acid coating on the optical properties of soot. Physical Chemistry Chemical Physics 11(36), 7869-7875.

Zelenyuk, A., Yang, J., Song, C., Zaveri, R.A., Imre, D., 2008. A New Real-Time Method for Determining Particles' Sphericity and Density: Application to Secondary Organic Aerosol Formed by Ozonolysis of alpha-Pinene. Environmental Science & Technology 42(21), 8033-8038.

Zhang, R.Y., Khalizov, A.F., Pagels, J., Zhang, D., Xue, H.X., McMurry, P.H., 2008b. Variability in morphology, hygroscopicity, and optical properties of soot aerosols during atmospheric processing. Proceedings of the National Academy of Sciences of the United States of America 105(30), 10291-10296.

Chapter 8: Multi-criteria decision analysis applied to compression ignition engine efficiency and gaseous, particulate and greenhouse gas emissions

Nicholas C. Surawski[a,b], Timothy A. Bodisco[b], Branka Miljevic[a], Richard J. Brown[b], Zoran D. Ristovski[a], Godwin A. Ayoko[c*]

[a]International Laboratory for Air Quality and Health, Queensland University of Technology, 2 George St, Brisbane QLD 4001, Australia

[b]School of Engineering Systems, Queensland University of Technology, 2 George St, Brisbane QLD 4001, Australia

[c]Discipline of Chemistry, Faculty of Science and Technology, Queensland University of Technology, 2 George St, Brisbane QLD 4001, Australia

Publication: Submission pending Environmental Science & Technology, 2011.

Contributor	Statement of contribution
Nicholas C. Surawski Signature Date 21/10/11	Undertook measurements that underpinned the PROMETHEE-GAIA analysis, wrote the manuscript, and interpreted the results.
Timothy A. Bodisco	Contributed to the experimental dataset for study 1, and reviewed the manuscript.
Branka Miljevic	Undertook the ROS measurements for experimental studies 1-3, and reviewed the manuscript.

Richard J. Brown	Involved in the experimental design for experimental study 1, and reviewed the manuscript.
Godwin A. Ayoko	Suggested and undertook the PROMETHEE-GAIA analysis. Helped to interpret the results and write the manuscript.
Zoran D. Ristovski	Involved in the experimental design of the measurements underpinning the PROMETHEE-GAIA analysis, assisting in interpreting the results and writing of the manuscript.

Principal Supervisor Confirmation

I have sighted email or other correspondence from all Co-authors confirming their certifying authorship.

Associate Professor Zoran Ristovski		21/10/11
Name	**Signature**	**Date**

Abstract

Compression ignition (CI) engine design is subject to many constraints which provides a multi-criteria optimisation problem that the engine researcher must solve. In particular, the modern CI engine must not only be efficient, but must also deliver low gaseous, particulate and life cycle greenhouse gas emissions so that its impact on urban air quality, human health, and global warming are minimised. Consequently, this study undertakes a multi-criteria analysis which seeks to identify alternative fuels, injection technologies and combustion strategies that could potentially satisfy these various CI engine design constraints. Three datasets are analysed with the Preference Ranking Organization Method for Enrichment Evaluations and Geometrical Analysis for Interactive Aid (PROMETHEE-GAIA) algorithm which explore the impact of 1): an ethanol fumigation system, 2): alternative fuels (20 % biodiesel and synthetic diesel) and alternative injection technologies (mechanical direct injection and common rail injection) and 3): various biodiesel fuels made from 3 feedstocks (i.e. soy, tallow, and canola) tested at several blend percentages (20-100 %) on the resulting emissions and efficiency profile of the various test engines. The results show that moderate ethanol substitutions (~20 % by energy) at moderate load, that high percentage soy blends (40-100 %), and that alternative fuels (biodiesel and synthetic diesel) provide an efficiency and emissions profile that yields the most "preferred" solutions to this multi-criteria engine design problem. Further research is, however, required to reduce Reactive Oxygen Species emissions with alternative fuels, and to deliver technologies that do not significantly reduce the median diameter of particle emissions.

8.1 Introduction

The CI, or diesel, engine is both a reliable and durable internal combustion engine type that is used ubiquitously for a range of on-road and off-road transportation purposes. The CI engine offers many design advantages compared to its spark ignition (SI), or petrol, engine counterpart (Heywood, 1988). Since the combustion process is initiated by compression, rather than from an electrical discharge from a spark plug, CI engines can be operated with a higher compression ratio relative to SI engines. The benefit of a higher compression ratio is that CI engines have a higher thermal efficiency compared to SI engines. In addition, since CI engines are not throttled, they typically operate under lean air-fuel ratios; which reduces emissions of Carbon monoxide (CO) and Hydrocarbons (HCs). In direct comparison, SI engines typically operate under near stoichiometric air-fuel ratios which exacerbates CO and HC emissions. Despite these design advantages, CI engines are noisy, have higher Nitrogen Oxide (NOx) emissions than SI engines, and without after-treatment, emit significantly more

particulate matter from the tailpipe. As a result, modern CI engine design is confronted with many challenges that aim to minimise its impact on human health, urban air quality, and global climate (Majewski and Khair, 2006).

From the noted list of CI engine disadvantages, the issue of Diesel Particulate Matter (DPM) emissions has been the subject of considerable research and development, and at present remains an unresolved problem (Eastwood, 2008b). Whilst alternative fuels, injection technologies, and combustion strategies can be used as a tool to reduce DPM emissions, investigating these technologies could improve other aspects related to the impact of CI engines, such as: reducing gaseous emissions, improving engine efficiency, and in the case of alternative fuels, could significantly reduce the environmental footprint (or life cycle greenhouse gas emissions) of transportation fuels.

Life cycle analysis (LCA) of a transport fuel (also known as wells-to-wheels emissions) takes into account the total greenhouse gas emissions associated with a given transportation task. A critical point with LCA is that it considers not only tailpipe greenhouse gas emissions, but it also accounts for the pre-combustion greenhouse gas emissions (also known as upstream emissions) associated with extraction, production, transport, processing, conversion and distribution of a given fuel (Beer et al., 2002). The regulated gaseous emissions discussed above (CO, HCs, and NO) primarily affect human health; however, CI engines are also responsible for emitting greenhouse gases that play a role in global warming. The three greenhouse gases included in the life-cycle assessment were carbon dioxide (CO_2), methane (CH_4), and nitrous oxide (N_2O). Whilst technically, N_2O is a nitrogen oxide and CH_4 a hydrocarbon, these compounds are treated separately due to their strong greenhouse forcing potential. Relative to carbon dioxide (global warming potential of 1), N_2O has a 100 year global warming potential of 298 and CH_4 has a global warming potential of 25 (Intergovernmental Panel on Climate Change, 2007). To minimise the environmental footprint of transportation fuels, clearly, reductions in both tailpipe and upstream greenhouse gas emissions are desired.

To assess whether alternative fuels, injection technologies and combustion strategies can improve the gaseous, particulate and life-cycle greenhouse gas emissions profile from a CI engine, whilst simultaneously maintaining or improving engine efficiency, offers a multi-faceted, multi-criteria optimisation problem that the engine researcher must solve. The

Operations Research (OR) literature is populated with techniques that are able to provide "optimal" solutions to problems characterised by a uni-variate (or multi-variate) objective function which requires optimisation subject to several constraints (Winston, 2004). However, in multi-criteria problems the notion of an "optimal" solution breaks down, meaning that the decision maker is not able to use the standard techniques available in the OR literature (such as the simplex method and derivative based optimisation techniques) (Brans and Vincke, 1985). A way around this problem is to utilise techniques based on preference rather than "optimal" solutions.

There are a variety of multi-criteria decision analysis (MCDA) algorithms which vary in complexity from the elementary (e.g. weighted sum method) to methods which include the notion of outranking (Guitouni and Martel, 1998); such as ELECTRE, PROMETHEE and REGIME. A review of the MCDA literature revealed that the PROMETHEE-GAIA approach proved quite useful in environmental applications (Behzadian et al., 2010). A significant advantage of the PROMETHEE-GAIA algorithm (compared to other MCDA methods) is that it facilitates a rational decision making process. This is achieved by virtue of a decision vector that directs the decision maker towards "preferred" solutions (Brans and Mareschal, 1994).

This study applies the PROMETHEE-GAIA algorithm to 3 experimental datasets that explored alternative fuels, injection technologies, and combustion strategies to assess the impact of these techniques on the gaseous, particulate and life-cycle greenhouse gas emissions from CI engines. Engine efficiency was monitored during all experiments, enabling the impact of these techniques on brake thermal efficiency to be assessed. Consequently, this study aims to identify (potentially) viable engine technologies that may simultaneously enable these various design constraints (i.e. gaseous, particulate, and life-cycle greenhouse gas emissions, and engine efficiency) to be satisfied.

8.2 Methods

8.2.1 The PROMETHEE-GAIA algorithm

The theory of the PROMETHEE-GAIA algorithm is well described in the literature. The explanation of the algorithm provided in this section is based on the works conducted by the developers in: Brans and Vincke (1985), Brans et al. (1986), Mareschal and Brans (1988), Brans and Mareschal (1994). Note that the absence of references in the ensuing section denotes that the discussion of the algorithm follows that presented in the above listed

publications. The interested reader is also directed to a paper by Behzadian et al. (2010) for a review of the history and the fields of application for this algorithm.

The PROMETHEE-GAIA algorithm permits solution of MCDA problems of the following form:

$$\text{Max}\{f_1(a), \cdots, f_{1k}(a) | \text{a} \in \text{A}\},$$

where A is a set of n alternatives which are evaluated through k criteria $(f_1, \cdots, f_k)$.

In this study, alternatives entail the application of different techniques to mitigate the impacts of a CI engine, such as alternative fuels, injection technologies and combustion strategies. Alternatively, the criteria against which alternatives are assessed involve factors such as low gaseous and particulate emissions, low life cycle greenhouse gas emissions with each chosen fuel, whilst also making sure that the engine efficiency is maximised.

PROMETHEE-GAIA accepts a real valued evaluation table ($f_i \in \mathbb{R}, \forall i$, see Table 8.1) as a numerical input to the algorithm in the following form (i.e. categorical data cannot be analysed):

Table 8.1: The PROMETHEE-GAIA evaluation table.

	$f_1(.)$	⋯	$f_{k(.)}$
a_1	$f_1(a_1)$	⋯	$f_k(a_1)$
⋯	⋯	⋯	⋯
a_n	$f_1(a_n)$	⋯	$f_k(a_n)$

If we take a particular criterion (say f_i) that has to be maximised, pairwise comparison between alternatives lead to the following preference structure ($\forall a, b \in A$):

$$\begin{cases} f_i(a) > f_i(b) \Leftrightarrow a \; P \; b, \\ f_i(a) = f_i(b) \Leftrightarrow a \; I \; b, \end{cases}$$

where P and I denote preference and indifference, respectively.

To take into account the relative scale of the criteria, a generalised criterion must be applied to each criterion. This is achieved with the preference function $P(a, b)$ which takes into account the preference of a over b for criterion f_i. The preference function $P(a, b)$ is

usually expressed in terms of the relative difference $d = f_i(a) - f_i(b)$, and is a normalised quantity such that $0 \leq P(a,b) \leq 1$. The preference function offers the following structure:

$$\begin{cases} P(a,b) = 0, \ if \ d \leq 0, & \text{no preference or indifference} \\ P(a,b) \approx 0, if \ d > 0, & \text{weak preference} \\ P(a,b) \approx 1, if \ d \gg 0, & \text{strong preference} \\ P(a,b) = 1, if \ d \gg\gg 0, & \text{strict preference.} \end{cases}$$

The preference function $P(a,b)$ is required to be a strictly monotonically increasing function of d, being similar in form to that presented in Figure 8.1.

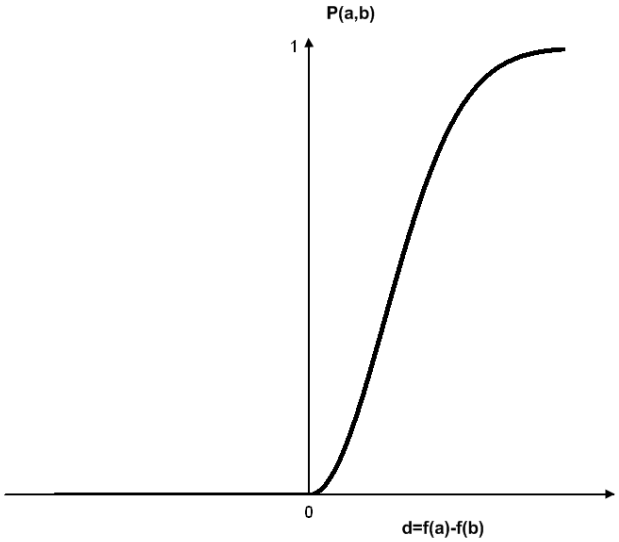

Figure 8.1: PROMETHEE-GAIA preference function.

A total of 6 preference functions are available to the PROMETHEE-GAIA user, and include functions such as: linear, V-shaped, Gaussian and other preference functions with varying thresholds. A V-shaped preference function was used in this study, with the maximum value of an alternative (for a particular criterion) used as a threshold value.

Once a generalised criterion (through the preference function) has been applied to each criterion (f_i), a multi-criteria preference index $\pi(a,b)$ for a compared to b (for all criteria) can be computed via:

$$\pi(a,b) = \sum_{j=1}^{k} w_j P_j\,(a,b), \quad \sum_{j=1}^{k} w_j = 1,$$

where $w_j > 0 \ \forall j$, are the weights assigned to each criterion with $w_j \in \mathbb{R}$, noting well that the weights sum to unity.

Under the assumption of equal weights the preference index simplifies to:

$$\pi(a,b) = \frac{1}{k}\sum_{j=1}^{k} P_j\,(a,b),$$

however, it is possible to undertake a sensitivity analysis with a un-equal weights applied to each criterion (Dağdeviren, 2008). A sensitivity analysis has not been undertaken in this study, and all criteria are given equal weights.

To aid in the decision making process, the algorithm then computes the positive outranking flow:

$$\phi^{+}(a) = \frac{1}{n-1}\sum_{x\in A} \pi(a,x),$$

and also the negative outranking flow:

$$\phi^{-}(a) = \frac{1}{n-1}\sum_{x\in A} \pi(x,a).$$

The positive outranking flow quantifies how much a given alternative outranks the others, with a higher value of $\phi^{+}(a)$ indicating a more preferred alternative. Conversely, the negative outranking flow quantifies how a given alternative is outranked by other alternatives. A smaller value of $\phi^{-}(a)$ is preferred.

A ranking of alternatives is available to the PROMETHEE-GAIA decision maker by considering the difference between the positive and negative outranking flows by considering the net outranking flow given by:

$$\phi(a) = \phi^{+}(a) - \phi^{-}(\text{a}).$$

A higher value of the net outranking flow indicates a more preferable alternative.

Most MCDA problems involve several criteria. As a result, the solution to the problem exists in a multi-dimensional space. The GAIA component of the PROMETHEE-GAIA algorithm then performs Principal Component Analysis (PCA) to reduce the dimensionality of the problem to 2 spatial dimensions (called the GAIA plane) for visual interpretation of the problem. The projection error associated with PCA is governed by the 2 dominant eigenvalues (λ_1, λ_2) of the variance-covariance matrix (C) associated with the uni-criterion (ϕ_j) net flows. The proportion of information retained after PCA (δ) is given by:

$$\delta = (\lambda_1 + \lambda_2) \Big/ \sum_{j=1}^{k} \lambda_j,$$

where: λ_k are the k eigenvalues of C. Typically, δ is greater than 60%, but often exceeds 80% for MCDA problems, so the GAIA plane retains a reasonable fraction of useful information.

Unlike PCA, PROMETHEE-GAIA has the critical difference that it provides a decision vector for the analyst. This enables the decision maker to view different alternatives in the GAIA plane, and to be directed towards preferred solutions by the decision vector. The decision vector is computed by calculating the projection of the different alternatives (α_i) onto the weights of the problem (w) which is achieved via:

$$(\alpha_i, w) = \sum_{j=1}^{k} w_i \phi_j (a_i) = \phi(a_i).$$

A decision vector that is long and not orthogonal to the GAIA plane is preferred for strong decision making power. Figure 8.2 shows the relationship between criteria in the GAIA plane. Correlated criteria lie close to each other in the GAIA plane (-45-45 ^{o}, left panel), anti-correlated criteria lie in roughly opposite directions (135-225 ^{o}, middle panel), whilst independent, or un-correlated criteria, lie in a roughly orthogonal direction (45-135 ^{o}, right panel) in the GAIA plane (Espinasse et al., 1997).

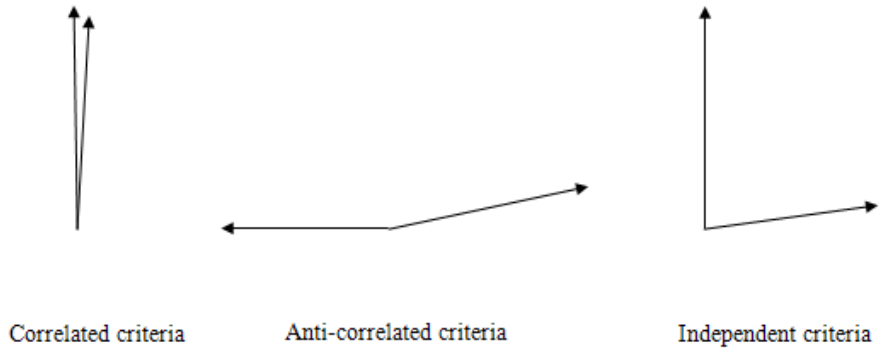

Figure 8.2: Relationships between criteria in the GAIA plane.

8.2.2 The datasets analysed

The gaseous and particulate emissions datasets investigated in this study were the subject of several recent publications (Surawski et al., 2010b; Surawski et al., 2011a; Surawski et al., 2011c; Surawski et al., 2011d). In this above set of studies, gaseous emissions, engine

efficiency and the physico-chemistry of DPM emissions were investigated in 3 distinctly different experimental study designs.

In the first study, an ethanol fumigation system was equipped to a direct injection diesel engine (Surawski et al., 2010b; Surawski et al., 2011d). The objective of this study was to investigate the impact of an alternative fuel (ethanol) and an alternative combustion strategy (fumigation - a type of pre-mixed compression ignition) on the resulting emissions profile from the test engine.

In the second study, an engine was tested with 2 injection configurations (mechanical direct injection, and common rail injection) and 3 fuels (ultra-low sulphur diesel (ULSD), 20% biodiesel blend, and a synthetic diesel) to explore the role of fuel type and injection configuration on the emission profile from the test engine (Surawski et al., 2011c).

The third study investigated the role of different biodiesel fuels made from different feedstocks (i.e. soy, tallow, and canola) tested at a range of different blend percentages (20-100 %), using the results from ULSD as baseline for comparison on the emissions profile from the test engine (Surawski et al., 2011a).

Table 8.2 provides an overview of the experimental data which formed the basis for application of the PROMETHEE-GAIA algorithm. The following parameters were calculated in all 3 studies listed above (Surawski et al., 2010b; Surawski et al., 2011a; Surawski et al., 2011c; Surawski et al., 2011d); namely: regulated emissions (CO, HCs, NO, and PM), unregulated emissions (particle number emissions, particle surface area emissions, Count Median Diameter (CMD) (derived from an SMPS size distribution), Reactive Oxygen Species (ROS) concentrations, and the organic volume percentage of particles. Other unregulated emissions that were measured included measuring: the percentage of volatile particles (PVP) for the ethanol fumigation study, and measuring either total polycyclic aromatic hydrocarbon emission (mg/kWh) (alternative fuels and injection technologies study), or measuring particle phase and vapour phase polycyclic aromatic hydrocarbons separately (alternative fuels study with 3 biodiesel feedstocks).

Table 8.2: An overview of the measurements conducted in the 3 datasets analysed with the PROMETHEE-GAIA algorithm. Each column refers to a different study, and each row refers to a different CI engine parameter that was measured or calculated. "X" denotes that a given parameter was measured or calculated in a particular study, whereas "-" denotes that this parameter was not measured or calculated.

		Study number		
		1	2	3
	Techniques investigated	**Alternative fuels** (ethanol) **Alternative combustion strategy** (fumigation)	**Alternative fuels** (biodiesel, synthetic diesel) **Alternative injection technologies** (mechanical direct injection, common rail injection)	**Alternative fuels** (biodiesel fuels made from soy, tallow and canola tested at different blend percentages 20-100 %)
Regulated emissions	Carbon monoxide (CO) (g/kWh)	X	X	X
	Hydrocarbons (HCs) (g/kWh)	X	X	X
	Nitric oxide (NO) (g/kWh)	X	X	X
	Particulate Matter (PM) (g/kWh)	X	X	X
Unregulated emissions	Particle number emissions (#/kWh)	X	X	X
	Count median diameter (CMD) (nm)	X	X	X
	Particle surface area (nm^2/cm^3)	X	X	X
	Reactive oxygen species (ROS) (nmol/mg)	X	X	X
	Particle organic volume percentage (%)	X (Only determined at 80 nm with a V-TDMA system)	X	X
	Percentage of volatile particles (%) (PVP)	X	-	-

	Total polycyclic Aromatic Hydrocarbons (PAHs) (mg/kWh)	-	X	X
	Particle phase polycyclic Aromatic Hydrocarbons (PAHs) (mg/kWh)	-	-	X
	Vapour phase polycyclic Aromatic Hydrocarbons (PAHs) (mg/kWh)	-	-	X
Engine performance	Brake thermal efficiency (-)	X	X	X
	Brake specific energy consumption (MJ/kWh)	X	X	X
	Pre-mixed combustion percentage (%)	X	-	-
	Diffusion flame combustion percentage (%)	X	-	-
Sustainability measure	Life-cycle greenhouse gas emissions (g/km)	X	X	X

Engine performance measures were also recorded during all 3 experiments. The two engine performance measures calculated were brake thermal efficiency and Brake Specific Energy consumption (BSEC).

The brake thermal efficiency was calculated according to (Heywood, 1988):

$$\eta_f = \frac{P_b}{\dot{m}_f Q_{LHV}}, \tag{8.1}$$

where P_b is the brake power output of the engine (measured with a dynamometer), $\dot{m}_f$ is the fuel mass flow rate, and Q_{LHV} is the lower heating value of the fuel.

In the first study (ethanol fumigation study), access to in-cylinder pressure versus crank angle data was available. By undertaking a combustion analysis with the AVL Boost program (AVL List GmbH, 2008a), heat release versus crank angle could be computed using the first law of thermodynamics. This enabled the percentage of heat released in the pre-mixed, and diffusion flame phases of combustion to be computed. These two engine performance measures were included in the first study to assess their impact on the overall emissions profile.

BSEC (MJ/kWh) was calculated according to:

$$BSEC = \frac{Q_{LHV} \times \dot{m}_f \times 3600}{P_b}. \quad (8.2)$$

Another quantity that was computed in all 3 experiments was the life-cycle greenhouse gas emissions for each transportation fuel investigated. Upstream greenhouse gas emissions estimates for N_2O, CH_4 and CO_2 associated with extraction, production, transport, processing, conversion and distribution of various Australian alternative fuels are taken from published data by Beer et al. (2001) and Beer et al. (2007). The same information source was used to obtain tailpipe (i.e. post combustion) emissions for N_2O and CH_4. Tailpipe CO_2 emissions factors were calculated using the data collected as part of the 3 studies described above. The total life cycle greenhouse gas emissions (g/km) were obtained by multiplying the raw emissions factor by its IPCC Global Warming Potential factor (Intergovernmental Panel on Climate Change, 2007) and then summing the results for the pre-combustion (i.e. upstream) and post-combustion (i.e. tailpipe) emissions contributions.

The only parameters listed in Table 8.2 that were maximised included: brake thermal efficiency, the count median diameter of particles, and the pre-mixed combustion percentage. All other criteria were minimised as they relate to gaseous, particulate and life-cycle greenhouse emissions which the engine designer wants to eliminate. The decision made about how to treat all the different criteria (i.e. maximise or minimise) gives an overall "metric" that needs to be optimised to satisfy CI engine design requirements.

8.3 Results and discussion

Figure 8.3 shows the PROMETHEE II outranking for all 3 datasets, which involves ranking the alternatives (for all 3 studies) from highest to lowest based on the value of their net outranking flow (ϕ). For the first study, second and third studies, the range of ϕ is 0.44, 0.29, and 0.70 and respectively. Thus, the range of ϕ gives an indication as to how well the PROMETHEE II outranking can distinguish between alternatives, where it is noted that the alternatives are closely grouped for the second study, but some clear differences in ranking are observed for the first and third study.

Another result to emerge from the PROMETHEE II outranking is how the algorithm gives greater preference to alternative fuels. In the first study, ϕ achieves a greater value for tests involving ethanol fumigation at all load settings except idle. In the second study, the

distinguishing power of the outranking is reduced (due to a limited ϕ range); however, we still observe that the algorithm ranks the alternative fuels in the order: synthetic diesel > biodiesel > ULSD. In the third study, 12 of the biodiesel blends are more highly preferred to ULSD. Indeed, only a single biodiesel blend (80% canola biodiesel) is less preferred to ULSD.

Other preferences emerge from the PROMETHEE II outranking. In the first study, the use of an alternative injection strategy (i.e. fumigation) is preferred over conventional diesel injection. This can be observed due to the higher ϕ values achieved when using intake manifold injection of ethanol for a fixed load setting relative to conventional diesel injection.

In the second study, the impact of injection technology (for a fixed fuel setting) is a little more difficult to determine. The trends in ϕ are mixed, with direct injection being favoured to common rail injection for synthetic diesel and ULSD for the intermediate and rated speed tests at half; whereas, common rail injection is preferred to direct injection with synthetic diesel at rated speed and full load, and with ULSD at intermediate speed and half load. With biodiesel, the outranking is not sensitive to the injection technology used, which is suggestive of compatibility of injection configuration alterations with this fuel type.

Overall, the PROMETHEE II outranking results are a promising sign for the use of alternative fuels, and combustion strategies. The results with alternative injection technologies are mixed; however, with the use of biodiesel changing the injection set-up does not adversely affect the final outranking. The results suggest a switch away from ULSD, but the specific alternatives (e.g. speed/load setting, fuel type etc) that are recommended need to be identified, which is attempted next.

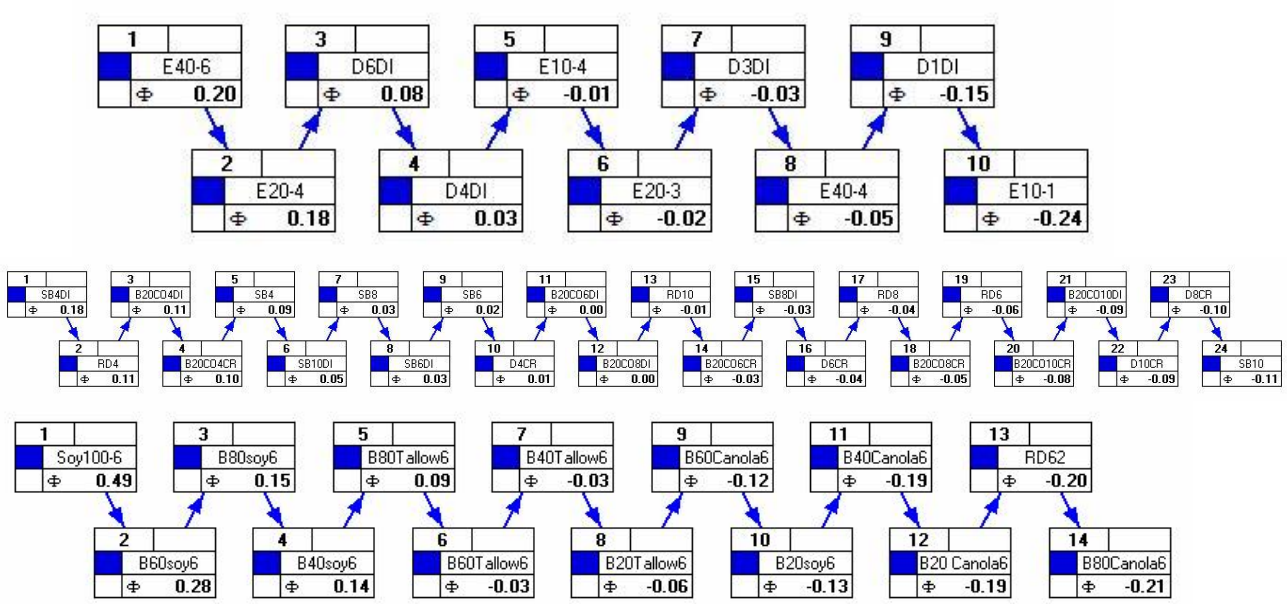

Figure 8.3: PROMETHEE II outranking for all 3 datasets. Top panel: alternative fuels and combustion strategy study, middle panel: alternative fuels and injection technologies study, bottom panel: alternative fuels study.

Figure 8.4 shows a GAIA biplot of alternatives for each of the 3 studies. In interpreting these results, the length of the decision vector (pi) is critical, as a longer decision vector indicates greater decision making power (Espinasse et al., 1997). From Figure 8.4, we observe that decision vector is short for the first two studies, but a longer decision vector is observed with the third study.

In the first study (top panel), only one alternative emerges from the alternatives GAIA biplot as a candidate for employing the ethanol fumigation approach. The E20 test at half load is located with 45 ^{o} of the decision vector and is located reasonably far from the origin of the GAIA alternatives plane. This is a valuable result for two main reasons. Previous research has suggested that ethanol fumigation is generally more successful under moderate load (i.e. not full or low load) conditions (Ecklund et al., 1984c), and that when implemented a 20 % ethanol substitution (by energy) is close to the optimal level of secondary fuel substitution (Abu-Qudais et al., 2000). The E40 test at full load is also located in close proximity to the decision vector, but it is difficult to recommend such a high level of ethanol substitution at this load, when the corresponding ULSD test at full load is located roughly in the direction of the decision vector much further from the origin. The analysis also identifies ethanol substitutions that should not be undertaken, such as the 20 % substitution at quarter load, and also the 10 % substitution at idle. This decision is reached, as these two alternatives are

located roughly in the opposite direction of the decision vector (135-225 ^{o}) - meaning that these alternatives are in conflict with the proposed engine design "metric". From a mechanical perspective, previous research explains this result (Ecklund et al., 1984c; Abu-Qudais et al., 2000), as the problem of flame quenching is encountered with ethanol fumigation under low load conditions.

In the second study (middle panel), the decision vector is quite short which limits the conclusions that can be drawn. Only 8 alternatives (out of 24) are located within close proximity to the decision vector; however, it is interesting to note that 6 of these alternatives are for alternative fuels (3 for biodiesel and 3 for synthetic diesel). The 8 alternatives are equally split between direct injection (4) and common rail injection (4). This fact combined with the limited $\boldsymbol{\phi}$ range for the analysis does not enable clear recommendations to be drawn from the second study.

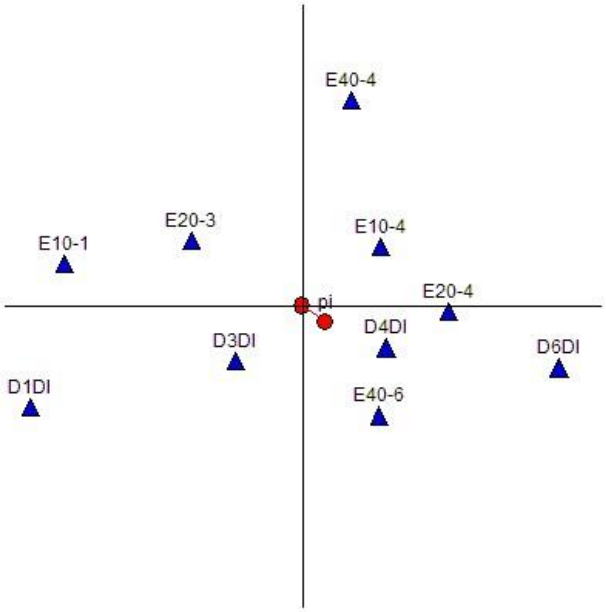
E40-4
E20-3
E10-1
E10-4
pi
E20-4
D4DI
D3DI
D6DI
D1DI
E40-6

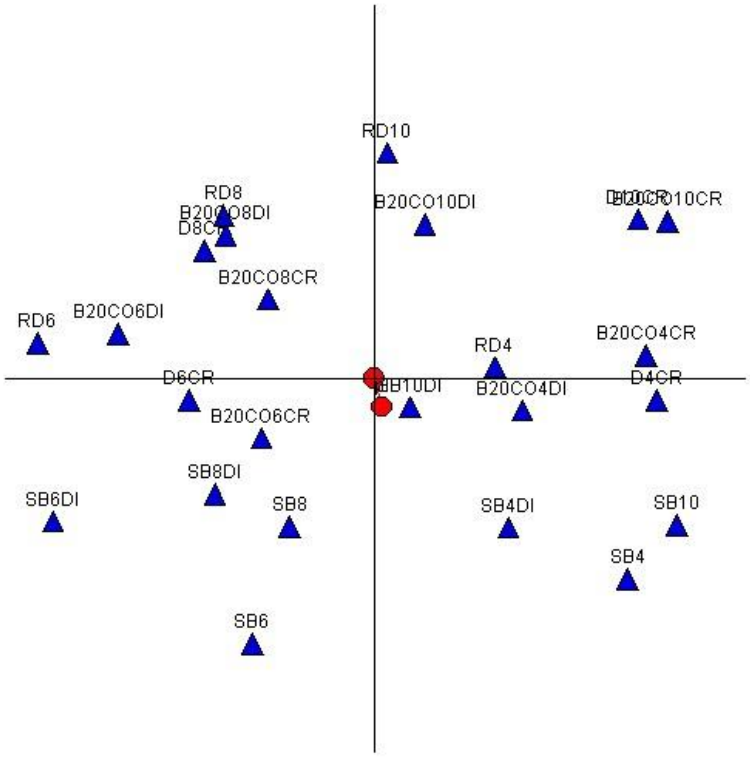
RD10
RD8
B20CO10DI
B20CO8DI
D8CR
B20CO8CR
RD6
B20CO6DI
B20CO4CR
RD4
D6CR
B20CO4DI
D4CR
B20CO6CR
SB8DI
SB6DI
SB8
SB4DI
SB10
SB4
SB6

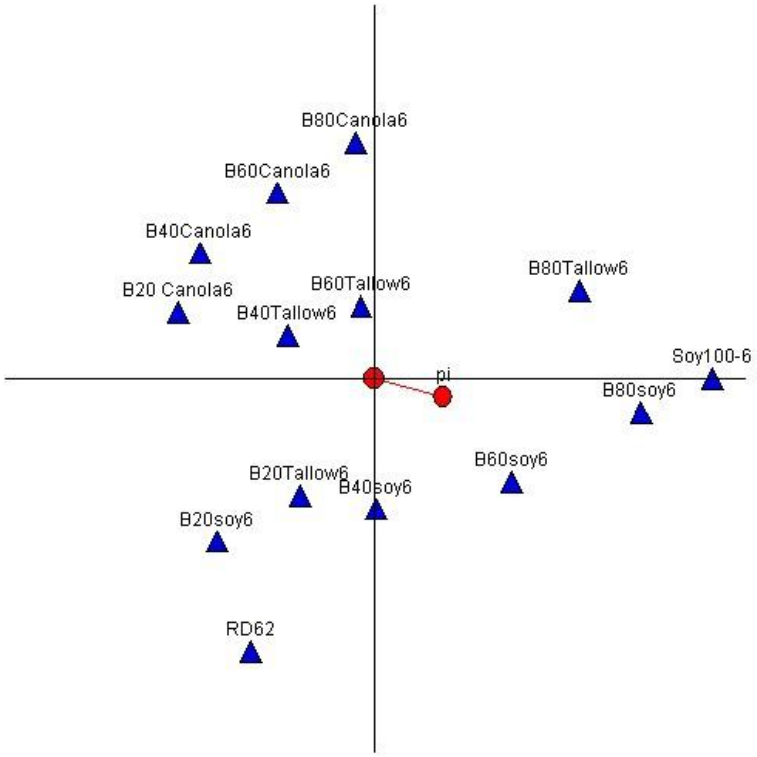

Figure 8.4: GAIA biplot of alternatives for all 3 datasets. Top panel: alternative fuels and combustion strategy study, middle panel: alternative fuels and injection technologies study, bottom panel: alternative fuels study. Principal components 1 and 2 explained 76.4 % (top panel), 66.4 % (middle panel), and 68.9 % (bottom panel) of the variance in the 3 datasets respectively.

In the third study (bottom panel), the decision vector is long and a clear separation of alternatives can be seen in the GAIA plane. 5 alternatives are located roughly in the direction of the decision vector (-45-45 ^{o}) pi. These 5 alternatives are the 80% tallow blend, and the 40, 60, 80, and 100 % soy blends. All four canola blends lie roughly in the opposite direction to the decision vector, as well as the 40 and 60 % tallow blends. All other fuel alternatives are roughly orthogonal to the decision vector, which indicates that these alternatives are not correlated with the criteria against which alternatives are optimised. A clear conclusion to emerge from the third study is that high percentage soy blends are preferred at full load for the test engine investigated.

Several results are evident from the GAIA plane which indicate criteria that are in conflict (i.e. are orthogonal to) with the decision vector for the problem. For example, finding techniques for maximising the CMD of particles (subject to the other constraints) was not

possible. This can be seen due to the CMD vector always being roughly orthogonal to the decision vector. Another parameter that was roughly orthogonal to the decision vector was the life-cycle greenhouse gas emissions. This result suggests that the selection of a sustainable fuel is usually in conflict with the other criteria (i.e. emissions and efficiency) against which alternative engine technologies are assessed. The GAIA plane shows also that alternative engine technologies are capable of delivering improvement in the physical characteristics of particles (such as reduced mass, number, and surface, but not increased CMD) especially for the third study. However, the improvements in the physical characteristics of particles were achieved by making the unregulated chemistry of the particles worse. This can be observed due to the roughly orthogonal nature of the particle physical and chemical characteristics in the GAIA plane. ROS emission increases were observed with all alternative fuels, and ROS increases were also observed with common rail injection, so this particular pollutant emerges from this analysis as an unregulated pollutant requiring reduction with alternative engine technologies.

In conclusion, this study has investigated common alternative engine technologies (i.e. fuels, combustion strategies, and injection technologies) that are applied in CI engines in an attempt to reduce their impact on urban air quality, human health and global warming. The results show that alternative combustion strategies (such as ethanol fumigation) are recommended at moderate load with ethanol substitutions around 20 %. The third study shows a clear preference for high percentage soy blends 40-100 % at full load. Alternatively, the second study does not exhibit strong preferences; however, biodiesel and synthetic diesel are preferred to ULSD, and direct injection is generally preferred to common rail injection. Whilst the results show that alternative engine technologies are capable of improving the nature of the CI engines emissions profile, further research is required to deliver technologies that minimise the impact of CI engines. Specifically, reducing ROS emissions with alternative fuels emerges as one problem requiring further research attention, along with finding that alternative engine technologies that do not significantly reduce the CMD of particles.

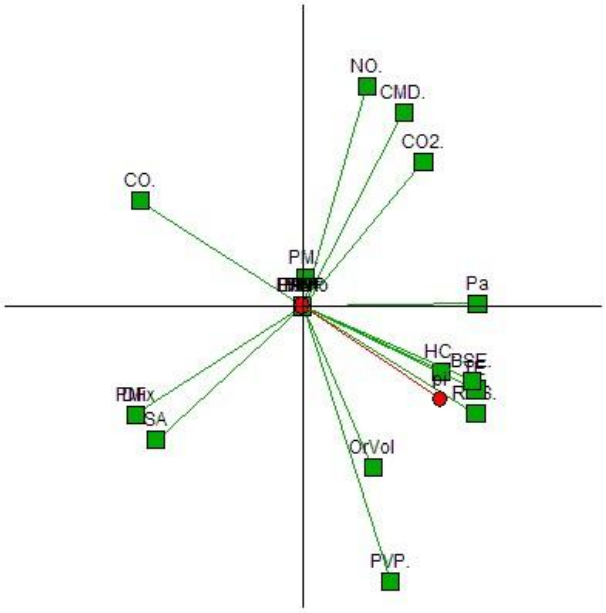
NO.
CMD.
CO2.
CO.
PM.
Pa
HC
SA
OrVol
PVP.

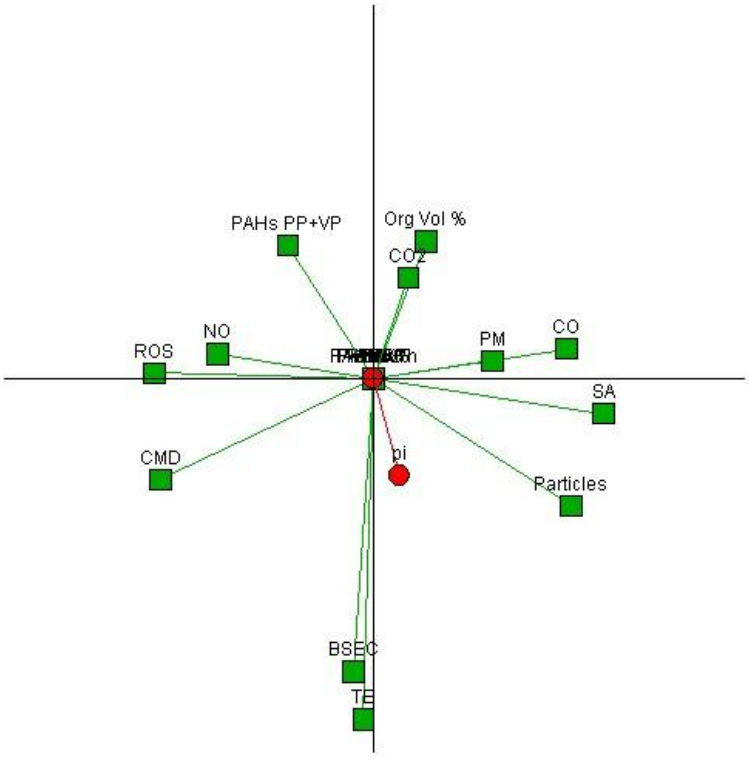
PAHs PP+VP
Org Vol %
CO2
NO
ROS
PM
CO
SA
CMD
pi
Particles
BSEC
TE

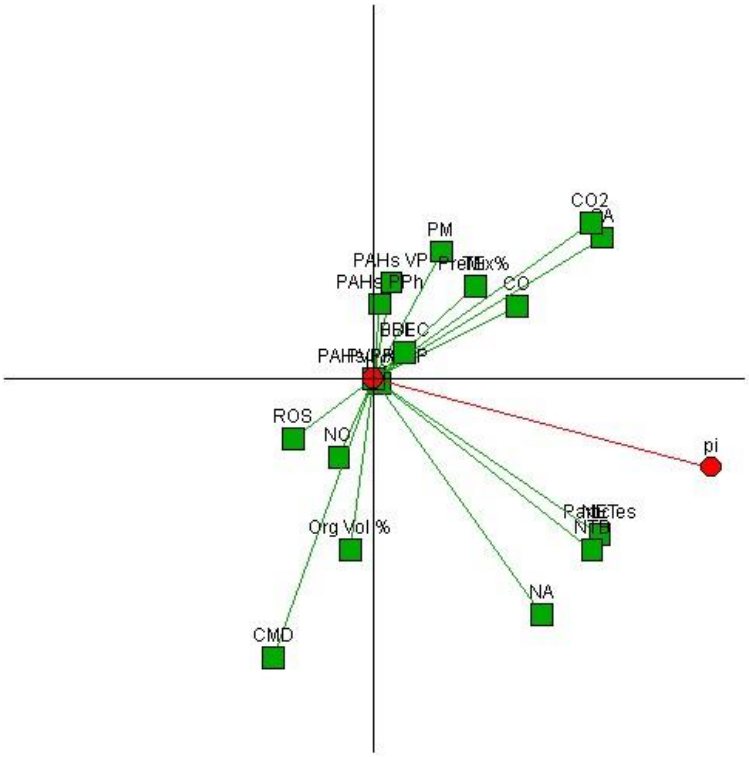

Figure 8.5: GAIA biplot of criteria of the 3 datasets. Top panel: alternative fuels and combustion strategy study, middle panel: alternative fuels and injection technologies study, bottom panel: alternative fuels study.

8.4 References

Abu-Qudais, M., Haddad, O., Qudaisat, M., 2000. The effect of alcohol fumigation on diesel engine performance and emissions. Energy Conversion and Management 41(4), 389-399.

AVL List GmbH, 2008. AVL BOOST v5.1, Graz, Austria.

Beer, T., Grant, T., Campbell, P.K., 2007. The greenhouse and air quality emissions of biodiesel blends in Australia. CSIRO Report Number KS54C/1/F2.27, pp. 1-126.

Beer, T., Grant, T., Morgan, G., Lapszewicz, J., Anyon, P., Edwards, J., Nelson, P., Watson, H., Williams, D., 2001. Comparison of transport fuels, Final Report (EV45A/2/F3C), to the Australian Greenhouse Office, on the Stage 2 study of Life-cycle Emissions Analysis of Alternative Fuels for Heavy Vehicles. CSIRO, pp. 1-463.

Beer, T., Grant, T., Williams, D., Watson, H., 2002. Fuel-cycle greenhouse gas emissions from alternative fuels in Australian heavy vehicles. Atmospheric Environment 36(4), 753-763.

Behzadian, M., Kazemadeh, R.B., Albadvi, A., Aghdasi, M., 2010. PROMETHEE: a comprehensive literature review on methodologies and applications. European Journal of Operational Research 200(1), 198-215.

Biswas, S., Verma, V., Schauer, J.J., Cassee, F.R., Cho, A.K., Sioutas, C., 2009. Oxidative Potential of Semi-Volatile and Non Volatile Particulate Matter (PM) from Heavy-Duty Vehicles Retrofitted with Emission Control Technologies. Environmental Science & Technology 43(10), 3905-3912.

Brans, J.P., Mareschal, B., 1994. The PROMCALC & GAIA decision-support system for multicriteria decision aid. Decision Support Systems 12(4-5), 297-310.

Brans, J.P., Vincke, P.H., 1985. A preference ranking organization method - (The PROMETHEE method for multiple criteria decision-making) Management Science 31(6), 647-656.

Brans, J.P., Vincke, P.H., Mareschal, B., 1986. How to select and how to rank projects - the PROMETHEE method. European Journal of Operational Research 24(2), 228-238.

Dağdeviren, M., 2008. Decision making in equipment selection: an integrated approach with AHP and PROMETHEE. Journal of Intelligent Manufacturing 19(4), 397-406.

Eastwood, P., 2008. Particulate emissions from vehicles. John Wiley & Sons, Ltd, Chichester, pp. 1-493.

Ecklund, E.E., Bechtold, R.L., Timbario, T.J., McCallum, P.W., 1984. State-of-the-art report on the use of alcohols in diesel engines. Society of Automotive Engineers, SAE Paper NO. 840118.

Espinasse, B., Picolet, G., Chouraqui, E., 1997. Negotiation support systems: a multi-criteria and multi-agent approach. European Journal of Operational Research 103(2), 389-409.

Guitouni, A., Martel, J.M., 1998. Tentative guidelines to help choosing an appropriate MCDA method. European Journal of Operational Research 109(2), 501-521.

Heywood, J.B., 1988. Internal combustion engine fundamentals. McGraw-Hill, Inc, New York, pp. 1-930.

Intergovernmental Panel on Climate Change, 2007. Climate change 2007: the physical science basis, contribution of Working Group I to the Fourth Assessment Report of the Intergovernmental Panel on Climate Change, IPCC Fourth Assessment Report (AR4), in: Solomon, S., Qin, D., Manning, M., Chen, Z., Marquis, M., Averyt, K.B., Tignor, M., Miller, H.L. (Eds.). IPCC, Cambridge, United Kingdom, pp. 1-996.

Majewski, W.A., Khair, M.K., 2006. Diesel emissions and their control. SAE International, Warrendale, pp. 1-561.

Mareschal, B., Brans, J.P., 1988. Geometrical representations for MCDA European Journal of Operational Research 34(1), 69-77.

Miljevic, B., Heringa, M.F., Keller, A., Meyer, N.K., Good, J., Lauber, A., Decarlo, P.F., Fairfull-Smith, K.E., Nussbaumer, T., Burtscher, H., Prevot, A.S.H., Baltensperger, U., Bottle, S.E., Ristovski, Z.D., 2010. Oxidative potential of logwood and pellet burning

particles assessed by a novel profluorescent nitroxide probe. Environmental Science & Technology 44(17), 6601-6607.

Surawski, N.C., Miljevic, B., Ayoko, G.A., Elbagir, S., Stevanovic, S., Fairfull-Smith, K.E., Bottle, S.E., Ristovski, Z.D., 2011a. A physico-chemical characterisation of particulate emissions from a compression ignition engine: the influence of biodiesel feedstock. Under review Environmental Science & Technology.

Surawski, N.C., Miljevic, B., Ayoko, G.A., Roberts, B.A., Elbagir, S., Fairfull-Smith, K.E., Bottle, S.E., Ristovski, Z.D., 2011b. Physicochemical Characterization of Particulate Emissions from a Compression Ignition Engine Employing Two Injection Technologies and Three Fuels. Environmental Science & Technology 45(13), 5498-5505.

Surawski, N.C., Miljevic, B., Roberts, B.A., Modini, R.L., Situ, R., Brown, R.J., Bottle, S.E., Ristovski, Z.D., 2010. Particle emissions, volatility, and toxicity from an ethanol fumigated compression ignition engine. Environmental Science & Technology 44(1), 229-235.

Surawski, N.C., Ristovski, Z.D., Brown, R.J., Situ, R., 2011c. Gaseous and particle emissions from an ethanol fumigated compression ignition engine. Submitted to Energy Conversion & Management.

Winston, W.L., 2004. Operations research: applications and algorithms, fourth edition. Brooks/Cole - Thomson Learning, Toronto, pp. 1-1418.

Chapter 9: Conclusions and further research

9.1 Conclusions arising from this study

This research program has made a significant contribution to our understanding of the physico-chemical properties of DPM with a range of DPM mitigation strategies. The measurements conducted in this thesis have relevance for the human health effects of DPM and also urban air quality and global climate. The CI engine is a major contributor to the ambient PM problem (Robinson et al., 2010), where DPM is associated with cardiovascular and respiratory morbidity and mortality (Pope and Dockery, 2006), and also influences global climate through its ability to absorb and scatter light (Jacobson, 2001). DPM emissions should, therefore, be investigated in a fundamental manner for the dual purposes of minimising human health impacts and also for mitigating global warming as has been done in this thesis.

This thesis has investigated a range of different DPM mitigation strategies primarily to ascertain their impact on its physico-chemical properties; however, these techniques also have ramifications for gaseous emissions, engine efficiency, and also the environmental footprint of a given transportation fuel. The introduction of new DPM mitigation strategies such as alternative fuels, injection technologies and combustion strategies should be conducted in such a way that all risk factors be minimised. As previously mentioned, risk factors associated with DPM mitigation strategies have human health and environmental aspects involved. Overall, the results from this thesis have identified several areas requiring improvement in terms of the emissions profile from CI engines employing a range of different DPM mitigation techniques.

The first manuscript which investigated gaseous and particle emissions from an ethanol fumigated CI engine showed that significant increases occurred in CO and HC emissions with this technology at all load settings other than idle. Whilst a previous study has shown particle number reductions with ethanol fumigation (Zhang et al., 2011), in direct contrast this thesis has shown that particle number emissions increases occur. Strategies should therefore be developed to mitigate CO, HC and particle number increases with ethanol fumigation technology in older CI engines (i.e. without after-treatment and turbocharging); which is a topic discussed in the research recommendations arising from this thesis.

The second manuscript explored in more detail the mechanism behind particle number increases with ethanol fumigation. This paper showed that ethanol fumigation was very effective at reducing DPM mass emissions, by virtue of vastly reducing the accumulation mode surface area. Since the ethanol fumigation approach delivered more volatile gas phase material, this led to conditions making the nucleation of volatile material more likely. A V-TDMA analysis confirmed that at high load accumulation mode particles were coated with a lot more volatile organic material, and at lower loads a very high percentage of particles were purely volatile. Nucleation of volatile material appears to be the mechanism behind particle number increases with ethanol fumigation, resulting in the formation of essentially organic nucleation modes. This manuscript also showed a relationship between the semi-volatile fraction of DPM (through the V-TDMA analysis) and the emissions of particle bound ROS.

The third manuscript investigated DPM emissions using two injection configurations with both injection systems being tested with 3 fuels. Both alternative fuels were effective at reducing DPM mass and number emissions (except for synthetic diesel with mechanical direct injection); however, injection technology was a more important factor for reducing DPM mass and number emissions. Common rail injection proved to be a very effective technique for reducing DPM mass and number emissions; however, with this approach DPM was coated with far more genotoxic compounds, such as PAHs and ROS.

This result has implications for the use of CI engines in an underground mine – which is an environment characterised by limited dilution conditions. The ventilation requirements for diesel powered equipment in underground mines are dictated by DPM mass emissions. Employing a common rail injection CI engine in this environment would lead to a reduction in an engines ventilation requirement (based on DPM mass) even though more toxic material is present on the DPM particle surface. Therefore, strategies need to be developed for reducing the semi-volatile fraction of DPM from common rail injection engines.

The fourth manuscript investigated DPM physico-chemical properties with a direct injection engine using biodiesel fuels made from 3 different feedstocks each tested with at least 4 blend percentages. All biodiesel fuel types and blend percentages were very effective at reducing DPM mass, although the DPM number results exhibited more complicated trends. Whilst larger soy and tallow biodiesel blend percentages reduced particle number emissions, other fuel types (especially canola blends) increased the number of particles emitted. For all

biodiesel fuel types investigated, as the biodiesel blend percentage was increased, the particles were internally mixed with more ROS on the particle surface. As a result, the factors leading to increased ROS emissions with oxygenated fuels needs to be explored in further detail to achieve reductions in this pollutant.

A combination of results from these 4 manuscripts identifies aspects of gaseous and DPM emissions requiring improvement to minimise the impact of alternative transportation fuels on human health.

A reduction in median particle size for a fixed engine load was observed for most alternative fuels. The fifth paper in this thesis investigated the morphological restructuring of a range of combustion aerosols (e.g. DPM, petrol exhaust, candle smoke etc) exposed to a range of different solvents with different surface tensions (e.g. DMSO, hexane, water etc) to explore a hypotheses enabling combustion aerosol restructuring to be explained. This study showed that restructuring occurred due to the ability of organic vapours to "wet" the particle surface. In particular, the role of surface tension, and the role of organics in flocculating elemental carbon containing primary particles were not found to be responsible.

The sixth manuscript in this thesis employed an MCDA technique (PROMETHEE-GAIA) to make recommendations about which DPM mitigation techniques (if any) are suitable for reducing the health impacts associated with gaseous and DPM emissions, whilst simultaneously achieving good thermal efficiency for each test engine, and making sure that life cycle greenhouse gas emissions are not increased. Based on the PROMETHEE II outranking, the results from this paper show strong preference for the usage of alternative fuels in CI engines given the constraints provided to the algorithm. Preference towards alternative combustion strategies (i.e. ethanol fumigation) was also indicated by the analysis; however, no clear preference was given to alternative injection strategies (i.e. common rail injection). A strong caveat to keep in mind from the PROMETHEE-GAIA results is that a strong separation in the GAIA plane is observed for the physical and chemical properties of DPM. Whilst the physical DPM properties are favourable with alternative fuels, injection and combustion strategies (e.g. particle mass/number etc), the chemical properties of DPM are particularly troublesome; especially ROS emissions. Furthermore, alternative engine technologies that do not significantly reduce the median diameter of particles need to be identified in future research.

A finding from the literature which was emphasised in Chapter 2 of this thesis was the importance of the semi-volatile component of DPM. The fourth manuscript published as part of this thesis demonstrated a strong correlation between the semi-volatile component of DPM and ROS emissions. ROS are implicated in oxidative stress occurring *in vivo* and are believed to be a precursor to a range of adverse cardiovascular and respiratory health effects (Pope and Dockery, 2006). The semi-volatile fraction of DPM is therefore a very good predictor of the likely health effects associated with DPM given its correlation with ROS emissions and associated oxidative stress. This point was emphasised in Chapter 2 of this thesis, with parts of this chapter being published in a seventh manuscript on the properties and health effects of DPM.

9.2 Recommendations for future research

Whilst predicting transportation futures is undoubtedly a difficult task (Moriarty and Honnery, 2004), it is quite likely that the CI engine will be a dominant transportation power source for the foreseeable future; either in its current configuration (with after-treatment), in hybrid format, or as a range extender for electric vehicles. Considering that intensive development work on CI engine efficiency and emissions is likely to continue for some time, there is therefore a strong justification for further research to improve the gaseous and DPM emissions profile from this type of internal combustion engine. Additionally, considering that India and China are currently experiencing rapid economic growth, there is the possibility of extensive automobile dependency to occur in the countries. Due to improved fuel efficiency, it is possible that the CI engine will become the power-train of choice. A future transportation scenario along these lines provides additional motivation for improvement of the CI engine emissions profile. To acceptably resolve the CI engine emissions problem will, therefore, require much further work, and close collaboration between many branches of science and engineering.

Several suggestions for future research are indicated below.

Alternative fuels research: gaseous emissions

This thesis has demonstrated that ethanol fumigation in CI engines leads to rather significant increases in CO and HC emissions. It is expected that this result is an inherent characteristic of the fumigation approach, rather than being simply a fuel based phenomenon. Therefore, elimination of CO and HC emissions using the fumigation approach in CI engines is a critical research need. Two solutions to this problem are proposed. The first approach would be a

complete re-design of the fumigation system that was used in this study. This thesis fumigated secondary fuels through a single low pressure injector in the intake manifold of the test engine. As a result, all cylinders of this engine are delivered secondary fuel from a single supplementary fuel injector. A major disadvantage of this approach is that secondary fuel is still being injected during the valve overlap period, when both the intake and exhaust valves are open. A corollary of this is that unburnt fuel can escape from the exhaust valve during the valve overlap period which could be a contributing factor to the large CO and HC emissions using the fumigation approach. It is proposed that future fumigation experiments should be conducted with a system whereby each cylinder is supplied supplementary fuel with a separate injector. The advantage of this approach is that more control is achieved with the secondary fuel injection process, enabling no secondary fuel to be injected during the valve overlap period for each cylinder. Thus a fundamental re-design of the fumigation approach adopted in this thesis could help to mitigate CO and HC emissions. Alternatively, if a re-designed fumigation system is not used, an oxidation catalyst emerges as an indispensable part of any fumigation system to mitigate CO and HC emissions. A diesel oxidation catalyst would also be a suitable after-treatment device for reducing the number of particles emitted with CI engines equipped with ethanol fumigation systems.

A range of biodiesel feedstocks and blends were investigated to assess their ability to reduce regulated emissions. Increased NOx emissions were observed with many of the biodiesel blends and feedstocks; especially with mechanical direct injection. Resolving the increased NOx emissions with biodiesel is therefore a critical research need. The use of a retarded injection timing with mechanical direct injection, or the use of an additive (such as ethanol) with a high latent heat of vaporisation could potentially play a role in biodiesel NOx mitigation (Zhu et al., 2010).

Alternative fuels research: DPM emissions

This thesis has shown that the use of biofuels (such as ethanol and biodiesel) in CI engines consistently led to increases in the semi-volatile fraction of DPM, and a correlation between the semi-volatile fraction of DPM and ROS emissions was demonstrated. Considering that ROS emissions are (potentially) a precursor to a range of adverse cardiovascular and respiratory health problems makes elimination of the semi-volatile fraction from biofuel DPM emissions a critical research need. After-treatment techniques could be used to eliminate this fraction of DPM (such as with a catalysed DPF) (Biswas et al., 2009), however, it should be noted that after-treatment is a "brute force" solution. It is anticipated that a more

elegant solution is required. A technique enabling the use of hydrogen in CI engines as a supplementary fuel could prove to be a fruitful avenue for future research to eliminate the semi-volatile fraction of DPM.

Instrumentation

Whilst a physico-chemical characterisation of DPM with various alternative fuels, injection technologies, and combustion strategies was successfully undertaken in this thesis using an SMPS-TD approach, a noted disadvantage of this technique is that it is limited by the rather lengthy SMPS scan time, which is typically of the order of several (~2-3) minutes. As a result, the development of near real-time instrumentation capable of resolving the non-volatile (EC) and semi-volatile (OC) fraction of DPM is a critical research need. The development of an instrument with these capabilities is recommended for two primary reasons. Firstly, it would potentially enable physico-chemical DPM monitoring under transient conditions - which are typically associated with spikes in the particle number concentration emitted by CI engines (Jayaratne et al., 2010). Secondly, the health effects of DPM involve physical effects (i.e. surface area of DPM) and chemical effects (i.e. semi-volatile mass), so measurements of this type would have relevance from a DPM health effects perspective (Giechaskiel et al., 2009).

In recent years, Matter Aerosol have developed a DiscMini instrument which is capable of measuring the number of particles emitted, their median diameter, and alveolar deposited surface area in near real time (~ 1 Hz) (Fierz et al., 2011). It is possible that further development of this rather useful instrument could be undertaken to provide near real-time information on the surface chemistry of particles. There are two ways that this could be achieved. The first approach involves developing a miniaturised TD to be used in conjunction with the DiscMini to investigate the semi-volatile fraction of DPM. The second approach is to split the aerosol into two streams, with the first stream being analysed by the existing DiscMini instrument, whilst the second stream being passed through a UV ionisation device which could yield information on (for example) polycyclic aromatic hydrocarbons adsorbed or condensed on the DPM surface through the emission of photoelectrons (Burtscher, 1992).

Another potential benefit of such an approach is measurement accuracy. The measurements conducted in this thesis show clearly that using a physical method (e.g. volatility) to explore

the chemical properties of DPM (e.g. presence of organics) is subject to less experimental error.

Certification measurements

A solid (> 23 nm) particle number standard has been recently introduced in the European Union (via the PMP program) for light duty diesel vehicles. Solid particles are able to be measured in a reproducible manner which is quite advantageous from a measurement science perspective (Giechaskiel et al., 2010b). Recent publications have shown that the PMP methodology rather effectively removes semi-volatile material not only from the nucleation mode but also organics adsorbed or condensed on the DPM surface (Giechaskiel et al., 2010a). This thesis has shown though that even in the absence of nucleation, an adsorbed semi-volatile coating on particles could be very deleterious to human health (through its correlation with ROS emissions). This finding questions the necessity of employing both heated dilution as well as the subsequent evaporation tube in the PMP methodology. Heated dilution is necessary to avoid the formation of volatile nucleation modes; however, the necessity of subsequently passing the particles through an evaporation tube is questionable. Removing the evaporation tube from the PMP methodology will still prevent the formation of volatile nucleation modes from forming, but will enable DPM to be coated with a small semi-volatile coating. Removal of the evaporation tube would not affect the measurement science fundamentals of the PMP methodology (i.e. repeatability/reproducibility etc), but would deliver a measurement system with far more relevance from a health perspective. Future research could (perhaps) assess the merits of removing the evaporation tube in this sampling methodology to investigate whether a reproducible particle number measurement is still obtained albeit with an adsorbed organic layer on particles.

9.3 Concluding remark

It is interesting to note that one of the world's most dominant transportation power sources (i.e. the CI engine) shares many design features with that used in the commercial production of carbon black (Eastwood, 2008b). Given how the internal combustion engine operates, it is unlikely that developments in combustion science nor DPM after-treatment could ever produce a truly particle free engine. We are, apparently, slaved to a relic from the industrial revolution for our transportation purposes. Taking a futuristic view, it is sincerely hoped that human ingenuity can develop a far more sustainable transportation power source, confining the CI engine to its rightful place in the modern age – namely, to a dusty museum.

9.4 References

Biswas, S., Verma, V., Schauer, J.J., Cassee, F.R., Cho, A.K., Sioutas, C., 2009. Oxidative Potential of Semi-Volatile and Non Volatile Particulate Matter (PM) from Heavy-Duty Vehicles Retrofitted with Emission Control Technologies. Environmental Science & Technology 43(10), 3905-3912.

Burtscher, H., 1992. Measurement and characteristics of combustion aerosols with special consideration of photoelectric charging and charging by flame ions. Journal of aerosol science 23(6), 549-595.

Eastwood, P., 2008. Particulate emissions from vehicles. John Wiley & Sons, Ltd, Chichester, pp. 1-493.

Fierz, M., Houle, C., Steigmeier, P., Burtscher, H., 2011. Design, calibration, and field performance of a miniature diffusion size classifier. Aerosol Science and Technology 45(1), 1-10.

Giechaskiel, B., Alföldy, B., Drossinos, Y., 2009. A metric for health effects studies of diesel exhaust particles. Journal of aerosol science 40(8), 639-651.

Giechaskiel, B., Chirico, R., DeCarlo, P.F., Clairotte, M., Adam, T., Martini, G., Heringa, M.F., Richter, R., Prevot, A.S.H., Baltensperger, U., Astorga, C., 2010a. Evaluation of the particle measurement programme (PMP) protocol to remove the vehicles' exhaust aerosol volatile phase. Science of the Total Environment 408(21), 5106-5116.

Giechaskiel, B., Cresnoverh, M., Jörgl, H., Bergmann, A., 2010b. Calibration and accuracy of a particle number measurement system. Measurement Science & Technology 21(4), Article Number 045102.

Jacobson, M.Z., 2001. Strong radiative heating due to the mixing state of black carbon in atmospheric aerosols. Nature 409(6821), 695-697.

Jayaratne, E.R., Meyer, N.K., Ristovski, Z.D., Morawska, L., Miljevic, B., 2010. Critical analysis of high particle number emissions from accelerating compressed natural gas buses. Environmental Science & Technology 44(10), 3724-3731.

Moriarty, P., Honnery, D., 2004. Forecasting world transport in the year 2050. International Journal of Vehicle Design 35(1-2), 151-165.

Pope, C.A., III, Dockery, D.W., 2006. Health effects of fine particulate air pollution: lines that connect. Journal of the Air & Waste Management Association 56(6), 709-742.

Robinson, A.L., Grieshop, A.P., Donahue, N.M., Hunt, S.W., 2010. Updating the conceptual model for fine particle mass emissions from combustion systems. Journal of the Air & Waste Management Association 60(10), 1204-1222.

Zhang, Z.H., Tsang, K.S., Cheung, C.S., Chan, T.L., Yao, C.D., 2011. Effect of fumigation methanol and ethanol on the gaseous and particulate emissions of a direct-injection diesel engine. Atmospheric Environment 45(11), 2001-2008.

Zhu, L., Cheung, C.S., Zhang, W.G., Huang, Z., 2010. Emissions characteristics of a diesel engine operating on biodiesel and biodiesel blended with ethanol and methanol. Science of the Total Environment 408(4), 914-921.